

ORGANISATION EUROPÉENNE POUR LA RECHERCHE NUCLÉAIRE
CERN EUROPEAN ORGANIZATION FOR NUCLEAR RESEARCH

SECOND ADVANCED ICFA BEAM DYNAMICS WORKSHOP
on Aperture-Related Limitations of the Performance
and Beam Lifetime in Storage Rings

Lugano, Switzerland
11-16 April 1988

PROCEEDINGS
Editors: J. Hagel and E. Keil



International Committee for Future Accelerators
Sponsored by the Particles and Fields Commission of IUPAP

GENEVA
1988

© Copyright CERN, Genève, 1988

Propriété littéraire et scientifique réservée pour tous les pays du monde. Ce document ne peut être reproduit ou traduit en tout ou en partie sans l'autorisation écrite du Directeur général du CERN, titulaire du droit d'auteur. Dans les cas appropriés, et s'il s'agit d'utiliser le document à des fins non commerciales, cette autorisation sera volontiers accordée.

Le CERN ne revendique pas la propriété des inventions brevetables et dessins ou modèles susceptibles de dépôt qui pourraient être décrits dans le présent document; ceux-ci peuvent être librement utilisés par les instituts de recherche, les industriels et autres intéressés. Cependant, le CERN se réserve le droit de s'opposer à toute revendication qu'un usager pourrait faire de la propriété scientifique ou industrielle de toute invention et tout dessin ou modèle décrits dans le présent document.

Literary and scientific copyrights reserved in all countries of the world. This report, or any part of it, may not be reprinted or translated without written permission of the copyright holder, the Director-General of CERN. However, permission will be freely granted for appropriate non-commercial use.

If any patentable invention or registrable design is described in the report, CERN makes no claim to property rights in it but offers it for the free use of research institutions, manufacturers and others. CERN, however, may oppose any attempt by a user to claim any proprietary or patent rights in such inventions or designs as may be described in the present document.

ISSN 0007-8328
ISBN 92-9083-003-6

ABSTRACT

These proceedings contain the papers presented at the 'Second Advanced Beam Dynamics Workshop on Aperture-Related Limitations of the Performance and Beam Lifetime in Storage Rings', which was organized in Lugano, Switzerland, from 11 to 16 April 1988, by the Beam Dynamics Panel of the International Committee for Future Accelerators (ICFA). The papers cover experiments on existing accelerators, analytical methods for determining amplitude limitations, criteria for the properties of the circulating beam and for the quality of accelerator components, and compensation schemes for field defects.

PREFACE

The Workshop on 'Aperture-Related Limitations of the Performance and Beam Lifetime in Storage Rings' was held at the Hôtel de la Paix in Lugano, from 11 to 16 April 1988. It was the second workshop in a series which is being organized by the Beam Dynamics Panel of the International Committee for Future Accelerators (ICFA). The first workshop was held in March 1987 in Brookhaven National Laboratory on 'Production of Low-Emittance Electron and Positron Beams'; the third workshop will be held at the Institute of Nuclear Physics in Novosibirsk from 29 May to June 1989 on 'Beam-Beam Effects in Circular Colliders'.

The Workshop started with a few review talks. The work was organized in four working groups on the following topics:

1. Experiments on existing accelerators, and the lessons to be learned for the planning of future experiments and the design of future machines, coordinated by J. Gareyte.
2. Analytical methods for determining amplitude limitations and diffusion rates in the tails of circulating beams, coordinated by S. Chattopadhyay.
3. Criteria for the properties of the circulating beam, i.e. tune spreads etc., and the resulting criteria for the quality of the storage ring components, coordinated by A. Chao.
4. Compensation schemes for field defects, coordinated by F. Willeke.

The working group coordinators gave summary talks at the end.

These proceedings contain the review talks, the summary talks, and contributions of the participants, arranged according to the working groups.

We should like to thank CERN for support and all the participants, in particular the working group coordinators, for their hard work and for submitting their contributions mostly within the deadline. We should also like to thank Mrs. S. Maio and Mr. J.C. Vialis for their help with the practical arrangements.

J. Hagel and E. Keil
Editors

ORGANIZING COMMITTEE

E.	Keil (Chairman)	T.	Katayama
V.I.	Balbekov	A.A.	Kolomensky
A.	Chao	C.	Leemann
N.	Dikansky	C.	Pellegrini
B.P.	Dmitrievsky	A.	Piwinski
S.-X.	Fang	T.	Suzuki
J.	Hagel (Scientific Secretary)	R.	Talman
C.-S.	Hsue	S.	Tazzari
E.	Kaiser (Secretary)		

CONTENTS

	Page No.
PREFACE	v
THEORY AND ANALYSIS OF NONLINEAR DYNAMICS AND STABILITY IN STORAGE RINGS—A WORKING GROUP SUMMARY	1
<i>S. Chattopadhyay</i>	
A STRATEGY FOR A THOROUGH BEAM STABILITY AND APERTURE ANALYSIS FOR A STORAGE RING FROM DESIGN CONSIDERATIONS	12
<i>S. Chattopadhyay</i>	
OVERVIEW OF METHODS TO DEFINE CONDITIONS FOR BOUNDED MOTION	17
<i>G. Guignard</i>	
PERIODIC SOLUTIONS OF THE HAMILTON-JACOBI EQUATION BY THE SHOOTING METHOD: A TECHNIQUE FOR BEAM DYNAMICS	33
<i>W.E. Gabella</i>	
ANALYTIC APPROACH OF DYNAMIC APERTURE BY SECULAR PERTURBATION THEORY	42
<i>J. Hagel and H. Moshhammer</i>	
CANONICAL DESCRIPTION OF A SECOND-ORDER ACHROMAT	52
<i>S.A. Kheifets, T.H. Fieguth and R.D. Ruth</i>	
AN INTRODUCTION TO SAD	62
<i>K. Hirata</i>	
CALCULATIONS OF THE PARTICLE DYNAMICS IN ACCELERATORS BEYOND THE USUAL PERTURBATION TECHNIQUES	66
<i>H. Mais</i>	

ASYMPTOTIC PROPERTIES OF BIRKHOFF NORMAL FORMS	72
<i>A. Bazzani and G. Turchetti</i>	
COMMENT ON SOME ANALYTICAL METHODS TRYING TO APPROACH THE LIMIT OF STABILITY FROM BELOW	76
<i>G. Guignard</i>	
BEAM DYNAMICS AND TRACKING	79
<i>S.A. Heifets</i>	
A POSSIBLE WAY TO COOL ANTIPROTONS	84
<i>Y.F. Orlov</i>	
SUMMARY REPORT OF THE WORKING GROUP ON EXPERIMENTS	87
<i>J. Crawford, D.A. Edwards, K. Hirata, J. Gareyte, P. Krejcik, P. Kuske, S. Peggs, J.P. Potier, J. Rossbach, T. Sherwood, G. von Holtey</i>	
AN OVERVIEW OF EXPERIMENT E778	95
<i>D.A. Edwards and M.J. Syphers</i>	
DYNAMICAL APERTURE AT THE SPS	105
<i>A. Hilaire</i>	
THE DYNAMIC APERTURE OF BESSY	120
<i>B. Simon and P. Kuske</i>	
HAMILTONIAN THEORY OF THE E778 NONLINEAR DYNAMICS EXPERIMENT	131
<i>S.G. Peggs</i>	
DYNAMIC APERTURE AND INVARIANCE BEHAVIOUR IN THE CERN ANTIPROTON COLLECTOR	145
<i>P. Krejcik</i>	
THE CRITERIA WORKING GROUP SUMMARY	152
<i>P. Audy, M. Cornacchia, A. Chao, M. Harrison, A. Hilaire, C.S. Hsue, H. Kugler, S. Ohnuma, C. Planner, B. Simon, S. Thomson and A. Verdier</i>	
APERTURE AND MULTIPOLE CRITERIA FOR LEP	162
<i>A. Verdier</i>	

SUMMARY OF WORKING GROUP ON COMPENSATION SCHEMES <i>F. Willeke</i>	164
THE APERTURE OF THE HERA PROTON RING <i>F. Willeke</i>	174
MULTIPOLE CORRECTION IN LARGE SYNCHROTRONS <i>D. Neuffer</i>	179
CHROMATICITY CORRECTION FOR LEP: HOW DID WE GET THERE <i>A. Verdier</i>	186
SECOND ORDER TUNE SHIFT IN A COMPENSATED SUPER CELL <i>A. Autin and F. Willeke</i>	192
CORRECTION OF SEXTUPOLAR BEAM ENVELOPE DISTORTION <i>B. Autin</i>	197
PERSISTENT CURRENT FIELD ERRORS AND DYNAMIC APERTURE OF THE HERA PROTON RING <i>R. Brinkmann and F. Willeke</i>	203
CHROMATIC CORRECTIONS AND DYNAMIC APERTURE IN THE HERA ELECTRON RING <i>R. Brinkmann and F. Willeke</i>	208
RECENT WORK ON ERROR CORRECTION AND RELATED ISSUES AT THE SSC <i>R. Talman</i>	213
FREQUENCY-DOMAIN CONSIDERATIONS IN MAGNET SORTING <i>S. Ohnuma</i>	218
SEXTUPOLE CORRECTION SCHEME FOR THE ESRF <i>A. Ropert</i>	223
List of Participants	228

THEORY AND ANALYSIS OF NONLINEAR DYNAMICS AND STABILITY IN STORAGE RINGS - A WORKING GROUP SUMMARY

Swapan Chattopadhyay

LBL, Berkeley, California, USA

P. Audy (Saturne), E.D. Courant (BNL), E. Forest (LBL), G. Guignard (CERN), J. Hagel (CERN), S. Heifets (CEBAF), E. Keil (CERN), S. Kheifets (SLAC), H. Mais (DESY), H. Moshhammer (ITP, Graz), C. Pellegrini (BNL), F. Pilat (CERN), T. Suzuki (KEK), G. Turchetti (U. Bologna), and R.L. Warnock (SLAC).

I. INTRODUCTION

In this report we summarize the efforts and discussions of the Working Group on Theoretical and Analytical Studies at the second ICFA Advanced Beam Dynamics Workshop on "Aperture Limitations in Storage Rings," held in Lugano, Switzerland, April 11-16, 1988. The working group identified several major issues to be addressed during the workshop. These are:

1. Comparison and contrast of different analytical methods used to date for determining Dynamic Aperture in Storage Rings.
2. A model lattice cell to compare these different methods.
3. Other approaches to accurate analytic computation of dynamical distortions to very high orders of nonlinearity.
4. Remainder estimation, long-term weak diffusion rates and all that (Nekhoroshev's theorem).
5. A strategy for a thorough beam stability and aperture analysis from design considerations.

In addition, questions regarding the dependence of the suitable methods on the goals of achieving a certain stability criterion, simple criteria and "scaling laws" for "stable aperture," the definition of "linear aperture" and "SMEAR," and approach to the "border of stability" from above (diffusion rates in the chaotic region by Melnikov's method) were raised and vigorously discussed and debated during the workshop. Various members of the group gave expository talks on many of these issues throughout the workshop. We discuss issues 1 through 4 below, followed by a summary of the major conclusions. Issue 5 is discussed in detail in a companion paper in these proceedings [1]. Nonlinear dynamics with damping and noise is a specialized topic and although discussed during the workshop, is not addressed in this summary. The presence of strong radiation damping in an electron storage ring allows questions regarding long-term stability beyond the damping time to be answered comfortably anyway.

II. ANALYTICAL METHODS FOR DETERMINING DYNAMIC APERTURE - A BRIEF COMMENTARY

We are concerned with different analytical methods dealing with amplitude limitations of stable motion in storage rings. All the methods studied in detail so far approach the limit of stability from 'below' i.e. from the side where the motion is still stable because the initial amplitude is not yet too large. A summary describing these methods is provided by G. Guignard [2] in these workshop proceedings. In a companion paper in these same proceedings, G. Guignard [3] also provides some comments on the advantages and limitations of these various methods. The reader should refer to these papers for a complete exposition.

Most of these methods are based on perturbation techniques of some kind. There are methods using perturbation theory in the Hamiltonian formalism e.g. Poincaré-von Zeipel-Moser procedure, Deprit's algorithm using Lie Transforms, etc. There are perturbation treatments by iterations on the equations of motion directly and successive linearizations thereof. There is the secular perturbation theory based on Lindstedt-Poincaré technique, using power series expansion of the solution in the nonlinear perturbation strength parameter and removing secular terms in each order of perturbation by selecting frequencies appropriately; and others. All these methods strive to compute perturbatively, to as high an order as feasible, nonlinear distortions of the phase-space at an amplitude of motion as large as possible e.g. distortion ΔI of the invariant action (or equivalently emittance), nonlinear detuning (i.e. amplitude-dependent tune shift), resonance widths, etc. The border of stability is then conjectured, in a somewhat ad hoc manner, to be associated with that value of the action J_0 or amplitude x_0 , for which one or more of the following conditions are satisfied: (i) the relative nonlinear distortion of action at amplitude x_0 , computed to certain order, becomes greater than or equal to unity, $\Delta I(x_0)/J_0 \geq 1$; (ii) the nonlinear action becomes negative, $J_0 = I_0 + \Delta I(x_0) \leq 0$; (iii) the nonlinear action becomes infinitely large; (iv) the perturbation solution fails to converge for amplitudes $x \geq x_0$, etc. We should note that the agreement of any one of these conjectures with the onset of large-scale global chaos supposedly associated with the dynamic aperture cannot be proven rigorously. These methods thus do not provide estimates of the true dynamic aperture in the strictest sense. Indeed for an arbitrary and general nonlinear lattice the limit arrived at this way could be very far from the true border of stability. These limits however have practical value in the sense that they do indicate the amplitude at which the phase-space topology gets highly complicated and, conservatively speaking, thus provide a necessary, although not sufficient condition for unstable motion. Under certain fortuitous circumstances, these limits may even be arbitrarily close to the dynamic aperture, as numerical tracking has suggested in a few simple cases [2,4].

In most of these methods, the analytical developments become cumbersome after a few low order calculations in the perturbation series, linearizations, iterations, etc. The convergence of the perturbation procedure, even when good, can not be proved mathematically. In many cases the generalization to magnetic multipole elements other than sextupoles has not been achieved and in some cases the extensions to two-dimensions even remains to be done. Often the validity of these methods is also restricted to a limited range of the linear-optics parameter space e.g. tunes etc. The Hagel-Moshhammer approach [4] using techniques of secular perturbation theory has been the most successful one, leading to reasonable approximate estimation of the dynamic aperture for systems as complex as the LEP collider.

Amongst nonperturbative methods, one can consider applying the numerically derived Residue Criterion of Green and McKay. However, the validity of this criterion has not been demonstrated beyond one-dimensional 'standard' and 'quadratic' maps. It can be applied exactly and directly to the stability of longitudinal synchrotron motion. For one-dimensional transverse betatron motion, it at best confirms Chirikov's resonance overlap criterion for the onset of chaos. Application of this method for extracting analytic expressions for the stability limit in a realistic, general, nonlinear two-dimensional map representing a storage ring is not obvious.

Another nonperturbative method, proposed by Gabella, Ruth and Warnock [5], is based on the direct solution of the two-dimensional Hamilton-Jacobi equation. This method allows computation of distorted invariant tori at amplitudes close to the dynamic aperture and looks for the singularities of the implicit equations defining the orbits via the generating function. There are indications that the breakdown of the generating function via a singularity is related to the residue criterion and can be generalized to higher dimensions. This seems to be one of the most promising analytic Hamiltonian approaches so far.

One can also attempt to approach the border of stability from 'above' i.e., from the region of large-scale global chaos in phase space. One may look at various stochastic diffusion processes e.g., Arnold diffusion, etc. using existing mathematical techniques such as Melnikov's method, etc. Not much progress has been made along these directions in storage ring dynamics. Comments on these approaches are provided by H. Mais [6] in his contributions to these proceedings.

III. A MODEL LATTICE FOR COMPARING DIFFERENT ANALYTICAL METHODS TO CALCULATE THE DYNAMIC APERTURE

For convenience and standardization, it was felt that one should focus on a model standard lattice cell on which to compare, contrast and numerically test the different analytical methods for calculating the Dynamic Aperture. The Lattice should be modestly nonlinear and yet be simple enough in structure with relatively known dynamic properties in order for it to be useful.

A FODO-lattice with superimposed quadrupoles and sextupoles separated by drift spaces of equal lengths was chosen as such a model. The lattice configuration is shown in Fig. 1.

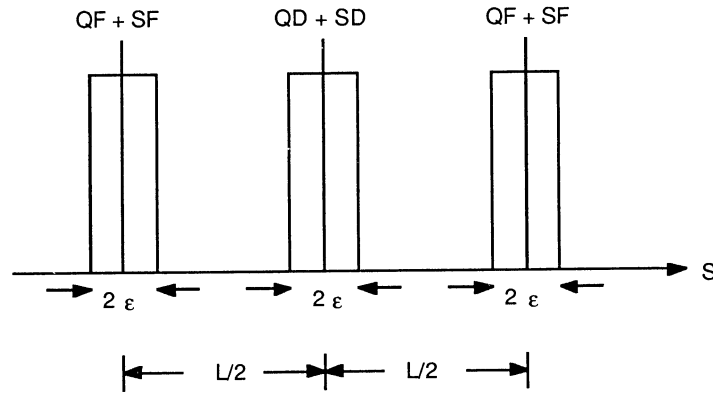


Fig. 1

The integrated strengths of each quadrupole (QF or QD) is chosen to be:

$$(K\ell) = \frac{4}{L} \sin\left(\frac{\mu}{2}\right) \quad (1)$$

where $\mu = 2\pi Q$ is the phase advance across the cell. The sextupole strengths could be chosen either arbitrarily or such as to correct the natural chromaticities ξ_x, ξ_y to vanishing values. In the latter case, the sextupole strengths should be chosen as:

$$(K'\ell)_F = \frac{(K\ell)}{\eta_F} \quad (2)$$

$$(K'\ell)_D = \frac{(K\ell)}{\eta_D} \quad (3)$$

where $\eta_{F,D} = \frac{L^2 n}{8 \sin^2\left(\frac{\mu}{2}\right)} \left[2 \pm \sin\left(\frac{\mu}{2}\right) \right]$ and $n = 1/\rho$.

As an example of the parameter values, one can consider the identical LEP cell lattice:

$$L = 79 \text{ m}; \quad \mu = \pi/3; \quad \rho = 3100 \text{ m}.$$

For comparison with numerical tracking, one could use initial or starting condition $\dot{x}(0) = \dot{y}(0) = 0$ and $x(0) = x_0, y(0) = y_0$. One could then ask what is the maximum value of the (x_0, y_0) pair, (x_0^{\max}, y_0^{\max}) , for which the motion is stable and bounded?

It was also suggested during the workshop that one could use any one of the high-brightness, low-emittance lattices envisaged for the many third generation synchrotron radiation sources around the world (Berkeley, Trieste, Taiwan, etc.) as test cases. These lattices are sufficiently nonlinear at modest amplitudes to put the analyses to a real test of their computational power and practicality.

IV. ANOTHER ANALYTIC APPROACH - HAMILTONIAN-FREE ANALYSIS ON EXACT MAPS

We have noted that analytic developments using the Hamiltonian approach become increasingly cumbersome as we go to higher orders in perturbation theory at large amplitudes of motion. It is indeed an ambitious goal to be able to derive explicit analytic expressions for the Dynamic Aperture (i.e. border of stability) for any arbitrary nonlinear two (and three) dimensional Hamiltonian system, such as is represented by a real storage ring. We shy away from such a goal of trying to reach the border of stability in one leap. Instead we ask a more practical and modest question: Do we have analytic tools to understand the phase space topology and compute with enough accuracy dynamical distortions (e.g. distortion of invariant tori of action, nonlinear resonance widths, amplitude-dependent tune-shifts etc.) at large amplitudes close to the Dynamic Aperture for a real three-dimensional storage ring lattice? The answer is yes and this tool is based on extracting exact "maps" for the accelerator lattice (rather than a Hamiltonian) and doing analysis (perturbative or otherwise) on these maps.

Hamiltonian formalism and exact equations of motion derived from them, are natural and useful tools for simple situations like a few objects moving in a rather "smooth" potential well. The Hamiltonian corresponding to a storage ring is a rather complicated beast, involving periodic delta-function-like objects corresponding to localized electromagnetic elements and time-dependence as well. A storage ring is intrinsically "modular", affecting a large number of "almost discrete" transformations on a particle's phase space coordinates. A description of beam dynamics with "maps" seems more natural. A map M transforms a point z_i of phase space at azimuth s_i on the reference orbit into a point z_f at azimuth s_f :

$$z_f = M(z_i; s_f, s_i) . \quad (4)$$

A full turn map $M(s)$ at azimuth s for a storage ring of circumference C corresponds to $s_i = s, s_f = s + C$; a multi-turn (n -turn) map $M_n(s)$ to $s_f = s + nC$. Insofar as one does not care to look at the phase-space topology at any other azimuth between s_i and s_f , the same "map" can be derived from a large number of Hamiltonians belonging to a certain "class", up to a certain order of nonlinearities of the map.

Maps have been used as standard tools to describe linear storage ring lattices for a long time. In the particular case of linear motion, maps are amenable to representations in terms of matrices. Indeed, transport matrices through linear elements involving Twiss parameters are all too familiar in the standard theory of betatron

motion in circular accelerators, one of the greatest triumphs of Courant-Snyder formalism. These matrices (i.e. maps) summarize the results of integrating the equations of motion and provide stability analysis directly. In the same spirit one could foresee great virtue in generalizing this formalism to the nonlinear case, using nonlinear maps. For this purpose, one needs to construct these maps in a sufficiently simple, reliable and accurate way. We will discuss the construction of maps later in the section. Once an accurate map is obtained, one could either use it to perform numerical tracking by iteration (thus saving computation time, since most of the work has already been done in extracting the map thus effectively eliminating redundant integrations) or could simply use a full-turn map to do analysis, perturbative or otherwise, on it to extract nonlinearly distorted dynamical quantities such as distortions of invariant tori (i.e. action or emittance), nonlinear tune-shifts, resonance analysis, etc. We turn to this latter issue of Hamiltonian-free analysis on exact maps for the moment.

A full-turn map allows the study of phase-space topology (e.g. invariant surfaces, etc.) without explicit reference to the underlying Hamiltonian. This is achieved either through the Normal Form Analysis [7,8,9] based on perturbation theory or through the solution of a functional equation for the invariant surface by an appropriate iterative method [5,10].

The Normal Form analysis is based on perturbation theory on exact maps and phase advances. It is the nonlinear map analogue of the linear Courant-Snyder solution:

$$\begin{bmatrix} x(s) \\ \dot{x}(s) \end{bmatrix} = U(s) R[\psi(s)] U^{-1}(0) \begin{bmatrix} x(0) \\ \dot{x}(0) \end{bmatrix} \quad (5)$$

where

$$U(s) = \begin{pmatrix} \sqrt{\beta(s)} & 0 \\ \gamma(s) & \frac{1}{\sqrt{\beta(s)}} \end{pmatrix}; \quad \gamma(s) = \dot{\beta}(s)/2\sqrt{\beta(s)}, \quad (6)$$

$$\beta(0) = \beta(C) \Rightarrow U(0) = U(C); \quad \psi(C) = 2\pi\nu \quad (7)$$

and R is the rotation matrix corresponding to phase advance $\psi(s)$, ν being the total tune and $\beta(s)$ the lattice beta-function.

Using the complex notation $z = x + ip$ for phase space coordinates under the transformation $z' = M(z, z^*)$, the Normal Form analysis uses symplectic transformations close to identity:

$$\{z, z^*\} \rightarrow \{\xi, \xi^*\} : z = \Phi(\xi, \xi^*) = \sum_{n \geq 1} \Phi_n(\xi, \xi^*) \quad (8)$$

where Φ_n 's are homogeneous polynomials of degree n in ξ, ξ^* to bring the map M to the Normal Form:

$$M = \Phi e^{i\Omega(\xi, \xi^*)} \Phi^{-1} \quad (9)$$

analogous to Eq. (5) for the linear case, where Ω is also of degree $\leq n+1$ and is determined recursively, together with Φ . Simply stated, this analysis transforms the phase-space to coordinates where the map is a pure rotation, with nonconstant amplitude-dependent angle however (Ω depends on $|\xi|^2 = \xi\xi^*$):

$$\xi' = e^{i\Omega(\xi, \xi^*)} \xi \quad (10)$$

It can be best visualized pictorially as in Fig. 2.

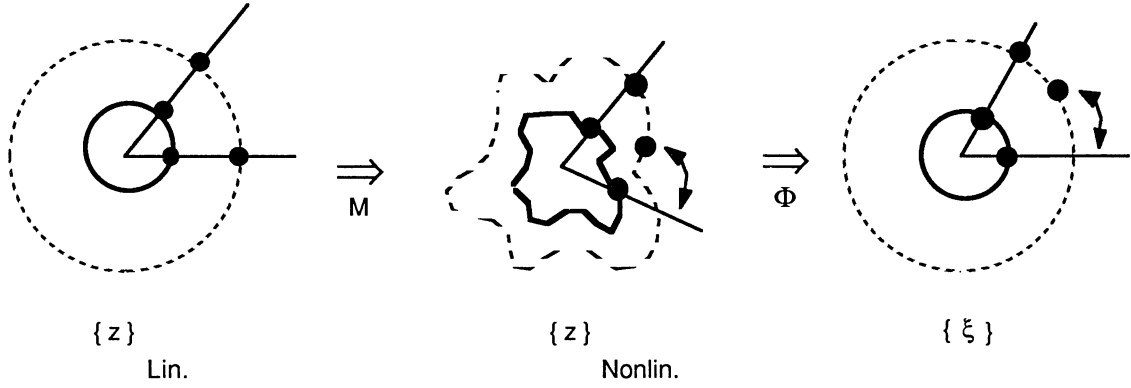


Fig. 2

After t -iterations, the map simply reads:

$$M^t = \Phi e^{it\Omega(\xi\xi^*)} \Phi^{-1} \quad (11)$$

The analysis extends up to an arbitrary order in Φ . If M is only an order N symplectic truncation, the normal form does not change up to the same order.

From Normal Forms, one can compute a whole host of dynamical quantities related to nonlinear phase-space distortions in a straightforward way. For example perturbative "tune-shifts" and distortion of invariant action or "SMEAR" can be simply computed as:

$$\text{Tune Shift: } \delta\nu = \frac{1}{2\pi} \Omega(\rho) - \nu_0 \quad (12)$$

$$\text{SMEAR: } \sigma = \frac{\langle (R - \langle R \rangle)^2 \rangle^{1/2}}{\langle R \rangle} \quad (13)$$

$$\text{where } \langle R \rangle = \frac{1}{2\pi} \int_0^{2\pi} R(\theta) d\theta \quad (14)$$

$$\text{and } R(\theta) = |z| = |\Phi(\xi, \xi^*)| = |\Phi(\rho e^{i\theta}, \rho e^{-i\theta})| \quad (15)$$

$$\rho = |\xi| = |\Phi^{-1}(z, z^*)| = |z| + \dots \quad (16)$$

One can also compute σ_n , the sum of the strengths of all n -th order resonances. One can write the full-turn map, explicitly delineating the linear map M_L , as:

$$M = M_L e^{\hat{g}_3} e^{\hat{g}_4} \dots e^{\hat{g}_n} \dots \quad (17)$$

$$\text{where } g_n = \sum_{\substack{j+k=n \\ |j|+|k| \leq n}} A_{jk} \epsilon_j^{j/2} \epsilon_k^{k/2} 2^{(j+k)/2} e^{i(\mathcal{L}\psi_x + m\psi_y)} \quad (18)$$

One can then construct resonance strengths at a certain amplitude $A_0 = \epsilon_0^{1/2}$ as follows:

$$\sigma_n = \sum_{\substack{j+k=n \\ |j|+|k|\leq n}} |A_{jk\ell m} A_{jk\ell m}^*| \epsilon_0^{n/2} \quad (19)$$

where ϵ_0 is a typical emittance of the particle. The σ_n 's are a full figure of merit of nonlinearity, containing tune-shifts, resonances and nonlinear distortion. They are also a measure of the resonance widths and are "invariant" under the linear map. What is more, one can mathematically subtract the nonlinear detuning or amplitude-dependent tune-shift, thus obtaining a quantity σ_n^* , which is a measure of "pure distortion" of invariant tori contributed by all n-th order resonances:

$$\sigma_n^* = [\sigma_n - \text{Tune shifts}] \quad \text{"Nonlinear Distortion"} \quad (20)$$

While σ_n is affected by the full nonlinear map, σ_n^* is affected by the "Coherent Nonlinear Map". This is depicted in Fig. 3 below. Quantities $\{\sigma_n\}$ and $\{\sigma_n^*\}$ allow us to disentangle linear vs. nonlinear and nonlinear detuning vs. nonlinear distortion effects in a machine in a most effective way.

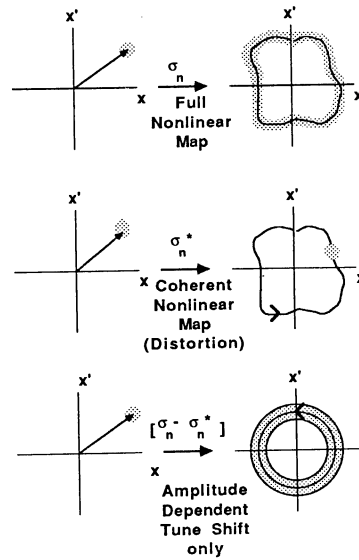


Fig. 3

The alternative nonperturbative method [5,10] of solving the functional equation for the invariant surface exploits the power of Newton's method to study invariant surfaces very close to unstable regions of phase space. From such a calculation again, one obtains nonlinear tune-shifts and Fourier analysis of the invariant surface to reveal the spectrum of contributing resonances.

Both these Hamiltonian free analysis tools on exact maps are powerful and complement each other. While it may be sufficient to use the Normal Form Analysis in many cases yielding quick and accurate quantitative phase-space analysis at large amplitudes, solving the functional equation for invariant surfaces may have a wider range of utility however, since it does not depend on perturbation theory.

Modular maps on a storage ring provide the advantage that any point in the ring is just as good for analytic manipulations on maps: any other point in the ring can be obtained by simple phase-advances, etc. One could also combine full-turn maps with maps describing localized effects such as the beam-beam interaction, r.f. kicks, undulators, etc., thus allowing studies of the effect of variations of the local effect in an otherwise unchanged full-turn lattice. One can even envision combining noise or dissipation (as in electron storage rings) with the symplectic maps considered here. Maps are also smooth functions of tunes, nonlinear magnet strengths, particle energy etc., in general. One can thus store maps for a few values of these parameters and use some kind of interpolation to reach other parameter values, thus allowing an efficient way to explore tune space, etc. All these favorable attributes, combined with the ability to track particles and existence of the above two powerful analysis tools to find invariant surfaces and compute accurately nonlinear phase-space distortions in greatly reduced computation time even at large amplitudes approaching the border of stability, point to great promise in the use of analysis based on exact maps and should allow us to take a significantly long leap forward in quantitatively thorough beam stability studies....provided we have tools to extract maps to any desired accuracy efficiently. We turn to this point next.

In spite of the recognition of the usefulness of nonlinear maps, their full power has not been fully exploited until recently, due to the difficulties associated with extraction of accurate maps. Representing the map $M(z; s_f, s_i)$ as a truncated Taylor series in the components of z :

$$M: z_f = z_i + Lz_i^2 + Tz_i^3 + \dots + Wz_i^N \quad (21)$$

one needs accurate computation of the Taylor coefficients, which involve increasingly higher order derivatives $W = [\partial^{N-1} z_f / \partial z_i^{N-1}]_0$ on any reference closed orbit. Such computations become increasingly inaccurate with N ,

involving high order ratios of vanishing numbers. This has tended to limit accuracy, since even with the help of Lie algebraic methods and symbolic manipulation, it was not practical to compute these coefficients beyond the first few orders. A significant recent development has resulted in a superbly improved technique [9] for calculation of derivatives, exact up to the computing machine precision, using Differential Algebra. This innovation, by M. Berz, finally can provide maps of the desired accuracy and can work to arbitrary order, limited only by computer storage and time.

In some extremely nonlinear cases with large amplitudes, one may hit a practical limitation even with differential algebraic techniques - it may simply be not feasible to compute a sufficient number of Taylor coefficients, the storage and computing time beginning to increase catastrophically beyond a certain order. Considerable progress is being made in a complementary and alternative approach [10] involving a global approximation of a map with "spline functions" (in 'action') and orthogonal basis functions (Fourier analysis in 'angle'). The coefficients in this representation can be obtained in an elementary way by running a tracking code for one turn starting from a set of initial values on a suitable mesh in action-angle space and then by proper fitting with the above functions. No derivatives of the map M are required. If the tracking code is symplectic, the resulting map will typically be symplectic to good accuracy. A small modification makes the map symplectic to any required precision. This method of Warnock et al. [10] although at a development stage, also seems quite promising with respect to accuracy, simplicity and computation time.

V. REMAINDER ESTIMATION, LONG-TERM WEAK DIFFUSION RATES AND ALL THAT

At every stage of Normal Form Analysis as a function of amplitude, the Birkhoff asymptotic perturbation series fails to converge beyond a certain number of symplectic normal form transformations. There is a

"remainder" that is left over at the penultimate convergence stage, which is a measure of the remaining fluctuation in the Hamiltonian or action ($\Delta J/J$) and is a measure of the weak diffusion rate at that amplitude resulting from the infinitely many thin stochastic layers in the phase space enclosed by that amplitude. Typically, inverse of these residual fluctuations is a broad measure of the lifetime τ_{life} of the particle resulting from these diffusion mechanisms. The situation is illustrated pictorially in Fig. 4.

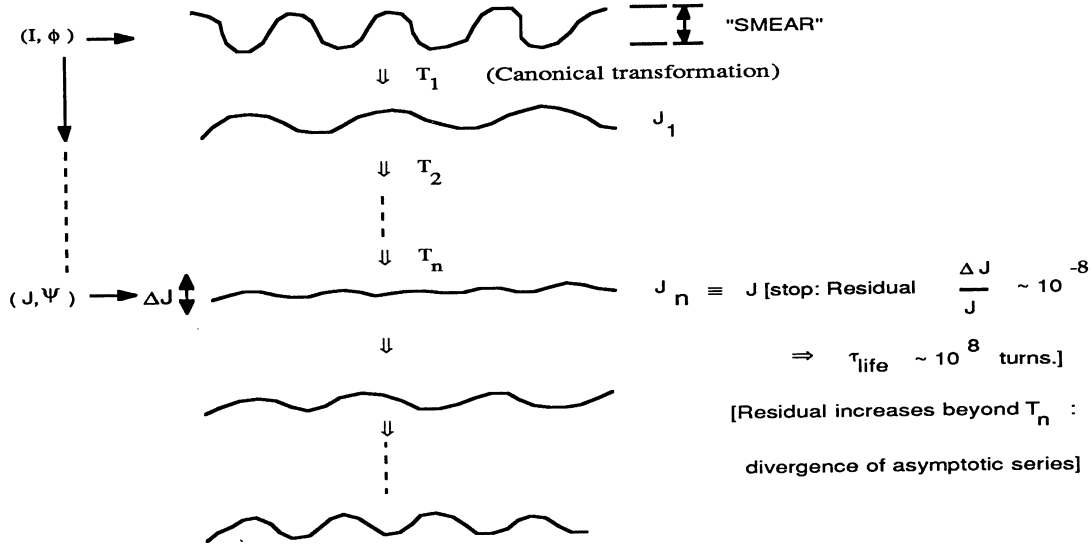


Fig. 4

If the remainder could be estimated accurately, we could estimate the weak diffusion rate accurately as well. Rigorous results in multidimensions exist only for autonomous (time-independent) Hamiltonian maps. No such rigorous result exists for nonautonomous (time-dependent) Hamiltonian maps, as for storage rings. However in the one-dimensional case in a phase plane, similar estimates hold. There are still arbitrary constants in these estimates and the results have to be used with extreme care. However, these estimates may still be useful for relative "scaling" of rates with amplitudes (emittances), etc. The mathematics is intricately related to Nekhoroshev's theorem and is exposed in the contribution of Bazzani and Turchetti [8] in these proceedings.

VI. CONCLUSIONS

We find that a global analytic expression and simple "scaling laws" for the Dynamic Aperture of an arbitrary nonlinear storage ring are hard, if not impossible, to find. Under some fortunate and very special circumstances for particular lattices, certain analytic methods using low order perturbation theory in the Hamiltonian formalism as outlined in Section II can, at best, point to a limiting amplitude of motion, around and beyond which the motion and the phase space structure itself get pathologically complicated. These limiting amplitudes, when analytically expressed (and if believed to be relevant and applicable), are cumbersome enough to be of little practical use. Often, they have to be numerically evaluated and simple "scaling" with parameters is not obvious, except under special circumstances. For simple situations with modest nonlinearity however, they have practical value in the sense that they provide a first guess at the pathological region of phase space.

Considerable progress has been made however, thanks to some powerful newly-developed computational tools as outlined in Section III of this report, in the ability to perform nonlinear computational analysis, perturbative or otherwise, at impressively large three dimensional amplitudes on any nonlinear lattice for which a tracking code exists without compromising unduly on accuracy, faithfulness and economy of time. These analytical methods allow one to penetrate deep into the nonlinear phase space, with accurate knowledge of the nonlinear optical distortions (distortion of invariant surfaces, nonlinear resonance spectrum, their strengths and widths, amplitude-dependent tune-shifts, etc.) at every stage, ultimately reaching amplitudes so close to the real border of stability or Dynamic Aperture that they can be accepted as the limiting amplitude for all practical purposes. Significant milestones in this development have been techniques to extract exact full-turn maps and technique to analyze these maps. In the former category, the algorithm to extract exact maps by computing derivatives with Differential Algebra is a significant innovation by M. Berz and is surely to be recognized as an unusually powerful tool. It will certainly find even more widespread application in the future. The other method of map extraction from an arbitrary tracking code using 'spline' and 'Fourier' fitting, as proposed by Warnock et al. recently, also holds significant promise and complements Berz's method in extremely nonlinear situations where storage and computation time become catastrophic. In the latter category of 'analysis of maps', E. Forest and others have resurrected the Normal Form analysis, known since Birkhoff, to a level where it provides computational capability orders of magnitude superior to any other methods that were used before. In parallel, the nonperturbative solution of the functional equation for the generating function, proposed by Warnock et al., provides another attractive and promising alternative, to be explored further in the future. These developments have been a significant step towards the thoroughness of beam stability analysis and computational analytic estimates of the border of stability, without involving the practically difficult long-term tracking.

The question of ultimate long-term stability (after 10^{10} turns, say) was vigorously discussed during the workshop. Both the numerically tracked short-term Dynamic Aperture and the above analyses have little to do with long-term stability. There exist no strict mathematical theorems applicable to a three dimensional storage ring. Estimation of the 'remainder' and weak diffusion rates, in the spirit of Nekhoroshev's theorem as discussed in Section IV, holds a very weak promise in this direction. This issue and possible alternatives to long-term tracking are discussed in companion papers [1] and [11] in these proceedings. A strategy for a thorough beam stability and aperture analysis for a storage ring from design considerations, taking into account the methods and recent developments outlined in this report, is discussed in reference [1].

ACKNOWLEDGMENT

This work was supported by the Office of Energy Research, Office of Basic Energy Sciences, Department of Energy under Contract No. DE-AC03-76SF00098.

REFERENCES

- [1] S. Chattopadhyay, "A Strategy for a Thorough Beam Stability and Aperture Analysis for a Storage Ring from Design Considerations," these proceedings.
- [2] G. Guignard, "Overview of the Methods to Define Conditions for Bounded Motion," these proceedings.
- [3] G. Guignard, "Comment on Some Analytic Methods Trying to Approach the Limit of Stability from Below," these proceedings.

- [4] J. Hagel and H. Moshhammer, "Analytic Approach of Dynamic Aperture by Secular Perturbation Theory," these proceedings.
- [5] W. E. Gabella, R.D. Ruth and R.L. Warnock, "Periodic Solutions of the Hamiltonian-Jacobi Equation by the Shooting Method: A Technique for Beam Dynamics," these proceedings.
- [6] H. Mais, "Calculations of the Particle Dynamics in Accelerators Beyond the Usual Perturbation Techniques," these proceedings.
- [7] A. Bazzani et al., "Normal Forms for Hamiltonian Maps and Nonlinear Effects in a LHC Model," CERN SPS/88-2 (AMS), LHC Note 66.
- [8] A. Bazzani and G. Turchetti, "Asymptotic Properties of Birkhoff Normal Forms," these proceedings.
- [9] E. Forest, M. Berz and J. Irwin, "Exact Computation of Derivatives with Differential Algebra and Applications to Beam Dynamics," SSC-166, submitted to Particle Accelerators.
- [10] R.L. Warnock, W. Gabella and R.D. Ruth, "Construction of Symplectic Full-turn Maps by Application of an Arbitrary Tracking Code," manuscript under preparation.
- [11] S.A. Heifets, "Beam Dynamics and Tracking," these proceedings.

A STRATEGY FOR A THOROUGH BEAM STABILITY AND APERTURE ANALYSIS FOR A STORAGE RING FROM DESIGN CONSIDERATIONS

Swapan Chattopadhyay

LBL, Berkeley, California, USA

We attempt in this report to outline a reasonable approach to understanding and analyzing beam stability and related aperture as thoroughly as one can, using tracking and all the available analytic tools mentioned in a companion summary report [1], while designing any particular storage ring. The approach might consist of the following sequential stages:

1. Determine the "Needed Aperture": Estimate the size of stable aperture of "good behavior", (x_0, y_0) , needed for beam injection, operation, lifetime etc. in both planes - usually prescribed as certain specifications by the users and builders of beam optical systems. Often one may want to specify the maximum tolerable optical aberrations (geometric and chromatic) and dynamical distortions at the border of the needed aperture as well. We note that the needed aperture is a machine and technology dependent concept.
2. Quickly estimate the short-term "Dynamic Aperture" by tracking over a few hundred turns (typically 400) with a good tracking code, both for the ideal machine and then with realistically "guessed" magnet errors. This Dynamic Aperture (A_0, B_0) better be much larger than the "Needed Aperture" (x_0, y_0) and preferably comparable to or larger than the physical size of the beam chamber. See Fig. 1.

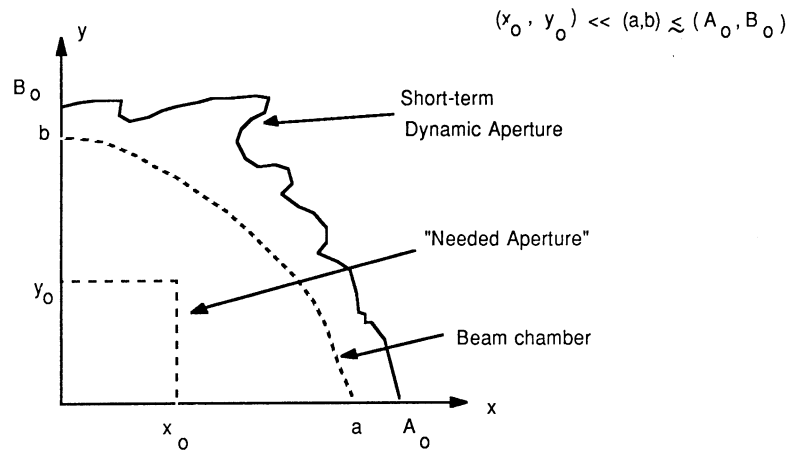


Fig. 1

The 400-turns "Dynamic Aperture" is admittedly a rather elusive concept, with very little to do with long-time stability in most cases. However, ensuring the above hierarchy of magnitudes in apertures is a necessary, although not sufficient, condition for beam stability. For small electron machines, tracking over a few "radiation damping times" may be sufficient for estimating Dynamic Aperture for long-time stability. For example, for synchrotron storage rings like the one being designed at Berkeley, the damping time $\tau_D \simeq 10$ ms corresponds to approximately 10,000 turns. Tracking over twenty or thirty thousand turns is still feasible. Long term tracking for large hadron machines is however almost impractical due to the hundreds of thousands of turns required for that purpose.

3. Once the "needed aperture" has been defined and short-and/or long-term "Dynamic Aperture" has been established by tracking, systematically explore the phase space structure and topology from small amplitudes to as large an amplitude as possible, in order to establish what we call the "Understandable Aperture". The "Needed Aperture" must lie within the "Understandable Aperture". The "Understandable Aperture" must be not only smaller than the "Dynamic Aperture", however determined by tracking, but must enclose a region of phase space where one or more of the relevant dynamical distortions (e.g., SMEAR, tune shifts, resonance widths, etc.), must stay bounded and reasonably finite and exhibit relatively understandable stable trends under small perturbations of the machine or the initial conditions. All the words "small perturbations", "relevant dynamical distortions", "bounded and reasonably finite", "relatively understandable stable trends", etc. are machine dependent and ought to be clearly understood and defined, tailored to a specific machine. For example, the concept of "Linear Aperture", defined as that within which the famous "SMEAR" must be less than a certain percentage ($< 10\%$), was elected as the definition of "understandable aperture" for the design of the SSC. It is a conservative and safe criterion and has tremendous practical value in the design of any machine. One should remember however that the prescription of a maximum percentage of fluctuation in the linear invariants is only a necessary but insufficient criterion for the long-term stability in any machine.

Instead of "linear", we have used the word "understandable". This is to imply that unlike the SSC at injection, many machines (all third generation synchrotron radiation sources and damping rings for example) have a nonlinear ideal sextupole lattice as the unperturbed starting point. Nevertheless, thanks to some powerful newly-developed computational tools as outlined in the summary report on theoretical and analytical studies [1], we are in a position to perform nonlinear analysis, perturbative or otherwise, at impressively large amplitudes, on any lattice for which a tracking code exists, without compromising on accuracy and faithfulness.

To perform such analysis, one first constructs the one-turn map "M" of the machine as precisely as one can to the desired level of accuracy (computer precision) either via the differential algebraic technique of M. Berz [1,2] or via a few-turn tracking data a la Warnock, et al. [1,3]. If successful, one has done most of the work. One can then analyze these maps either through Normal Form perturbative analysis [1,2,4,5] or through the nonperturbative iterative solution of the functional equation for the invariant surface itself [3,6], to compute quantities containing the detailed information of the nonlinear optics. Most of it is contained in the resonance strengths (or widths). Knowing the strengths of all resonances of all orders, in principle, implies knowing the entire nonlinear optical map. In practice however, one is limited to only a small number of figures of merit to be computed to characterize the nonlinear machine e.g. $\sigma_n(A)$ = sum of the strengths of all n-th order resonances at amplitude A, $\sigma_n^*(A)$ = contribution of all n-th order resonances to pure distortion [1], nonlinear tune shift $\Delta\nu(A)$, distortion of invariant tori or SMEAR $\sigma(A)$, etc. Using these, one can try to 'creep into' the nonlinear region as far as one can.

4. One can then look for trends in these nonlinear optical distortions as a function of amplitude A and resonance order ' n '. Criteria for "good behavior" should then be decided upon by imposing judicious constraints on the upper bounds and patterns of these quantities, specific to any particular machine. Possible criteria could be various combinations of the following:

- (i) $|\Delta v(A)| \leq .01$ or $.001$, etc.
- (ii) convergence and/or regularity of $\sigma_n(A)$
- (iii) sensitivity of $\Delta v(A)$ and $\sigma_n(A)$ to amplitude (i.e., $\sigma'_n(A) \equiv d\sigma_n(A)/dA$, $\Delta v'(A)$, etc).
- (iv) $|\sigma_n| \leq \dots$, $n > n_0$.
- (v) $\text{SMEAR} = \sigma(A) < (\text{certain percentage}) \sim 10\%$ (imposes constraint on $\sum_n \sigma_n^*(A)$).

Pattern of the resonance strengths $\sigma_n(A)$ in tune units as a function of order ' n ' and amplitude A (.001 to .005 in suitable units) expected for the bare lattice of the Advanced Light Source being designed at Berkeley, for example, is shown in Fig. 2. It shows the usual convergence pattern of falling off by an order of magnitude per each increasing order of the resonance at small amplitudes (.001). Pattern gets worse with higher amplitudes, with no systematic trend or convergence expected close to the Dynamic Aperture.

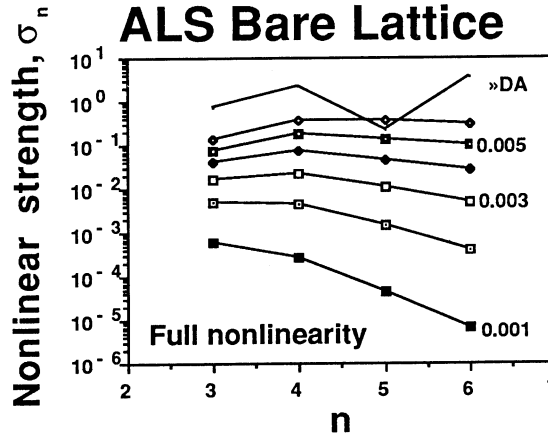


Fig. 2

5. Finally, one would want to compare the "Needed Aperture" with these behavior criteria. Hopefully, one can correlate the storage ring behavior with these nonlinear optical distortions as outlined above. The final aim is some kind of visualization of contours of constant "dynamical quality" in the amplitude plane, as sketched in Fig. 3 and choice of a certain nonlinearly distorted but understandable and controllable amplitude contour A_c as the aperture limit. Once chosen, $\Delta v(A_c)$, $\sigma(A_c)$, $\sigma_n(A_c)$, $\sigma_n^*(A_c)$, $\sigma'_n(A_c)$ etc. will then dictate tolerances on magnetic multipole components of the machine.

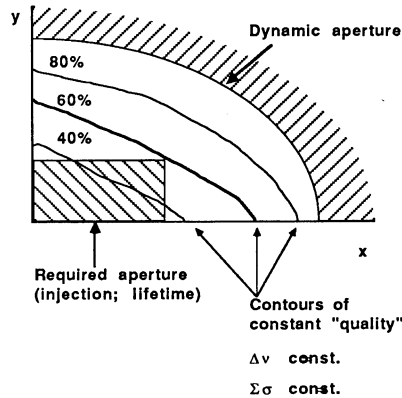


Fig. 3

Further details of choosing the aperture criteria for various machines are exposed in detail in the Criteria Working Group Summary by A. Chao [7] in these proceedings.

6. Now then, how about ultimate long-term stability (after 10^{10} turns, say)? Both the short-term Dynamic Aperture and the above analysis have little connection with long-term stability. What is worse, no precise statement in this regard can be made, since no general theorem exists. The KAM theorem only predicts bounded motion for "small" amplitudes in one dimension. In practice, this small amplitude is so small as to be useless for stability considerations in storage rings. Moreover, particles really move in three dimensions and due to Arnold diffusion and other semi-quantitative concepts, it is clear that some particles very close to the origin will nevertheless escape. The position in phase space of these particles is extremely machine dependent and the most insignificant change in modeling a machine sometimes may turn an unstable particle into a stable one and vice versa. Nothing, not even the powerful mathematical theorems like the KAM, seems to rescue particles from possible long term loss, except electrons where there is radiation damping. But then for electrons one can track over thirty thousand turns or so to determine numerically the Dynamic Aperture. This leads us to long term tracking for protons (hundreds of thousands of turns), which may not be feasible.

For protons, a relevant question to ask instead is: what is the expected lifetime of a beam having a certain maximum amplitude of motion? For this purpose, one may attempt to estimate, in the spirit of Nekhoroshev's theorem [1,5], the "remainder" at that amplitude, the weak diffusion rate due to these stochastic layers and their enhancement by external noise, modulation by synchrotron oscillation, etc. One can use any or all of these qualitative methods including Arnold diffusion rate, Chirikov criterion, modulation diffusion, etc. to arrive at some estimate of beam lifetime τ_L expected from nonlinear dynamics. This has to be compared with expected beam lifetime τ_M from other considerations by carefully looking at mechanisms of other beam losses and their various time scales: noise, beam-beam, Touschek and Intrabeam scattering, Luminosity etc. All one has to ensure is that $\tau_L > \tau_M$.

We note that it is nontrivial, if not impossible, to compute τ_L accurately. Qualitative estimates may be off from reality by several orders of magnitude owing to arbitrary constant parameters appearing in the remainder estimates [1,5]. Considerations along these lines and the possibility of simulating long-term tracking with short-term tracking using finitely many particles and imposed noise, is exposed in detail in the contribution of Heifets [8], in these proceedings.

Given the importance of this issue in the design of a real storage ring and the difficulty and lack of any quick sound method of determining the border of stability directly in one step, the above systematic, lengthy and somewhat painful process seems to be the only approach to a comfortable design of a storage ring, safeguarding the understandability and controllability of the beam dynamics, even under extremely nonlinear situations.

ACKNOWLEDGMENTS:

The author has benefited from numerous illuminating discussions with R. L. Warnock, G. Turchetti and especially E. Forest (with whom he is fortunate to have continuous dialogues as a colleague) on maps, analysis on maps and general Hamiltonian analysis. He is also thankful to E. Forest for providing the data in Fig. 2 and to M. S. Zisman for providing some of the illustrations.

The work was supported by the Office of Energy Research, Office of Basic Energy Sciences, Department of Energy under Contract No. DE-AC03-76SF00098.

REFERENCES:

- [1] S. Chattopadhyay, "Theory and Analysis of Nonlinear Dynamics and Stability in Storage Rings - A Working Group Summary," these proceedings.
- [2] E. Forest, M. Berz, and J. Irwin, "Exact Computation of Derivatives with Differential Algebra and Applications to Beam Dynamics," SSC-166, submitted to *Particle Accelerators*.
- [3] R. L. Warnock, W. Gabella and R. D. Ruth, "Construction of Symplectic Full-turn Maps by Application of an Arbitrary Tracking Code," manuscript under preparation.
- [4] A. Bazzani et al., "Normal Forms for Hamiltonian Maps and Nonlinear Effects in a LHC Model," CERN SPS/88-2 (AMS), LHC Note 66.
- [5] A. Bazzani and G. Turchetti, "Asymptotic Properties of Birkhoff Normal Forms," these proceedings.
- [6] W. E. Gabella, R. D. Ruth, and R. L. Warnock, "Periodic Solutions of the Hamilton-Jacobi Equation by the Shooting Method: A Technique for Beam Dynamics," these proceedings.
- [7] A. Chao, "The Criteria Working Group Summary," these proceedings.
- [8] S. A. Heifets, "Beam Dynamics and Tracking," these proceedings.

OVERVIEW OF METHODS TO DEFINE CONDITIONS FOR BOUNDED MOTION

G. Guignard

CERN, Geneva, Switzerland

ABSTRACT

This paper is a summary of the talk we were asked to present at the ICFA Beam Dynamics Workshop which dealt with aperture-related limitations of the performance in storage rings. The purpose of the talk was to give an overview of the analytical methods known by the author and developed recently, with the hope to obtain closed expressions for either invariant distortions or amplitude limits up to which the motion remains bounded. Since the progress in this field is very rapid, the author begs the indulgence of the reader if a method he does not know about was not mentioned in this overview. The methods retained are all based on the Hamiltonian formalism and the related equations of motion; perturbation treatment restricted to low orders is used to analyse the effects of nonlinearities and estimate the limit at which such methods fail to describe correctly the actual motion. The present overview does not treat of Hamiltonian-free perturbation theories based on exact maps and using normal forms. Most of the methods described have been applied to particular models and compared to tracking; the results obtained are encouraging for as well one-dimensional as two-dimensional motions.

1. CHAOTIC TRANSITION FOR HENON-HEILES POTENTIAL

It is possible to study the transition to chaos for particular autonomous systems by looking at the Liapunov exponents around the transition boundary surfaces [1]. Considering an accelerator containing quadrupoles for transverse focusing and sextupoles for chromaticity correction, the Hamiltonian for a particle is given as :

$$H = \frac{1}{2} [\dot{x}^2 + K(s)x^2 + \dot{z}^2 - K(s)z^2] + K'(s) [xz^2 - \frac{1}{3} x^3] \quad (1)$$

A crude approximation consists in averaging over one superperiod only the strengths of the quadrupoles and sextupoles which are focusing in one transverse direction [1]. The s -dependence is then suppressed :

$$\bar{H} = \frac{1}{2} [\dot{x}^2 + \bar{K} x^2 + \dot{z}^2 + \bar{K} z^2] + \bar{K}' (xz^2 - \frac{1}{3} x^3) \quad (2)$$

At this point, a change of variables from (x,z) to (ξ,ζ) allows to transform \bar{H} into the Henon-Heiles potential [2], noted G hereafter.

$$\xi = x \bar{K}'/\bar{K} \quad \zeta = z \bar{K}'/\bar{K}$$

$$G = \bar{H} \bar{K}'^2/\bar{K}^3 = \frac{1}{2} (\dot{\xi}^2 + \xi^2 + \dot{\zeta}^2 + \zeta^2) + (\xi\zeta^2 - \frac{1}{3} \xi^3) \quad (3)$$

The stability of G can be studied analytically by linearising the motion around one trajectory and looking for the eigenvalues λ of the associated Jacobian matrix. The stability of the system requires that the real parts of λ are negative on the invariants. Using the energy defined by (3) and associated with initial conditions such that $\xi_0 = \zeta_0 = A_0$ and $\dot{\xi}_0 = \dot{\zeta}_0 = 0$, i.e. :

$$G = A_0^2 + \frac{2}{3} A_0^3 \quad (4)$$

the real parts of λ are found to be negative provided $G < 1/12$ (tracking results give in comparison $G < 1/14.74$). Eq. (4) and the stability condition on G give an estimate of the critical amplitude, i.e. $A_0 = 0.266$.

This has been applied for instance to a simple structure made of FODO cells, corresponding to the LEP lattice [3] and containing sextupoles of equal but opposite strengths alternatively, to compensate the natural chromaticity. Using thin-lens approximation, the critical value of x_0 is deduced from the transformation (3) from (x,z) to (ξ,ζ) and the limit for A_0 .

$$x_0 = 0.266 \bar{K}/\bar{K}'$$

$$\frac{\bar{K}}{\bar{K}'} = \frac{L \theta (1 + 1/2 \sin^2 \mu/2)}{4 (\sin^2 \mu/2)} \quad (5)$$

The cell-length L is 79 m, the bending angle per cell θ is 21.613 mrad and the phase advance μ is used as the variable. The resulting variation of x_0 as a function of μ is given in Fig. 1, together with the limit coming from numerical integration or tracking and from other methods summarised hereafter.

2. NONLINEAR PERTURBATION AND HAMILTONIAN FORMALISM

We will consider here the betatron oscillations described by H_0 and perturbed by nonlinear fields contained in H_1 . Following the general treatment given in Ref. 4, the total Hamiltonian can be expressed as :

$$H = H_0(\underline{I}) + H_1(\underline{I}, \underline{\phi})$$

$$H_0 = Q_X I_X + Q_Z I_Z = \underline{Q} \cdot \underline{I} \quad (6)$$

with

$$H_1 = \sum_{jklm} h_{jklm} I_x^{(j+k)/2} I_z^{(l+m)/2} \exp\{i[(j-k)(\phi_x + Q_x \theta) + (l-m)(\phi_z + Q_z \theta)]\}$$

$$h_{jklm} = h_C \sim \beta_x^{(j+k)/2} \beta_z^{(l+m)/2} \frac{\partial^{N-1} B_z}{\partial x^{(N-1)}} \exp\{i[(j-k)(\phi_x - Q_x \theta) + (l-m)(\phi_z - Q_z \theta)]\}$$

The two-dimensional vectors \underline{I} and $\underline{\phi}$ are the transverse actions and angles. The components of the vector \underline{Q} are the tunes. The Fourier harmonics of h_C are noted h_{Cp} .

2.1 Averaging procedure of Poincaré-von Zeipel

Canonical transformations are used to eliminate non-resonant periodic terms [5]. They are generated by a function S_t connecting the exact variables $(\underline{I}, \underline{\phi})$ to the averaged variables $(\underline{J}, \underline{\psi})$. The function S_t is written in a mixed set of variables :

$$S_t(\underline{\phi}, \underline{J}, \theta) = \underline{\phi} \cdot \underline{J} + S(\underline{\phi}, \underline{J}, \theta) \quad (7)$$

The relations between the variables as well as the Hamilton-Jacobi equation for the transformed Hamiltonian G are :

$$\underline{I} = \underline{J} + \partial S_{\underline{\phi}} \quad \underline{\psi} = \underline{\phi} + \partial S_{\underline{J}}$$

$$G(\underline{J}, \underline{\psi}, \theta) = H(\underline{I}, \underline{\phi}, \theta) + \partial S(\underline{\phi}, \underline{J}, \theta) / \partial \theta \quad (8)$$

where H is given by Eqs. (6) and the coefficients h_{Cp} . The periodicity in $\underline{\phi}$, $\underline{\psi}$ and θ for a circular accelerator implies that the forms of G and S can be the same as the one of H , and respective coefficients g_{Cp} and s_{Cp} can be used. Using Taylor's expansion to express G and H in the set of S -variables gives for the Hamilton-Jacobi equation :

$$G(\underline{J}, \underline{\psi}, \theta) = G(\underline{J}, \underline{\phi}, \theta) + \partial G_{\underline{\psi}} \cdot \partial S_{\underline{J}} + \dots = H_0(\underline{J}) + \underline{Q} \cdot \partial S_{\underline{\phi}} + H_1(\underline{J}, \underline{\phi}, \theta) + \partial S_{\theta} + \partial H_{1\underline{I}} \cdot \partial S_{\underline{\phi}} + \dots (9)$$

Using the Fourier series for H , G and S and the harmonic coefficients h_{Cp} , g_{Cp} and s_{Cp} , Eq. (9) can be replaced by a set of relations noted by their harmonic number p . Each relation can then be solved for the coefficients of the generating function S to first or second order in the perturbation. Formally, the first and second order solutions can be written as follows :

$$s_{Cp}^{(1)} = i \frac{h_{Cp} - g_{Cp}}{\underline{n} \cdot \underline{Q} - p}$$

$$s_{Cp}^{(2)} = s_{Cp}^{(1)} + \sum_{C''p'} \frac{r' n''}{2} \frac{g_{C''p-p'} s_{C'p'}^{(1)} - h_{C'p-p'} s_{C''p'}^{(1)}}{\underline{n} \cdot \underline{Q} - p} \quad (10)$$

Eqs. (10) are solvable by iteration. In first order, there are resonant terms for which we must have $h_{Cp} = g_{Cp}$ for S to converge; for the non-resonant terms, we can simply choose $g_{Cp} = 0$. In second order, the expressions of $s_{Cp}^{(1)}$ are introduced in the right hand side of $s_{Cp}^{(2)}$. The generating function S can then be written to second order :

$$S = \sum_{C,p} s_{Cp}^{(2)} J_x^{(j+k)/2} J_z^{(l+m)/2} \exp[i \underline{n} \cdot (\underline{\phi} + \underline{Q}\theta) - ip\theta] \quad (11)$$

The relations (8) between the variables give finally analytical expressions for the distortions of the phase space trajectories, to that order of the perturbation [6,7] :

$$\begin{aligned} \underline{I} &= \underline{J} - \sum_{Cp} \underline{n} |s_{Cp}^{(2)}| J_x^{(j+k)/2} J_z^{(l+m)/2} \exp[i \underline{n} \cdot (\underline{\phi} + \underline{Q}\theta) - ip\theta] \\ \delta \underline{\phi} &= \underline{\psi} - \underline{\phi} = \sum_{Cp} \frac{r}{2\underline{J}} s_{Cp}^{(2)} J_x^{(j+k)/2} J_z^{(l+m)/2} \exp[i \underline{n} \cdot (\underline{\psi} - \delta \underline{\phi} + \underline{Q}\theta) - ip\theta] \end{aligned} \quad (12)$$

The new constants of the motion \underline{J} serve as parameters in Eqs. (12). However, to completely treat the problem for given initial conditions $(\underline{I}_0, \underline{\phi}_0)$, we must solve nonlinear algebraic equations of the form $\underline{I}_0 = \underline{I}_0(\underline{J}, \underline{\phi}_0)$. The distortions of the "invariants" \underline{I} have been calculated using Eqs. (12) and compared with tracking results [8] for the Tevatron lattice containing one sextupole represented by five kicks. Fig. 2 shows the comparison and the reasonable agreement for $\Delta I < 1/2 I_{\max}$.

The validity of the present analytical approach implies $\underline{I} > 0$ in such a way that the amplitudes x and z stay real. As a consequence, the method fails when $\Delta I > \underline{J}$ by virtue of Eqs. (12) and these equations give therefore a crude estimate of the limit of validity and stability.

2.2 Averaging procedure using Lie transforms

Let us begin by expanding H , G and S as power series of ϵ , which is here a control parameter for the perturbation [9] :

$$H = \sum_0^{\infty} \frac{\epsilon^n}{n!} H_n \quad S = \sum_0^{\infty} \frac{\epsilon^n}{n!} S_{n+1} \quad G = \sum_0^{\infty} \frac{\epsilon^n}{n!} G_n \quad (13)$$

The functions H_n are known; it is required to find all G_n and S_n order by order, S being the transform needed to get the averaged orbit and no growth term. This is done by recursive algorithm based on the D-operator, defined as the total derivative along the local H_0 -orbits,

$$Dg = \frac{\partial g}{\partial \theta} + L(H_0)g \quad (14)$$

where $L(H_0)$ is the Lie-operator associated with H_0 and acting on the function g in the following way : $L(H_0)g = \{g, H_0\}$.

The recursion based on the Hamilton-Jacobi equation gives the following equations for the lower orders :

$$\begin{aligned} \text{0th order} \quad & G_0 = H_0 \\ \text{1st order} \quad & DS_1 + G_1 = H_1 \\ \text{2nd order} \quad & DS_2 + G_2 = H_2 + \{H_1, S_1\} + \{G_1, S_1\} \end{aligned} \quad (15)$$

where $\{, \}$ is the Poisson bracket. For any order n , the n th-equation can be constructed explicitly and expressed in terms of lower orders G_k and S_k ; there are exactly two unknown functions G_n and S_n at each order. The determination of G_n comes from the condition that S must converge and stay bounded; to suppress any growth, G_n must cancel the average of the right hand side (r.h.s.) of Eqs. (15). The second function S_n is then the solution of a partial differential equation which can be formally written as follows :

$$DS_n = (r.h.s.)_n - G_n \quad (16)$$

where all terms are known explicitly, except S_n . According to the definition of D , S_n is given by the integration of $(r.h.s.)_n - G_n$ along the H_0 -orbits, which are defined by $H_0(I)$ and $Q = \partial H_0 / \partial I$. Therefore, the phase ϕ must be replaced by $\phi + Q(\theta' - \theta)$ in the known terms of Eq. (16), before integration. In this way, one gets explicit expressions for all the S_n and any n . Consequently, the distorted orbits associated with the Hamiltonian H can also be written explicitly as a power series of the parameter ϵ .

This approach has been used to depict the effects of arbitrary harmonics of sextupoles and octupoles for instance [9], but not to speculate about the divergence of Lie series and the onset of chaos.

3. SUCCESSIVE LINEARIZATION OF THE EQUATION OF MOTION

In the case of one-dimensional horizontal betatron motion with sextupole fields, the equation of motion becomes :

$$\ddot{x} + K(s)x - K'(s)x^2 = 0 \quad (17)$$

In practical applications, the nonlinear part of (17) is small compared with the linear one. Therefore, an approximate solution is obtained by the first linearization :

$$\ddot{x}^{(0)} + K(s)x^{(0)} = 0 \quad (18)$$

and the solution of (18) is well known. Now one writes the complete solution as $x(s) = x^{(0)}(s) + u(s)$ and the corresponding equation for $u(s)$ can be expressed as [7] :

$$\ddot{u}^* + [K(s) - 2K'(s)x^{(0)}]u = K'(s)[x^{(0)^2} + u^2] \quad (19)$$

The next step consists in dropping the quadratic term u^2 and this is called the second linearization :

$$\ddot{u}^*(0) + [K(s) - 2K'(s)x^{(0)}]u^{(0)} = K'(s) x^{(0)^2} \quad (20)$$

After two linearizations, the approximation of x becomes $x^{(0)}(s) + u^{(0)}(s)$ and the stability of the motion is unequivocally related to the condition that $u^{(0)}$ is bounded. Let us therefore consider Eq. (20). The inhomogeneous part is the source of distinct resonances at which the motion can become unbounded. However, if the homogeneous part of Eq. (20) corresponds to unbounded motion, then $u^{(0)}$ is necessarily unbounded. Hence, the complete information about the stability limit is, in general, contained in the homogeneous part. This is related to the following mechanism : a parametric resonance at small amplitudes drives the solution to large amplitudes where selfamplification occurs. The equation of interest is therefore the following one :

$$\ddot{u}^*(0) + [K(s) - 2K'(s)x^{(0)}]u^{(0)} = 0 \quad (21)$$

Since $x^{(0)}(s)$ is not periodic over one magnetic period, Eq. (21) can only be reduced to a vector recurrence with a nonconstant transfer matrix.

$$\begin{pmatrix} u^{(0)} \\ \dot{u}^{(0)} \end{pmatrix}_{n+1} = M_n \begin{pmatrix} u^{(0)} \\ \dot{u}^{(0)} \end{pmatrix}_n \quad (22)$$

However, if the linear phase advance $\mu/2\pi$ is rational, i.e. equal to p/q , $x^{(0)}(s)$ becomes periodic over q magnetic periods. Hence, Eq. (21) is Hill's equation again with an associated matrix defined over this new period and independent of n :

$$R = \prod_{i=0}^{q-1} M_i \quad (23)$$

The coefficients of R are polynoms in the initial values x_0 and \dot{x}_0 .

The linear theory tells us that the solution $u^{(0)}$ will be bounded if the condition $|\text{Tr}(R)| < 2$ is fulfilled. This can be used for a direct estimation of the stability limit to that order of the approximation (2nd linearization). Fig. 3 shows the limit obtained by this method for the LEP lattice and variable μ [7]. Results are also reproduced in Fig. 1 for comparison.

4. INVARIANTS AND LIMIT OF STABILITY THROUGH DIRECT SOLUTION OF HAMILTON-JACOBI EQUATION

We start again from the Hamiltonian of Eq. (6), the canonical transformation defined by the function (7) and the relations (8) which include the Hamilton-Jacobi equation. Once S is known, the invariant surfaces come from the first equation (8), i.e.

$\underline{I} = \underline{J} + \partial S_{\underline{\phi}} = \underline{I}(\underline{\phi}, \theta)$, and the orbits are given by the functions $\underline{I}(\theta)$ and $\underline{\phi}(\theta)$, where $\underline{\phi} = \underline{\psi} - \partial S_{\underline{J}} = \underline{\phi}(\underline{J}, \underline{\psi}, \theta)$. S is a real and periodic function, describing stable motion :

$$\begin{aligned} S(\underline{\phi}, \underline{J}, \theta) &= \sum_{n,p} s_{np}(\underline{J}) \exp[i(\underline{n} \cdot \underline{\phi} - p\theta)] \\ \partial S_{\underline{\phi}}(\underline{\phi}, \underline{J}, \theta) &= \sum_{n,p} i \underline{n} s_{np}(\underline{J}) \exp[i(\underline{n} \cdot \underline{\phi} - p\theta)] \end{aligned} \quad (24)$$

The Hamilton-Jacobi equation (9) must be satisfied by S and can be rewritten by separating the part independent of θ from the rest which is small by definition,

$$\partial H_0 \underline{J} \cdot \partial S_{\underline{\phi}} + \partial S_{\theta} = [G(\underline{J}) - H_0(\underline{J})] - [H_0(\underline{J} + \partial S_{\underline{\phi}}) - H_0(\underline{J}) - \partial H_0 \underline{J} \cdot \partial S_{\underline{\phi}} + H_1] \quad (25)$$

The function S must be such that G depends only on the actions and \underline{J} become the constants of the motion. The idea worked out in Ref. 10 consists in looking for a system of equations for the $s_{np}(\underline{J})$ in order to obtain a direct solution of Eq. (25). The Fourier transform of Eq. (25) and the introduction of the unperturbed frequency $\underline{\omega}_0 = \partial H_0 \underline{J}$ give the next relations :

$$\begin{aligned} \underline{n} \neq 0 \quad i(\underline{n} \cdot \underline{\omega}_0 - p) s_{np} &= - \frac{1}{(2\pi)^{m+1}} \int \dots \int_0^{2\pi} d\underline{\phi} d\theta \exp[-i(\underline{n} \cdot \underline{\phi} - p\theta)] \times \\ &\times [H_0(\underline{J} + \partial S_{\underline{\phi}}) - H_0(\underline{J}) - \underline{\omega}_0 \cdot \partial S_{\underline{\phi}} + H_1] \\ \underline{n} = 0 \quad i p s_{0p} &= \frac{1}{(2\pi)^{m+1}} \int \dots \int_0^{2\pi} d\underline{\phi} d\theta e^{ip\theta} [H_0(\underline{J} + \partial S_{\underline{\phi}}) + H_1] \end{aligned} \quad (26)$$

in which the identities (24) have been used. This set of equations may be summarized succinctly as :

$$s = A(s), \quad \text{where } s = [s_{np}] \text{ is the vector made of the Fourier amplitudes of } S, \\ \text{and } A = A_{np} \text{ are given by the integrals in (26).} \quad (27)$$

This general form (27) has to be reduced to a version having only a finite number of Fourier modes before to be solved. Provided that the Hamiltonian is suitably restricted and $\underline{n} \cdot \underline{\omega}_0 \neq p$ on the modes included, the reduced version of (27) can be solved by iteration.

$$s(k+1) = A(s(k)) \quad \text{with } s^{(0)} = 0 \quad (28)$$

in such a way that $s^{(k)}$ tends towards the solution s when n goes to infinity. The first iterate $s^{(1)} = A(0)$ is the usual result for s in the lowest order perturbation theory. In order to improve the convergence, the Newton iteration is considered. Defining

$$F(s)_{np} = i(\underline{n} \cdot \underline{\omega_0} - p) [s - A(s)]_{np} \quad (29)$$

the method implies that :

$$\partial F_s(s(k)) [s(k+1) - s(k)] + F(s(k)) = 0 \quad (30)$$

where ∂F_s is the Jacobian matrix made of the partial derivatives of F with respect to the Fourier amplitudes of S . At each iteration, one calculates from (30) the quantity $\delta s = s(k+1) - s(k)$ and then $s(k+1)$ is computed as $s(k+1) = s(k) + \delta s$. This method involves all orders at each iterate.

This approach was used to calculate the separatrices for a single isolated resonance (Fig. 4), which were obtained after nine iterations using about 130 modes in n and 30 in p . The arrival of stochasticity was also studied [10] from the stability side; the onset of chaos can be recognized from the fact that the Eq. (8) for $\underline{\psi}$ develops a singularity. In this case, it is impossible to solve for $\underline{\phi} = \underline{\phi}(\underline{J}, \underline{\psi}, \theta)$ and this happens if the Jacobian

$$\frac{\partial \underline{\psi}}{\partial \underline{\phi}} = 1 + \partial^2 S_{J\phi} \quad (31)$$

has zeros. Fig. 5 shows the Jacobian (31) calculated for the two-resonance model, near transition to chaos.

5. GENERALISED INVARIANT AND STABILITY

Using the normalised amplitude $q = x/\sqrt{\beta}$ and its conjugate momentum p , the equation of motion (17) valid in the presence of sextupoles becomes :

$$\begin{aligned} q' &= p \\ p' &= -Q^2 q - f(\theta) q^2 \end{aligned} \quad (32)$$

where $f(\theta)$ describes the distribution of the sextupoles around the ring. Eliminating the variable θ from (32), we obtain :

$$\frac{dp}{dq} p + Q^2 q + f\left(\int \frac{dq}{p}\right) q^2 = 0 \quad (33)$$

The idea [11] consists in integrating (33) to obtain an invariant containing the integral of algebraic expressions :

$$p^2 + Q^2 q^2 + 2 \int q^2 f \left(\int \frac{dq}{p} \right) dq = 2C, \quad (34)$$

rewriting (34) by using the action-angle variables

$$I(\phi) + \frac{2}{Q^2} \int I \cos^2 \phi f \left(\int \frac{dq}{p} \right) d(\sqrt{I} \cos \phi) = \frac{2C}{Q^2} \quad (35)$$

and finding approximate solutions of (35) by iterations of the type

$$I^{(k+1)}(\phi) = \frac{2C}{Q^2} - F[\phi, I^{(k)}(\phi)]. \quad (36)$$

In (36), $F(\phi, I)$ replaces the integral of Eq. (35) multiplied by $2/Q^2$. The iteration (36) begins with the lowest approximation $I^{(0)}$ given by the linear equation ($F \equiv 0$). The problem is hence reduced to integrations. Considering only the first iteration, Eq. (36) simplifies to

$$I^{(1)}(\phi) = I^{(0)} + I^{(0)^{3/2}} \frac{2}{Q^2} \int \cos^2 \phi \sin \phi f\left(-\frac{\phi}{Q}\right) d\phi \quad (37)$$

and the initial conditions must satisfy the following relation :

$$0 = I^{(0)} + I^{(0)^{3/2}} \frac{2}{Q^2} F_1(0) - q^2(0) \quad (38)$$

in which $F_1(\phi)$ is the integral of Eq. (37). The stability limit is by definition the largest amplitude $q(0)$ such that the motion remains bounded. The transformation $q = \sqrt{I} \cos \phi$ implies real and positive values for I when the motion is bounded. Hence, if $I^{(1)}$ becomes negative or if Eq. (38) has no real solution, the action is not real and positive anymore, \sqrt{I} becomes complex and q is not bounded (exponential behaviour). This means that, at the $q(0)$ value for which this happens, the actual motion is not described correctly by the retained approximation; one suspects that this is due to the onset of instability.

This was applied to a regular lattice made of FODO cells, with two sextupole families [11]. Fig. 6 shows the results (dots) obtained as a function of $\mu/2\pi$ after one iteration and compares them with tracking (full line). Results for the LEP lattice, compensated for chromaticity, are drawn in Fig. 1. In order to reproduce the effect of the 4th-order resonance, another iteration is needed and can be achieved more easily by modifying the approach. The invariant (35) can indeed be rewritten by using q , q' and the independent variable θ inside the integral :

$$Q^2 I(\theta) + 2\epsilon \int q^2 f(\theta) q'(\theta) d\theta = Q^2 q_0^2 \quad (39)$$

The solution q to be inserted in the integral is expanded as a power series of the control parameter ϵ :

$$q = \sum_{n=0}^{\infty} \epsilon^n q(n) \quad (40)$$

The $q(n)$ are solutions of linear inhomogeneous differential equations of the following type :

$$q(n)'' + Q^2 q(n) = F(n)(q(0), q(1), q(2), \dots, q(n-1)) \quad (41)$$

where F is a superposition of trigonometric functions and can be expressed as a function of the lower order solution. For instance, $F(0) = 0$ and $F(1) = -q_0^2 f(\theta) \cos^2(Q\theta)$. At each order, the frequency is adjusted to cancel the secular terms and the contribution $q(n)$ can be written analytically. Hence, the integral of the generalised invariant (39) is calculable to any order n and the result is usable for an estimation of the action $I(n+1)$ (to next order).

$$Q^2 I(n+1) = Q^2 q_0^2 - 2\epsilon \int_0^\theta q(n)^2 f(\theta) q(n)'(\theta) d\theta \quad (42)$$

Using the functions $F(0)$ and $F(1)$ defined above and solving the corresponding equations (41) gives the explicit forms of $q(0)$ and $q(1)$. These solutions are then inserted in the recurrence (42) to calculate the action $I(2)$ after two iterations.

The criterion for unbounded motion remains the same, i.e. $I(2) < 0$. The results obtained after 2 iterations for the same FODO lattice as before, are shown in Fig. 7. Third and fourth order resonances are now visible, and the agreement with tracking is good. Fig. 8 illustrates similar results computed for a complete LEP structure with a reduced number of cells per arc and variable phase advance per superperiod. In this comparison with tracking, it appears that analytical estimate does not reproduce the effect of the 5th-order resonance, as expected from two iterations.

6. SECULAR PERTURBATION AND OTHER METHODS

In the last section, we would like to briefly mention other promising methods and recent developments. Let us first recall the Greene's conjectures [12] which postulate a relationship between the existence of invariants for a motion with irrational frequency ω and the linear stability of near-periodic orbits of frequency $\omega_r = p/q$ close to and converging on ω . From studies on standard and quadratic maps, it was observed that the invariant tori break up if the residues of the tangent map associated to the near-periodic orbits tend towards 0.25 when ω_r tends to ω . This break up corresponds to a transition of loss of smoothness and instability. The method was used to study resonance overlap [13] and synchrotron motion in stationary buckets [14], since the change in phase and energy at each cavity traversal is described by the standard map.

$$I_{n+1} - I_n = K \sin \phi_n \quad \phi_{n+1} - \phi_n = I_{n+1} \quad (43)$$

with

$$I_n = \left(\frac{\delta E}{h \omega_s} \right)_n \quad \frac{2\pi h^2 \alpha_c}{N R_s p_s} \quad K = \frac{2\pi h \alpha_c e V_{RF}}{N^2 R_s p_s \omega_s}$$

The change in energy per traversal through each of the N cavities is δE and the parameter K is proportional to Q_s^2 . The Greene's conjectures indicate that the onset of stochasticity appears for $K = 0.9716$.

In a recent work [15], the method summarized in Sect. 4 of finding periodic solutions by formulating the Hamilton-Jacobi equation as an integral equation has been modified to make use of a more efficient technique. The generating function S is expanded in a Fourier series for ϕ , but not for θ . The periodicity of the Fourier coefficients s_n with θ is enforced by a shooting algorithm which leads to solutions such that $s_n(0) = s_n(2\pi)$. An application to the Berkeley Advanced Light Source shows the good accuracy and large region of convergence of the method.

Let us finally point out the possible application of secular perturbation theory to the nonlinear betatron motion [16]. The starting point is again the expansion (40) of the normalised amplitude q and the use of the explicit solutions $q^{(n)}$ of the differential equations (41). Then, the integral which appears in (39) and contains q and q' is developed in a power series of ϵ :

$$\int f(\theta) q^2(\theta) q'(\theta) d\theta = \sum_{n=0}^{\infty} \epsilon^n T(n) \quad (44)$$

The following steps consist in finding approximations for $T(n)$ and applying a convergence criterion for the sum. The criterion is based on the same conjectures already explained in previous sections. The actual solution is not correctly described anymore when the perturbation leads to $I < 0$ and chaotic motion takes place when the perturbation series does not converge. The convergence of (44) can be studied analytically if the perturbation is restricted to second order. In this case the development (44) can be formally written as :

$$\sum \epsilon^n T(n) = T^{(0)} \sum \epsilon^n G_0(n) + T^{(1)} \sum \epsilon^n G_1(n) \quad (45)$$

The two series on $G_0(n)$ and $G_1(n)$ have the same radius of convergence and the d'Alembert's criterion can directly be applied to any of them. This gives a closed expression for the estimate of the dynamic aperture. The result was used to calculate again the stability limit of a regular lattice as function of the phase advance per cell. The curve obtained is shown in Fig. 1 for comparison with the other methods and tracking. The agreement with tracking is good. The method has also been generalised to two-dimensional motion and the result applied to the LEP structure.

REFERENCES

1. S.Y. Lee and S. Tepikian, The chaotic dynamical aperture, IEEE Trans. Nucl. Sci. NS-32 (1985) 2225.
2. M. Henon and C. Heiles, The applicability of the third integral of motion, Astron. Jour. 69 (1964) 73.
3. G. Guignard, Parameter list for LEP Phase 1, LEP Parameter Note 9, CERN (1986).
4. G. Guignard, General theory of sum and difference resonances in a 3d magnetic field, CERN 76-06 (1976).
5. J. Moser, Stabilitätsverhalten kanonischer Differentialgleichungssysteme, Nach. Akad. Wiss. Gottingen IIA (6), (1955) 87.
6. A. Ando, Distortion of emittance with nonlinear magnetic field, KEK Preprint 83-30 (1984).
7. G. Guignard and H. Hagel, Sextupole correction and dynamic aperture : Numerical and analytical tools, Part. Accel., Vol. 18 (1986) 129.
8. F. Willeke, Analytical study of the Tevatron nonlinear dynamics, FNAL, FN-422 (1985).
9. L. Michelotti, Moser-like transformations using the Lie transform, Part. Accel., Vol. 16 (1985) 233.
10. R.L. Warnock and R.D. Ruth, Invariant Tori through direct solution of Hamilton-Jacobi equation, SLAC-PUB-3865, LBL-21709 (1986).
11. J. Hagel, Invariants of betatron motion and dynamic aperture; an analytical approach, CERN/LEP-TH/86-22 (1986).
12. J.M. Greene, A method for determining a stochastic transition, Jour. Math. Phys. 20 (1979) 1183.
13. G. Guignard, Phase space dynamics, in Lecture Notes in Physics 296, Proc. on Frontiers of Particle Beams, Texas 1986, Ed. M. Month and S. Turner, Springer-Verlag.
14. F. Pilat, Nonlinear and chaotic effects in the longitudinal phase space of an accelerator, Ph. D. Thesis, Trieste Univ. (1986).
15. W.E. Gabella, R.D. Ruth and R.L. Warnock, Periodic solutions of the Hamilton-Jacobi equation by the shooting method, this ICFA Workshop.
16. H. Moshhammer and J. Hagel, Secular perturbation theory and dynamical aperture, this ICFA Workshop.

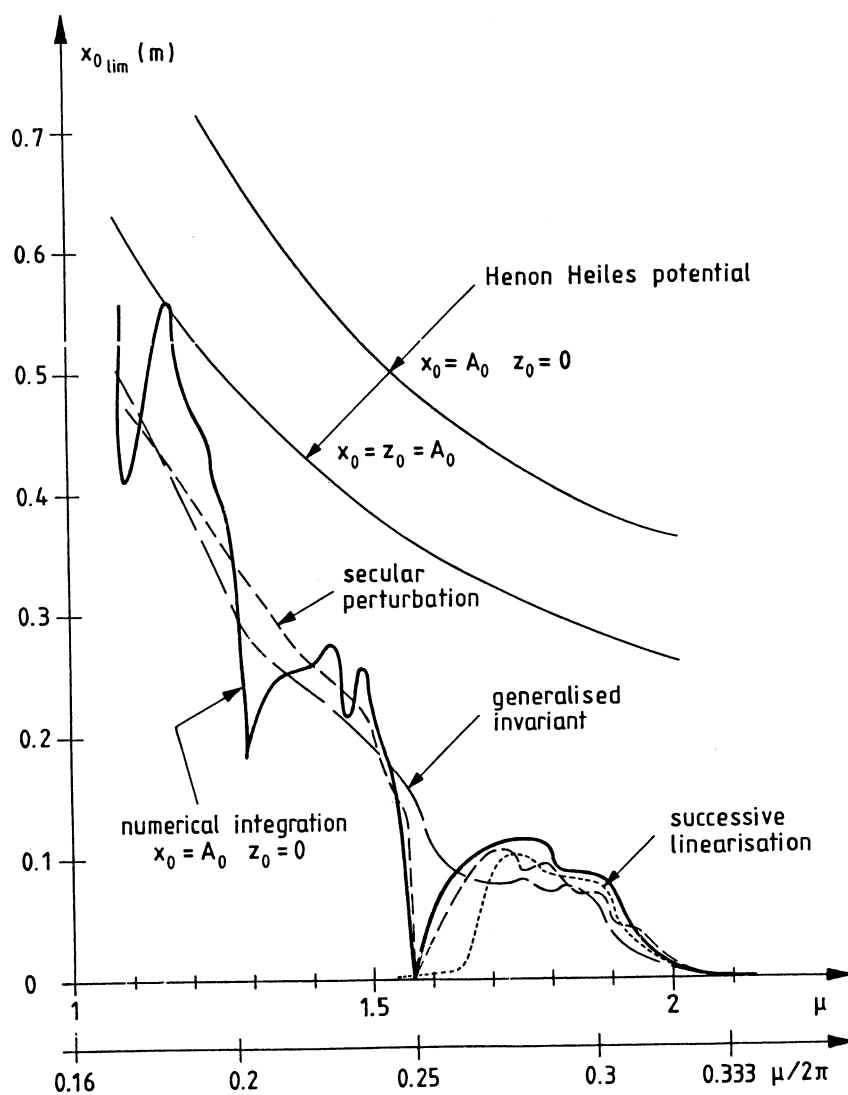


Fig. 1 - Limit of stability as a function of the phase advance in FODO cells, using different methods of calculation.

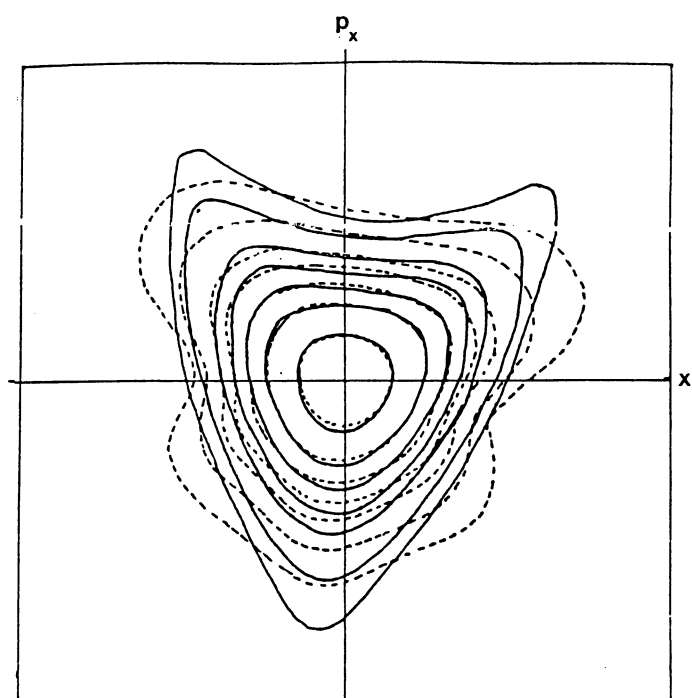


Fig. 2 - Invariant distortions with sextupoles calculated by using the average procedure of Poincaré-von Zeipel.

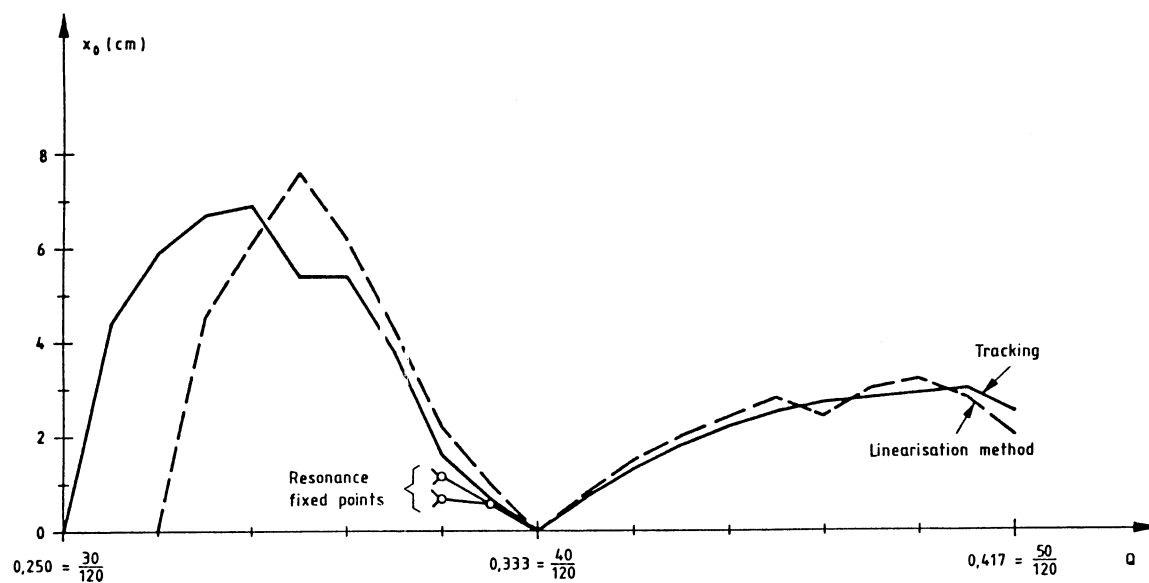


Fig. 3 - Limit of stability for the LEP lattice, using two successive linearizations.

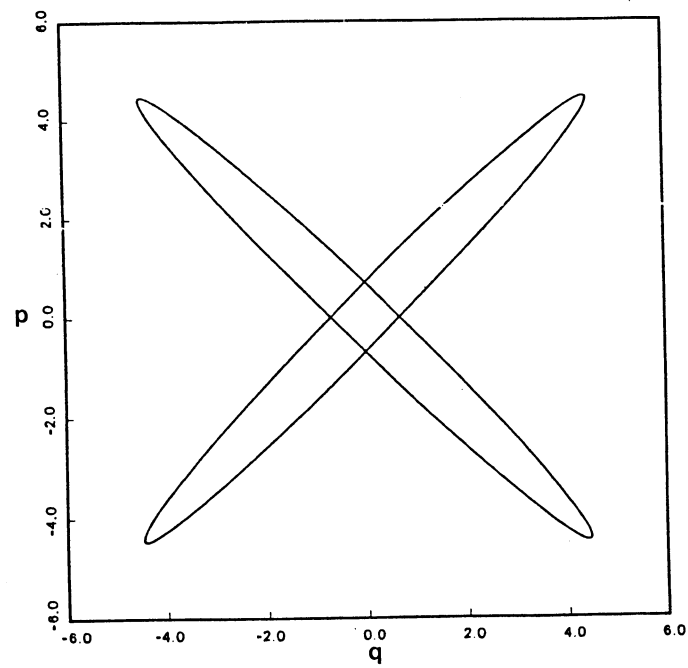


Fig. 4 - Separatrices of a single resonance obtained by solving the Hamilton-Jacobi equation.

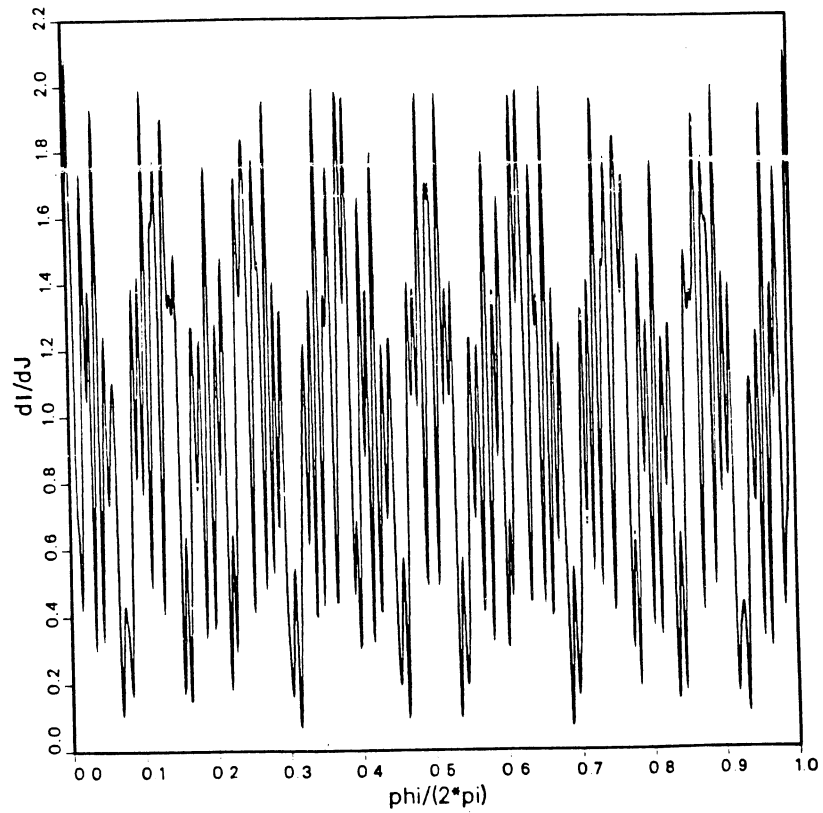


Fig. 5 - Jacobian variations for the two-resonance model, near transition to chaos.

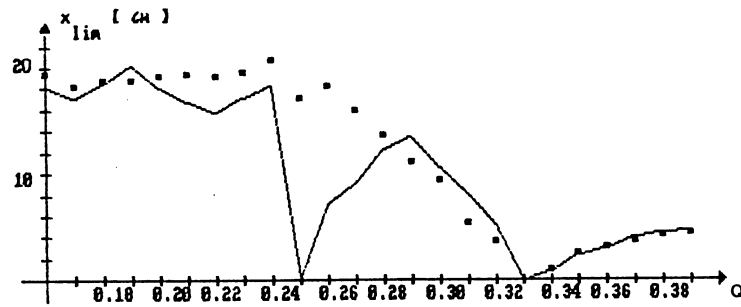


Fig. 6 - Limit of stability for FODO cells, using one iteration to find an approximation of the generalised invariant.

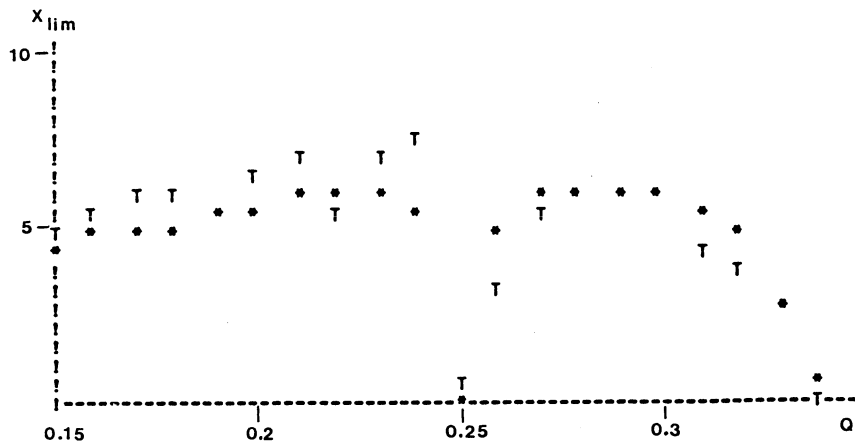


Fig. 7 - Limit of stability for a FODO cells after two iterations in the generalised-invariant method.

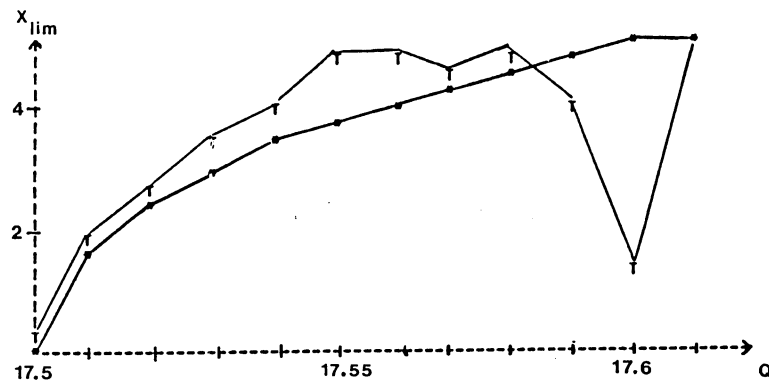


Fig. 8 - Limit of stability for a LEP structure after two iterations in the generalised-invariant method.

PERIODIC SOLUTIONS OF THE HAMILTON-JACOBI EQUATION BY THE SHOOTING METHOD: A TECHNIQUE FOR BEAM DYNAMICS*

W.E. Gabella[†]

University of Colorado, Boulder, Colorado, USA

R.D. Ruth and R.L. Warnock

SLAC, Stanford University, Stanford, California, USA

ABSTRACT

Periodic solutions of the Hamilton–Jacobi equation determine invariant tori in phase space. The Fourier spectrum of a torus with respect to angular coordinates gives useful information about nonlinear resonances and their potential for causing instabilities. We describe a method to solve the Hamilton–Jacobi equation for an arbitrary accelerator lattice. The method works with Fourier modes of the generating function, and imposes periodicity in the machine azimuth by a shooting method. We give examples leading to three-dimensional plots in a surface of section. It is expected that the technique will be useful in lattice optimization.

1. INTRODUCTION

In earlier papers, we proposed direct numerical solution of the Hamilton–Jacobi equation as a method to study particle beam dynamics [1-4]. There are two aspects of the proposal. First, one can compute invariant surfaces in phase space (tori) by finding solutions that are periodic in s , the arc length along a reference trajectory [3]. This is in the spirit of canonical perturbation theory, but is more accurate and simpler to implement, especially at large amplitudes. Second, one can use nonperiodic solutions of the Hamilton–Jacobi equation to construct symplectic maps for long-term particle tracking [3,4].

In Ref. [3], we found periodic solutions for accelerator lattices by formulating the Hamilton–Jacobi equation as an integral equation. In the present paper, we introduce a more efficient technique for finding periodic solutions, based on an iterative shooting procedure.

Other proposals for studying invariant surfaces for accelerators have been pursued in recent years. Dragt et al. [5], Forest [6], and Forest, Berz and Irwin [7] have developed a perturbative algorithm to extract normal forms from evolution maps. Guignard and Hagel [8] have worked with successive linearizations of the equations of motion in Lagrangian form. Michelotti [9] has applied the Deprit form of perturbation theory. Moshhammer and Hagel [10] have implemented secular perturbation theory applied to the equations of motion. It is difficult to compare efficacy of the various methods since they have not all been implemented to the same degree, and comparable results on performance are not readily available. The features of our method that we find appealing are generality, accuracy, large region of convergence and simplicity of programming.

2. THE HAMILTONIAN

We write the Hamiltonian for two transverse degrees of freedom as follows:

$$H(\mathbf{I}, \Phi, s) = \beta^{-1}(s) \cdot \mathbf{I} + f(s)V(\mathbf{I}, \Phi) \quad , \quad (2.1)$$

where β^{-1} is a two-component vector formed from Twiss parameters,

$$\beta^{-1}(s) = \begin{pmatrix} 1/\beta_1(s) \\ 1/\beta_2(s) \end{pmatrix} \quad . \quad (2.2)$$

*Work supported by the Department of Energy, contracts DE-AC03-76SF00515 and DE-FG02-86ER40302.

[†]Current address: Stanford Linear Accelerator Center, Stanford University, Stanford, California 94309.

The action and angle variables, $\mathbf{I} = (I_1, I_2)$, $\Phi = (\phi_1, \phi_2)$, are related to transverse momenta and coordinates by [11]

$$p_i = -(2I_i/\beta_i(s))^{1/2} \left[\sin \phi_i - \frac{\beta_i'(s)}{2} \cos \phi_i \right] , \quad (2.3)$$

$$x_i = (2I_i\beta_i(s))^{1/2} \cos \phi_i . \quad (2.4)$$

The function $f(s)$ consists of a series of unit steps; it is equal to 1 over the extent of each nonlinear magnet or skew quadrupole and zero elsewhere. For each multipole, V is a polynomial in the x_i . For a sextupole,

$$V(\mathbf{I}, \Phi) = \frac{S}{6} (x_1^3 - 3x_1x_2^2) , \quad (2.5)$$

where S is constant with dimensions (length) $^{-3}$. For a skew quadrupole,

$$V(\mathbf{I}, \Phi) = Mx_1x_2 . \quad (2.6)$$

Although the Hamiltonian as described is not entirely general, our method does allow virtually any function $V(\mathbf{I}, \Phi, s)$ in place of the second term of (2.1). We can account for Maxwellian fringe fields and curvature effects. It is not necessary to expand the square root in the original relativistic form of the Hamiltonian.

To account for departures from the design momentum, deviations from the off-momentum closed orbit are used as canonical coordinates. To represent the Hamiltonian, there are two possible avenues, which we call the “explicit” and “implicit” approaches. In the explicit scheme, we use the β functions for the design orbit and a dispersion function $D(s)$ to represent the momentum dependence of the Hamiltonian explicitly, as in Eq. (6.12) of Ref. [11]. This gives chromatic terms that are quadratic in the coordinates, which can be treated as part of the perturbation. In the implicit scheme, we simply use the Hamiltonian in its original form (2.1), but with a different closed reference orbit and different β functions and multipole strengths for each momentum. The closed orbits and lattice functions are determined anew from an auxiliary lattice program each time the momentum is changed. For the present account, we suppose that the implicit scheme is used.

3. HAMILTON-JACOBI EQUATION

To find invariant surfaces in phase space, we seek a canonical transformation $(\mathbf{I}, \Phi) \rightarrow (\mathbf{J}, \Psi)$ such that the transformed Hamiltonian H_1 is a function of \mathbf{J} alone. For such a transformation, $\partial \mathbf{J} / \partial s = 0$ and $\partial \Psi / \partial s = \nabla H_1(\mathbf{J})$, so that \mathbf{J} is invariant and Ψ advances linearly with s . We obtain the transformation from a generating function $G(\mathbf{J}, \Phi, s)$ such that

$$\mathbf{I} = \mathbf{J} + G_\Phi(\mathbf{J}, \Phi, s) , \quad (3.1)$$

$$\Psi = \Phi + G_J(\mathbf{J}, \Phi, s) , \quad (3.2)$$

where subscripts denote partial derivatives.

The Hamilton-Jacobi equation is the requirement that the new Hamiltonian H_1 indeed depend only on \mathbf{J} , namely,

$$H(\mathbf{J} + G_\Phi(\mathbf{J}, \Phi, s), \Phi, s) + G_s(\mathbf{J}, \Phi, s) = H_1(\mathbf{J}) . \quad (3.3)$$

Once the appropriate periodic solution of this partial differential equation for G is known, the invariant surface is given by (3.1) in explicit form. To represent the surface graphically, we can take a surface of section at fixed s , and plot $\mathbf{I}(\Phi, s)$ versus Φ . The invariant \mathbf{J} is a fixed parameter chosen at the start.

To find a solution of (3.3), our first step is to expand G in a Fourier series:

$$G(\mathbf{J}, \Phi, s) = \sum_{\mathbf{m}} e^{i\mathbf{m} \cdot \Phi} g_{\mathbf{m}}(\mathbf{J}, s) \quad . \quad (3.4)$$

This is a natural step, since by (3.1) and (2.3, 2.4), the generator G must be periodic in Φ with period 2π . Let us now substitute (3.4) in (3.3), choosing (2.1) to be the Hamiltonian. Next, take the inverse Fourier transform of the resulting equation. We find [writing $g_{\mathbf{m}}(s)$ for $g_{\mathbf{m}}(\mathbf{J}, s)$]

$$\begin{aligned} & \left(\frac{\partial}{\partial s} + i\mathbf{m} \cdot \beta^{-1}(s) \right) g_{\mathbf{m}}(s) \\ &= -f(s) \frac{1}{(2\pi)^2} \int_0^{2\pi} d\Phi e^{-i\mathbf{m} \cdot \Phi} V(\mathbf{J} + G_{\Phi}(\Phi, s), \Phi) \\ &+ (H_1(\mathbf{J}) - \mathbf{J} \cdot \beta^{-1}(s)) \delta_{\mathbf{m}0} \end{aligned} \quad (3.5)$$

where

$$G_{\Phi}(\Phi, s) = \sum_{\mathbf{m}} i\mathbf{m} e^{i\mathbf{m} \cdot \Phi} g_{\mathbf{m}}(s) \quad . \quad (3.6)$$

Since (3.6) has no term with $\mathbf{m} = 0$, the set of equations (3.5, 3.6) is a closed system for determination of the amplitudes $g_{\mathbf{m}}(s)$, $\mathbf{m} \neq 0$, which does not depend on the still unknown function $H_1(\mathbf{J})$. In (3.5) the presence of the action \mathbf{J} , a fixed parameter to be chosen at the start, induces \mathbf{J} -dependence of the solution $g_{\mathbf{m}}$.

We truncate the series (3.6), so that (3.5, 3.6) becomes a finite set of ordinary differential equations, which may be integrated by a standard numerical algorithm. For the integration, it is convenient to pass to the "interaction representation" by the change of variable

$$h_{\mathbf{m}}(s) = e^{i\mathbf{m} \cdot \Psi(s)} g_{\mathbf{m}}(s) \quad , \quad (3.7)$$

$$\Psi(s) = \int_0^s \beta^{-1}(u) du \quad . \quad (3.8)$$

These variables obey, for $\mathbf{m} \neq 0$,

$$\frac{\partial h_{\mathbf{m}}}{\partial s} = -f(s) \frac{e^{-i\mathbf{m} \cdot \Psi(s)}}{(2\pi)^2} \int_0^{2\pi} d\Phi e^{-i\mathbf{m} \cdot \Phi} V(\mathbf{J} + G_{\Phi}(\Phi, s), \Phi) \quad , \quad (3.9)$$

$$G_{\Phi} = \sum_{\mathbf{m} \in B} i\mathbf{m} e^{i\mathbf{m} \cdot (\Phi - \Psi(s))} h_{\mathbf{m}}(s) \quad . \quad (3.10)$$

Here B is a finite set of modes. The property $h_{\mathbf{m}} = h_{-\mathbf{m}}^*$ reduces the set of amplitudes that must be considered. A suitable set of independent amplitudes is

$$\begin{aligned} & h_{m_1, m_2}, h_{-m_1, m_2}, h_{m_1, 0}, h_{0, m_2} \\ & 1 \leq m_i \leq M_i, i = 1, 2 \quad . \end{aligned} \quad (3.11)$$

The $h_{\mathbf{m}}$ are constant between magnets where $f(s) = 0$, so that the region of integration reduces to the support of $f(s)$.

The determination of $H_1(\mathbf{J})$ and $g_0(s)$ is discussed at the end of Section 4.

4. PERIODICITY, CONTRACTIVE PROPAGATORS AND THE SHOOTING METHOD

Let C denote the circumference of the reference trajectory. Since (3.1) expresses the invariant surface $I(\Phi, s)$, and the points s and $s + C$ are physically identical, the generator G must be periodic in s . Thus, we must find solutions of (3.9, 3.10) such that

$$g_m(0) = g_m(C) \quad . \quad (4.1)$$

We enforce periodicity by a shooting algorithm, that is, by an iterative procedure in which we sequentially adjust the initial value $h_m(0) = g_m(0)$ until $h_m(C) = e^{i m \cdot \Psi(C)} g_m(C)$ satisfies

$$h_m(C) = e^{2\pi i m \cdot \nu} h_m(0) \quad , \quad (4.2)$$

which is equivalent to (4.1). Here $\nu = \Psi(C)/2\pi$ is the unperturbed tune.

One requirement on an acceptable shooting algorithm is that it be certain to converge when the perturbation V is sufficiently weak (and $m_1\nu_1 + m_2\nu_2$ differs from an integer for all m_1, m_2 in the mode set chosen). This requirement is not met by a naive iteration

$$g^{(0)}(0) \rightarrow g^{(0)}(C) = g^{(1)}(0) \rightarrow g^{(1)}(C) = g^{(2)}(0) \rightarrow \dots \quad , \quad (4.3)$$

where the arrow indicates one integration through the lattice. Here and in the following discussion, we suppress the subscript m , letting $g = \{g_m\}$ or $h = \{h_m\}$ stand for a vector with Fourier amplitudes as components.

We form a shooting algorithm that will converge for small V by virtue of the contraction mapping principle [12]. Let us recall the latter. In a finite-dimensional vector space, let S_b consist of all vectors x with $\|x\| \leq b$; S_b is a complete metric space with metric $d(x - y) = \|x - y\|$, where double bars denote any vector norm. Suppose that an operator A , in general nonlinear, maps S_b into itself

$$\|A(x)\| \leq b \quad , \quad (4.4)$$

for all x in S_b . Suppose also that A is contractive, i.e.,

$$\|A(x) - A(y)\| \leq \alpha \|x - y\|, \quad 0 < \alpha < 1 \quad , \quad (4.5)$$

for all x, y in S_b . Then

$$x = A(x) \quad (4.6)$$

has a unique solution in S_b . Furthermore, that solution may be computed by iteration, beginning with any point x_0 in S_b :

$$x_{p+1} = A(x_p) \quad , \quad p = 0, 1, 2, \dots \quad , \quad x_0 \in S_b \quad , \quad x_p \rightarrow x \quad , \quad p \rightarrow \infty \quad . \quad (4.7)$$

We wish to put the shooting problem in the form (4.6), so that it can be solved by iteration. The unknown x will be $h(0)$, the value of h at the beginning of the lattice.

We exploit the fact that the propagation operator U for h is small and contractive at small V . This operator is defined by

$$U(h(0)) = h(C) - h(0) \quad . \quad (4.8)$$

To compute $U(h(0))$ one has to integrate the differential equation (3.9) through the lattice, taking $h(0)$ as initial value. It is clear that $U(h(0))$ vanishes as $V \rightarrow 0$. Also, by considering the integral equation equivalent to (3.9), one can show that U is contractive when $\partial V / \partial J$ is sufficiently small [13]. Note that V and $\partial V / \partial J$ are simultaneously small in the limit of vanishing magnet strength.

We substitute the definition (4.7) in the periodicity condition (4.2) and rearrange to obtain

$$h_m(0) = \frac{1}{e^{2\pi i m \cdot \nu} - 1} U_m(h(0)) \quad , \quad (4.9)$$

which may be written as

$$h(0) = A(h(0)) \quad . \quad (4.10)$$

Now if $e^{2\pi i m \cdot \nu} \neq 1$ for all $m \in B$, we can apply the contraction mapping theorem to (4.10) if the magnet strengths are sufficiently small. For small strengths, A maps some set S_b into itself, and is contractive on that set.

Note that the corresponding propagator for g , defined as $g(C) - g(0)$, is not small and contractive for weak magnets, owing to the term $i m \cdot \beta^{-1} g$ in (3.5). An important step was to pass to the interaction picture, to eliminate this term.

It is not surprising that the “small divisor,” $e^{2\pi i m \cdot \nu} - 1$, appears in (4.9). Such divisors are intrinsic to the problem of determining invariant tori. They make it impossible to expand the mode set B without limit; they become arbitrarily small at large m , whatever the value of ν , and spoil convergence of an iterative solution. In order to expand the mode set indefinitely, it is necessary to invoke a sequence of canonical transformations rather than just one [2]. We find, however, that we can take B so large as to get acceptably accurate results with one transformation, provided that we do not work too close to regions where invariant tori fail to exist.

Having determined $g_m(s)$, $m \neq 0$, we can use (3.5) to determine the new Hamiltonian $H_1(J)$. We put $m = 0$ in (3.5) and integrate on s from 0 to C . The requirement $g_0(0) = g_0(C)$ immediately gives a formula for $H_1(J)$. Inserting that expression for $H_1(J)$, and integrating (3.5) for $m = 0$ from 0 to s , we obtain $g_0(s)$. The initial value $g_0(0)$ is arbitrary; it corresponds to an arbitrary offset of Ψ with respect to Φ at $s = 0$, as is seen from (3.2). Knowing $H_1(J)$, one can calculate the perturbed tune $\nu_1 = \nabla H_1(J)$ by numerical differentiation.

5. NUMERICAL METHOD

We wish to solve (4.9) for $h(0)$. To find $U(h(0))$, we integrate the differential equations (3.9) over the interval $[0, C]$, with initial value $h(0)$, using the fourth-order Runge-Kutta method. The sum in (3.10) and the integral over Φ in (3.9) are evaluated by the Fast Fourier Transform (FFT). The Φ integral is first discretized with a number of mesh points for Φ_i at least equal to $2 M_i$, where M_i is the maximum mode number defined in (3.11). Usually we take $2 M_i$ mesh points for a first try, and $4 M_i$ for refinement; see Ref. [2], Section 5, for remarks on discretization error.

We find that $g_m(s)$ has rather simple behavior as a function of s over the extent of one magnet. For instance, in the case of one transverse degree of freedom at moderate amplitudes, $g_m(s)$ is nearly a quadratic function of s over the extent of a single sextupole, for each m . This implies that the number of Runge-Kutta steps per magnet can be rather small. One or two steps [four or eight evaluations of the right hand side in (3.9)] proved to be sufficient in good regions of phase space. As the dynamic aperture is approached, and more Fourier modes are included, it is necessary to increase the number of steps.

To solve (4.9), we have used simple iteration, as in the contraction mapping theorem, taking as zeroth iterate the result of lowest order perturbation theory. The iteration converges provided that the invariant action J is not too large. At large J , we apply Newton's method to solve (4.9), obtaining convergence up to the dynamic aperture in cases studied to date. The Jacobian matrix required for the multi-dimensional Newton method was approximated by calculating partial derivatives as divided differences. That is, with

$$F_m(h(0)) = h_m(0) - \frac{1}{e^{2\pi i m \cdot \nu} - 1} U_m(h(0)) \quad (5.1)$$

we computed divided differences

$$\frac{F(h(0) + \Delta h e) - F(h(0))}{\Delta h} \quad (5.2)$$

for some small scalar Δh . A succession of unit vectors \mathbf{e} in the various coordinate directions produces the full set of partial derivatives making up the Jacobian. This requires one integration through the lattice for each \mathbf{e} , and therefore is expensive for large problems.

6. EXAMPLES

We give results for one cell of the Berkeley Advanced Light Source (ALS). The ALS has very strong sextupoles, and therefore is a demanding case in which to test our method. The cell contains four sextupoles, and has lattice parameters as given in Table 1. The values stated are for s at the leading edge of a magnet.

We first show results for motion in the horizontal plane only. The formalism described above was transcribed for one degree of freedom. We plot $I(\phi)$ versus $\phi/2\pi$ in the surface of section at $s = 0$. In each plot, we show the invariant curve, obtained by solving (4.9), and also points obtained from single-particle tracking. The points from tracking are all on a single trajectory, starting at the point $(I, \phi) = (I(0), 0)$ on the invariant curve. Tracking was done by means of a fourth-order explicit symplectic integrator [14].

Table 1. Berkeley ALS Cell.

s (leading edge)	$\beta_{x,y}$	$\alpha_{x,y}$	$\psi_{x,y}$	S	Δs
5.775	1.4724	-1.7791	2.4799	-88.09	.20
	10.6957	8.4007	.8658		
6.875	3.9837	2.2722	2.8191	115.615	.20
	1.5798	.4167	1.2217		
9.325	3.1367	-1.9628	4.5996	115.615	.20
	1.4428	-.2681	2.9279		
10.425	2.2972	2.3448	4.8865	-88.09	.20
	7.6031	-7.0624	3.3945		

Circumference $C = 16.4$, Tunes $\nu_x = 1.189735$, $\nu_y = .681577$

s, β, C in meters; S in (meters)⁻³

Length of sextupole = Δs

Figure 1 shows the result of simple iterative solution of (4.9) at invariant action $J = 9 \cdot 10^{-7}$ m. This corresponds to maximum horizontal displacement at $s = 0$ of $x_{\max} = 4.5$ mm. The calculation was done with 15 Fourier modes, $1 \leq |m| \leq 15$, and two Runge-Kutta steps per magnet. The agreement of invariant curve and tracking is very close. To check the agreement quantitatively, we took 600 points (I_i^t, ϕ_i^t) from tracking, and compared them with the corresponding points $(I(\phi_i^t), \phi_i^t)$ on our computed invariant curve. We formed the measure of error

$$\epsilon = \frac{\sum_{i=1}^{600} |I(\phi_i^t) - I_i^t|}{\sum_{i=1}^{600} |I(\phi_i^t) - J|}, \quad (6.1)$$

and found $\epsilon = 4.4 \cdot 10^{-5}$. This is a demanding error test, since the normalizing divisor in (6.1) is formed from distortions, i.e., departures from invariant action, rather than the invariant action itself. If the denominator in (6.1) were replaced by $600 J$, the value of ϵ would be considerably smaller.

To judge convergence of an iterative solution of (4.9), we calculate the quantity

$$r^{(p+1)} = \frac{\|\mathbf{h}^{(p+1)}(0) - \mathbf{h}^{(p)}(0)\|}{\|\mathbf{h}^{(p)}(0)\|}, \quad (6.2)$$

where $\|\mathbf{h}\|$ denotes the sum of the absolute values of the independent Fourier components of \mathbf{h} . The index p denotes the p^{th} iterate, whether obtained in simple iteration or in Newton's iteration.

The run of Fig. 1 is for a value of J close to the largest that gives unambiguous convergence in the solution of (4.9) by plain iteration. Consequently, the convergence as measured by $r^{(p)}$ was fairly slow: we found $r^{(5)} = 7.6 \cdot 10^{-4}$, $r^{(10)} = 7.7 \cdot 10^{-5}$, $r^{(15)} = 1.6 \cdot 10^{-5}$, ... $r^{(60)} = 3.9 \cdot 10^{-11}$. The time for 60 iterations in double precision was less than two minutes on a MicroVAX. The pattern of convergence was in accord with expectations based on the contraction mapping principle, with α in (4.5) around 0.7.

The horizontal dynamic aperture of the ALS as determined by tracking is around 22 mm at $s = 0$. To reach such large values, where the nonlinearities are very strong, we find it imperative to solve (4.9) by Newton's method. In Fig. 2 we show results from a Newton iteration at $J = 2.22 \cdot 10^{-6}$, which corresponds to $x_{\max} = 7.1$ mm at $s = 0$; this is roughly the aperture required for injection. The calculation was done with 15 modes, and 12 Runge-Kutta steps per magnet, the latter being much more than necessary. Agreement with tracking is still good, with $\epsilon = 5.2 \cdot 10^{-5}$. Convergence was rapid: $r^{(1)} = 1.2 \cdot 10^{-5}$, $r^{(2)} = 4.2 \cdot 10^{-11}$, $r^{(3)} = 4.1 \cdot 10^{-16}$, $r^{(4)} = 3.7 \cdot 10^{-17}$. The computing time was about 6.5 minutes for two iterations; this could be divided by 3 if four Runge-Kutta steps per magnet were used, probably an adequate number.

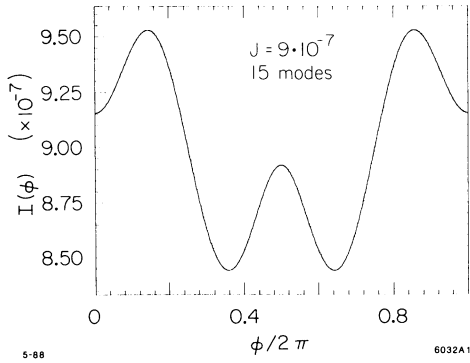


Figure 1.

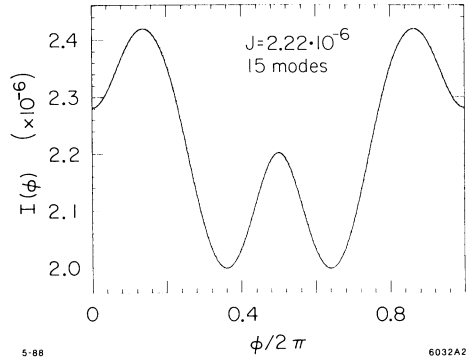


Figure 2.

In Fig. 3 we show a run very close to the dynamic aperture, with $J = 2 \cdot 10^{-5}$ m and $x_{\max} = 22.4$ mm at $s = 0$. Again, we take 15 modes and 12 Runge-Kutta steps per magnet. Agreement with tracking is only fair; $\epsilon = 4.4 \cdot 10^{-2}$. Convergence is still impressive: $r^{(1)} = 1.8 \cdot 10^{-2}$, $r^{(2)} = 1.8 \cdot 10^{-4}$, $r^{(3)} = 8.1 \cdot 10^{-9}$, $r^{(4)} = 2.2 \cdot 10^{-16}$. The 4% disagreement with tracking arises from taking too few modes. In Fig. 4, we repeat the case of Fig. 3 but include 63 modes, again with 12 Runge-Kutta steps, and obtain $\epsilon = 4.8 \cdot 10^{-3}$. Convergence is slightly slower, $r^{(4)} = 7.7 \cdot 10^{-12}$, $r^{(5)} = 9.7 \cdot 10^{-17}$.

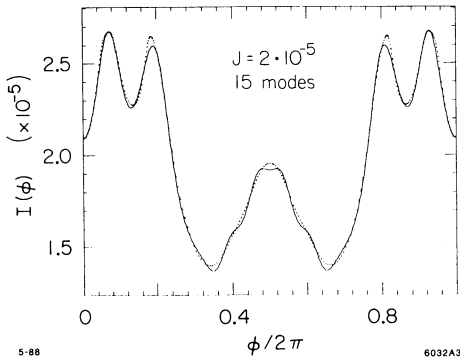


Figure 3.

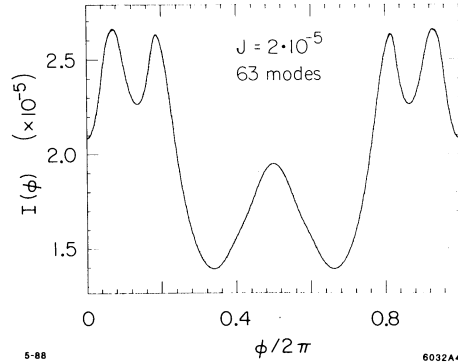


Figure 4.

With large mode sets at large amplitudes, as in the case of Fig. 4, it is necessary to use relatively many integration steps. For instance, the run of Fig. 4 failed to converge when we tried only five Runge-Kutta steps per magnet. At large amplitudes, the differential equations (3.9) appear to have a property reminiscent of stiffness, the allowable step size being determined by the high modes, even though they play a minor role in the solution.

In Figs. 5 and 6 we show results for motion in two degrees of freedom. The phase space is now five-dimensional (coordinates $I_1, \phi_1, I_2, \phi_2, s$). There are two invariants J_1, J_2 for an invariant surface, which is a three-torus. Taking a surface of section at $s = 0$, we see that the points (I_1, ϕ_1, ϕ_2) , or the points (I_2, ϕ_1, ϕ_2) , lie on a two-dimensional surface, which we may plot in three dimensions [1]. In Figs. 5 and 6 we plot I_1/J_1 and I_2/J_2 , respectively, each versus $(\phi_1, \phi_2)/2\pi$. Here 1 (2) denotes the horizontal (vertical) plane of motion.

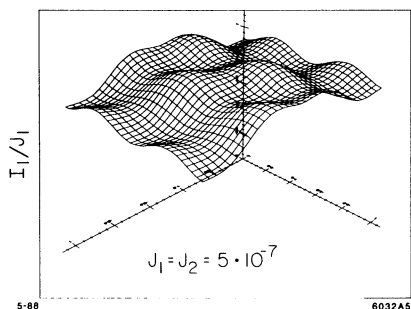


Figure 5.

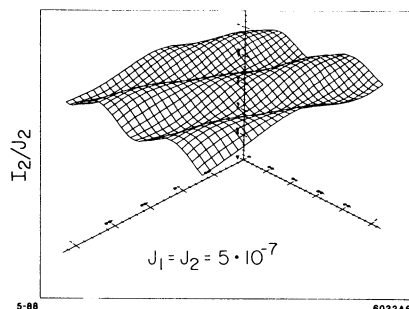


Figure 6.

The results shown are for $J_1 = J_2 = 5 \cdot 10^{-7}$ m, and were obtained by plain iteration using Fourier modes with $|m| \leq 7$ in each variable, and two Runge-Kutta steps per magnet. The agreement with tracking is quite good in spite of the relatively small mode set: $\epsilon_1 = 4.01 \cdot 10^{-4}$, $\epsilon_2 = 4.07 \cdot 10^{-4}$. The iteration gave $r^{(p)}$ decreasing slowly to $3.7 \cdot 10^{-5}$ at $p = 25$; at larger p it began to increase. The 25 iterations required 25.5 minutes on the MicroVAX. Notice that the intersection of coordinate axes is at 0 in the plots; the departure of the surfaces from planarity is quite large.

In two degrees of freedom, the convergence is somewhat poorer than in one at comparable amplitudes. Moreover, the use of Newton's method is expensive in two degrees of freedom. We are studying ways to reduce expense by modified Newton procedures. Another possibility is to avoid Newton's method by making successive canonical transformations so as to reduce the magnitude of the perturbation, along the lines suggested in Ref. [2]. This approach seems promising.

It goes without saying that all results in computation of invariant surfaces are strongly dependent on tunes. We have used the tunes of Table 1. Slightly different tunes could give better or poorer convergence of our iterative method.

7. CONCLUSION

We have tested our method in a difficult example, and have found that it gives good accuracy and a large region of convergence. Further efforts are needed to reduce computation expense at large amplitudes in strongly nonlinear lattices, especially in two degrees of freedom. There are good prospects for improvements through modified Newton methods or successive canonical transforms.

REFERENCES

1. R. D. Ruth, T. Raubenheimer and R. L. Warnock, IEEE Trans. Nucl. Sci. NS-32 (1985) 2206.
2. R. L. Warnock and R. D. Ruth, Physica 26D (1987) 1.
3. R. L. Warnock and R. D. Ruth, *Proceedings of the 1987 IEEE Particle Accelerator Conference*, p. 1263.
4. R. L. Warnock, R. Ruth and W. Gabella, *Symplectic Maps for Accelerator Lattices*, Workshop on Symplectic Integration, Los Alamos National Laboratory, March 19-21, 1988.
5. For a review, see A. J. Dragt, F. Neri, G. Rangarajan, D. R. Douglas, L. M. Healy and R. D. Ryne, *Lie Algebraic Treatment of Linear and Nonlinear Beam Dynamics*, University of Maryland preprint, to be published in Annual Review of Nuclear and Particle Science.
6. E. Forest, Particle Accelerators 22 (1987) 15.
7. E. Forest, M. Berz and J. Irwin, SSC Central Design Group report SSC-166, Lawrence Berkeley Laboratory, March 1988.
8. G. Guignard and J. Hagel, Particle Accelerators 18 (1986) 129.
9. L. Michelotti, Particle Accelerators 16 (1985) 233.
10. H. Moshhammer and J. Hagel, *Proceedings of the Second Advanced ICFA Beam Dynamics Workshop*, Lugano, April 11-16, 1988.
11. R. D. Ruth in *Physics of Particle Accelerators*, AIP Conference Proceedings, Number 153 (Amer. Inst. Phys., 1987).
12. T. L. Saaty and J. Bram, *Nonlinear Mathematics* (McGraw-Hill, 1964).
13. We shall give the proof in a forthcoming paper. For the present, we merely note that the claim is consistent with numerical results.
14. R. D. Ruth and E. Forest, in preparation. A similar third-order symplectic integrator was described by R. D. Ruth, IEEE Trans. Nucl. Sci. NS-30 (1983) 2669.

ANALYTIC APPROACH OF DYNAMIC APERTURE BY SECULAR PERTURBATION THEORY

J. Hagel and H. Moshhammer

CERN, Geneva, Switzerland and
Institut für Theoretische Physik TU Graz, Austria

Secular perturbation theory (or Lindstedt - Poincaré technique) is applied to the equation of motion of a single charged particle in a storage ring. Nonlinearities are generated by higher order magnetic multipoles. From existing theories of non-linear dynamics we expect the convergency of the expansion to break down at a certain strength of the non - linear perturbation due to the onset of unbounded or chaotic motion. We derive a criterion for the divergence of the perturbation expansion which yields to a closed formula for the maximum initial amplitude leading to bounded motion.

1 Introduction

We study the equation of motion of a single charged particle under the influence of external magnetic fields. Although we restrict ourselves in this report to non - linear effects generated by sextupoles, the method here presented may be applied without serious problems to higher order magnetic multipoles.

It is well known that initial values may decide the character of the non - linear motion. The aim of our work is to estimate a lower limit for maximum initial values that lead to bounded trajectories in phase space. We approach the solution of the equation of motion using secular perturbation theory which yields an expansion of the solution in bounded functions. The divergence of this expansion has to be related very closely to the dynamic aperture. We neglect the effect of Arnold's diffusion in the transvers motion in two degrees of freedom (four dimensional phase space).

Other proposals for estimating analytically the dynamical aperture have been developed in recent years [3],[4],[12] and [13].

2 Equation of motion

From [2] we obtain the Hamiltonian for two transverse degrees of freedom as follows:

$$\tilde{H} = \left[-K_1 \frac{\hat{x}^2}{2} + K_1 \frac{\hat{y}^2}{2} \right] + \frac{p_{\hat{x}}^2}{2} + \frac{p_{\hat{y}}^2}{2} - \frac{\dot{K}(s)}{6} (\hat{x}^3 - 3\hat{x}\hat{y}^2)$$

where

$$K_1(s) = \frac{e}{p_0 c} \frac{\partial B_y}{\partial \hat{x}}$$

$$\dot{K}(s) = -\frac{e}{p_0 c} \frac{\partial^2 B_y}{\partial \hat{x}^2}$$

are taken from a Taylor series expansion of the magnetic field strength at the reference orbit ($\hat{x}, \hat{y} = 0$). Using Hamilton equations we find:

$$\frac{d^2 \hat{x}}{ds^2} - K_1(s) \hat{x} - \frac{\dot{K}(s)}{2} (\hat{x}^2 - \hat{y}^2) = 0 \quad (1)$$

$$\frac{d^2 \hat{y}}{ds^2} + K_1(s) \hat{y} + \dot{K}(s) \hat{x} \hat{y} = 0 \quad (2)$$

Let C denote the circumference of the reference trajectory. Since the points s and $s + C$ are physically identical we find

$$K_1(s) = K(s + C) \quad , \quad \dot{K}(s + C) = \dot{K}(s);$$

and the linear parts of the differential equations are of Hill's type. We now transform the dependent - as well as the independent variables:

$$\hat{x}(s) = x(\theta_x) \beta_x^{1/2}(s) \quad ,$$

$$\hat{y}(s) = y(\theta_y) \beta_y^{1/2}(s) \quad ,$$

$$\theta_x = \frac{1}{Q_x} \int_0^s \frac{d\tilde{s}}{\beta_x(\tilde{s})} \quad ,$$

$$\theta_y = \frac{1}{Q_y} \int_0^s \frac{d\tilde{s}}{\beta_y(\tilde{s})} \quad ;$$

where

$$Q_x = \frac{1}{2\pi} \int_0^C \frac{ds}{\beta_x(s)} \quad ,$$

$$Q_y = \frac{1}{2\pi} \int_0^C \frac{ds}{\beta_y(s)} \quad ;$$

and finally obtain finally from Eqs.(1) and (2):

$$\frac{d^2 x}{d\theta_x^2} + Q_x^2 x - \frac{1}{2} \dot{K}(s) \beta_x^{3/2}(s) Q_x^2 [\beta_x(s) x^2 - \beta_y(s) y^2] = 0 \quad (3)$$

$$\frac{d^2 y}{d\theta_y^2} + Q_y^2 y + \dot{K}(s) \beta_y^2(s) \beta_x^{1/2}(s) Q_y^2 x y = 0 \quad . \quad (4)$$

The advantage of these equations is the very simple representation of the solution of the linear parts. On the other hand we have to deal with two variables θ_x, θ_y which are linearly independent.

3 The horizontal motion

In this section we consider the one dimensional motion in the horizontal plane of a storage ring. Using the following initial conditions,

$$y(0) = 0, \quad y'(0) = 0$$

we obtain pure horizontal motion from Eqs (3) and (4):

$$\frac{d^2x}{d\theta_x^2} + Q_x^2 x + \epsilon f(\theta_x) x^2 = 0 \quad (5)$$

where

$$f(\theta_x) = \frac{1}{2} Q_x^2 \dot{K}(s) \beta_x^{\frac{5}{2}}(s) \quad (6)$$

is a periodic function with respect to the circumference of the ring. Although ϵ is equal to unity in the above equation it is used as a parameter for the series expansion. The fundamental idea of secular perturbation theory is based on the fact that one of the effects of non - linear terms is to shift the frequency of the system from Q , of the linear theory to \tilde{Q} . According to this method, which is one of the earliest techniques that yielded uniform expansions of the solutions of such problems, both the dependant variable x and the frequency of the system are expanded in powers of ϵ ; see Refs. [11] and [9].

$$x = x_0 + \epsilon x_1 + \epsilon^2 x_2 + \dots + \epsilon^n x_n \quad (7)$$

$$\dot{x} = \dot{x}_0 + \epsilon \dot{x}_1 + \epsilon^2 \dot{x}_2 + \dots + \epsilon^n \dot{x}_n$$

$$\tilde{Q} = Q\omega$$

$$\tilde{\theta}_x = \theta_x \omega$$

$$\omega = 1 + \epsilon \omega_1 + \epsilon^2 \omega_2 + \dots + \epsilon^n \omega_n ; \quad (8)$$

We define the quadratic form:

$$\Omega_n = \sum_{i=0}^n \omega_i \omega_{n-i} .$$

From Eq.(5) we obtain:

$$\ddot{x} \omega^2 + Q^2 x + \epsilon f(\tilde{\theta}_x) x^2 = 0 . \quad (9)$$

where the dot denotes the derivative with respect to $\tilde{\theta}_x$. Next, we insert Eq.(7) in the transformed equation, equate coefficients of like powers of ϵ , and obtain linear equations that can be solved successively.

$$\ddot{x}_0 + Q^2 x_0 = 0 \quad (10)$$

$$\ddot{x}_1 + Q^2 x_1 = -f(\tilde{\theta}_x) x_0^2 - 2\omega_1 \ddot{x}_0 \quad (11)$$

$$\ddot{x}_2 + Q^2 x_2 = -f(\tilde{\theta}_x) 2x_1 x_0 - (\omega_1^2 + 2\omega_2) \ddot{x}_0 - 2\omega_1 \ddot{x}_1 \quad (12)$$

$$\ddot{x}_3 + Q^2 x_3 = -f(\tilde{\theta}_x)(2x_0x_2 + x_1^2) - \Omega_3\ddot{x}_0 - \Omega_2\ddot{x}_1 - \Omega_1\ddot{x}_2 \quad (13)$$

\vdots

$$\ddot{x}_n + Q^2 x_n = -f(\tilde{\theta}_x) \sum_{j=0}^{n-1} x_j x_{n-1-j} - \sum_{j=0}^{n-1} \ddot{x}_j \Omega_{n-j} \quad (14)$$

Each of these equations contains one free parameter ω_n which is chosen to eliminate the secular terms. For simplicity we deal with initial conditons of the following form

$$x(0) = A , \quad \dot{x}(0) = 0 ;$$

The initial conditions are fully imposed to the unperturbed equation.

$$x_0(0) = A , \quad \dot{x}_0(0) = 0 ,$$

$$x_n(0) = 0 , \quad \dot{x}_n(0) = 0 ;$$

which yields the solutions of Eqs. (11) - (14) as partial solutions of the inhomogeneous equation plus the homogeneous parts.

$$x_n = -x_n^p(0) \cos(Q\tilde{\theta}) + x_n^p(\tilde{\theta}) \quad n > 0$$

Because of our requirement of cancelling secular terms, the particular solutions are unique. If we substitute these equations into Eqs. (11) - (14) we realize that the solution of the n^{th} order equation contains all solutions of the lower orders. Thus as a second step we may expand the particular solution of Eq. (14) into a set of n basis- functions:

$$x_n^p(\tilde{\theta}_x) = \sum_{l=1}^n c_l^n q_l(\tilde{\theta}_x) . \quad (15)$$

where c_l^n are constant coefficients and the basis functions q_n are particular solutions of the following system of differential equations:

$$\ddot{x} + Q^2 x = -f(\tilde{\theta}_x) \sum_{j=0}^{n-1} q_j q_{n-1-j} - \frac{1}{A^{n+1}} \sum_{j=0}^{n-1} \ddot{x}_j \Omega_{n-j} . \quad (16)$$

Up to the third order we find the following coefficients:

$$\begin{aligned} c_1^1 &= A^2 ; \\ c_1^2 &= -2A^3 q_1(0) , \quad c_2^2 = A^3 ; \\ c_1^3 &= -2A^4 q_2(0) + 5A^4 q_1^2(0) , \quad c_2^3 = -3A^4 q_1(0) , \quad c_3^3 = A^4 . \end{aligned}$$

For an arbitrary n we have:

$$\begin{aligned} c_l^n &= A^{n+1} \sum_{m=0}^{m=n-1} (-1)^m \frac{(n+m)!}{(n+1)!} \times \\ &\frac{(l+1)}{k_1! k_2! k_3! \dots k_{n-1}!} \left(q_1^{k_1}(0) q_2^{k_2}(0) q_3^{k_3}(0) \dots q_{n-1}^{k_{n-1}}(0) \right) ; \end{aligned} \quad (17)$$

with the additional conditions:

$$n = l + \sum_{j=1}^{n-1} j k_j , \quad m = \sum_{j=1}^{n-1} k_j .$$

This formula may be prooved by induction. With the following definitions:

$$q_0 = \cos(Q\tilde{\theta}) \quad , \quad c_0^n = - \sum_{l=1}^{\infty} c_l^n q_l(0)$$

for $n \geq 1$ we obtain:

$$x_n = \sum_{l=0}^{\infty} c_l^n q_l(\tilde{\theta}) \quad (18)$$

and finally

$$x = A \cos(Q\tilde{\theta}) + \sum_{n=1}^{\infty} \sum_{l=0}^{\infty} c_l^n q_l(\tilde{\theta}) \quad (19)$$

which may be regarded as a double series expansion. Eq. (19) may be written as:

$$x = A \cos(Q\tilde{\theta}) + q_0(\tilde{\theta}) \sum_{n=1}^{\infty} c_0^n + q_1(\tilde{\theta}) \sum_{n=1}^{\infty} c_1^n + q_2(\tilde{\theta}) \sum_{n=1}^{\infty} c_2^n + \dots \quad (20)$$

Since the basis- functions are linearly independent divergency of one of these series is a sufficient condition for the secular perturbation theory to break down. We find an lower limit for the divergency of this series expansion using d'Alembert's convergency- criterion. We restrict ourselves in Eq. (17) on contributions up to the order 2 and obtain as an lower limit for the dynamic aperture:

$$A_{limit} = \left| \frac{1}{q_1(0)\sqrt{G(\lambda)}} \right| \quad \lambda = -\frac{q_2(0)}{q_1(0)^2} \quad (21)$$

with the additional function:

$$G(\lambda) = \left| \lim_{l \rightarrow \infty} \frac{1}{(2l+3)(2l+4)} \frac{1 + \sum_{k=0}^{l+1} \frac{(3l+k+4)!(2l+2)!}{(l+1-k)!(4l+5)!(2k)!} \lambda^{-k}}{\sum_{k=0}^l \frac{(3l+k+1)!(2l+2)!}{(l-k)!(4l+5)!(2k)!} \lambda^{-k}} \right| \quad (22)$$

Note that this function does not contain the initial amplitude A . $G(\lambda)$ may be evaluated numerically. Two properties of this function could be derived analytically:

$$G(0) = 16$$

$$\lim_{\lambda \rightarrow \infty} G(\lambda) = \frac{27}{4} \lambda$$

Equation (21) contains information about the third and the fourth integer resonances. The fifth integer resonance arises in $q_3(0)$ whose contribution was neglected in this calculation.

We apply this method to the horizontal motion of a storage ring. Using the periodicity of $f(\tilde{\theta})$ this function is expanded in a fourier series.

$$f(\tilde{\theta}) = \sum_{n=0}^{\infty} a_n \cos(n\tilde{\theta}) + \sum_{n=0}^{\infty} b_n \sin(n\tilde{\theta}) = \frac{1}{2} Q_x^2 \dot{K}(s) \beta_x^{\frac{5}{2}}(s) \quad (23)$$

As an example we consider the horizontal motion in LEP including sextupole perturbation. The results of our analytic approach which yields a

lower limit of the dynamical aperture is compared with tracking over 400 turns. In figure 1 we vary the horizontal tune from 17.25 over the default value 17.58 to 17.75. Tracking shows an additional fifth integer resonance at $Q_x = 17.60$, which could not be dedected by formula (21) since it does not contain the term $q_3(0)$.

4 Non - linear motion in two dimensions

We expand the dependant variables x, y as well as the two tunes in powerseries of ϵ . The independant variables are transformed according to the shift of frequency :

$$\tilde{\theta}_x = \omega^x \tilde{\theta} \quad , \quad \check{\theta}_y = \omega^y \check{\theta}$$

With Eqs. (3) and (4) we obtain the following system of differential equations.

$$\begin{aligned} \ddot{x}_0 + Q_x^2 x_0 &= 0 \\ \ddot{x}_1 + Q_x^2 x_1 &= +\frac{1}{2} Q_x^2 \dot{K}(s) \beta_x^{3/2}(s) \left[\beta_x(s) x_0^2(\tilde{\theta}_x) - \beta_y(s) y_0^2(\check{\theta}_y) \right] - \\ &\quad - 2\omega_1^x \ddot{x}_0(\tilde{\theta}_x) \\ &\quad \vdots \\ \ddot{x}_n + Q_x^2 x_n &= +\frac{1}{2} Q_x^2 \dot{K}(s) \beta_x^{3/2}(s) \left[\beta_x(s) \sum_{j=0}^{n-1} x_{n-j-1} x_j(\tilde{\theta}_x) - \beta_y(s) \sum_{j=0}^{n-1} y_{n-j-1} y_j(\check{\theta}_y) \right] - \\ &\quad - \sum_{j=1}^n \ddot{x}_{n-j}(\tilde{\theta}_x) \Omega_j^x, \\ \\ \ddot{y}_0 + Q_y^2 y_0 &= 0 \\ \ddot{y}_1 + Q_y^2 y_1 &= -Q_y^2 \dot{K}(s) \beta_y(s) \beta_x(s)^{1/2} y_0(\check{\theta}_y) x_0(\tilde{\theta}_x) - \\ &\quad - 2\omega_1^y \ddot{y}_0(\check{\theta}_y) \\ &\quad \vdots \\ \ddot{y}_n + Q_y^2 y_n &= -Q_y^2 \dot{K}(s) \beta_y(s) \beta_x(s)^{1/2} \sum_{j=0}^{n-1} x_{n-j-1}(\tilde{\theta}_x) y_j(\check{\theta}_y) - \\ &\quad - \sum_{j=1}^n \ddot{y}_{n-j}(\check{\theta}_y) \Omega_j^y; \end{aligned}$$

The initial conditions

$$\begin{aligned} x(0) &= A \quad , \quad \dot{x}(0) = 0 \\ y(0) &= B \quad , \quad \dot{y}(0) = 0 \end{aligned}$$

are imposed to the lowest order equations.

$$x_0(0) = A \quad , \quad y_0(0) = B \tag{24}$$

We define 7 basis- functions as particular solutions of the following equations.

$$\begin{aligned}
q_{11}(\tilde{\theta}_x) : \quad \ddot{x} + Q_x^2 x &= \frac{1}{2} Q_x^2 \dot{K}(s) \beta_x^{5/2}(s) \cos^2(Q_x \tilde{\theta}_x) \\
q_{12}(\tilde{\theta}_x) : \quad \ddot{x} + Q_x^2 x &= -\frac{1}{2} Q_x^2 \dot{K}(s) \beta_x^{3/2}(s) \beta_y(s) \cos^2(Q_y \check{\theta}_y) \\
p_{11}(\check{\theta}_y) : \quad \ddot{y} + Q_y^2 y &= -Q_y^2 \dot{K}(s) \beta_y^2(s) \beta_x^{1/2}(s) \cos(Q_x \tilde{\theta}_x) \cos(Q_y \check{\theta}_y) \\
q_{21}(\tilde{\theta}_x) : \quad \ddot{x} + Q_x^2 x &= Q_x^2 \dot{K}(s) \beta_x^{5/2}(s) q_{11}(\tilde{\theta}_x) \cos(Q_x \tilde{\theta}_x) \\
q_{22}(\tilde{\theta}_x) : \quad \ddot{x} + Q_x^2 x &= -Q_x^2 \dot{K}(s) \beta_x^{3/2}(s) \\
&\times [\beta_x(s) q_{12}(\tilde{\theta}_x) \cos(Q_x \tilde{\theta}_x) + \beta_y(s) p_{11}(\check{\theta}_y) \cos(Q_y \check{\theta}_y)] \\
p_{21}(\check{\theta}_y) : \quad \ddot{y} + Q_y^2 y &= -Q_y^2 \dot{K}(s) \beta_y^2(s) \beta_x^{1/2}(s) \\
&\times [q_{11}(\tilde{\theta}_x) \cos(Q_y \check{\theta}_y) + p_{11}(\check{\theta}_y) \cos(Q_x \tilde{\theta}_x)] \\
p_{22}(\check{\theta}_y) : \quad \ddot{y} + Q_y^2 y &= -Q_y^2 \dot{K}(s) \beta_y^2(s) \beta_x^{1/2}(s) q_{12}(\tilde{\theta}_x) \cos(Q_y \check{\theta}_y)
\end{aligned}$$

Now we may expand the particular solutions of the n^{th} order equations into these basis- functions.

$$x_n^p(\tilde{\theta}) = c_{11}^n q_{11}(\tilde{\theta}) + c_{12}^n q_{12}(\tilde{\theta}) + c_{21}^n q_{21}(\tilde{\theta}) + c_{22}^n q_{22}(\tilde{\theta}) + x_n^\perp \quad (25)$$

$$y_n^p(\check{\theta}) = d_{11}^n p_{11}(\check{\theta}) + d_{21}^n p_{21}(\check{\theta}) + d_{22}^n p_{22}(\check{\theta}) + y_n^\perp \quad (26)$$

The last terms in each equation x_n^\perp, y_n^\perp are elements of the complementary subspace. For the coefficients we find:

$$\begin{aligned}
c_{11}^n &= -\sum_{j=0}^{n-1} x_j^p(0) x_{n-1-j}^p(0) \\
c_{12}^n &= +\sum_{j=0}^{n-1} x_j^p(0) y_{n-1-j}^p(0) \\
d_{11}^n &= +\sum_{j=0}^{n-1} x_j^p(0) y_{n-1-j}^p(0) \\
c_{21}^n &= -\sum_{j=0}^{n-2} x_j^p(0) c_{11}^{n-1-j} \\
c_{22}^n &= -\sum_{j=0}^{n-2} x_j^p(0) c_{12}^{n-1-j} \\
d_{21}^n &= -\sum_{j=0}^{n-2} x_j^p(0) d_{11}^{n-1-j} \\
d_{22}^n &= -\sum_{j=0}^{n-2} y_j^p(0) c_{12}^{n-1-j}
\end{aligned}$$

Introducing again Eqs. (25) and (26) in the upper equations we find the explicit formula for the coefficients. For example :

$$\begin{aligned}
c_{11}^n &= \sum_k \sum_l \sum_m \sum_o \sum_p \sum_i \sum_j A^{2+m+k+2j+2o-l} B^{2l+2p+2i} \times \\
&(-1)^{k+m+j+o} \frac{2(2l+2i)(1+m+i+2k+3j+2o)!(m+o+2l+2i+3p-1)!}{q!m!p!k!l!j!i!o!(2+m+k+2j+2o-l)!(2p+2l+2i)!} \times \\
&q_{11}^k(0) q_{12}^l(0) q_{21}^j(0) q_{22}^i(0) p_{11}^m(0) p_{21}^o(0) p_{22}^p(0)
\end{aligned}$$

The divergence of the expansion is again dedected by d'Alemdert's criterion. This leads to the following eight conditions for maximum initial values A and B:

$$A_{lim} = |4q_{11}(0)|^{-1} \quad (27)$$

$$A_{lim} = 2 |27q_{21}(0)|^{-\frac{1}{2}} \quad (28)$$

$$B_{lim} = |q_{22}(0)|^{-\frac{1}{2}} \quad (29)$$

$$A_{lim} = |p_{11}(0)|^{-1} \quad (30)$$

$$A_{lim} = |p_{21}(0)|^{-\frac{1}{2}} \quad (31)$$

$$B_{lim} = 2 |27p_{22}(0)|^{-\frac{1}{2}} \quad (32)$$

$$B_{lim} = 2 | 27p_{11}(0)q_{12}(0) |^{-\frac{1}{2}} \quad (33)$$

$$B_{lim} = | 4q_{11}(0)q_{12}(0) |^{-\frac{1}{2}} \quad (34)$$

As final limit we choose the minimum result for A and B obtained from Eqs. (27) - (34). As an application we treated the transvers motion of the LEP storage ring. In figure 2 we have varied the sextupole strength of a defocussing sextupole comparing the analytic approach with tracking results. The initial condition has been chosen on the vertical axis.

5 Remarks

The here presented method yields to a lower limit for the dynamic aperture. For reliable application of this method, either the possible distance between this lower limit and the real dynamic aperture has to be estimated, or we may add an upper limit, approaching the problem from the area of unbounded motion. Secondly we have to supply a criterion whether a resonance appears or not.

The representation of two dimensional equations of motion in Eqs. (3) and (4) leads to very complicated calculations of the basis functions (not in the one dimensional case!). On the other hand we had been looking for a simple and clear algorithm to estimate the dynamical aperture. As a future activity we try to extend this method of double expansion on Eqs. (1) and (2).

References

- [1] E.D. Courant, R.D. Ruth, W.T. Weng: *Stability in Dynamical Systems*, SLAC-Publication **3415**, (1984).
- [2] G. Guignard: *A general Treatment of Resonances in Accelerators*, CERN/78-11, (1978).
- [3] G. Guignard, J. Hagel: *Dynamical Aperture: Analytic Derivation and Sextupole Algorithms*, Nonlinear Dynamics Aspects of Particle Accelerators, Lecture Notes in Physics 247, Springer (1986).
- [4] J. Hagel: *Invariants of Betatron Motion and Dynamic Aperture - an Analytic Approach*, CERN LEP-TH/86-22, (1986).
- [5] J. Hagel: *DYNAP - A Programm for Estimating the Dynamical Aperture in Storage Rings*, CERN LEP-TH/86-23, (1987).
- [6] H. Moshhammer: *Analytische Berechnung der Dynamischen Apertur in der nichtlinearen Fokussierungsstruktur von Speicherringen* Thesis, Technical University Graz, (1988).
- [7] R.G. Littlejohn: *Noncanonical Hamilton Mechanics*, Particle Accelerators, **19**, (1986) [221].

- [8] R.S. Mackay: *Transition to Chaos for Area-Preserving Maps*, Non-linear Dynamics Aspects of Particle Accelerators, Lecture Notes in Physics 247, Springer (1986).
- [9] R.E. Mickens: *An Introduction to Nonlinear Oscillations*, Cambridge University Press, Cambridge (1981).
- [10] J. Moser: *Break-Down of Stability*, Nonlinear Dynamics Aspects of Particle Accelerators, Lecture Notes in Physics 247, Springer (1986).
- [11] A.H. Nayfeh: *Problems in Perturbation*, John Wiley a. Sons, New York (1985).
- [12] R.D. Ruth : *Single Particle Dynamics and Nonlinear Resonances in Circular Accelerators*, Nonlinear Dynamics Aspects of Particle Accelerators, Lecture Notes in Physics 247, Springer (1986).
- [13] J.F. Schonfeld: *A new Approach to Dynamic Aperture Problems*, Particle Accelerators, **20**, (1986) [121].
- [14] R.L. Warnock R.D. Ruth: *Invariant Tori through direct Solution of the Hamilton-Jacobi Equation*, Physica **26D**, (1987) [1].

* * *

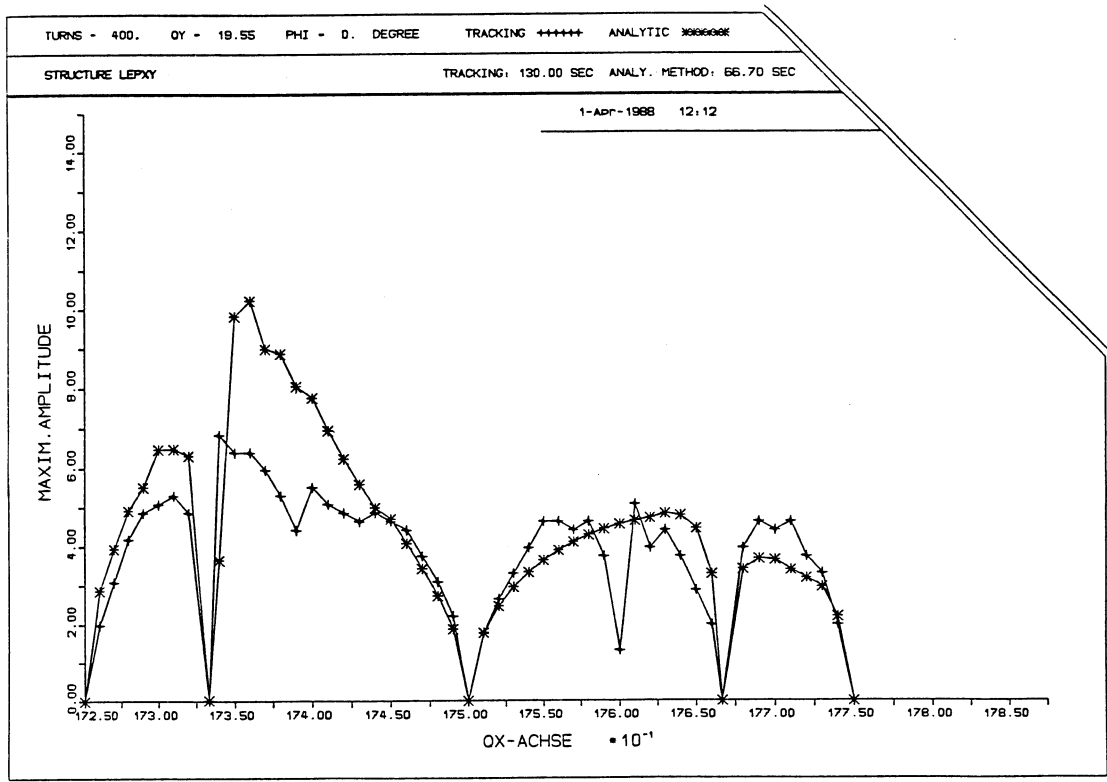


Fig. 1

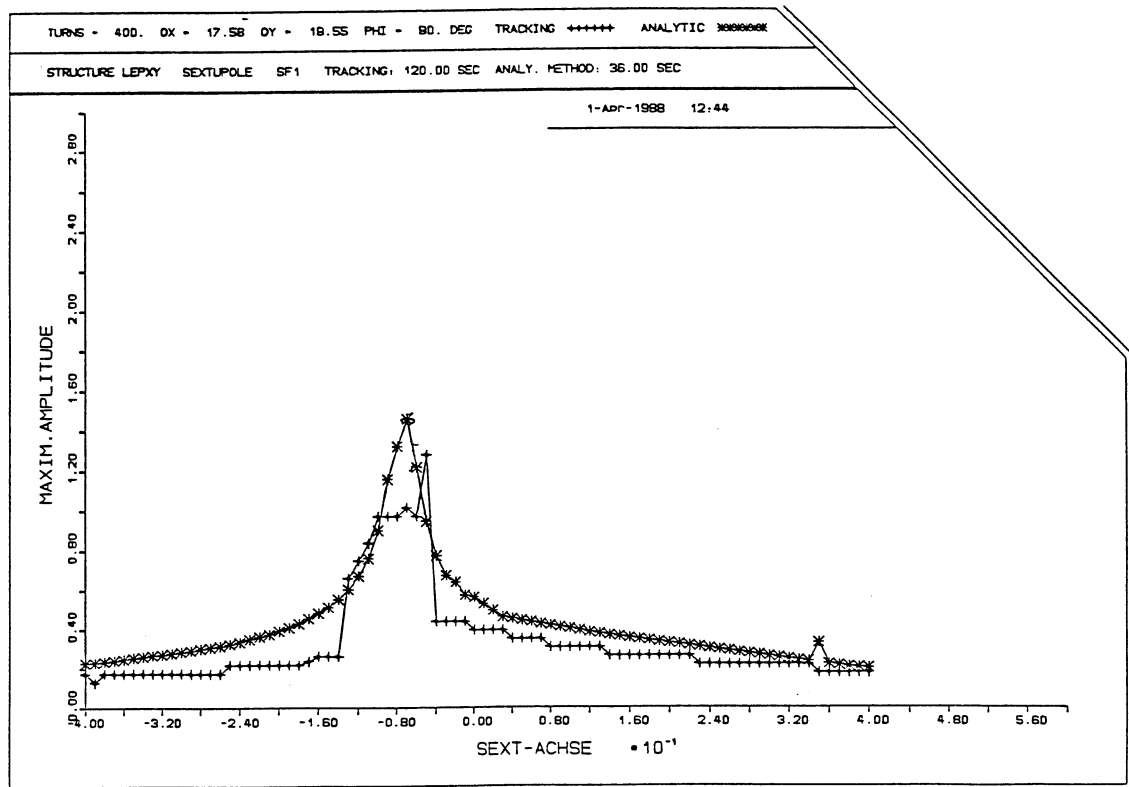


Fig. 2

CANONICAL DESCRIPTION OF A SECOND-ORDER ACHROMAT*

S.A. Kheifets, T.H. Fieguth and R.D. Ruth

SLAC, Stanford University, Stanford, California, USA

ABSTRACT

Charged particle motion in a second-order magnetic optical achromat is described using a canonical perturbation theory. Necessary and sufficient conditions for the existence of such a device are presented. Given these conditions, the second-order matrix elements at the end of the achromat are found explicitly. It is shown that all geometric matrix elements are equal to zero and all chromatic matrix elements are either also equal to zero or proportional to the corresponding chromaticity. Thus all second-order matrix elements vanish simultaneously when the two chromaticities are made to be equal to zero.

1. INTRODUCTION

A fascinating property of the second-order achromat invented by K. L. Brown [1] is that all the matrix elements describing both *geometric* and *chromatic* aberrations (with the exception of the elements connected to the path length of a particle trajectory) of the second-order matrix *simultaneously* vanish at the achromat exit provided that certain conditions are satisfied.

The proof of such a property for a second-order achromat with respect to the geometric aberrations was given by K. L. Brown in Ref. [1]. This paper also contains a practical recipe for constructing a second-order achromat.

On the other hand, a proof pertaining to *chromatic aberrations* is much more difficult. The first attempt of such a proof belongs to D. Carey [2], who showed that the recipe works.

Here we use a canonical perturbation theory to describe the particle motion in a beam line [3]. This approach brings us in a natural way to the formulation of the *necessary and sufficient* conditions for the existence of the second-order achromat. We show *why* the second-order achromat works and provide the reader with a simple physical explanation of the underlying reasons for its existence. By calculating the second-order matrix elements directly we show why they vanish when the achromatic conditions are fulfilled.

This paper will proceed as follows. In Section 2 the canonical formalism [4] for a particle motion in a magnetic field is described. The particle motion is separated into betatron and synchrotron parts. In Section 3 the betatron motion is described using canonical (angle-action) variables. We obtain formulae for horizontal and vertical chromaticities which agree with results obtained by M. Bassetti [5]. We then proceed to give the solution of the Hamilton's equations up to the second-order terms. Section 4 contains calculation of the second-order matrix elements. In particular, the chromatic matrix elements are found explicitly. The necessary and sufficient conditions for a second-order achromat are derived in Section 5. A special case of an achromat built from identical cells is considered.

This paper is in essence a short version of the paper [6], where more detailed calculations can be found.

*Work supported by the Department of Energy, contract DE-AC03-76SF00515.

2. THE HAMILTONIAN FOR THE MOTION OF A CHARGED PARTICLE IN A MAGNETIC FIELD

In the vicinity of a planar reference curve which follows the path of a particle with the reference momentum P_o in a guiding magnetic field, the motion of an arbitrary particle is governed by a Hamiltonian [4] which we represent here with all the terms up to and including those which are cubic in coordinates and momenta:

$$H_1(x, p_x, y, p_y; s) = -eA_s/cP_o - (1 + xh)(1 + \delta) + (1 + xh)(p_x^2 + p_y^2)/2(1 + \delta) \quad (1)$$

Here we use the notation $h = 1/\rho$, where ρ is local radius of curvature of the reference trajectory. The coordinate x is the horizontal (in the plane of the reference trajectory) deviation from the reference trajectory while y is the vertical deviation. The canonically conjugate momenta are p_x and p_y , respectively. The fractional difference of the particle momentum P from that of the reference momentum P_o defines δ : $P = P_o(1 + \delta)$. The distance s along the reference curve measured from an arbitrary point serves as an independent variable.

The quantity A_s which appears in Eq. (1) is the *canonical* vector potential [4] representing the guide field. Again retaining the terms up to and including those which are cubic in the coordinates, A_s is given by the following expression [7]:

$$\begin{aligned} \frac{-e}{cP_o} A_s(x, y, s) = & xh(1 + hx/2) + K_1(s)(x^2 - y^2)/2 \\ & + K_1(s)(hx^3/3 - hxy^2/2 - h^2y^4/24) + K_2(s)(x^3 - 3xy^2)/6 \quad , \end{aligned} \quad (2)$$

where $K_1 = \frac{h}{B_o} \frac{\partial B_y}{\partial x}$ and $K_2 = \frac{h}{B_o} \frac{\partial^2 B_y}{\partial x^2}$ are local (at the location s) strengths of the quadrupole and sextupole components of the magnetic field B_y , respectively.

The term linear in x in the Hamiltonian (1) makes the equation of motion for the x -plane inhomogeneous. The particular solution of this inhomogeneous equation gives the *equilibrium orbit* of the off-momentum particle. The reference orbit is but a special case of the more general equilibrium orbit for which $\delta = 0$. The solution of the homogeneous equation describes (in case of stable motion) *betatron oscillations*. An off-momentum particle performs betatron oscillations about its corresponding equilibrium orbit.

To describe the horizontal betatron motion of the off-momentum particle one can use a canonical transformation from x, p_x, y, p_y to x_β, p_β, y, p_y to eliminate linear terms in the Hamiltonian. New coordinates and momenta are connected to the old ones by $x_\beta = x - D(s)\delta$, $p_x = p_\beta + \zeta(s)\delta$.

As shown in Ref. [8], functions $D(s)$ and $\zeta = D'(1 + \delta)/(1 + hD\delta)$ can be found from a solution of the following second-order differential equation:

$$D'' = (1 + hD\delta)(h - h^2D - K_1D - K_1hD^2\delta - K_2D^2\delta/2)/(1 + \delta) + h(D')^2/2(1 + hD\delta) \quad (3)$$

Equation (3), together with corresponding initial conditions, defines the *dispersion function* which describes the equilibrium orbit for an off-momentum particle. For δ small, a solution of Eq. (3) can be found as an expansion in δ

$$D(s) = D_o(s) + \delta D_1(s) + \dots \quad , \quad (4)$$

where the *zero-th* order function D_o is a solution of the equation

$$D_o'' + (K_1 + h^2)D_o = h \quad ; \quad (5)$$

the *first-order* function D_1 is a solution of the equation

$$D_1'' + (K_1 + h^2)D_1 = (K_1 + 2h^2)D_o - h - 2K_1hD_o^2 - K_2D_o^2/2 - h^3D_o^2 + h(D_o')^2/2 \quad , \quad (6)$$

and so on.

The particular *zero-th* order dispersion function $d(s)$ which has the special initial conditions $d(0) = d'(0) = 0$ defines the first-order matrix elements $R_1^6(s)$ and $R_2^6(s)$ [9] which couple x and x' to δ [10].

On the other hand, for periodic systems with period l it may be convenient to define a periodic dispersion function. Such a dispersion function is called *the matched dispersion*. One should distinguish the matched dispersion from functions $D(s)$ with other possible initial conditions. We will denote the *zero-th* order matched dispersion as $\eta(s)$: $\eta(s+l) = \eta(s)$, $\eta'(s+l) = \eta'(s)$. It can be found as solution of Eq. (5) with the following boundary conditions: $\eta(l) = \eta(0)$, $\eta'(l) = \eta'(0)$.

Any *zero-th* order dispersion function $D_o(s)$ with arbitrary initial conditions $D_o(0)$ and $D_o'(0)$ (including the matched dispersion) is connected to function $d(s)$ by the following matrix expression:

$$\begin{pmatrix} D_o(s) \\ D_o'(s) \\ 1 \end{pmatrix} = \begin{pmatrix} R_1^1(s) & R_1^2(s) & d(s) \\ R_2^1(s) & R_2^2(s) & d'(s) \\ 0 & 0 & 1 \end{pmatrix} \begin{pmatrix} D_o(0) \\ D_o'(0) \\ 1 \end{pmatrix}, \quad (7)$$

where R_i^k are the first-order matrix elements for transition from an arbitrary point 0 to an arbitrary point s of the system. This feature will be used below for calculation of the second-order chromatic matrix elements.

3. BETATRON MOTION

In the new variables x_β, p_β, y, p_y the Hamiltonian has no linear terms and describes betatron motion of a particle with respect to its corresponding equilibrium orbit:

$$\begin{aligned} H_2 = & (p_\beta^2 + p_y^2)/2(1+\delta) + K_x x_\beta^2/2 + K_y y^2/2 \\ & + K_{2x} D\delta x_\beta^2/2 - K_{2y} D\delta y^2/2 + (K_{2x} x_\beta^3 - 3K_{2y} x_\beta y^2)/6 \\ & + h x_\beta (p_\beta^2 + p_y^2)/2(1+\delta) + h D\delta (p_\beta^2 + p_y^2)/2(1+\delta) + h\zeta\delta p_\beta x_\beta/(1+\delta), \end{aligned} \quad (8)$$

where the following notations are used: $K_x = K_1 + h^2$, $K_y = -K_1$, $K_{2x} = K_2 + 2hK_1$, $K_{2y} = K_2 + hK_1$.

As in Ref. [4] we now perform a canonical transformation to the action-angle variables J_x, ϕ_x, J_y, ϕ_y . The old coordinates and momenta are expressed in terms of the new ones as

$$x_\beta = \sqrt{\frac{2J_x\beta_x}{(1+\delta)}} \cos \phi_x, \quad p_\beta = -\sqrt{\frac{2J_x(1+\delta)}{\beta_x}} (\sin \phi_x + \alpha_x \cos \phi_x) \quad (9)$$

and similar expressions for y, p_y . The new Hamiltonian is

$$H_3(J_x, \phi_x, J_y, \phi_y; s) = \frac{J_x}{\beta_x} + \frac{J_y}{\beta_y} + C_{0,0}^{1,0} J_x + C_{0,0}^{0,1} J_y + V(J_x, \phi_x, J_y, \phi_y; s), \quad (10)$$

where

$$V(J_x, \phi_x, J_y, \phi_y; s) = \sum_{m,n,k,l} J_x^{k/2} J_y^{l/2} [C_{m,n}^{k,l} \cos(m\phi_x + n\phi_y) + S_{m,n}^{k,l} \sin(m\phi_x + n\phi_y)] \quad (11)$$

(k, l, m and n are all integers.) All non-zero coefficients $C_{m,n}^{k,l}$ and $S_{m,n}^{k,l}$ are given in Table 1. The functions $\beta(s)$ and $\alpha(s) = -\beta'/2$, used to describe the modulated betatron oscillations are *the matched functions* for the system under consideration. For a periodic system the matched β -function is also periodic as required by Floquet's theorem [11]. For a nonperiodic system the matched function is defined by the condition that the final values for the function and its derivative are the same as the initial values. Of course, it would be possible to parametrize the motion in terms of unmatched β -functions. In this case, the following results for the second-order achromat are unchanged; however, the proofs are somewhat

Table 1.
Non-Zero Coefficients of the Second-Order Hamiltonian

Notations:
 $H = \frac{J_x}{\beta_x} + \frac{J_y}{\beta_y} + \sum_{m,n,k,l} J_x^{k/2} J_y^{l/2} [C_{m,n}^{k,l} \cos(m\phi_x + n\phi_y) + S_{m,n}^{k,l} \sin(m\phi_x + n\phi_y)], \Delta = 1 + \delta.$

N	Coefficient	
1	$C_{0,0}^{1,0}$	$(K_{2x}D - K_x)\delta\beta_x/2\Delta + hD\delta\gamma_x/2 - h\zeta\delta\alpha_x/\Delta$
2	$C_{0,0}^{0,1}$	$-(K_{2y}D + K_y)\delta\beta_y/2\Delta + hD\delta\gamma_y/2$
3	$C_{2,0}^{1,0}$	$(K_{2x}D - K_x)\delta\beta_x/2\Delta + hD\delta(1 - \alpha_x^2)/2\beta_x - h\zeta\delta\alpha_x/\Delta$
4	$S_{2,0}^{1,0}$	$hD\delta\alpha_x/\beta_x - h\zeta\delta/\Delta$
5	$C_{0,2}^{0,1}$	$-(K_{2y}D + K_y)\delta\beta_y/2\Delta - hD\delta(1 - \alpha_y^2)/2\beta_y$
6	$S_{0,2}^{0,1}$	$hD\delta\alpha_y/\beta_y$
7	$C_{3,0}^{3,0}$	$K_{2x}\beta_x^{3/2}/6\sqrt{2}\Delta^{3/2} - h(1 - \alpha_x^2)/\sqrt{2}\beta_x\Delta$
8	$C_{1,0}^{3,0}$	$K_{2x}\beta_x^{3/2}/2\sqrt{2}\Delta^{3/2} + \sqrt{2}h(1 + \alpha_x^2)/\sqrt{\beta_x\Delta} - h(1 - \alpha_x^2)/\sqrt{2}\beta_x\Delta$
9	$C_{1,0}^{1,2}$	$-K_{2y}\beta_x^{1/2}\beta_y/2\sqrt{2}\Delta^{3/2} + h\gamma_y\sqrt{2\beta_x/\Delta}$
10	$C_{1,2}^{1,2}$	$-K_{2y}\beta_x^{1/2}\beta_y/2\sqrt{2}\Delta^{3/2} - h(1 - \alpha_y^2)\sqrt{\beta_x/2\Delta}/\beta_y$
11	$C_{1,-2}^{1,2}$	$-K_{2y}\beta_x^{1/2}\beta_y/2\sqrt{2}\Delta^{3/2} - h(1 - \alpha_y^2)\sqrt{\beta_x/2\Delta}/\beta_y$
12	$S_{3,0}^{3,0}$	$h\alpha_x\sqrt{2/\beta_x\Delta}$
13	$S_{1,0}^{3,0}$	$h\alpha_x\sqrt{2/\beta_x\Delta}$
14	$S_{1,2}^{1,2}$	$h\alpha_y\sqrt{2\beta_x/\Delta}/\beta_y$
15	$S_{1,-2}^{1,2}$	$-h\alpha_y\sqrt{2\beta_x/\Delta}/\beta_y$

more complicated. Finally, we choose the β -function to be independent of momentum, treating all the terms in the Hamiltonian dependent on δ as perturbations.

Due to the explicit dependence of the Hamiltonian (10) on the angles ϕ_x and ϕ_y , J_x and J_y are not constants of motion as would be the case for the unperturbed Hamiltonian. Note, however, that the perturbation term V is zero when averaged over all values of the angle variables. This allows us to evaluate the effects due to the leading order terms (e.g., changes in phase advance of the betatron oscillations) by doing such averaging.

For a system of total length L we define a symbol $\langle \rangle$ for the averaging over the angle variables. From the equation of motion the horizontal phase advance is:

$$\phi_{xo}(s) \approx \phi_{xo} + \psi_x(s) + \Delta\psi_x(s) + \dots, \quad (12)$$

where ψ_{xo} is an initial phase of the horizontal betatron oscillation,

$$\psi_x(s) = \int_0^s \frac{ds'}{\beta_x(s')} \quad (13)$$

is the linear (unperturbed) horizontal betatron phase, and

$$\Delta\psi_x(s) = \frac{\delta}{2(1+\delta)} \int_0^s ds' [(K_{2x}D - K_x)\beta_x + \frac{hD(1+\delta)(1+\alpha_x^2)}{\beta_x} - 2h\zeta\alpha_x] \quad (14)$$

is the horizontal tune shift due to the nonlinear terms in the Hamiltonian. Similarly for the vertical tune, these quantities are given, respectively by:

$$\phi_{y0} \approx \phi_{y0} + \psi_y(s) + \Delta\psi_y(s) + \dots, \quad (15)$$

$$\psi_y(s) = \int_0^s \frac{ds'}{\beta_y(s')}, \quad (16)$$

$$\Delta\psi_y(s) = -\frac{\delta}{2(1+\delta)} \int_0^s ds' \left[(K_{2y}D + K_y)\beta_y - \frac{hD(1+\delta)(1+\alpha_y^2)}{\beta_y} \right]. \quad (17)$$

The *chromaticity* $\xi = (1/2\pi)(\partial\psi(L)/\partial\delta)_{\delta=0} \equiv (\partial\nu/\partial\delta)_{\delta=0}$ is a measure of the linear dependence of the tune on δ . From Eqs. (14) and (17) one finds:

$$\xi_x = \frac{1}{4\pi} \int_0^L ds' [(K_{2x}D_o - K_x)\beta_x + hD_o\gamma_x - 2hD_o'\alpha_x] \quad (18)$$

and

$$\xi_y = -\frac{1}{4\pi} \int_0^L ds' [(K_{2y}D_o + K_y)\beta_y - hD_o\gamma_y]. \quad (19)$$

Up to now the initial conditions for the dispersion function $D_o(s)$ which enters the above formulae has not been specified. Sometimes special initial conditions are appropriate. For example, for a system built of several identical cells the *periodic matched dispersion* η is convenient. Since β -functions are also periodic, the integrands in Eqs. (18) and (19) become periodic as well. In this case, it is sufficient to perform the integration over one period l :

$$\xi_x = \frac{1}{4\pi} \int_0^l ds' [(K_{2x}\eta - K_x)\beta_x + h\eta\gamma_x - 2h\eta'\alpha_x], \quad (20)$$

$$\xi_y = -\frac{1}{4\pi} \int_0^l ds' [(K_{2y}\eta + K_y)\beta_y - h\eta\gamma_y]. \quad (21)$$

Equations (20) and (21) were obtained by M. Bassetti [5] following a simple intuitive approach.

It is both interesting and important to note that it follows, from Eq. (7) and from the conditions (to be shown) required for a system to become a second-order achromat, that the values for chromaticities given by Eqs. (18) and (19) are independent of the initial conditions for the dispersion function.

Now we consider the perturbation V [Eq. (11)] in the Hamiltonian [Eq. (10)]. To describe the perturbed betatron motion of a particle we apply the canonical perturbation theory [3] and use the results obtained in Ref. [6]. The generating function which eliminates all the second-order terms from the Hamiltonian in Eq. (10) is given by the expression (see Appendix):

$$G(I_x, \phi_x, I_y, \phi_y, s) = - \int_0^s ds' \sum_{m,n,k,l} I_x^{k/2} I_y^{l/2} \left(C_{m,n}^{k,l} \cos[m(\phi_x + \tilde{\psi}_x' - \tilde{\psi}_x) + n(\phi_y + \tilde{\psi}_y' - \tilde{\psi}_y)] \right. \\ \left. + S_{m,n}^{k,l} \sin[m(\phi_x + \tilde{\psi}_x' - \tilde{\psi}_x) + n(\phi_y + \tilde{\psi}_y' - \tilde{\psi}_y)] \right), \quad (22)$$

where the *perturbed* phases are $\tilde{\psi}_{x,y} = \psi_{x,y}(s) + \Delta\psi_{x,y}(s)$, $\tilde{\psi}_{x,y}' = \psi_{x,y}(s') + \Delta\psi_{x,y}(s')$. The new invariants of the motion are $I_x = J_x - G_{\phi_x}$ and $I_y = J_y - G_{\phi_y}$, where a subscript in G indicates the partial differentiation with respect to the subscript.

The solution of the Hamilton's equations up to the second-order terms now is:

$$x_\beta(s) = \sqrt{\frac{2(I_x + G_{\phi_x})\beta_x}{(1 + \delta)}} \cos(\phi_{x0} + \psi_x + \Delta\psi_x - G_{J_x}) \quad , \quad (23)$$

$$x'_\beta(s) = -\sqrt{\frac{2(I_x + G_{\phi_x})}{\beta_x(1 + \delta)}} [\sin(\phi_{x0} + \psi_x + \Delta\psi_x - G_{J_x}) + \alpha_x \cos(\phi_{x0} + \psi_x + \Delta\psi_x - G_{J_x})] \quad , \quad (24)$$

and similar expressions for the vertical plane.

4. SECOND-ORDER MATRIX ELEMENTS

We will now apply the general results obtained in the previous section to the second order achromat as defined in Ref. [1] — a magnetic system for which all first-order terms represent the identity transformation and all second-order aberrations vanish at its end.

Let a single component of the vector in the phase space $(x_\beta, x'_\beta, y, y', \Delta I, \delta)$ be expressed by $X_i(s)$. Then, at each point s , component $X_i(s)$ can be represented as a power series in initial values $X_k(0)$ by expanding the following expressions:

$$x(s) = x_\beta(s) + D(s)\delta, \quad x'(s) = x'_\beta(s) + D'(s)\delta \quad , \quad (25)$$

$$y(s) = y_\beta, \quad y'(s) = y'_\beta \quad . \quad (26)$$

This gives, in general,

$$X_i(s) = R_i^k(s)X_k(0) + T_i^{kj}(s)X_k(0)X_j(0) \quad . \quad (27)$$

Here the summation from 1 to 6 over repeated indices (one upper and one lower) is to be understood. From definition (27) it follows that matrix T is symmetric in the upper indices: $T_i^{kj} = T_i^{jk}$. In order for the first order matrix $R_i^k(L)$ to be the unity matrix for a whole achromat the tunes ν_x and ν_y should be integers and $\sin 2\pi\nu_x = 0$, $\cos 2\pi\nu_x = 1$. Similar expressions hold for y -plane.

There are three categories of the second-order matrix elements $T_i^{kj}(s)$: a) *geometric* matrix elements, i.e., all T_i^{kj} with $i, k, j = 1, 2, 3, 4$; b) *single-chromatic* matrix elements, i.e., elements with k or $j = 6$ and c) *double-chromatic* matrix elements, i.e., with $k = j = 6$.

Equations in the form of Eq. (27) are obtained by expansions of Eqs. (23) and (24) for small G_{ϕ_x}, G_{J_x} and $\Delta\psi_x$ and of similar equations for the vertical plane. Introduce the amplitudes $a_x = \sqrt{2I_x/(1 + \delta)}$, $a_y = \sqrt{2I_y/(1 + \delta)}$ and express $x_i(L)$ in terms of $x_i(0)$ by excluding a_x, ϕ_x, a_y, ϕ_y .

a) Geometric matrix elements

All the second-order *geometric* matrix elements are proportional to one of the derivatives $G_{I_x}, G_{I_y}, G_{\phi_x}$ or G_{ϕ_y} . Therefore, if these derivatives vanish simultaneously at the point $s = L$, so will the second-order geometric matrix elements. Below we will find the conditions under which these derivatives vanish. For now suppose that these conditions are met.

b) Single-chromatic matrix elements

Consider now the terms which are proportional to $\Delta\psi_x$. These we expand in δ and keep terms linear in δ . That gives:

$$x(L) = x(0) + 2\pi\xi_x\delta[\beta_x(0)x'(0) + \alpha_x(0)x(0)] \quad , \quad (28)$$

$$x'(L) = x'(0) - 2\pi\xi_x\delta[\alpha_x(0)x'(0) + \gamma_x(0)x(0)] \quad . \quad (29)$$

Comparing Eqs. (28) and (29) with Eq. (27) we find:

$$\begin{pmatrix} T_1^{16} & T_1^{26} \\ T_2^{16} & T_2^{26} \end{pmatrix}_L = 2\pi\xi_x \begin{pmatrix} \alpha_x & \beta_x \\ -\gamma_x & -\alpha_x \end{pmatrix}_0, \quad (30)$$

$$\begin{pmatrix} T_3^{36} & T_3^{46} \\ T_4^{36} & T_4^{46} \end{pmatrix}_L = -2\pi\xi_y \begin{pmatrix} \alpha_y & \beta_y \\ -\gamma_y & -\alpha_y \end{pmatrix}_0. \quad (31)$$

Recall that for any lattice the initial values for the matched β , α and γ are uniquely defined. When the conditions $\xi_x = 0$ and $\xi_y = 0$ are met all the single-chromatic second-order matrix elements become zero simultaneously.

c) *Double-chromatic matrix elements*

From Eqs. (4) and (25) it follows that the double-chromatic matrix elements are: $T_1^{66}(L) = D_1(L)$, $T_2^{66}(L) = D_1'(L)$.

The solution of Eq. (6) for the zero initial conditions $D_1(0) = D_1'(0) = 0$ gives the following expressions for the second-order dispersion and its derivative at the exit of the achromat $s = L$:

$$D_1(L) = \sqrt{\beta_x(L)} \left(\sin \psi_x(L) \int_0^L ds' P_1(s') \sqrt{\beta_x(s')} \cos \psi'_x - \cos \psi_x(L) \int_0^L ds' P_1(s') \sqrt{\beta_x(s')} \sin \psi'_x \right), \quad (32)$$

$$\begin{aligned} D_1'(L) = \frac{1}{\sqrt{\beta_x(L)}} & \left([\cos \psi_x(L) - \alpha_x(L) \sin \psi_x(L)] \int_0^L ds' P_1(s') \sqrt{\beta_x(s')} \cos \psi'_x \right. \\ & \left. + [\sin \psi_x(L) + \alpha_x(L) \cos \psi_x(L)] \int_0^L ds' P_1(s') \sqrt{\beta_x(s')} \sin \psi'_x \right), \end{aligned} \quad (33)$$

where $P_1(s)$ is the right-hand side of Eq. (6):

$$P_1(s) = K_x(1 - hD_o)D_o - h - K_{2x}D_o^2/2 + h^2D_o + h(D_o')^2/2. \quad (34)$$

First consider the matched dispersion $D_o = \eta$. Then $P_1(s)$ is a periodic function and as is shown below for the second-order achromat, it follows that both $D_1(L)$ and $D_1'(L)$ and, consequently, $T_1^{66}(L)$ and $T_2^{66}(L)$ vanish.

Next consider a dispersion function D_o with arbitrary initial conditions. Then, using Eq. (7), D_o can be represented as a sum of an η -function and a free oscillation function. Again it will be shown below that contribution to $D_1(L)$ and $D_1'(L)$ due to this oscillation also vanishes. Hence, the second-order double-chromatic matrix elements become zeros at the end of an achromat independently of the initial conditions for the dispersion function.

5. SECOND-ORDER ACHROMAT

We have shown that in order for the geometric matrix elements to vanish the derivatives of the generating function G must be equal to zero at the end of an achromat. Now we will find the conditions under which that is true.

The generating function $G(s)$ as well as its derivatives over canonical variables I_x, I_y, ϕ_x and ϕ_y are sums of the terms which are linearly independent. In order for the sum to be zero for all possible values

of these variables, each term separately must be zero. Considering a typical term of those sums the following conditions should be satisfied:

$$\int_0^L ds' F_{mn}(s') \exp(i[m\tilde{\psi}'_x + n\tilde{\psi}'_y]) = 0 \quad , \quad (35)$$

where F_{mn} are the complex amplitudes obtained from Eq. (22) and Table 1.

Equations $\xi_x = 0, \xi_y = 0$, Eq. (35) and the conditions that the tunes ν_x and ν_y for a whole achromat should be integers constitute the most general set of the necessary and sufficient conditions for a system to be a second-order achromat.

Consider now a particular case of an achromat built out of N identical cells of length l and tunes per cell ν_x^c and ν_y^c . As for any second-order achromat the total tunes $N\nu_x^c = \text{integer}$, $N\nu_y^c = \text{integer}$. Assume that values for K_{2x} and K_{2y} have been found such that chromaticities ξ_x and ξ_y in Eqs. (20) and (21) are equal to zero. We will show that in this case Eq. (35) is satisfied, provided that the unperturbed tunes ν_x^c and ν_y^c both avoid the following resonance values:

$$m\nu_x^c + n\nu_y^c \neq \text{integer} \quad , \quad (36)$$

where $m = 1, 2$ or 3 for $n = 0$, and $m = 0$ or 1 for $n = 2$ or -2 .

Indeed, let us assume first that functions F_{mn} contain the matched dispersion function η and consequently they all are periodic functions with the period l . Then each integral can be evaluated in the following way

$$\begin{aligned} & \int_0^L ds' F_{mn}(s') \exp(im\tilde{\psi}'_x + in\tilde{\psi}'_y) \\ &= \int_0^l ds' F_{mn}(s') \exp(im\tilde{\psi}'_x + in\tilde{\psi}'_y) \frac{1 - \exp[2\pi i N(m\nu_x^c + n\nu_y^c)]}{1 - \exp[2\pi i(m\nu_x^c + n\nu_y^c)]} \quad . \end{aligned} \quad (37)$$

The unperturbed tunes are used here since the chromaticities are equal to zero. Restrictions in Eq. (36) follow from here.

Now consider the case where the dispersion function D is not periodic. As we discussed earlier it can be expressed as a sum of a periodic function and a free oscillation function [see Eq. (7)]. Examining Table 1 we find that the coefficients containing D give rise to terms already made to vanish by the conditions in Eq. (36).

If, as is usual for an optical magnetic line, $\nu_x^c = \nu_y^c = \nu^c$, all the essential conditions in Eq. (36) are reduced to only one requirement $3\nu^c \neq \text{integer}$. In this case, condition (36) is equivalent to the statement that the number of cells in the second-order achromat should be more than 3 ($N \geq 4$). In this particular form the conditions for the second-order achromat were originally formulated by K. Brown [1].

CONCLUSIONS

Using a canonical perturbation theory we have developed a complete theory of the second-order achromat. The necessary and sufficient conditions for the existence of such a device are given. We have shown the reason why all the second-order geometric matrix elements are zeros simultaneously when these conditions are met. The second-order chromatic matrix elements were found explicitly. It was shown that the double-chromatic elements are zeros and that the single chromatic elements are proportional to corresponding chromaticities and consequently vanish when the chromaticities were made equal to zero. We have also shown that for a second-order achromat all the formulae for the second-order matrix elements which explicitly contain the dispersion function do not depend on the initial conditions for that function.

ACKNOWLEDGMENTS

Discussions with many people were illuminating and useful and are appreciated. In particular, we are grateful to K. Brown, S. Heifets, J. Jowett, L. Rivkin and H. Zyngier for their valuable comments and interest to the present work.

REFERENCES

1. K. L. Brown, *A Second-Order Magnetic Optical Achromat*, Report SLAC-PUB-2257, SLAC, Stanford University, February 1979; IEEE Trans. Nucl. Sci. NS-26 (3), p. 3490 (1979).
2. D. C. Carey, *Why a Second-Order Magnetic Optical Achromat Works*, Fermilab Pub. 79/61-Exp 2042; Nucl. Instr. Meth. **189**, 365 (1981).
3. A. N. Kolmogorov, *On Conservation of Conditionally-Periodic Motions of a Small Change in Hamilton's Function*, Dokl. Acad. Nauk SSSR **98**, 4, 525 (1954).
4. R. D. Ruth, Single Particle Dynamics and Nonlinear Resonances in Circular Accelerators in the book *Linear Dynamics Aspects of Particle Accelerators*, Proceed. of the Joint US-CERN School on Particle Accelerators, Sardinia, 1985, Springer Verlag, p. 37.
5. M. Bassetti, *A Simple Derivation of Chromaticity Formulae*, LEP Note 504, Report CERN, Geneva, Switzerland, 18 June 1985.
6. S. A. Kheifets, T. H. Fieguth and R. D. Ruth, *Canonical Description of a Second-Order Achromat*, SLAC Note AP-56, SLAC, Stanford University, October 1986.
7. F. Ch. Iselin, *The MAD Program (Methodical Accelerator Design) Reference Manual*, Report CERN-LEP-TH/85-15, Geneva, Switzerland, 1985.
8. J. M. Jowett, *Non-Linear Dissipative Phenomena in Electron Storage Rings*, *ibid.* 4, p. 343.
9. K. L. Brown et al., *TRANSPORT—a Computer Program for Designing Charged Particle Beam Transport Systems*, Report SLAC-91, Rev. 2, UC-28, SLAC, Stanford University, May 1977.
10. K. L. Brown, *A First- and Second-Order Matrix Theory for Design of Beam Transport Systems and Charged Particle Spectrometers*, Report SLAC-75, SLAC, Stanford University, June 1982.
11. J. Stoker, *Non-Linear Vibrations*, Interscience, 1950.
12. A. N. Kolmogorov, *On Conservation of Conditionally-Periodic Motions of a Small Change in Hamilton's Function*, Dokl. Acad. Nauk SSSR **98**, 4, 525 (1954).
13. T. O. Raubenheimer and R. D. Ruth, *Superconvergent Tracking*, SLAC-PUB-4370, Stanford University, July 1987, to be published.

APPENDIX I

CANONICAL PERTURBATION THEORY

In this Appendix we derive the generating function (22) used to solve the Hamilton's equations with an accuracy up to the second order in perturbation. The method was developed by Kolmogorov and is known as *canonical perturbation theory* [12].

We start with the Hamiltonian Eq. (10):

$$H_3(\vec{J}, \vec{\phi}, s) = H_0(\vec{J}, s) + V(\vec{J}, \vec{\phi}, s) \quad . \quad (A.1)$$

All vectors here and in what follows are two-dimensional, for example, $\vec{J} \equiv (J_x, J_y)$. The nonlinear perturbation $V(\vec{J}, \vec{\phi}, s)$ is periodic in angles $\vec{\phi}$ and has zero average over these angles. Our goal is to find canonically conjugate new variables such that the new Hamiltonian is a function of the new generalized momenta alone plus terms of order V^2 .

Consider a canonical transformation from the variables $(\vec{J}, \vec{\phi})$ to new variables $(\vec{I}, \vec{\Phi})$ with the generating function of the new momenta and the old coordinates

$$F(\vec{I}, \vec{\phi}, s) = \vec{\phi} \cdot \vec{I} + G(\vec{I}, \vec{\phi}, s) \quad . \quad (A.2)$$

The new coordinates are defined by $\vec{\Phi} = \vec{\phi} + G_{\vec{I}}, \vec{J} = \vec{I} + G_{\vec{\phi}}$ and the new Hamiltonian is

$$H_4 = H_0(\vec{I} + G_{\vec{\phi}}, s) + V(\vec{I} + G_{\vec{\phi}}, \vec{\phi}, s) + G_s \quad , \quad (A.3)$$

where a subscript indicate partial differentiation with respect to the subscript. Since for a small perturbation V , the function G is also small, we can expand H_4

$$H_4 = H_0(\vec{I}, s) + \vec{\Omega} \cdot G_{\vec{\phi}} + G_{\vec{\phi}} \cdot \vec{\Omega}_{\vec{I}} \cdot G_{\vec{\phi}}/2 + V(\vec{I}, \vec{\phi}, s) + V_{\vec{I}} \cdot G_{\vec{\phi}} + G_s \quad , \quad (A.4)$$

where the angular "frequencies" denoted by $d\vec{\psi}/ds \equiv \vec{\Omega}(\vec{I}, s) = H_{0,\vec{I}}$ may be functions of both the amplitude \vec{I} and the independent variable s .

By choosing a function $G(\vec{I}, \vec{\phi}, s)$ to satisfy the equation

$$\vec{\Omega}(\vec{I}, s) \cdot G_{\vec{\phi}} + V(\vec{I}, \vec{\phi}, s) + G_s = 0 \quad (A.5)$$

we can eliminate from the Hamiltonian all the terms of the order of V . The new momenta \vec{I} then will be integrals of motion with the accuracy V^2 .

Equation (A.5) for G is a first order differential equation, the solution of which can be found using the fact that all functions are periodic in angles. Substituting into the Fourier expansions

$$V(\vec{I}, \vec{\phi}, s) = \sum_{\vec{m}} v_{\vec{m}}(\vec{I}, s) \exp(i\vec{m} \cdot \vec{\phi}) \quad , \quad G(\vec{I}, \vec{\phi}, s) = \sum_{\vec{m}} g_{\vec{m}}(\vec{I}, s) \exp(i\vec{m} \cdot \vec{\phi}) \quad , \quad (A.6)$$

where the vector of integer coefficients $\vec{m} = (m_x, m_y)$ is introduced, we find a system of equations which are equivalent to Eq. (A.5):

$$(i\vec{m} \cdot \vec{\Omega}(s) + \frac{d}{ds})g_{\vec{m}} = -v_{\vec{m}} \quad . \quad (A.7)$$

Hence, the function G with the initial condition $G(\vec{I}, \vec{\phi}, 0) = 0$ is [6,13]

$$G = - \sum_{\vec{m}} \int_0^s ds' v_{\vec{m}}(\vec{I}, s') \exp\{i\vec{m} \cdot [\vec{\phi} + \vec{\psi}(s') - \vec{\psi}(s)]\} \quad , \quad (A.8)$$

where $\vec{\psi}(s') = \int_0^{s'} ds'' \vec{\Omega}(s'')$, $\vec{\psi}(s) = \int_0^s ds' \vec{\Omega}(s')$. That is, in fact, the expression (22) which was given in the text.

AN INTRODUCTION TO SAD

*Kohji Hirata**

CERN, Geneva, Switzerland

ABSTRACT

SAD (Strategic Accelerator Design) is a group of computer codes for beam dynamics being developed in KEK. The plan and the present status are reviewed.

1. INTRODUCTION

A group of Fortran codes called SAD is being developed by a KEK group whose present members are : K. Hirata, S. Kamada, K. Oide, N. Yamamoto and K. Yokoya. The principal aim of the code is to provide all the necessary information on beam dynamics that can be generated by computer for the 'Accelerator Improvement, Development and Study' group of TRISTAN. It is hoped that it will also be useful to design and operate other machines.

SAD is composed of several parts. In the final stage of the construction, the user can organize these parts freely so that he can establish his own strategy to design an accelerator.

In the next section, some characteristic parts of the code will be introduced which are now complete. The final section summarizes future plans.

2. SOME FEATURES OF SAD

2.1 Input format of lattice parameters

The input format of SAD is similar to that of MAD [1] but not identical. The user can either directly write the format on a data file used for the central computer or send the lattice parameters of the TRISTAN main ring from the minicomputers used for control and operation.

He can also send the results of SAD to the minicomputers.

2.2 Calculation of equilibrium emittances

For electron machines, emittance calculation is important. We calculate these by taking only linear elements into account. Otherwise the meaning of these becomes ambiguous.

*) On leave from KEK, Ibaraki-ken, Japan.

We track the changes of standard deviations σ_{ij} (i and j stand for coordinates and angles) through each element around one turn : σ_{ij} is influenced by linear forces from magnets and cavities and also by synchrotron radiation. We decide emittances by finding the solution of $\sigma'_{ij} = \sigma_{ij}$, where σ'_{ij} is σ_{ij} after one turn. Consequently, our 'emittances' vary slightly around the ring. This is natural because we cannot, in general, diagonalize the diffusion and damping terms simultaneously in the linear difference equations describing the changes of σ_{ij} .

2.3 Coordinate system

The choice of the coordinate system becomes delicate when the accelerator is not planar. We employ a special system proposed by K. Yokoya [2] which is based on the parallel transport of the reference frame along the design orbit. This gives a locally defined coordinate system to each point on the ring. We start by defining x and y coordinates at one point in the ring and transport them parallel to the design orbit (see Fig. 1).

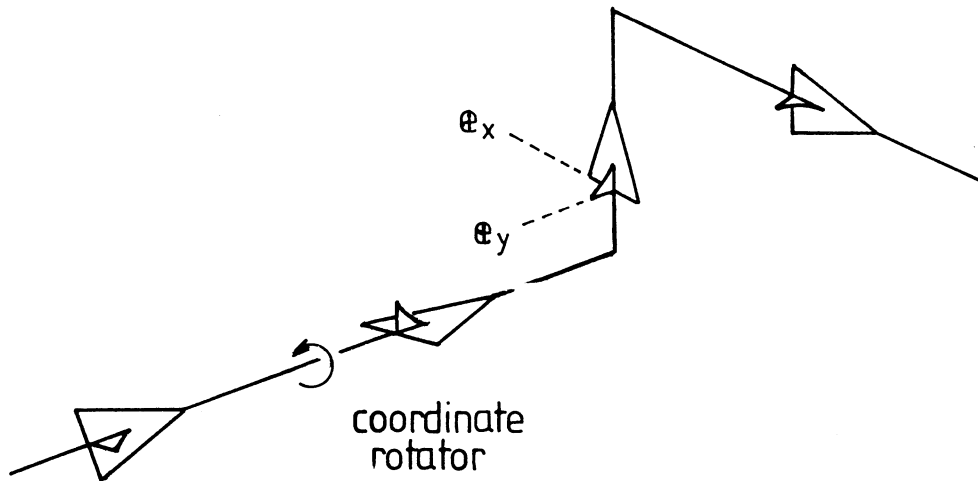


Fig. 1 Accelerator coordinates

This is nothing but what is implicitly assumed in, for example, alignment of elements. It also simplifies the equations of motion. One bad thing is that the system is defined only locally; after one turn, the x and y axes do not necessarily return to the original direction but in general rotate around the design orbit by some angle. This is determined by the curvature of the design orbit. This is, however, intrinsic to the non-planar design orbit. This coordinate system is very similar to that for the twisted torus which is one of the simplest, non-trivial fibre bundles [3].

2.4 Canonical perturbation

For a particle with small amplitude, perturbation provides enough information. Recently, a new formulation based on the Lie algebra was proposed⁴⁾. It is not only conceptually transparent but also suitable for computer calculation.

SAD uses it, for example, to give tunes as functions of action variables. The user can choose the degrees of freedom as follows:

- a) 2, for transverse dynamics
- b) 3, with longitudinal oscillation
- c) 2.5, for transverse with energy deviation as a parameter.

The tunes are expressed as functions of a) J_x and J_y , b) J_x , J_y and J_z and c) J_x , J_y and E , where J 's are the action variables and E is the energy deviation from the nominal value.

At present, SAD gives perturbation results up to 6th power of canonical variables. The highest order is limited by a table of Campbell-Baker-Hausdorff formula. It is easy and straightforward to extend the highest order if necessary.

2.5 Polarization calculation

The degree of equilibrium polarization in electron storage rings is much influenced by non-linear elements. Multiparticle tracking is not helpful enough in this case because of long damping times.

Recently, K. Yokoya found a systematic and analytical method⁵⁾ using Lie algebra, which SAD utilizes.

At present, SAD can predict the degree of polarization only when closed orbit is absent. This will soon be improved.

2.6 Particle tracking

SAD tracks particles in 2, 3 and 2.5 dimensions (see section 2.4), giving Poincaré plots, Fourier analysis and so on.

One useful point is that the Poincaré plots and Fourier analysis can be done in terms of the action-angle variables obtained by the perturbation calculation. By this, we can see whether or not the perturbation works well in certain regions of phase space and we can, to some extent, distinguish real chaos from seemingly chaotic behaviour coming from a projection of phase space on a plane.

The code is already vectorized so that it is easy to extend it to multi-particle tracking for electron rings (with damping and diffusion) by a vector computer.

2.7 Final focussing system design

SAD has subsidiary codes for designing the final focus system for linear colliders. The algorithm is based on a multi-dimensional Newton-Raphson method.

The variables are length of straight sections and strengths of quadrupole and sextupole magnets. It is possible to set several constraints for fitting.

It can also be used for a linear matching of a periodic structure (ring), although a more general matching code is planned.

3. PLANS FOR THE FUTURE

We will soon install codes for a general purpose linear matching and chromaticity correction by an iteration method. Radiation damping and sinusoidal deflection will be taken into account in the tracking code for the modelling of a tune measurement system in electron rings.

Following installation of these codes, a supervising code or a demand format will be established by which users can organize several parts of SAD along his own tactics. These subsets of SAD will be called TAD (Tactical Accelerator Design). For example, he can use, in his TAD, a feedback do-loop containing the linear matching and the perturbation to find a good operating point.

A more extended and detailed report will soon be available.

The author would like to thank all the members of the LEP Theory Group for their hospitality. In particular, Dr. J. Spencer is acknowledged for his help and advice in the preparation of this manuscript.

REFERENCES

1. F.C. Iselin, E. Keil, J. Niederer and J.M. Veuillen, 'The MAD Program, CERN/LEP-TH/87-60.
2. K. Yokoya, 'Beam Polarization in High Energy Electron Storage Rings', KEK Internal Report 85-7, 1985.
3. For example, N.E. Steenrod, 'The Topology of Fibre Bundles', Princeton Univ. Press, 1951.
4. E. Forest, Lie Algebraic Maps and Invariants produced by Tracking Codes, SSC-78 (July 1986).
5. K. Yokoya, Nucl. Instr. Meth. A 258 (1987) 149.

CALCULATIONS OF THE PARTICLE DYNAMICS IN ACCELERATORS BEYOND THE USUAL PERTURBATION TECHNIQUES

(Notes and References)

H. Mais

Deutsches Elektronen-Synchrotron (DESY), Hamburg, Federal Republic of Germany

The main purpose of this brief communication is to make some comments on the particle motion in the strongly nonlinear (chaotic) region of phase space and to give a list of references which - although far from being complete - can be helpful for investigating this problem.

Because of the presence of various nonlinear fields (higher order multipole fields caused by magnet errors, nonlinear cavity fields, nonlinear fields of the beam-beam interaction) a proton storage ring acts as a nonlinear device (see Fig. 1):

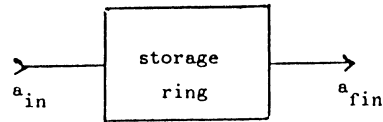


Fig. 1

a_{in} is some initial amplitude (which may be a combination of transverse and longitudinal coordinates) and a_{fin} is the amplitude after N ($\sim 10^8$ - 10^{10}) revolutions in the storage ring. Mathematically the accelerator is modelled by a nonlinear (nonintegrable) Hamiltonian

$$H = H_0(\underline{I}) + \varepsilon H_1(\underline{\theta}, \underline{I}, s)$$

with explicit time- (s -) dependence. H_0 is the integrable part, $\underline{I} = (I_1, I_2, I_3)$ are the action variables, $\underline{\theta} = (\theta_1, \theta_2, \theta_3)$ are the angle variables and εH_1 is a small perturbation.

According to a_{in} one can try to define different zones (see Fig. 2)

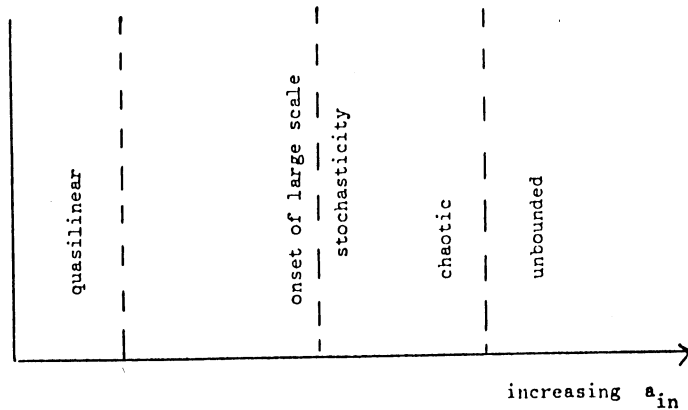


Fig. 2

For small amplitudes the storage ring behaves more or less like a linear element (at least for the time scales of interest i.e. 10-20 hours storage time) whereas for larger amplitudes the behaviour becomes more and more nonlinear (chaotic i.e. sensitively dependent on the initial conditions) and eventually unbounded (especially in the case of multipole nonlinearities). The main problem of accelerator dynamics is to make quantitative and reliable predictions of these different zones, or stated physically - to calculate quantities like the linear aperture and the dynamic aperture.

For this purpose various approximation schemes have been developed:

In the linear region perturbation methods are widely used (see G. Guignard's contribution to this workshop for a critical review).

The onset of large scale stochasticity can be calculated using for example Chirikov's resonance overlap criterion [1], [2], Greene's residue criterion [3], renormalization group methods [4], [5], [6] or finally a criterion derived in the framework of the direct integration of the Hamilton-Jacobi equation [7]. For two-dimensional nonlinear maps (i.e. one-dimensional nonautonomous Hamiltonians) these methods have been extensively used and compared with numerical simulations. However, in higher dimensions only the methods of Chirikov and Warnock and Ruth [7] are applicable and a systematic study and comparison with tracking is still missing, at least to the author's knowledge.

The situation is even more complex, if one wants to describe the particle motion in the chaotic region of phase space. On the other hand such a description could be extremely valuable as a supplementary information to the perturbation calculations valid only for small nonlinear perturbing terms.

For two-dimensional nonlinear (symplectic or area-preserving) mappings the break-up of invariant KAM tori and the particle motion across these broken barriers in phase space is well studied. Using transport-type theories and diffusion models one can calculate escape rates, see for example [6], [8], [9], [10], [11], [12], [13].

In the higher-dimensional case (four- and higher-dimensional nonlinear (symplectic) mappings) the situation is not so clear. Although there is common belief that there are also extended chaotic regions in phase space and that invariant tori break at certain

critical values of the perturbation strength ($\sim a_{in}$), there are some subtleties which are characteristic for this case.

First of all there is Arnold diffusion called after V. I. Arnold who first studied this phenomenon. Arnold diffusion is universal in that there is no critical perturbation strength for its presence (like a threshold-value for the breaking of KAM tori) although the diffusion rate vanishes with vanishing perturbation. There are a number of investigations of this phenomenon, see for example chapter six of the monograph of Lichtenberg and Lieberman [13], and [14], [15], [16], [17], [18], [20], [21] where further references can be found. Recently Arnold diffusion (sometimes also called thin layer diffusion [16]) has been studied by Marsden and Holmes [19] using Melnikov's method for pendulum-type Hamiltonians.

Although Arnold diffusion is usually associated with nonoverlapping resonances, it can be regarded as belonging to a larger class of phenomena with overlapping resonances which strongly enhance the rate of diffusion (sometimes called thick layer diffusion [16]). A particular example of diffusion along layers of overlapping resonances is that of modulational diffusion caused by a slow modulation of the driving perturbation, see for example [13], [16], [21], [22], [23]. Additional complicating effects like external noise can also be included [13].

Thus, summarizing one can say that diffusion models can be helpful in describing at least approximately the particle motion in the strongly nonlinear (chaotic) region of phase space. These models have been used for a variety of physical systems.

The aim of this contribution is not to provide new and final results but to stimulate future studies of the particle dynamics in accelerators concentrating on the chaotic regime of phase space (see also the contribution of S. Heifets to this workshop). These investigations can give supplementary information to the usual perturbation methods, which are valid only for small perturbation strengths.

Acknowledgement

The author wants to thank the organizers of this workshop, especially Dr. E. Keil, for a pleasant and interesting week in Lugano.

References

- [1] B.V. Chirikov
"A universal instability of many-dimensional oscillator systems"
Phys. Rep. 52, 263 (1979)

- [2] M. Tabor
"The onset of chaotic motion in dynamical systems"
Advances in Chemical Physics Vol. XLVI, p. 73 (1981)

- [3] J.M. Greene
"A method for determining a stochastic transition"
J. Math. Phys. 20, 1183 (1979)

- [4] D.F. Escande
"Dynamique Hamiltonienne" in "Structures et Instabilités"
Editeur Scientifique: C. Godrèche, 1985

- [5] D.F. Escande
"Stochasticity in classical Hamiltonian systems: universal aspects"
Phys. Rep. 121, 165 (1985)

- [6] R.S. MacKay
"Transition to chaos for area-preserving maps" in "Nonlinear Dynamics Aspects of Particle Accelerators"
Proc. Sardinia 1985 eds. J.M. Jowett, M. Month, S. Turner
Lecture Notes in Physics Vol. 247, Springer Verlag

- [7] R.L. Warnock, R.D. Ruth
"Invariant tori through direct solution of the Hamilton-Jacobi equation"
Physica 26D, 1 (1987)

- [8] L.P. Kadanoff
"From periodic motion to unbounded chaos: investigations of the simple pendulum"
Physica Scripta T9, 5 (1985)

- [9] D. Bensimon, L.P. Kadanoff
"Extended chaos and disappearance of KAM trajectories"
Physica 13D, 82 (1984)

- [10] S.J. Shenker, L.P. Kadanoff
"Critical behavior of a KAM surface: I. Empirical results"
J. Statist. Phys. 27, 631 (1982)

- [11] R.S. MacKay, J.D. Meiss, I.C. Percival
"Transport in Hamiltonian systems"
Physica 13D, 55 (1984)

- [12] J.D. Meiss
"Transport near the onset of stochasticity"
Part. Accel. 19, 9 (1986)

- [13] A.J. Lichtenberg, M.A. Lieberman
"Regular and Stochastic Motion"
Springer Verlag, 1983

- [14] M.A. Lieberman
"Many-dimensional Hamiltonian systems" in Proc.
US Summer School on High-Energy Particle Accelerators
AIP Conf Proc. Vol 153

- [15] G. Benettin, L. Galgani, A. Giorgilli
"Boltzmann's ultraviolet cutoff and Nekhoroshev's theorem on Arnold diffusion"
Nature 311, 444 (1984)

- [16] F. Vivaldi
"Weak instabilities in many-dimensional Hamiltonian systems"
Rev. Mod. Phys. 56, 737 (1984)

- [17] F.A. Salam, J.E. Marsden, P.P. Varaiya
"Chaos and Arnold diffusion in dynamical systems"
IEEE Trans. Circ. Syst. CAS-30, 697 (1983)

- [18] K. Kaneko, R.J. Bagley
"Arnold diffusion, ergodicity and intermittency in a coupled
standard mapping"
Phys. Lett. 110A, 435 (1985)

- [19] P.J. Holmes, J.E. Marsden
"Melnikov's method and Arnold diffusion for perturbations of
integrable Hamiltonian systems"
J. Math. Phys. 23, 669 (1982)

- [20] A.J. Lichtenberg
"Techniques of resonance analysis"
Part. Accel. 19, 197 (1986)

- [21] M.A. Lieberman
"Arnold diffusion in Hamiltonian systems with three degrees
of freedom" in "Nonlinear Dynamics" ed. R.H.G. Helleman,
New York Acad. Sci. Vol. 357 (1980)

- [22] B.V. Chirikov, M.A. Lieberman, D.L. Shepelyansky,
F.M. Vivaldi
"A theory of modulational diffusion"
Physica 14D, 289 (1985)

- [23] J. Tennyson
"The dynamics of the beam-beam interaction" in "Physics of
High Energy Particle Accelerators"
AIP Conf. Proc. Vol 87, 1982

ASYMPTOTIC PROPERTIES OF BIRKHOFF NORMAL FORMS

A. Bazzani

CERN, Geneva, Switzerland

Istituto Nazionale di Fisica Nucleare – Sezione di Padova, Italy

G. Turchetti

CERN, Geneva, Switzerland

Istituto Nazionale di Fisica Nucleare – Sezione di Bologna, Italy

Introduction. In the study of nonlinear effects in hadronic accelerators the use of normal forms has been recently proposed ^[1,2] as a promising alternative to the standard tracking methods. Analytical progress has been made which ^[3], combined with the algorithmic approach to the polynomial algebra ^[4,5,6], allows high perturbation orders to be reached and numerical estimates on the remainders to be obtained ^[7,8,9].

The Birkhoff series for the normal forms are known to diverge from the KAM theory; however they are also expected to exhibit an asymptotic character already since Poincaré. For the hamiltonian flows a rigorous estimate, leading to the exponential stability time of the Nekhoroshev's theorem ^[10], was recently given ^[11,12] providing accurate estimates in celestial mechanics ^[13]. For the area preserving maps numerical evidence of an asymptotic behavior was obtained and a theoretical explanation was given ^[7]. The numerical investigation of higher dimensional symplectic maps and the related analytical bounds on the remainders are in progress ^[8].

Hamiltonian flows. We consider the autonomous hamiltonian of anharmonic oscillators

$$h = \sum_{k=1}^d \omega_k (x_k^2 + p_k^2) + V(x, p) \quad (1)$$

Introducing the action-angle variables and a scaling parameter

$$x_k = \epsilon \sqrt{j_k} \sin \theta_k \quad p_k = \epsilon \sqrt{j_k} \cos \theta_k \quad h = \epsilon^2 H \quad (2)$$

one has

$$H(j, \theta; \epsilon) = \omega \cdot j + \epsilon V(j, \theta; \epsilon) \quad (3)$$

We consider the canonical transformation $(j, \theta) = \mathcal{C}(J, \Theta; \epsilon)$ to normal coordinates, \mathcal{C} being a polynomial map of order N in ϵ such that

$$H(\mathcal{C}(J, \Theta; \epsilon); \epsilon) = \sum_{m=0}^N \epsilon^m \hat{H}_m + \epsilon^{N+1} R_N(J, \Theta; \epsilon) \quad (4)$$

The last equation is solved recursively up to order N in ϵ and R_N denotes the remainder. The equations of motion then read

$$\frac{dJ}{dt} = \epsilon^{N+1} \frac{\partial R_N}{\partial \Theta} \quad (5)$$

If we assume $||\partial R_N/\partial\Theta|| < M_N$, a constant depending only on N , in some disk ($|J| < \rho$) then the variation of the action J is bounded by

$$|J(t) - J(0)| < M_N \epsilon^{(N+1)} t < \epsilon \sigma \quad (\epsilon \sigma < \rho) \quad (6)$$

for times not exceeding some $T_N(\epsilon)$

$$t < T_N(\epsilon) = \frac{\sigma}{M_N \epsilon^N} \quad (|J(0)| < \rho - \epsilon \sigma) \quad (7)$$

If one had $M_N = AB^N$ with $\epsilon < B^{-1}$, then $T_N(\epsilon) \rightarrow \infty$ as $N \rightarrow \infty$ and a convergence and stability condition would be achieved contradicting KAM theory. On the contrary it was proved that

$$M_N = A(BN)^{N\beta} \quad (8)$$

and consequently the error $E_N(\epsilon) = \epsilon^N M_N$, which gives the variation of the action for $t \sim 1/\epsilon$, diverges for any $\epsilon > 0$ when $N \rightarrow \infty$. However for fixed ϵ we can compute the value $N_{\text{opt}}(\epsilon)$ of N which minimizes the error

$$N_{\text{opt}}(\epsilon) = \frac{1}{\epsilon B \epsilon^{1/\beta}} \quad (9)$$

and the corresponding optimal error $E_{\text{opt}}(\epsilon)$ which reads

$$E_{\text{opt}}(\epsilon) = E_{N_{\text{opt}}(\epsilon)} = A \exp \left(- \left(\frac{\beta}{\epsilon B} \right) \epsilon^{-1/\beta} \right) \quad (10)$$

As a consequence the largest stability time $T_{\text{opt}}(\epsilon) = 1/E_{\text{opt}}(\epsilon)$ is exponentially large with exponent $\propto \epsilon^{-1/\beta}$. It is interesting to observe that a remarkable scaling law follows from the previous relations, independently of all the constants, except β , whose accurate computation is quite difficult. Assuming for simplicity $\beta = 1$ we have

$$\epsilon \rightarrow \epsilon/2 \implies T_{\text{opt}}(\epsilon) \rightarrow (T_{\text{opt}}(\epsilon))^2 \quad (11)$$

Hamiltonian maps. We consider hamiltonian symplectic maps of \mathbf{R}^{2d} which, letting $x_k + ip_k = \epsilon_k z_k$ so that $z_k = i\sqrt{j_k} e^{-i\theta_k}$, explicitly read

$$z' = F(z, z^*) = \epsilon^{i\omega} (z + \epsilon f_2(z, z^*) + \dots) \quad (12)$$

Letting

$$z = \Phi(Z, Z^*) = Z + \epsilon \Phi_2(Z, Z^*) + \dots + \epsilon^N \Phi_{N+1}(Z, Z^*) \quad (13)$$

be a symplectic transformation, close to the identity (where Φ_n are homogeneous polynomials of degree n in Z and Z^*), we consider the equation

$$\Phi^{-1} \circ F \circ \Phi = \epsilon^{i\Omega(ZZ^*)} [Z + \epsilon^{N+1} R_N(Z, Z^*)] \quad (14)$$

where Ω is also of degree $\leq N + 1$ and together with Φ is recursively determined. After t iterations equation (14) reads

$$\Phi^{-1} \circ F^t \circ \Phi = e^{it\Omega(ZZ^*)} \left[Z + \epsilon^{N+1} R_N^{(t)}(Z, Z^*) \right] \quad (15)$$

and supposing $\|R_N\| < M_N$ one has $\|R_N^{(t)}\| \leq t M_N$. If F is only an order N symplectic truncation, the normal form does not change up to the same order. Even though no result is yet available on M_N as for the flows, a strong evidence was obtained for its behaviour to be still given by (8).

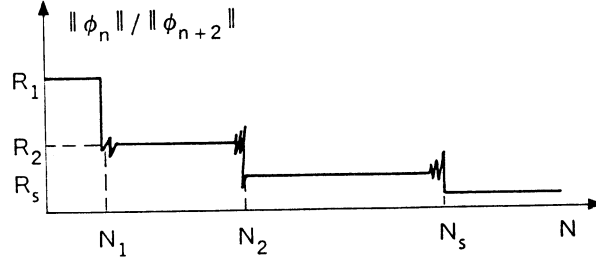
Letting M_s/N_s the sequence of leading resonances to $\omega/2\pi$, given by the continued fraction expansion when $\omega/2\pi$ is a quadratic irrational number, we have the estimates $|\omega/2\pi - M_s/N_s| \leq N_s^{-2}$. If we denote with r_s the value of ϵ for which the resonance N_s occurs

$$\Omega(r_s^2) = \omega + \Omega_2 r_s^2 + \dots = 2\pi \frac{M_s}{N_s} \implies r_s \simeq \frac{1}{|\Omega_2|^{1/2} N_s} \quad (16)$$

we find that the series $\|\Phi_n\|$ (where $\|\cdot\|$ denotes the L^2 average over the angles) satisfies the condition

$$\frac{\|\Phi_n\|}{\|\Phi_{n+2}\|} = r_s^2 \quad N_s < n < N_{s+1} \quad (17)$$

which can be explained observing that the leading divisor is $|1 - e^{i\omega N_s}|^{-1} \simeq N_s^2 \simeq r_s^{-2}$. This implies that the series $\|\Phi_n\|$ behaves as a geometric series whose convergence radii r_s tend to zero as s is increased to infinity as shown by figure :



As a consequence we have the following estimate

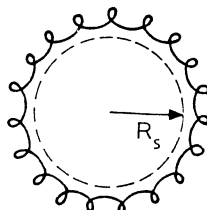
$$\|\Phi_{N_s}\| \sim \left(\frac{1}{r_1}\right)^{N_2 - N_1} \dots \left(\frac{1}{r_s}\right)^{N_{s+1} - N_s} \dots \simeq (BN_s)^{\beta N_s} \quad (18)$$

when $\omega/(2\pi) = (\sqrt{p^2 + 4} + p)/2$ is a quadratic irrational (p an integer), taking into account eq. (16) and $N_{s+1} \sim N_s \omega/(2\pi)$; it turns out that $\beta = [1 - (\omega/(2\pi))^{-1}]/\log(\omega/(2\pi))$. Since R_{N_s} is essentially $\|\Phi_{N_s+2}\|$ the estimate (8) for M_N follows.

If we stay within a disc $\epsilon \leq r_s$ the series behaves as a geometric series of radius r_s for $N_s < N < N_{s+1}$, but its convergent behaviour persists until considerably higher orders. Indeed if we fix $\epsilon = r_s$ the optimum value of the truncation is obtained for

$$N_{\text{opt}}(\epsilon) \sim \frac{|\Omega_2|^{1/2}}{\epsilon \beta} N_s^{1/\beta} \quad (19)$$

For $N > N_s$ if we increase ϵ sufficiently beyond r_s the divergent behaviour due to the resonance N_s , will appear in a dramatic way: indeed the image of a circle will become a curve with N_s loops and the 1-to-1 correspondence will be lost, as shown by figure .



Acknowledgments

We are grateful for the hospitality at the SPS division of CERN.

* * *

REFERENCES

- [1] A.Bazzani,P.Mazzanti,G.Servizi,G.Turchetti: *LHC note 66* – CERN SPS **88** 2 (1988)
- [2] E.Forrest: “*Hamiltonian-free perturbation theory*” – SSC -111preprint (1987)
- [3] A.Bazzani: “*Normal forms for symplectic maps in \mathbf{R}^{2n}* ” – Celestial Mechanics to be published (1987)
- [4] A.Bazzani,G.Servizi,G.Turchetti: “*POLYN: a program for algorithmic manipulation of polynomials*” – in preparation (1988)
- [5] A.Bazzani,G.Servizi,G.Turchetti: “*BIRKH: a program for computing the Birkhoff normal forms for symplectic maps of \mathbf{R}^{2n}* ” – in preparation (1988)
- [6] G.Servizi,G.Turchetti: – Computer Physic Communication **32** 201 (1984)
- [7] G. Servizi,G. Turchetti: – nuovo Cimento **95B** 121 (1986)
- [8] A.Bazzani, W. Scandale, G. Servizi, G.Turchetti : “*Description of nonlinear beam dynamics in the CERN Large Hadron Collider by using normal form alorithms*” – contribution to EPAC Conference **LP123** (1988)
- [9] G. Turchetti: “*Perturbative methods for hamiltonian maps*” – Proceedings of the Summer School of Medellin 1986 Ed by W.A. Saenz, World Scientific (1988)
- [10] N.N. Nekhoroshev: – Russ. Math. Surveys **32N6** 1 (1977)
- [11] G.Benettin, G. Gallavotti: – Journ. Stat. Phys. **44** 293 (1986)
- [12] A.Giorgilli L. Galgani: – Journ. Celestial Mechanics **37** 95 (1985)
- [13] A.Giorgilli et al. : – Dep. of Physics of Milano preprint (1988)

COMMENT ON SOME ANALYTICAL METHODS TRYING TO APPROACH THE LIMIT OF STABILITY FROM BELOW

G. Guignard

CERN, Geneva, Switzerland

ABSTRACT

In a tentative to clarify some of the questions raised during the discussion, we try to make comments on different analytical methods dealing with amplitude limitations. All the methods considered here approach the limit of stability from below, i.e. from the side where the motion is still stable because the initial amplitude is not yet too large. A summary description of these methods is given in the paper on the Overview of the Methods to Define Conditions for Bounded Motion, published in these proceedings, and the reader should refer to it.

The approach consisting in using a smooth model of the accelerator based on the averaging of the focusing and sextupole strength offers the advantage of dealing with autonomous system and Henon-Heiles potential. The stability of this potential written for two degrees of freedom has indeed been studied analytically by considering linearised motion around a trajectory. A simple criterion was derived from the fact that the real part of the eigenvalues of the Jacobian matrix must remain negative. In this way, a limit in amplitude for the stability can be deduced, but the quality of the approximation strongly depends on the necessity to average the forces and to a lesser extent on the method used to calculate this average. Obviously, the losses of aperture associated with isolated resonances at precise phase-advance values are not reproduced by this model, and between strong resonances the analytical approximation is likely optimistic since the stability limit can only be decreased by resonance effects. Nevertheless, the method gives an envelope for this limit as a function of the phase advance per superperiod.

Perturbation theory in the Hamiltonian formalism has been frequently used in order to study the effects of two-dimensional nonlinearities in accelerators. The Poincaré-von Zeipel-Moser procedure to first and second order was indeed extensively applied to field components. To first order it allows to analyse multipole effects near specific resonances, derive expressions for the invariants in their neighbourhood and define the bandwidths so often used to characterize the perturbation. To second order, this procedure makes it possible to quantify some of the effects associated with the presence of sextupoles; integrals can indeed be written for computing the strengths of the associated octupole terms, the tune shifts with the amplitude, the variations of the Twiss parameters with the momentum deviation and the distortions of the invariants in a wider range of values for the phase advances. This of course means that these analytical expressions can also be used to minimize adverse effects of sextupoles. The approximation obtained for the invariants is valuable provided the distortions characterized by $\Delta I/J$ do not become too large (< 0.5).

Pushing this approach to its limit of validity, a rough estimate of the initial amplitude at which the stability limit is possibly reached comes out from the condition $\Delta I(x_0) \approx J$. To improve the validity of the criterion and the description of the tori the procedure can in principle be applied to higher orders. In practice however, it is difficult to go above the second order, since the canonical transformation uses a mixed set of variables and consequently the equations of the orbits are implicit. Concerning the convergence of the procedure, a mathematical proof exists for very small perturbation, but the actual convergence goes beyond the value proven mathematically. The other procedure interesting to consider is based on Deprit's algorithm and Lie transforms. It has the advantage to use a canonical set of variables and to give explicit expressions for the generating function as well as the orbits. The procedure can therefore be applied conveniently up to high orders and examples of applications including order six exist. The problem of the convergence of this procedure is similar to the one mentioned above and the approach has not been used to speculate on the amplitude limits at which the motion becomes unbounded. With both the procedures, the results may depend on the characteristics of the linear optics, like the tunes.

The direct solution of the two-dimensional Hamilton-Jacobi equation brings the advantage of avoiding to work order by order, as with perturbation theory. It makes it possible to look for the singularities of the implicit equations defining the orbits and the condition for these singularities to occur seems related to the residue criterion associated with Greene's conjectures. Orbit singularities are of course connected with motion instability and the results of the method can be used to estimate the stability limits as well as other properties such as the tune shifts. Because this technique is based on the analysis in Fourier series of the generating function, difficulties are associated with the truncation to a finite number of modes for numerical calculations. In particular, the convergence near the stability limit depends critically on this number. This approach opens the possibility of new developments. The Fourier analysis on the independent variable can be replaced by a shooting method forcing the solution to be closed over one turn. In the presence of one degree of freedom, this new method ensures convergence very close to dynamic aperture, with plain iteration for mildly nonlinear systems and with Newton's method for strongly nonlinear systems. With two degrees of freedom, plain iteration gives good solutions at modest amplitudes and the authors are yet working on making Newton's method successful for strongly nonlinear systems.

The residue criterion is based on the calculation of the residue $R = [2 - \text{Tr}(M)]/4$ associated with the one-dimensional tangent map M . Numerical results of detailed studies upon the stability of the standard and quadratic maps brought up the Greene conjecture; the invariant tori break up when the value of R tends towards 0.25 and this corresponds to an instability. This criterion can directly be applied to one-dimensional transverse motion around stable fixed points and to synchrotron motion inside stationary buckets. The first application gives a possible criterion for the onset of chaos corresponding approximately to resonance overlap while the second application allows to estimate the longitudinal dynamic aperture associated with different frequencies, in particular the most irrational one called golden number. However, for more general two-dimensional maps, the application

of the method is not evident. It is for instance not obvious how to use this criterion for a system as complicated as an accelerator structure containing sextupoles and/or perhaps other multipoles, and to deduce from it an analytic expression for the limit in amplitude.

Perturbation treatments by iterations on the equations of motion have recently been studied for the particular case of an accelerator structure containing only sextupoles as nonlinear elements. Successive linearisation was applied to the one-dimensional system associated with the horizontal betatron motion. Even if the analytical developments become cumbersome after two linearisations, the method is interesting since it converges rapidly at each iteration which contains contributions of all orders in the perturbation. Furthermore, the linearisation makes it possible to bring back the nonlinear equation of motion to Hill's equation, and hence to apply the well-known condition on the trace of the associated matrix. However, there exists no proof of the convergence of these iterations and difficulties are associated with the appearance of non-physical parametric resonances when the average of the function describing the nonlinear sextupole fields is different from zero. This arte fact restricts the range of values of the linear-optics parameters inside which the method can actually be used. It has also to be noted that the successive linearisation method has not yet been generalised to magnetic elements other than sextupoles and that the extension to two-dimensional systems remains to be done.

Another method is based on the expansion of the solution for the motion as a power series of the parameter ϵ which serves the control of the perturbation. For each function of this series, it is possible to write an inhomogeneous linear differential equation which contains a superposition of trigonometric functions. Each equation contains one free frequency-parameter which can be used to eliminate secular terms. Explicit solutions can then in principle be written for the amplitudes at each step of the iteration. In this approach, the shift in frequency from the linear value, resulting from the nonlinear terms in the equation of motion, is taken into account. Criteria are then applied to determine approximately when the solution is unbounded. On the one hand, if the action becomes negative the iterations cannot converge to the exact solution and the motion becomes chaotic with high probability. This makes it possible to deduce a first criterion to be satisfied by looking for a zero of the action I after restricting the perturbation to first order only. On the other hand, if the first criterion does not make sense because the convergence is not satisfied to first order, the condition for bounded motion implies that I must never become infinite. This allows to find out a limit for the initial amplitude up to which the solution converges while pushing the perturbation to second order. These criteria give a closed expression of the limiting amplitude as a function of the important machine parameters. This expression is so complicated that it has to be calculated numerically, but it nevertheless leads to reasonable approximate estimation of the dynamic aperture for systems as complex as the LEP collider. It has to be noted that the conjecture that the convergence breakdown of the perturbation series always agrees with the onset of chaos could not be proven rigorously up to now. If this method has been extended for two-dimensional systems, the generalisation to nonlinear elements other than sextupoles does not yet exist.

BEAM DYNAMICS AND TRACKING

S.A. Heifets

Continuous Electron Beam Accelerator Facility, Newport News, Virginia, USA

ABSTRACT

The study of beam dynamics in a storage ring is described as a multistep process with emphasis on optimization of the long term tracking.

Analysis of the stability of particles in a storage ring includes several steps.

1. Rough analysis of the structure of series of a perturbation theory shows^[1], that there is a dimensional parameter of expansion λ_k

$$\lambda_k \approx b_k A^{k-1} \beta \quad (1)$$

where b_k is the k -th multipole coefficient ($k=2$ for sextupole), A is the amplitude of betatron oscillations, and β is the average β -function. (More detailed analysis gives an additional factor which depends on whether the multipoles are random or systematic, and on their distribution along the ring). This parameter defines the order of magnitude of the main nonlinear effects driven by the nonlinearity λ_k : width of nonlinear resonances, tune shift, the geometric aberrations, etc.

The stable motion can be expected (but not necessarily exists) only within the dynamic aperture, which can be roughly estimated from the condition $\lambda_k \approx 1$. For the SSC, for a multipole with a unit strength $b_k \approx 10^{-4} \text{cm}^{-k}$ and $\beta = 300 \text{m}$, the parameter $\lambda_k = 1$ for the amplitude $A = 3 \text{mm}$. Obviously, the perturbation theory is not applicable for amplitudes/nonlinearities for which $\lambda_k > 1$. That cannot be improved by any modification of a perturbation theory, because for amplitudes $\lambda_k > 1$, stochastic motion is typical. It means that for such amplitudes most of the KAM invariant tori are destroyed and most of the trajectories behave randomly. The study of the beam dynamics, therefore, makes sense only for amplitudes where $\lambda_k < 1$, which corresponds to the concepts of the dynamic aperture in the SSC design report.^[2]

2. For the part of phase space where $\lambda_k < 1$, there is hierarchy of the resonances: the widths of the higher-order resonances which appear in the n -th order of perturbation theory, are proportional to λ_k^n , and go down exponentially with n as $\exp(-n \ln 1/\lambda_k)$. Because the number of resonances increases with n only as n^2 , the resonances of any order do not overlap as far as there is no overlapping of the separatrices of the resonances of the first order of perturbation theory. According to Chirikov criterion, it means that most of the KAM tori are preserved, and the typical trajectory corresponds to quasiperiodic motion.

For the linear aperture^[2], where $\lambda_k \ll 1$, say $\lambda_k \approx 0.1$, the beam dynamics is dominated by low-order resonances and can be analyzed with a perturbation theory. It is easy to give the analytic expressions for the tune shift of the first and second order of a perturbation theory, the width of the resonances and geometric aberrations in this case, and they can be found elsewhere. The corresponding formulas, obtained by the method of canonical transformation, for example, are given in.^[3] The magnitude of the nonlinear effects depends on the details of the lattice functions and character of the nonlinearities in the ring. The use of these formulas requires, of course, some numeric analysis. The exact size of the dynamic aperture may also be found by the short-term tracking, which usually means several hundred turns. Needless to say, all nonlinearities have to be analyzed together to take into account the cross-talk between them.

3. The beam dynamics for most interesting small amplitudes can be studied in particular with the Green-MacKay residue criterion.^[4] In perturbation theory, the criterion asserts that KAM invariant tori

are preserved and the trajectories with the tune $\nu(A) < k/m$ are confined, if the width of $\Delta\nu = 4\Omega/m$ of the nearest to $\nu(0)$ resonance $m\nu = k$ is small $m^2\Delta\nu < 2/3$ or $m\Omega < 1/6$. That gives even tougher constrain on Ω for higher order resonances than Arnold diffusion.

To my knowledge, the criterion has not been formulated for the 2-D time dependent case yet. In^[8] the attempt has been done to find the maximum stable amplitude based on the residue criterion, which was understood for the resonance $m_x\nu_x + m_y\nu_y = k$ as

$$m\Omega < 1/6 \quad \text{with} \quad m = \sqrt{m_x^2 + m_y^2}.$$

The resonances have been found, driven by random multipoles b_k , $k = 2, \dots, 12$ in the SSC-type lattice. The values of random b_k were set by the condition that the tune shift and the emittance distortion correspond to the linear aperture constraints up to the amplitude 5mm. The width of all resonances of the first order in b_k have been calculated with and without correlation between the multipoles, given by the fixed total field distortion. The amplitude dependence of a tune was given by the tune shift of the first and second order. In Fig. 1 the residue parameter $\xi = (3/2)m^2\Delta\nu$ is plotted vs. amplitude $A = \sqrt{A_x^2 + A_y^2}$. The amplitude at which $\xi = 1$ is considered to be the maximum stable amplitude. The results are in good agreement with the results of tracking.^[2]

4. The analysis of the low order resonances allows us to optimize the lattice and provides the detail structure of the phase space as it is given by low order resonances. However, as it is well known, there are thin stochastic layers in the vicinity of all separatrices of nonlinear resonances, which are responsible for "weak instability."^[6] The long term stability depends on the diffusion rate in this stochastic component of the phase space. Nevertheless, some mechanisms of the weak instability are well known and the rate can be estimated analytically. For example, the average rate of Arnold's diffusion in the vicinity of the resonance $m\nu = k$, depends on the frequency of small oscillations Ω in the separatrix:

$$D_\nu = \frac{1}{2} \frac{\partial}{\partial(s/R)} \langle \nu^2 \rangle = 16\pi e^{-\pi/\Omega}.$$

Ω is related to the width of the resonance: $\Delta\nu = 4\Omega/m$. For the SSC the rate gives rms tune diffusion $\Delta\nu \approx 0.01$ during 10^8 turns, if $\Omega < 0.09$.

Another factor limiting a particle life time is noise in the system due to intrabeam scattering, synchrotron radiation, residual gas, ripples of power supply, Schottky noise of the beam-beam interaction, etc. The rate of the noise induced diffusion can be enhanced by the nonlinear resonances.^[6] Let H_r be the Hamiltonian which describes a nonlinear resonance $m\nu = k$, and D be the rate of the diffusion induced by the noise in the system. Then the interaction between nonlinear resonances and the noise can be described as crossing of the resonances similar to the crossing of the nonlinear resonances in modulation diffusion with the Hamiltonian

$$H = H_r + \left(\frac{D}{m}\right)\psi.$$

The crossing rate is

$$v = \nu D / m\Omega^2$$

where Ω is the frequency of small oscillations in the resonance. For the SSC parameters $v \ll 1$. Successive crossings of the nonlinear resonances within the dynamic aperture with an average distance between them of $\delta\nu$, give additional diffusion with the rate

$$\frac{\partial}{\partial(s/R)} \langle \nu^2 \rangle = 2Q_* \Omega^2 v^2 \ln^2(1/v)$$

with

$$Q_* = \frac{4\pi D}{\delta\nu} \left(\frac{\partial\nu}{\partial\epsilon}\right)$$

For the SSC the effect is very small.

5. Tracking is the favorite method to study the long term stability today. The tracking is performed as a two step process which includes preparation of a single turn map, and tracking with the map some number of particles N_p for the number of turns N_t , which has to be comparable with the luminosity life time.

Generally speaking, because the measure of the stochastic component is exponentially small, an arbitrary chosen trajectory does not display any instability even in the long-term tracking. This argument shows that the long-term tracking has to be done with very large number N_p of particles to represent the effect of the stochastic component. The product $N_p * N_t$ defines the CPU time necessary for tracking and is always limited. Therefore, the initial conditions of few trajectories for tracking have to be chosen very carefully, based on the structure of the phase space within the linear aperture obtained in previous steps. An alternative approach can be based on numeric experiments which start as short term tracking with large N_p to find the initial conditions producing the largest modulation of the amplitudes (or smear). On the next step the tracking is repeated only with these initial conditions but larger N_t and so on, until we are able to specify the initial conditions for the long term tracking.

6. The only known remedy which can reduce CPU time is concatenation of the elements in a ring. There is no clear answer on how the concatenation effects the results of tracking. Obviously, it reduces time needed for tracking. The CPU time required to generate and run the n -turn map for the lattice with M elements in a ring is of order of

$$t \approx t_e M n + \left(\frac{N_t}{n}\right) t_{tr} N_p$$

where t_e is the time necessary to generate a map for a single element, and t_{tr} is the time for a one turn mapping. If $t_e \approx t_{tr}$, the optimum n is

$$n \approx \sqrt{\frac{N_t N_p}{M}}$$

and can be very large. For the SSC $M \approx 10^8$, $N_t \approx 10^8$ and $n \approx 10^4$, if $N_p \approx M$. Of course, the accuracy decreases with n . The acceptable accuracy of the map may not be better than the accuracy of the magnetic field measurements, although the differential algebra method allows, in principal, for a much higher accuracy to be obtained. To some extent, for the long term tracking there is no need to know the exact map, as far as the map which is used in tracking corresponds to a nonintegrable Hamiltonian and generates nonlinear resonances with the same average density and widths as the exact Hamiltonian. The accuracy of a map for long term tracking is limited practically by the accuracy of the tracking code used for concatenation of different elements of the ring.^[7] If the tracking code neglects terms of order of A^m , A is a dimensionless amplitude and has accuracy ϵA^m for each element, the accuracy of the n -turn map is $\Delta \approx M n \epsilon A^m$. The map does not describe higher order nonlinearities correctly. However, as we discussed above, probably the most important stochastic layers within the linear aperture are associated with the resonances of the lowest order. The nonlinear resonances which the map takes into account give the diffusion rate of order of

$$D \sim \sum_{k=2}^m k^2 \exp\left(-\frac{\pi}{\Omega_2 A^{k-2}}\right)$$

where the pre-exponential factor gives the number of resonances of k -th order and the widths of the resonances are scaled according to Eq. (1). The neglected higher order resonances can give the diffusion rate of order of

$$D \sim \sum_{k=m+1}^{nm} k^2 \exp\left(-\frac{\pi}{\Omega_2 A^{k-2}}\right)$$

If the amplitude A is sufficiently small, the first sum dominates in spite of the larger number of higher order resonances. From this point of view, it may suffice to have the map with accuracy $\Delta \approx M \epsilon A^l$, with $l < m$. That means $n < A^{l-m}$. For example, if $m = 5$ (MARYLIE), $l = 2$ (sextupole) and $A \approx 0.1$ (linear aperture), then n can be as big as 1000. These estimations pursue only the goal of raising the question rather than of giving an exact number for n , but they show that an optimal map is a many turn map.

7. Singular dependence of the behaviour of a trajectory on the initial conditions is smoothed out to some extent by the noise of round-off errors of a computer.

Artificial noise can also be implemented in tracking to generate a certain rate of diffusion.^[1] If the implemented rate is small, it enables us to do tracking with a very large number of turns, but to the contrary with the usual tracking, the behaviour of the trajectory does not depend on the choice of the initial conditions. Hence, the tracking with a single trajectory may reveal the average properties of the phase space although fluctuations may require tracking of more than one particle.

Deviation of the experimental diffusion rate from the rate due to artificially implemented noise may give information on the density of the nonlinear resonances in this area. This method has been demonstrated on a model^[1] and can be easily implemented in the existing tracking codes as a random kick of small amplitude per turn.

8. The synchro oscillations and periodic ripples of power supply add additional modulation resonances which can be studied in the same way as resonances driven by the lattice nonlinearities. The distance between the synchro-betatron resonances in frequency is equal to the tune Q_s of the synchrotron oscillations. The significant number of the resonances is $\delta\nu/Q_s$ and depends on the betatron tune modulation $\delta\nu$. If the linear chromaticity of the storage ring is cancelled out, the tune modulation is proportional to the second power of energy spread. For the SSC it is less or of order of Q_s . Hence, the synchrotron oscillations may add only a few new resonances within the dynamic aperture and cannot change the long-term stability substantially. The low frequency periodic ripples of dipole power supply can give tune modulation of the first order, but they can be suppressed by a feedback system.

Acknowledgement

I am thankful to A. Chao, E. Courant, D. Douglas and E. Forest for useful discussions. This work was supported by the U.S. Department of Energy under contract DE-AC05-84ER40150.

References

1. S. Heifets, "Long-Run Stability and the Noise," Preprint UH-IBPD-011-86.
2. "SSC Conceptual Design," SSC-SR-2020, March 1986.
3. S. Heifets, "The lattice nonlinearities and the long term stability of the SSC," 1987 IEEE Particle Accelerator Conference, Washington, 1987, p.1207; Preprint CEBAF-PR-87-027.
4. R. S. MacKay, "Transition to Chaos for Area-Preserving Maps" in **Nonlinear Dynamics Aspects of Particle Accelerators**, Sardinia, 1985.
5. F. Vivaldy, "Weak Instability in many-dimensional Hamiltonian Systems," **Rev. of Modern Physics**, 56, 4, 1984.
6. H. G. Hereward, "Diffusion in the presence of resonances" CERN/ISR-DI/72-26; D. Neuffer, A. Riddiford, A. Ruggiero, "Enhancement of diffusion by a nonlinear force," FERMILAB TM-1007, 2040, (1980).
7. E. Forest, private communication, Lugano Workshop, 1988.
8. D. Douglas, "Dynamic Aperture Calculations for Circular Accelerators and Storage Rings," AIP Conference Proceedings, Proceedings of Particle Accelerators, 1987.

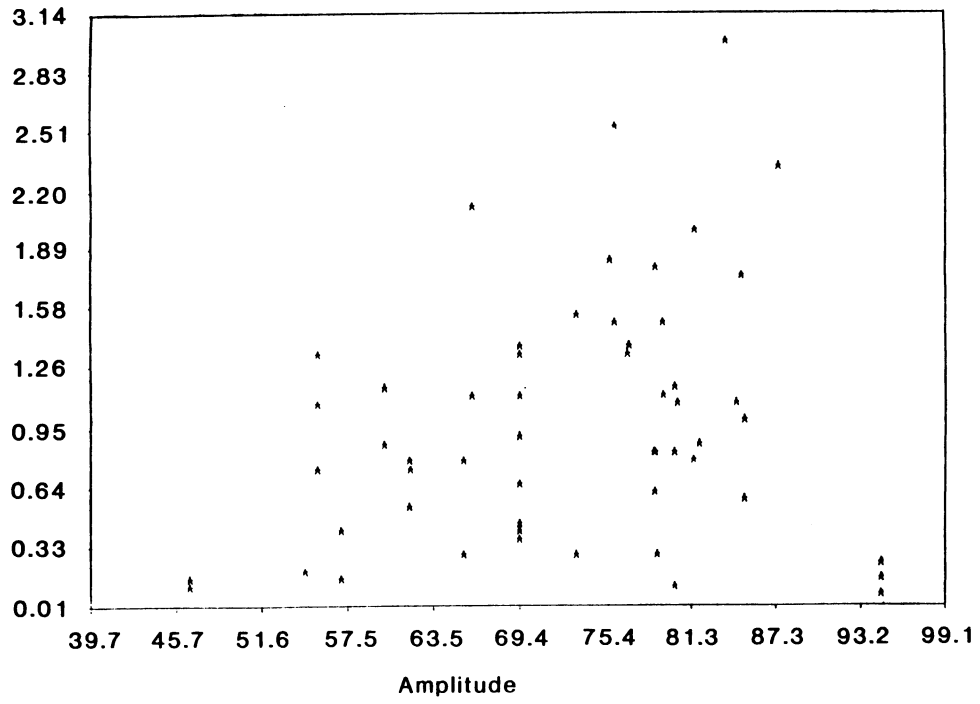


Figure 1a

The residue parameter vs. amplitude with uncorrelated random multipoles.

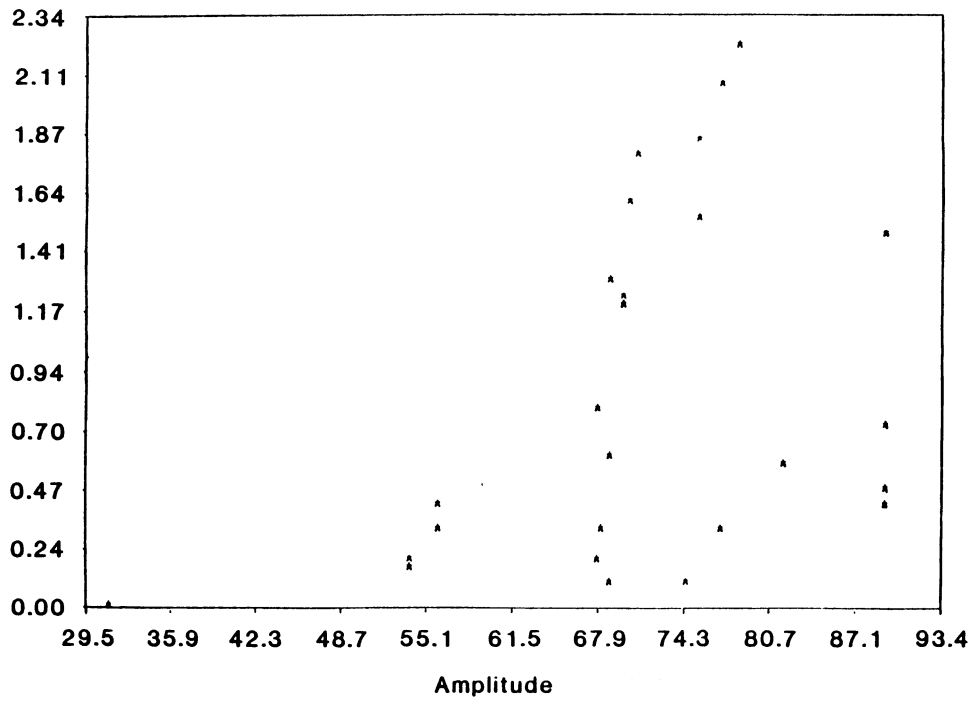


Figure 1b

The same as Fig. 1a, but with correlation given by constrain on the total variation of the magnet field $\Delta B/B < 10^{-4}$.

A POSSIBLE WAY TO COOL ANTIPROTONS

Yuri F. Orlov

F.R. Newman Laboratory, Cornell University, Ithaca, NY, USA

I will consider whether it is possible to create for antiprotons something like synchrotron radiation damping of electrons. Obviously, for heavy particles, only coherent losses of energy can be essential. We therefore need to increase individual energy losses of every antiproton with the help of some coherent process. Let us suppose that N_{coh} particles (a "coherent bunch") is involved in some process of coherent energy loss when passing through a special structure disposed on the storage ring (Fig. 1). The loss of energy, e , of each particle of the coherent bunch is proportional to N_{coh} :

$$e = A N_{\text{coh}} \quad (1)$$

The damping constant $1/\tau$ (for radial oscillations in the case of Fig. 1) can be proportional to e/E , $1/\tau = Be/2E$, if a special structure for the energy loss is chose properly and if every particle loses its energy independently. But we must remember that only one degree of freedom (from $2N_{\text{coh}}$ degrees of freedom of the coherent bunch) has independent loss of energy: an antiproton in the center of the mass of the coherent bunch will have a damping rate proportional to $e/2E$. Therefore, if we repeatedly produce coherent energy losses by passing new bunches through our special structure, then we will obtain an average damping constant of

$$1/\tau = Be/(2EN_p) \quad (2)$$

If $N_{\text{coh}} = N_p^-$, i.e., the coherent bunch contains antiprotons only, we have $1/\tau = AB/2E$, i.e., τ is independent of the number of coherent particles. The result is the same as for individual losses of energy; there is no gain of damping from coherency. This result is to be expected.

I suggest using mixed electron-antiproton bunches to increase coherent energy losses of antiprotons. In such a case,

$$N_{\text{coh}}/N_p^- = 1 + (N_e/N_p^-) \quad (3)$$

where N_p^- is the number of antiprotons inside the bunch, N_e is the same for electrons.

In the case $N_e/N_p^- \gg 1$ the coherency increases the antiproton damping.

In Fig. 1, antiproton and electron bunches passing through the structure have a very small radial beta-function at point 0; so in the area of energy losses, the radial phase ellipse of the antiproton bunch is as shown in Fig. 2. Usually the longitudinal sizes of antiproton bunches are too big for remarkable coherent losses of energy. Therefore, I suggest using small dense electron bunches with the same velocity and the same common radial phase space as antiprotons. In Figs. 1 and 2, these additional electron bunches are denoted by black spots; the antiproton bunch is outlined. So that the fields created by the additional bunches have a relatively small influence on the antiprotons outside them, I suggest using resistive losses of bunches moving between two plates as shown in Fig. 3. In the case of infinitely conducting plates, the fields created by a single bunch

fall off exponentially for a distance of the order of the h (the interval between plates), and then fall off algebraically [1]. We must use electron bunches not shorter than h if we want to decrease their influence outside them. Resistive energy losses were calculated by V. K. Neil, D. L. Judd, and L. J. Laslett [2]. According to them, the value A in equation (1) is equal to

$$A = (4/3\pi^2) (q^2/\epsilon_0 h) (L/s) (\epsilon_0 c/\delta s)^{\frac{1}{2}} \quad (4)$$

where q is the charge of an electron or an antiproton, L is the length of the structure we use for resistive losses, s is the length of the electron bunch, δ is the conductivity of plates, and c is the velocity of light. In this expression, I took into account that the highest frequency important for resistance of the plates is defined by s , the length of the bunch.

The value of B in equation (3) is

$$B = n(1/T_0)b \quad (5)$$

where n is the number of structures for resistive losses, T_0 is the revolution time of antiprotons, and b is the ratio of the number of antiprotons inside the electron bunches to the total number of antiprotons. Finally,

$$1/\tau = An(1/2T_0E) [b + I_e / I_p] \quad (6)$$

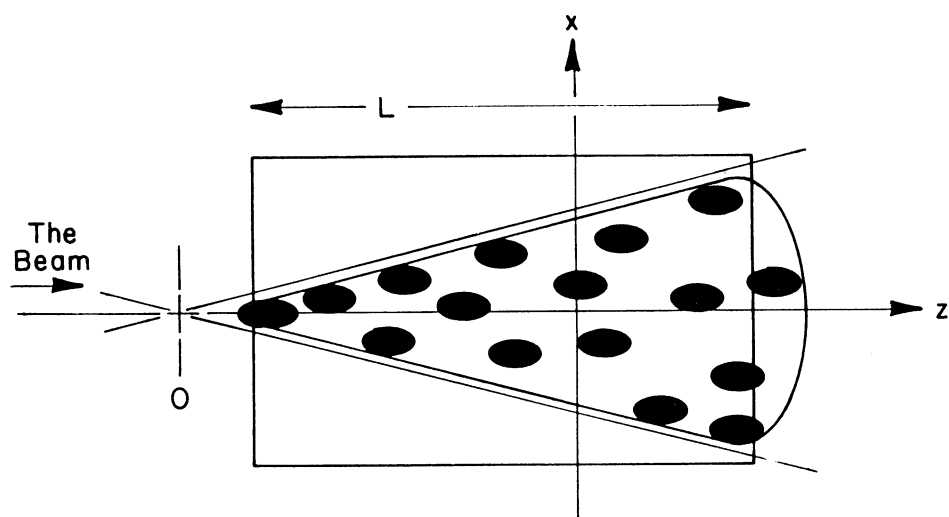
where I_e is the current of electrons passing through the structure, and I_p is the total current of antiprotons passing through the same structure. The coefficient before the square brackets is very small. But in the cases where $I_e / I_p \gg 1$, $1/\tau$ may be not so small.

The general conclusion is that such cooling is relatively weak although possible. (Instead of resistive losses, it is possible to use coherent radiations; in that case the damping effect will be much bigger. But this demands estimating the influence of electron bunches on antiprotons outside these bunches. Such an estimation remains to be done.)

* * *

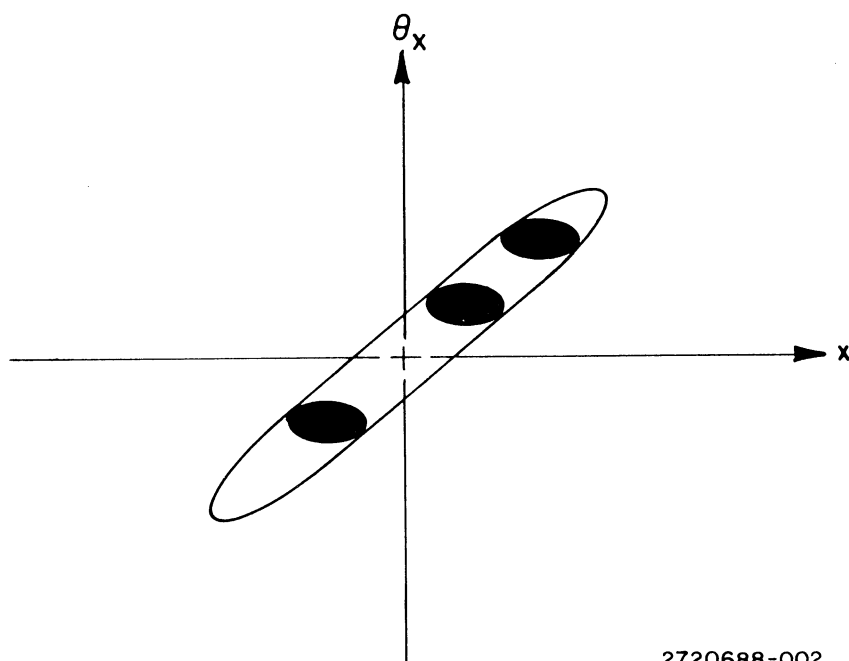
REFERENCES

- [1] P. L. Morton, V. K. Neil, and A. M. Sessler, Wake Fields of a Pulse of Charge Moving in a Highly Conducting Pipe of Circular Cross Section, Journal of Applied Physics, Vol. 37, No. 10, 3875-3883, September 1966.
- [2] V. Kelvin Neil, David Judd, and L. Jackson Laslett, Coherent Electromagnetic Effects in High Current Particle Accelerators: II. Electromagnetic Fields and Resistive Losses, The Review of Scientific Instruments, Vol. 32, No. 3, 267-276, March 1961.



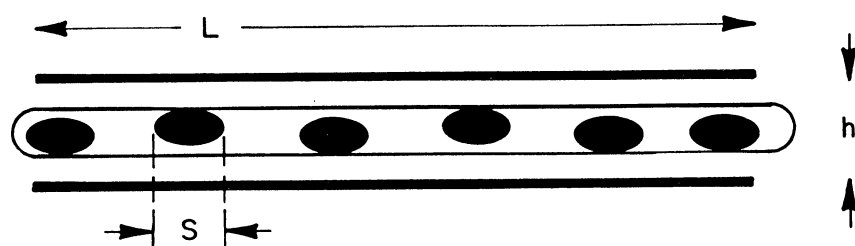
2720688-001

Fig. 1



2720688-002

Fig. 2



2720688-003

Fig. 3

SUMMARY REPORT OF THE WORKING GROUP ON EXPERIMENTS

*J. Crawford (SIN), D.A. Edwards (FNAL), K. Hirata (CERN), J. Gareyte (CERN),
P. Krejcik (CERN), P. Kuske (BESSY), S. Peggs (LBL), J.P. Potier (CERN),
J. Rossbach (DESY), T. Sherwood (CERN), G. von Holtey (CERN)*

(reported by J. Gareyte)

ABSTRACT

The new generation of storage rings will have to cope with unavoidable non linearities. This concerns the lepton as well as the large hadron projects. In order to better understand the practical implications of these effects, it is proposed to conduct specific experiments on existing machines.

1. INTRODUCTION

Despite considerable progress, Non Linear Dynamics is still incapable of predicting stability of particle orbits in accelerators.

With present day computers, tracking techniques are a very powerful tool and are used extensively in the design of new machines. However, their limits are dramatically revealed as soon as one tries to simulate real machines, which must operate sometimes for many hours, and in which many different phenomena conspire to slowly perturb the orbits of particles. As a matter of fact, Non Linear Dynamics is a very complicated subject in itself, but in the real world of accelerators it is just another complication added onto an already complicated system. Whereas the computing speed is expected to increase steadily in the future, the human ability to cleverly include all the relevant phenomena in the tracking models will probably evolve at a much slower pace.

In the foreseeable future one will therefore, as in the past, rely mainly on experience to make sound judgements about the validity of new projects. Progress in Non Linear Dynamics and tracking techniques should, however, be pursued vigorously since these are necessary ingredients for a better understanding of existing as well as of future machines. The aim of this working group was to analyse how the results of theoretical or tracking studies can be used to understand the real world of experimenters, and concurrently, how specific experiments can be devised to check the validity of these results, and their relevance to the problems of machine designers. The hope is that by comparing theoretical

or tracking results with experimental ones, it will be possible to define suitable criteria which, in turn, will considerably extend the predictive power of these techniques.

The work concentrates nowadays on two main classes of projects: the lepton machines in which performance relies on sophisticated lattices, with irregular betatron functions and strong chromaticity correcting sextupoles, and superconducting hadron colliders, which must operate for many hours with negligible beam losses, in spite of unavoidable non linear errors in their magnetic guiding field.

2. UNDERSTANDING EXISTING MACHINE

It would be adventurous to design new machines while existing ones are not fully understood. The first round of discussions was devoted to the review of how one understands the behaviour of existing machines as far as non linearities are concerned.

LEPTON MACHINES

In lepton machines it is sufficient to follow the trajectories of particles for a damping time, that is for about 10^3 turns, which is well within the reach of computer tracking. In this case one therefore expects a good agreement between predictions of computer tracking and experimental observations. Is this the case? The answer is: not always.

In Petra (Rossbach) the program Racetrack was used to evaluate the aperture in the presence of the mini beta insertion. The results indicated that the machine would not operate properly for a β^* smaller than 8 cm, which was indeed verified experimentally. Other features were less well explained. In KEK (Hirata) the apparent Dynamic Aperture (D.A.) at injection is much smaller than calculated by tracking. The observed tune dependence is not reproduced in tracking. In PEP, results sometimes agreed, sometimes not.

These discussions suggested the following remarks:

- A real machine is much more complicated than a model used in tracking codes.
- There are many other phenomena like synchrobetatron resonances, instabilities, ion trapping, which can change the experimental observations. For instance, in CESR, the aperture determined by orbit bumps was found to be current dependent (Peggs).

Therefore it may take a long time (many years) for the team of accelerator physicists looking after an operating machine to disentangle all these effects and just know what they are measuring.

- The betatron functions of a real machine are not accurately known. Where they can be measured, they are often found to depart from the theoretical values. This can be caused by an imperfect knowledge of the fields along the orbit (multipolar fringe fields in the case of short magnets, or short gaps in between magnets) or by spurious effects of another nature: for instance, a closed orbit crossing a strong quadrupole off-axis generates dispersion (Rossbach, Petra). When the orbit is corrected by displacing quadrupoles, this effect is systematically enhanced and it creates local variations of β 's, (Krejčík, CERN AC.) Variations of β 's of the order of 10% have been observed in Bessy (Kuske) as well as in the AC. As a second iteration one can use the measured functions to improve the model, but in any case there is always an uncertainty of the order of 5% on the measured values.

Two recommendations emerge from these remarks:

- one cannot stress too much the importance of understanding in detail the behaviour of existing machines. This is first to the benefit of their users, but also, since projects are blooming all over the world, to that of the community at large.
- At the design stage, it is imperative to test the sensitivity of tracking results to changes in optics functions, or any imperfection which is likely to show up in the real world.

HADRON MACHINES

There are only two hadron colliders in operation, the CERN S \bar{p} pS and the Fermilab Tevatron. Both are very linear machines, except in collision mode where their otherwise regular lattice is perturbed by the low beta insertions and the beam-beam effect provides strong non linearities. More experience has been gathered up to now in the S \bar{p} pS and it mainly concerns the beam-beam effect. The observations are the following:

In the presence of beam-beam collisions particles diffuse transversely out of the beam, faster in the tails of the distribution than in the core. This diffusion is attributed to the excitation of high order non linear resonances since when the beams are debunched the phenomenon

disappears (in this situation the effect is smoothed out azimuthally, resonances are not excited).

- If part of the beam straddles resonances of order 10 or less, the lifetime is so low that no useful operation is possible (lifetime less than half an hour). Higher order resonances up to order 16 have a clearly visible effect, but do not prevent a useful operation of the machine. As a consequence, since resonances of order 10 or less must be avoided, it is imperative that the tune spread in the beam stays below 0.02.
- Tracking studies have been made to try to explain the observations. Diffusion through stochastic layers in between high order resonance islands was demonstrated, but only when the beam-beam parameter was increased considerably above the value observed in the real machine. For values comparable to the real ones, the phase space looks perfectly stable, except if external random noise is added. In this case noise induced diffusion is considerably enhanced by the beam-beam effect. It is believed that this qualitatively explains the observations : it has been shown that by reducing the noise level in the machine (tune modulations, spurious microexcitations of the beams) the lifetime could be improved.
- Due to this diffusion process, collimators have to be placed permanently at suitable positions in order to catch the outgoing particles in a controlled way, thus preventing them from falling into the physics detectors (or the superconducting magnets in future cryogenic machines).

3. THE NEED FOR SPECIFIC EXPERIMENTS

Computer models are insufficient because they do not include many effects which are important in reality. Operating machines provide a wealth of information which can be exploited to bridge the gap between computer models or analytical calculations and reality, but are often difficult to understand in full detail, because of the complexity inherent in their operating modes.

The need for specific experiments in the domain of Non Linear Dynamics as well as in other domains of the Science of Accelerators is clearly perceived.

These experiments should be performed in machines which are already well understood, so that clear conditions can be defined, spurious

phenomena eliminated, and the effects under study carefully isolated. Doing similar experiments in different machines would be invaluable to help distinguish those results which are relevant to the problem studied, from those which are just a property of the machine used. Such experiments have been done recently at CERN and Fermilab on the subject of interest to this workshop and are reported in these proceedings.

The major difficulty, in the present environment, comes from the competition for machine time with the main machine users, because of a world shortage of facilities. It is therefore necessary to develop a concerted effort and work in a complementary way in different laboratories.

From the discussions around this subject two main classes of experiments emerged: the first is concerned with understanding the structure of the phase space produced by non linearities and evaluating the short term consequences (typically over 10^3 turns), the second addresses the problem of the long term consequences of non linearities (typically over 10^5 to 10^8 turns). The first category is of universal interest while the second only concerns the hadron colliders.

4. UNDERSTANDING THE PHASE SPACE

Poincarré surfaces of section are easy to obtain by tracking. Interesting parameters such as tune and smear can be calculated, but much more information is contained in these plots, like the resonance islands. Now the technique is ripe for an experimental measurement of these properties on real machines. This has been the main object of the Fermilab experiment E778 but is also being tried elsewhere. Krejcik (these proceedings) reported preliminary work done at the CERN AC to understand non linear coupling induced by sextupoles near $Q_H = Q_V$ with a view to correcting it in order to increase the machine acceptance. The two-dimensional plot of the invariants reveals the relative importance of the resonant terms in a very clear and spectacular way.

In order to obtain a faithful mapping of the phase space one should use a beam with initial dimensions much smaller than the D.A. which is to be explored. The beam is kicked onto the desired phase space trajectory and its position is followed on successive revolutions with at least two monitors separated by $(2k + 1)\pi/2$ in betatron phase. Such measurements can be done with hadrons, but lepton machines appear to be particularly well suited because the natural dimensions of the beams are usually much smaller than the machine aperture. However, situations in which radiation damping is not too strong would have to be selected.

In lepton machines a rough exploration of the phase space can be done in another way, which is well illustrated by the report from P. Kuske on measurements made at Bessy. In this machine the beam core dimension is extremely small but due to gas scattering, a very faint halo of particles extends up to the vacuum chamber walls. By introducing collimators inside the aperture the flow of particles at different amplitudes can be guessed from the drop in lifetime which is recorded. In a normal situation this technique just detects a sharp edge corresponding to the chamber wall, but when strong non linearities are introduced, for instance, by closing the pole pieces of the undulator magnet, more interesting structures are revealed: the apparent aperture (the D.A.?) is smaller than the geometrical aperture and there are regions of amplitudes where the flow rate of particles seems to be increased (transport by resonant islands?)

Synchrotron light monitors can also be used to explore phase space: by kicking the beam with the right amplitude a sufficient number of particles can be trapped in resonant islands which will then become visible.

5. LONG TERM STABILITY

Future superconducting hadron colliders will have to operate without particle losses or beam degradation for tens of minutes at injection energy and during ramping, and for tens of hours in collision mode. The consequences of magnet non linearities on this long-term behaviour is up to now largely unknown. Experience on beam-beam effects in the CERN SppS collider can give some clues in this domain but is certainly not sufficient to draw definite conclusions. The main reason for that is the marked difference in phase space topology between a machine dominated by beam-beam and a machine dominated by magnet non linearities. In addition some features shown by the SppS may be specific to this machine and less important in superconducting colliders, and vice-versa.

The only way to make progress in this area is therefore to devise and conduct clever experiments in order to better understand what are the most important mechanisms which govern the long-term behaviour of a beam, in the presence of a realistic, non linear phase space. Since a few hours of machine time means a few 10^8 turns, there is no hope in the foreseeable future to attack the problem through analytical calculations or computer tracking.

It is proposed to create known phase space topologies by powering non linear elements in otherwise linear machines, and to measure the diffusion rates as a function of amplitude under well controlled machine conditions: tune modulation, noise, and any realistic perturbation which can simulate real life.

Special beams can be used to enhance sensitivity for a given phenomenon. For instance, by kicking a beam with small initial dimensions onto a chain of islands pertaining to a high order resonance, one creates a hollow beam (in phase space) which only covers the region of interest. By applying noise in selected frequency bands one can explore diffusion rates in different phase space regions (Peggs).

6. EXPERIMENTS IN PROJECT

6.1 Fermilab

Experiment E778 will be pursued. Other sextupole configurations will be tested, and the techniques will be extended to two degrees of freedom. It is expected that learning how to handle the data, taking care of decoherence and extracting the relevant parameters will be much more difficult in two dimensions. On the other hand, it is believed that this step is necessary.

Studies of high order resonant islands and their modulation sidebands will be pursued. One will try to better detect the change of régime from ordered phase space to chaos.

6.2 CERN SPS

An effort is being made to experimentally measure the phase space. Measurements of short term stability (over a few seconds), as already reported here by Hilaire, are easy and will be pursued for different working points and different sextupole distributions. They should allow to better define the relation between the criteria used in the design of new machines, namely ΔQ and smear, and stability over a few 10^5 turns. This time scale is interesting because it is accessible both to experiment and to extended tracking.

Major efforts are planned to investigate long term stability. Lifetimes, diffusion rates should be measured for different phase space topologies. One can use sextupoles as well as a Non Linear Lens which consists of two current carrying copper bars placed on either side of the beam. This instrument generates a series of high order multipoles, whose relative strengths can be chosen in a certain domain by varying the distance between the bars.

6.3 Influence of low frequency noise

In Hera ground motion will make the two beams move with respect to each other, thus modulating the beam-beam effect. It is proposed to test

the importance of this effect in the CERN S \bar{p} pS where it is known that at high frequency (13 kHz) such spurious modulations have a very detrimental effect on the beam lifetime. It is hoped that at the lowest frequencies where ground motion has a significant contribution, the sensitivity of the beam is so much reduced that this will not pose a problem.

7. CONCLUSION

A concerted approach towards an experimental evaluation of the effect of non linearities in storage rings is felt necessary. Some experiments have already been done in a few machines, while others are being proposed and discussed. These experiments tend to promote new concepts and use up-to-date technology, two aspects which may help to operate future machines in a more difficult situation, when non linearities can no longer be neglected.

AN OVERVIEW OF EXPERIMENT E778

D.A. Edwards and M.J. Syphers

FNAL, Batavia, Illinois, USA

ABSTRACT

The nonlinear dynamics of transverse particle oscillation in the Tevatron is studied experimentally and compared with prediction. Sixteen superconducting sextupoles are used to produce an adjustable third-integer resonance driving term. Agreement between simulation and experiment for phase space distortion and amplitude dependence of tune is in general good. Trapping of particles in resonance islands is observed, and island properties studied.

1. INTRODUCTION

Experiment E778 at Fermilab had its origin in the need to subject the SSC magnet aperture criterion to experimental examination. It has developed into a collaborative effort in the study of nonlinear dynamics and beam diagnostics involving accelerator physicists from the SSC Central Design Group, Cornell, SLAC, CERN, and Fermilab. The overall report of the collaboration has been submitted for publication elsewhere.[1] In this report, we present an outline of the experiment, a summary of results to date, and some general comments.

The magnetic field quality specification used in the SSC Conceptual Design Report is based on the imposition of bounds to the departure from linear behavior in the oscillation of single particles about their closed orbits. The specification is physically reasonable, but it is important to give serious attention to the values assigned to the parameters in the criterion. This experiment (E778) is part of that effort.

If the betatron oscillations of a particle in a synchrotron are linear, then the oscillation amplitude will be a constant of the motion. If there is no coupling between the two transverse degrees of freedom, the projections of the amplitude on the horizontal and vertical planes will each be an invariant. A turn-by-turn plot of the vertical projection versus the horizontal projection will yield a single point.

Nonlinearities in the magnetic fields will lead to gradual (on the time scale of a betatron oscillation period) changes in the magnitudes of the transverse amplitude projections. The single point of the turn-by-turn plot will develop, in general, into an area. The distance of a point within this area to the mean position of all the points is a measure of the change of amplitude. The criterion places a limit on the ratio of this change to the mean amplitude. In particular, the rms value of this fractional excursion, termed the "smear," is to be less than 7% within the aperture used for routine beam operations.

The principal aims of experiment E778 are to (1) measure smear and tune shifts and compare the results with tracking calculations, (2) look for short time scale (e.g., injection) performance degradation with increase of nonlinear perturbation, (3) look for enhancement of long term beam loss or emittance increase with nonlinearities, all as steps toward improving the criterion. In addition, this activity serves as a focus for instrumentation improvement and the development of techniques to study more complex problems in phase space dynamics.

2. BACKGROUND FOR THE EXPERIMENTS

2.1 Phase Space Measurements

The original beam position monitor system in the Tevatron was capable of recording the motion of the center of charge of the beam for one thousand turns. An upgrade for this experiment extended the capability to the million turn level.[2] The positions at two neighboring monitors, coupled with a knowledge of the intervening optics, can be used to find the transverse velocity of the beam at either monitor. Thus, a phase space plot can be obtained for the turn-by-turn motion.

Figures 1a and 1c show turn-by-turn plots for one thousand turns in the Tevatron as recorded by two neighboring position monitors in the horizontal plane. A coherent betatron oscillation was induced in the circulating beam by firing a kicker magnet fifty turns after the beginning of the plot. That the decrease in amplitude is modest over the thousand turns is an indication of near-linear behavior. Figures 1b and 1d display the Fourier transforms of the two position signals, and give the fractional part of the betatron oscillation tune.

In Fig. 2, similar data is displayed in normalized phase space coordinates; the horizontal axis is position and the vertical is the appropriate conjugate variable so that the plot is the familiar circle of simple harmonic motion. If the position variable is x and the angle with respect to the unperturbed orbit is x' , then in terms of the conventional Courant-Snyder parameters, this conjugate variable is $\beta x' + \alpha x$.

In 1985, when this procedure for displaying phase space motion became routinely available in the control room at Fermilab, some initial studies were made of the perturbation of the motion by nonlinearities. In particular, eight sextupoles were used to excite the resonance at the betatron oscillation tune of $19 \frac{1}{3}$. Figure 3 shows a case in which the small amplitude tune was 19.34. A kicker produced an initial amplitude so that a particle at the centroid would perform stable motion close to the separatrix. As expected, the circle is deformed into the triangle characteristic of this resonance.

A natural extension of this technique employs four position monitors - two in each transverse degree of freedom - to obtain four dimensional phase space information. Though some preliminary data have been recorded in this mode, the studies to date have concentrated on one degree of freedom.

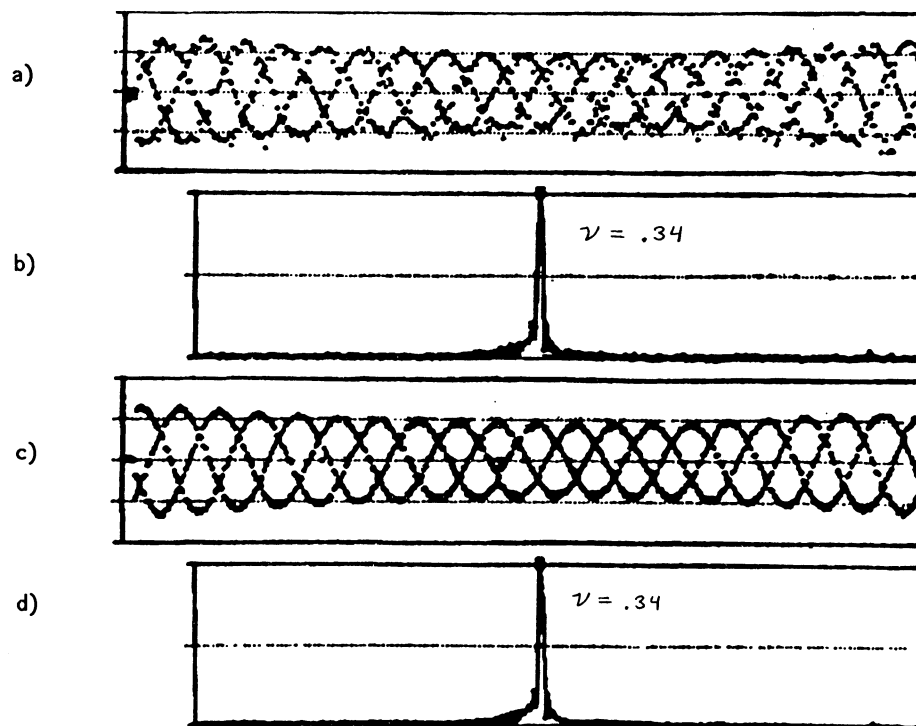


Fig. 1

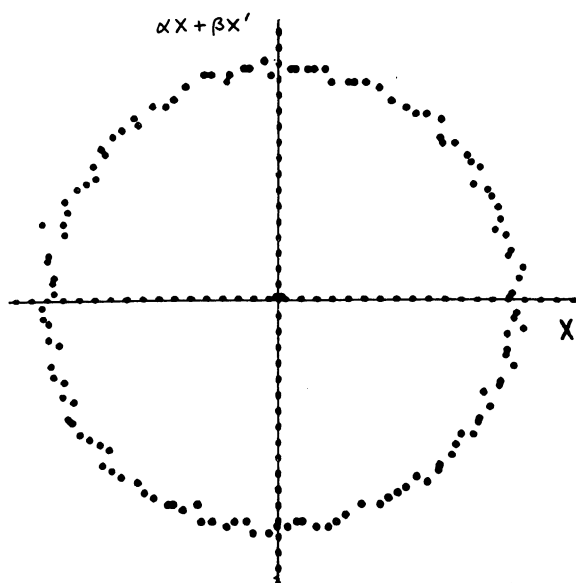


Fig. 2

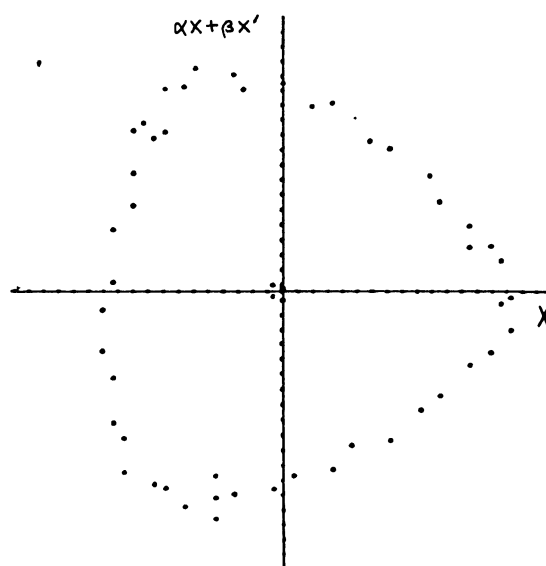


Fig. 3

2.2 Sextupoles Used in E778

For this experiment, 16 additional sextupoles were commissioned. The superconducting magnets themselves had been installed when the Tevatron was constructed, but cables, power supplies, and controls still needed to be supplied. Including the 8 elements used in the earlier studies, the resulting sextupole complement is 16 normal sextupoles at stations 22, 24, 26, 28, 32, 34, 36, 38 in C and F sectors and 8 skew sextupoles at stations 12, 14, 16, 18, 23, 27, 37, 43 in D sector. The skew sextupoles were not used in the studies reported here.

The normal sextupoles are powered in pairs by 8 supplies, so a variety of configurations is possible. For this run, it was elected to power them so as to produce a strong third-integer resonance driving term. Measurements were performed at tunes far from the $1/3$ resonance to study the more complicated phase space structure exhibited there than that examined in the earlier work. Figure 4 and Fig. 5 contrast the expected near-resonance and far-from-resonance behavior in the presence of only one sextupole as obtained from a tracking program. When the tune is near resonance - at 19.35, for example - the particle flow in phase space is along contours as exhibited in Fig. 4. Far from resonance, at a tune of 19.42, the phase space contours become those in Fig. 5.

The striking feature of Fig. 5 is the appearance of resonance "islands." Since the unperturbed betatron tune is 19.42 in this figure, the particle tune varies from 19.42 at the origin to 19.333 at the separatrix. (Technically, the separatrix only exists when the discrete sextupoles are replaced by a smooth approximation.) At an intermediate amplitude, the sextupole generates the five islands characteristic of a fifth-order resonance. The phase space of Fig. 4 also contains islands, but their orders are so large that they are difficult to see on the scale of the figure.

2.3 Measurements as Planned

All measurements were conducted at the Tevatron injection energy of 150 GeV. Necessary preliminaries included verification that the normalized emittance (95%) of the injected beam was at or below 15π mm-mrad, orbit adjustment at the nonlinearities to minimize tune shifts and other off-center effects, reduction of horizontal-vertical coupling by skew quadrupoles and tune split, reduction of chromaticity to 3 units or less, and minimization of coherent synchrotron oscillations at injection.

Four basic types of measurements were carried out. The first type of experiment consisted of injecting, then ramping the sextupoles up to the desired setting in 10 seconds. After a further 10 second delay, a coherent betatron oscillation was induced by firing the Tevatron injection kicker. At each of several values of the horizontal tune, a number of kick amplitudes were employed, bounded from above by the onset of beam loss in the bare Tevatron. The principal data recorded at each condition were the turn-by-turn signals from two monitors, and the beam intensity through the supercycle. This variety of data was analyzed to yield smear and tune values to be compared with simulation.

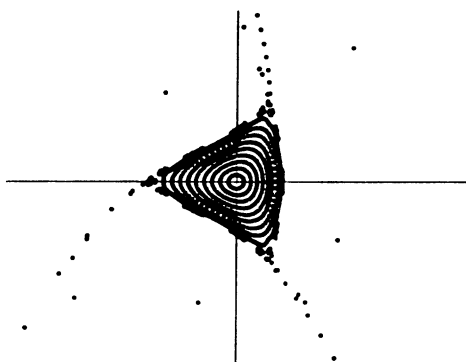


Fig. 4

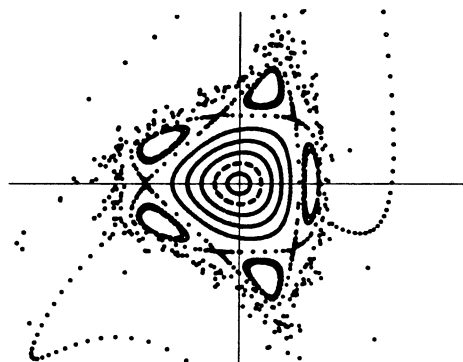


Fig. 5

In the second, the nonlinearities were on when beam was injected into the Tevatron and measurements were performed with intentional injection steering errors. Data recorded included first turn position monitor readings, closed orbit shortly after injection, turn-by-turn data at injection, beam profiles at injection and nine seconds later, and beam intensity versus time. This data was examined to find evidence for degradation in short-term beam behavior.

In the third, the emittance of the beam was slowly increased through the introduction of noise into the transverse dampers and the limiting emittance observed as a function of sextupole excitation. Beam profiles were recorded throughout this process. The limiting beam size was taken to be a measure of the dynamic aperture (when less than the physical aperture) and compared with simulation.

The fourth variety of measurements was associated with the study of resonance islands. The procedure was similar to that used in the first type of measurement, but with conditions adjusted for trapping of a portion of the beam in islands. It was this phase of the experiment that motivated the extension of the turn-by-turn capability to the million turn scale. Existing extraction system hardware was modified to permit a significant range of tune modulation in amplitude and frequency.

3. EXPERIMENTAL TECHNIQUES AND DATA REDUCTION

3.1 Single Particle Considerations

If the beam were a single particle, then at first glance the calculation of the smear would reduce to a simple matter of minimizing an appropriate least squares sum. The variables used in the minimization represent lattice functions and closed orbit offsets at the beam position monitors, which thereby are determined from the data.

To compensate for linear coupling between the two transverse degrees of freedom, the skew quadrupoles were adjusted so that less than 10% of the amplitude of a horizontal oscillation coupled over into the vertical when the tunes were split by approximately 0.1. The closed orbit was adjusted at each sextupole location so that both the closed orbit

distortion and the small amplitude tune shift caused by the sextupole excitation were adjudged to be negligible. Occasional changes in the chromaticity circuits were made to compensate for the time variation of the sextupole moment in the main bending magnets.

3.2 Multiparticle Considerations

The finite emittance and momentum spread of the real beam make for difficulties in both the experimental procedures and in the data analysis. In principle, the decoherence of the turn-by-turn signal that arises from chromaticity can be eliminated and indeed that is straightforward at zero excitation of the additional sextupoles. However, the additional sextupoles introduce non-negligible chromaticity on their own. Measurements were performed to calibrate and correct this effect.

But the dominant source of decoherence is the nonlinear tune variation with amplitude caused by the sextupoles. Figure 6 illustrates the loss of coherent beam centroid motion at a sextupole excitation of 15 Amperes. The extraction of the phase space distortion in the face of this effect relies on a reconstruction of a single-particle motion by fitting a Gaussian to the apparent amplitude reduction. Such a fit is shown in Fig. 7. By fitting over a variable number of turns, one can determine the smear and also its stability versus turn number. The result for one experimental condition is shown in Fig. 8.

The several corrections and fitting procedures of this and the preceding subsection are incorporated in a program, Tevex,[3] written specifically for this experiment. This is the principal program used in the reduction of the smear data.

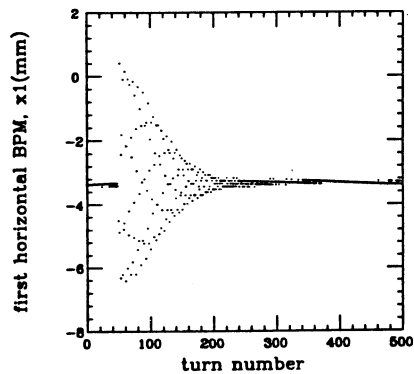


Fig. 6

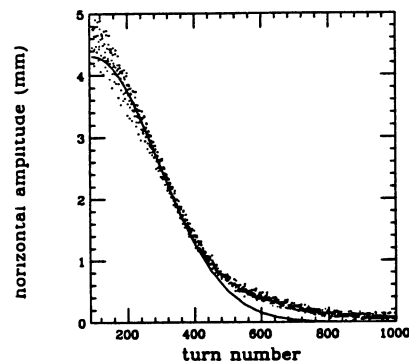


Fig. 7

4. RESULTS

4.1 Phase Space Distortion and Smear

The smear of the bare Tevatron is characterized by Fig. 9, confirming that in the absence of the additional sextupoles the smear is indeed small. At the time of this particular measurement, the finite resolution of the beam position monitors contributed about 1% to the observed smear. For the bare Tevatron measurements, this contribution was subtracted in quadrature to yield the results shown. This correction is negligible for the data taken with sextupoles energized.

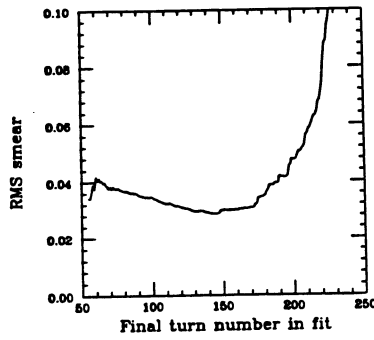


Fig. 8

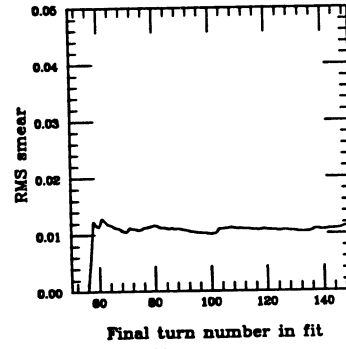


Fig. 9

Figure 10 displays smear versus sextupole current for a range of kick amplitudes with a tune of 19.38. For these data, the beam emittance had been reduced to less than 4π mm-mr by scraping the beam after injection. For this small emittance beam, the agreement between simulation and experiment is very good. As can be seen in Fig. 11, for higher emittance beams ($\geq 10 \pi$ mm-mr) the agreement deteriorates. This is especially true at lower tune values. The decoherence times for these data are shown in Fig. 12 and Fig. 13. As can be seen, the agreement between simulation and measurement is better for the lower emittance.

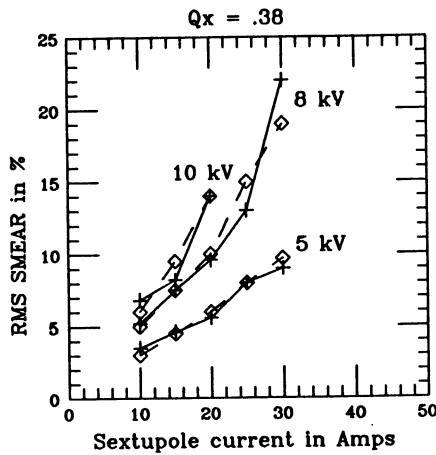


Fig. 10

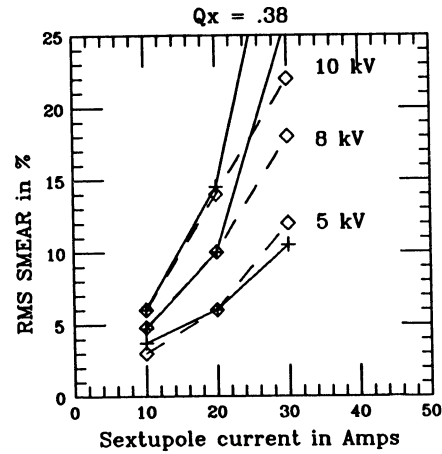


Fig. 11

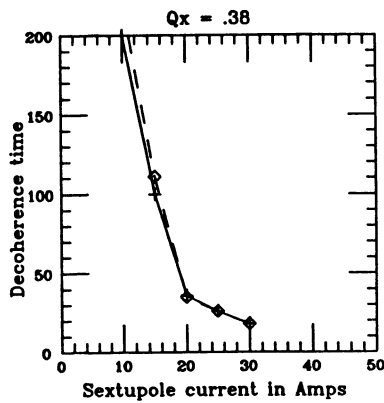


Fig. 12

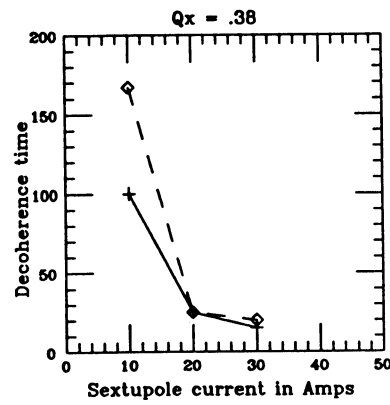


Fig. 13

4.2 Injection Experiment and Dynamic Aperture

Even at the highest sextupole excitations, no significant variation or deterioration in beam trajectory information was revealed. For instance, closed orbits a few milliseconds after injection differ by less than a millimeter for sextupole excitations of 0 and 45 amperes. The conclusion is that it would be possible to diagnose and correct injection problems in the presence of these strong nonlinearities.

Initial measurements revealed long term losses as indicated by Fig. 14. The fractional beam loss in the first five seconds after injection is plotted versus sextupole current. In each case, there was apparently a threshold sextupole current above which a slow loss was found. However, it was found that this loss could be dramatically reduced by turning off the RF cavities, and so it is unlikely that the loss is associated with a purely transverse process.

The straightforward dynamic aperture measurement yielded the results presented in Table 1. At 15 amperes, the calculated dynamic aperture is outside of the physical aperture; at the higher currents the experimental results are smaller than the prediction from short-term tracking of on-momentum particles.

Table 1

<u>Sextupole Current</u>	<u>Dynamic Aperture (full width, mm)</u>	
	<u>measured</u>	<u>calculated</u>
15 Amperes	13*	27
30 Amperes	10.5	13.5
50 Amperes	6.5	8

*physical aperture smaller
than dynamic aperture

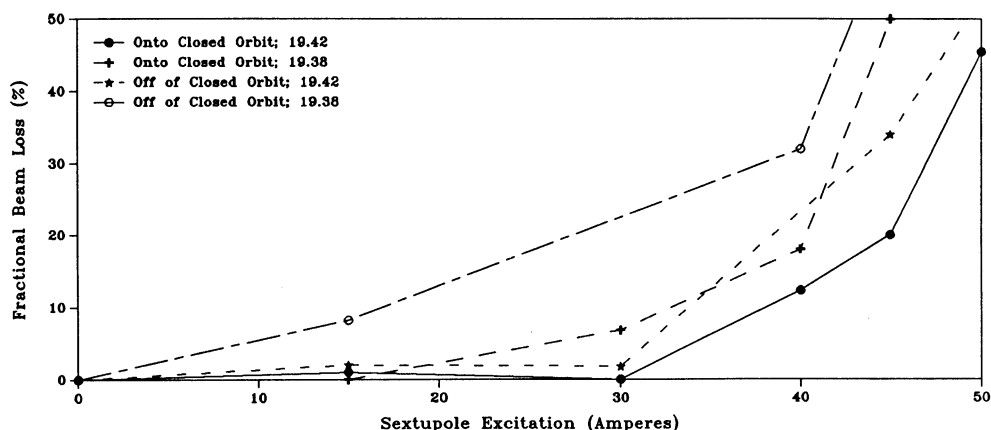


Fig. 14

4.3 Islands and Tune Modulation

Referring to Fig. 5, it is conceivable that with a particular kick amplitude and orientation, some fraction of the beam could become trapped in resonance islands. The detection of such trapping turned out to be surprisingly easy, for in the presence of decoherence of the rest of the beam, the trapped particles continue to oscillate in a coherent fashion, as is demonstrated in Fig. 15.

A spectrum analyzer verified that this coherent motion continued throughout the ten seconds before the sextupoles ramped down, though the signal strength gradually decayed with time indicating a leakage of particles from the islands. Both the turn-by-turn data and the spectrum analyzer showed that the sustained signals were associated with tunes whose fractional parts were $2/5$, $3/7$, $5/13$ as would be expected. As expected, the persistent signal at, for instance, $2/5$ was no longer present if the fractional part of the small amplitude tune was reduced below $2/5$.

The $2/5$ resonance was studied in further detail. Using the improved capabilities of the turn-by-turn system, the coherent motion of particles trapped in resonance islands were recorded for many thousands of consecutive turns. Figure 16 shows a phase space plot for such a case, the five islands being clearly visible. The star-shaped pattern in the corner of the plot is a demagnified view of the same data with successive points joined by straight lines, confirming the $2/5$ nature of the resonance.

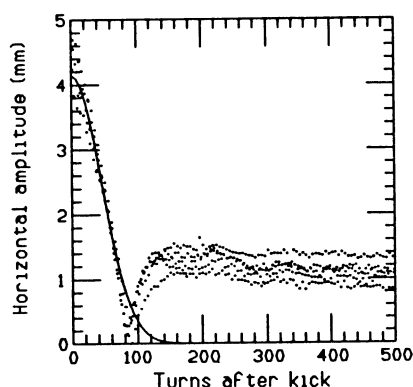
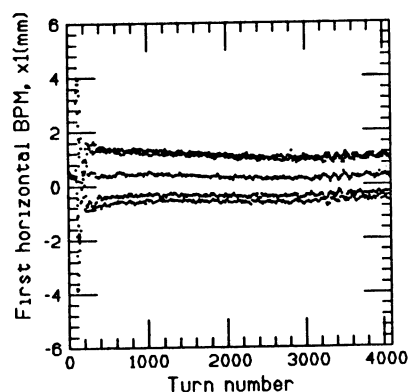


Fig. 15

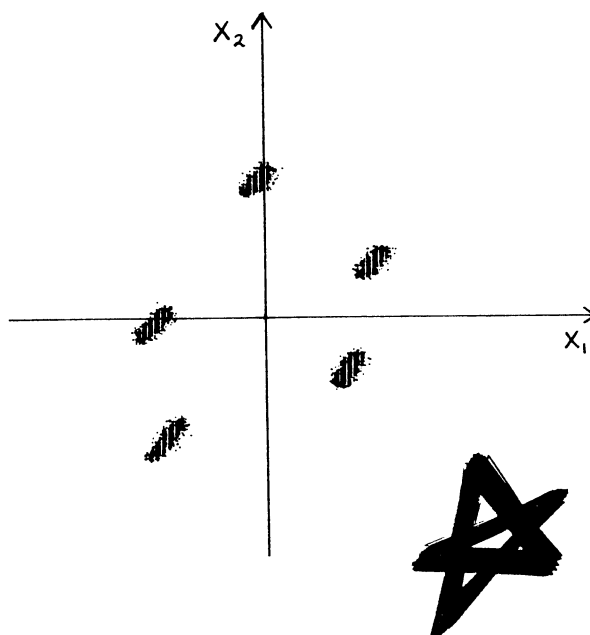


Fig. 16

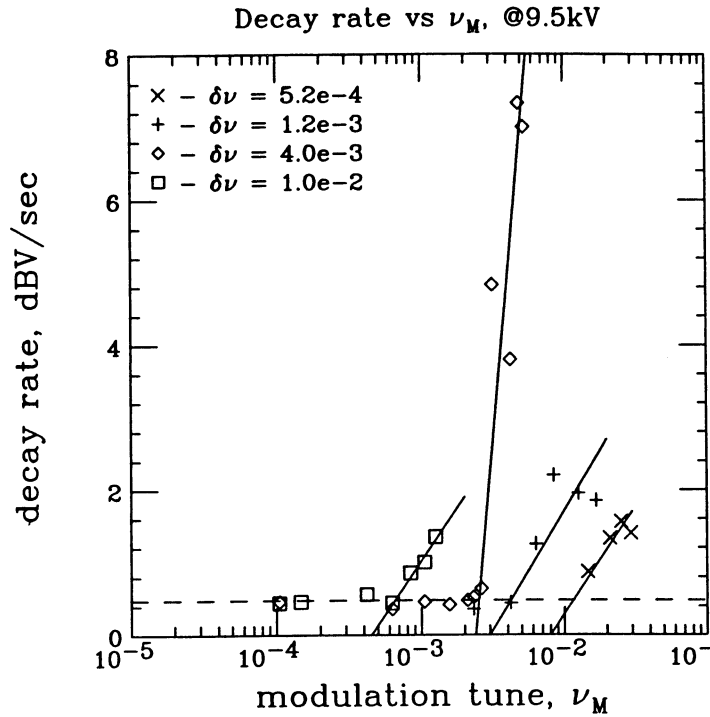


Fig. 17

Tune modulation was found to influence the lifetime of the persistent tune lines associated with particles trapped in islands. A particular set of results is shown in Fig. 17. The islands break up at the higher frequencies with the departure from adiabaticity. One would expect the break to appear at lower values of modulation frequency for higher values of modulation amplitude and this is what Fig. 17 indicates. The system is expected to exhibit other distinct phases; one chaotic and one non-chaotic, with the latter further subdivided into regions with and without sidebands. The analysis of this and other aspects of resonance islands is preliminary, but indicative of an interesting research direction.

* * *

REFERENCES

- [1] A. W. Chao et al, submitted to Phys. Rev. Letters.
- [2] S. Peggs, C. Saltmarsh, R. Talman, "Million Revolution Accelerator Beam Instrument for Logging and Evaluation," SSC-169, March 1988.
- [3] S. G. Peggs, contribution to these proceedings.

DYNAMICAL APERTURE AT THE SPS

A. Hilaire

CERN, Geneva, Switzerland

ABSTRACT

The dynamic aperture of the SPS has been measured in the presence of nonlinearities artificially introduced in order to simulate the operating conditions of future large superconducting colliders. These nonlinearities are produced either by strong lumped sextupoles or by a special Non Linear Lens consisting of two current carrying bars parallel to the beam. By comparing the measurements with extensive computer simulations the empirical criteria which are used in the design of superconducting colliders can be refined and their validity more firmly established.

1. INTRODUCTION

In the large Superconducting Hadron Colliders which are now under design the magnetic field contains nonlinearities related to the physical aperture of the magnets. As the aperture of the magnets has a strong influence on their cost, it is essential to have a good estimate of the maximum permissible deviation of the magnetic field from linearity. To do so some criteria are being used but the numerical values assigned to them has to be checked experimentally. To this aim an experiment has been performed at the SPS at CERN [1], the results of which are presented and analysed here.

2. AIM OF THE EXPERIMENT

Two criteria are used in the design of Large Superconducting Colliders based on the deviation from the linear motion due to magnetic imperfections.

The first one is the variation ΔQ of the tune due to the different amplitudes of motion of the particles in the beam. A maximum value is assigned to ΔQ in order to avoid low order resonances which would lead to a deterioration in the beam lifetime. A value of 0.005 has been proposed which would make it possible to avoid resonances of order less than 10.

In a perfectly linear machine, the amplitude of the particle, defined to be the Courant and Snyder invariant, remains unchanged from turn to turn. When nonlinearities are added, this amplitude will vary from turn to

turn. The relative change of this amplitude is taken as the second criterion. In order to eliminate the effect due to the linear coupling, one takes the sum of the horizontal and vertical amplitudes i.e.:

$$W_x = \beta_x x'^2 + 2\alpha_x x x' + \gamma_x x^2$$

$$W_y = \beta_y y'^2 + 2\alpha_y y y' + \gamma_y y^2$$

$$\overline{W_x} = \frac{1}{N} \sum_{i=1}^N W_{xi}$$

$$\overline{W_y} = \frac{1}{N} \sum_{i=1}^N W_{yi}$$

$$\text{Smear} = \frac{\frac{1}{N} \sum_{i=1}^N [(W_{xi} + W_{yi}) - (\overline{W_x} + \overline{W_y})]^2}{\overline{W_x} + \overline{W_y}}$$

The numerical value taken as a criterion for the Smear is 0.035.

The aim of the experiment was then to check the validity of the numerical values used for those criteria. To do so, we measured the reduction in the dynamical aperture of the SPS resulting from the introduction of well known nonlinearities in the machine.

The experimental results are then compared to tracking results incorporating the same nonlinearities.

3. CONDITIONS OF THE EXPERIMENT

In order to compare the experimental results with the tracking ones, the machine conditions have to be well known. For this reason, an energy range where the SPS is very linear has been chosen. Between 100 GeV/c and 250 GeV/c the remanent field effects are negligible as are the space charge effects, and the saturation effects in the magnets are not yet perceptible. An energy of 120 GeV/c has been chosen to benefit from the maximum strength for the added nonlinearities.

The beam intensity has been reduced to $2 \cdot 10^{12}$ protons per pulse in order to minimize the octupolar field necessary to suppress the resistive wall instabilities. In these conditions the total Landau damping octupole strength around the ring was:

$$\int \frac{B'''' dl}{6B\rho} = 3 \text{ m}^{-3}$$

The chromaticity of the Accelerator is corrected using 4 sextupole families. This allows to have an almost flat curve $Q = f(\frac{\Delta P}{P})$.

SPS Set up for Aperture Experiment

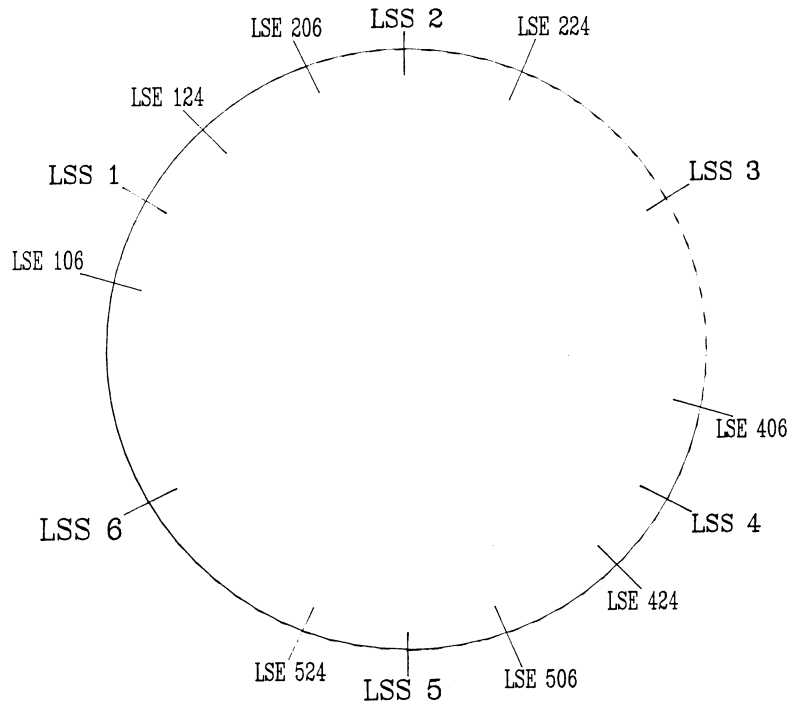


Fig. 1

The nonlinearity has been added by powering 8 sextupoles normally used for extraction purposes. As shown on Fig. 1, these sextupoles are almost regularly spaced around the SPS. During this experiment they have been powered with a current of 140 A which corresponds for each sextupole to a sextupolar strength.

$$\frac{B''l}{B\rho} = 0.28 \text{ m}^{-2}$$

Each of these sextupoles is powered independently so that the excitation pattern around the ring can be changed in order to excite more or less the third order resonance. The different patterns are chosen in any case so as to keep the chromaticity on the central orbit unchanged.

4. TRACKING PROCESS

In order to compare experimental results with calculations, the tracking program PATRAC [2] developed at the SPS has been used. This program uses a linear matrix code for elements up to the quadrupole and

thin lens approximation for higher order elements. The tune is obtained by FFT using up to 4096 turns. Closed orbit distortions can be simulated by randomly distributed displacements of the main quadrupoles.

As an output, together with the phase space plot, the program gives the tune diagram and the smear.

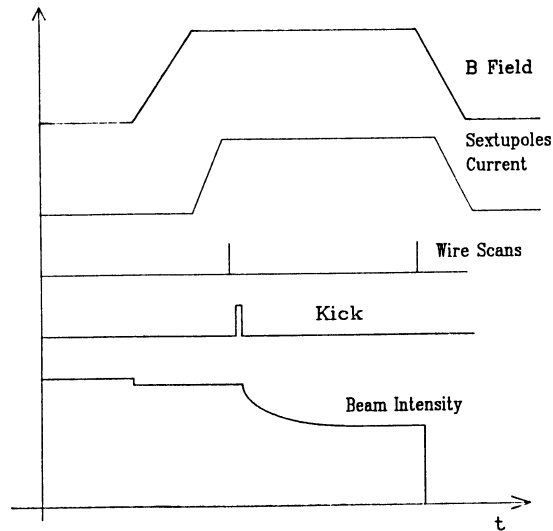
The simulations of the experimental conditions have been made under 4 conditions:

- a) Short term tracking (< 5000 turns) without synchrotron motion.
- b) Short term tracking with synchrotron motion.
- c) Long term tracking (up to 10^5 turns) with synchrotron motion.
- d) Long term tracking including closed orbit distortion.

The synchrotron motion is simulated by changing at the end of each turn the particle energy according to the formula:

$$\frac{\Delta p}{p} = \left(\frac{\Delta p}{p}\right)_0 + \delta p \cos(2\pi \cdot i \cdot Q_s)$$

where $\left(\frac{\Delta p}{p}\right)_0$ is the mean momentum of the particle
 δp is the amplitude of the energy oscillation
 i is the turn no.
 Q_s is the synchrotron tune



Procedure in Pulsed Mode

Fig. 2

5. EXPERIMENTAL PROCEDURE IN PULSED MODE

As it is shown on Fig. 2, after ramping the momentum to 120 GeV/c, the non linear elements are ramped to their nominal current. The beam then receives a kick in order to increase its emittance by a known factor.

One observes a slow loss starting and ending after the kick which ends after a few seconds (2 - 4 sec) and then the beam intensity remains more or less constant. The beam dimensions are measured before the kick and at the end of the flat top when the intensity is constant.

This last measurement gives the largest amplitude of the stable particles and hence the dynamical aperture under these conditions.

6. EXPERIMENTAL RESULTS IN PULSED MODE

The dynamical aperture of the SPS was first measured in the absence of nonlinearities. The vertical aperture has been found to be 14.7 mm (Fig. 3)

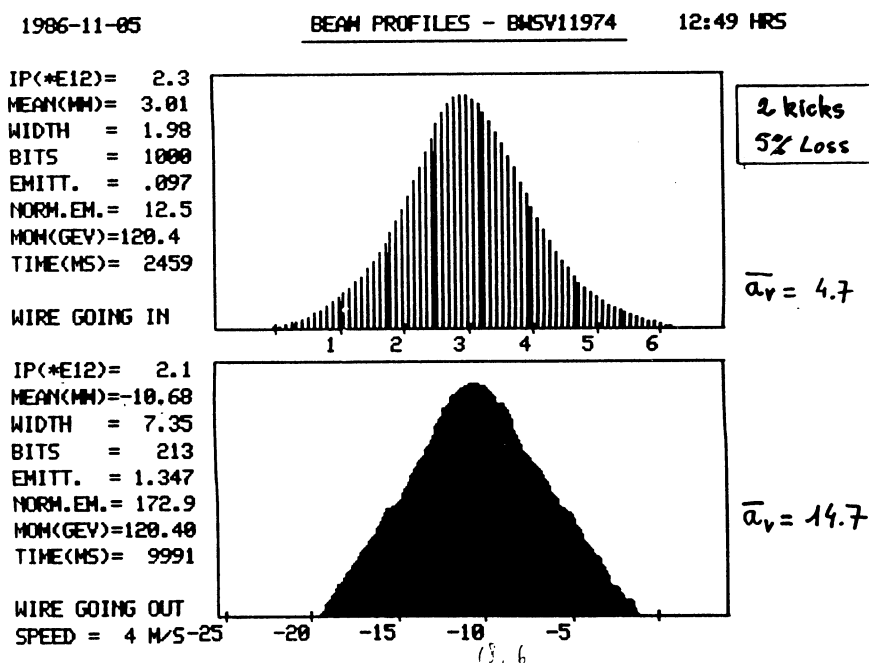


Fig. 3 Vertical Aperture without nonlinearities

(all dimensions are normalised to $\beta = 100\text{m}$). The vertical size of the vacuum chamber is 23 mm and this gives 8.3 mm of closed orbit distortion, misalignments, etc., which is perfectly reasonable at 120 GeV/c in the SPS

The horizontal aperture is far too big and cannot be measured under the same conditions due to coupling.

Without any kick, the beam dimensions are 5.8 mm horizontally and 4.7 mm vertically.

Non linearities were then introduced with a pattern as shown in Fig. 4.

First Sextupole Pattern

+ - - + + - - +

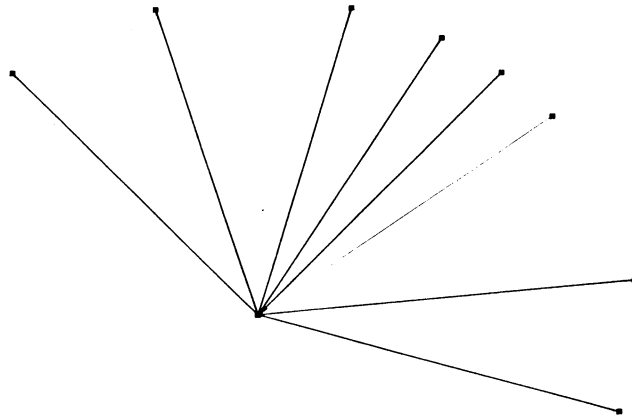
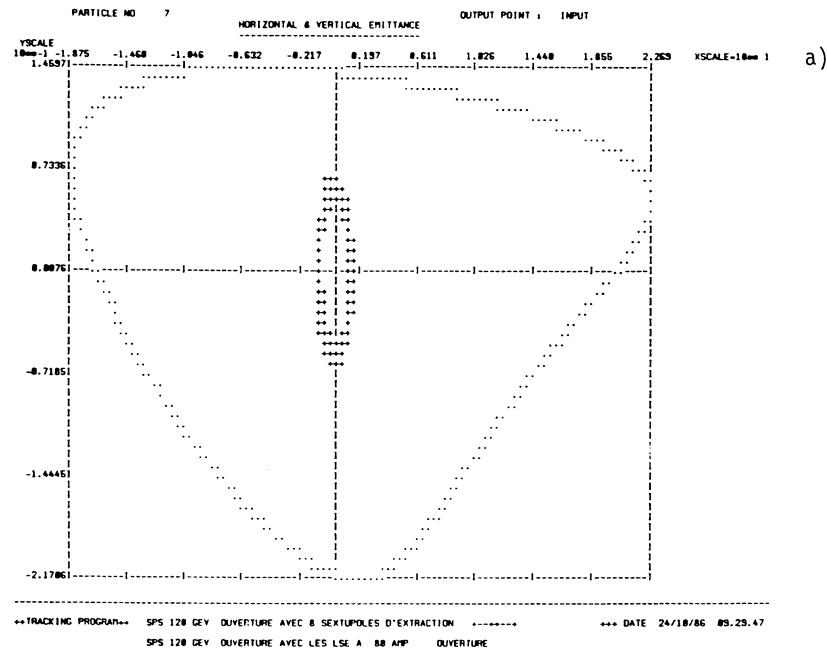


Fig. 4

On this figure, the strength of each sextupole is represented by a vector of which the amplitude is unity and the angle equal to $3\psi_h$ (ψ_h is the usual horizontal betatronic phase). This pattern strongly excites the $1/3$ integer resonance and this results in a triangular phase space as seen on the simulation (Fig. 5a) and visible as well on the flying wire profile (Fig. 5b). The experiment has been repeated for different Q's and different strengths of the nonlinear elements and the results are shown on Figs. 6-8. As expected the dynamical aperture is reduced when approaching the third integer stopband or when increasing the nonlinear strength. For all cases the apertures found by short term tracking are about a factor 2 larger than the experimental ones.

In order to better see the influence of higher order resonances a different pattern, shown on Fig. 9, has been used. This pattern does not excite the third order stopband.



b)

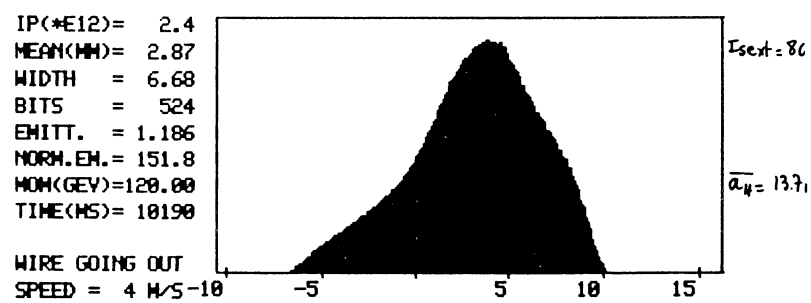


Fig. 5 Phase space from tracking and beam profile

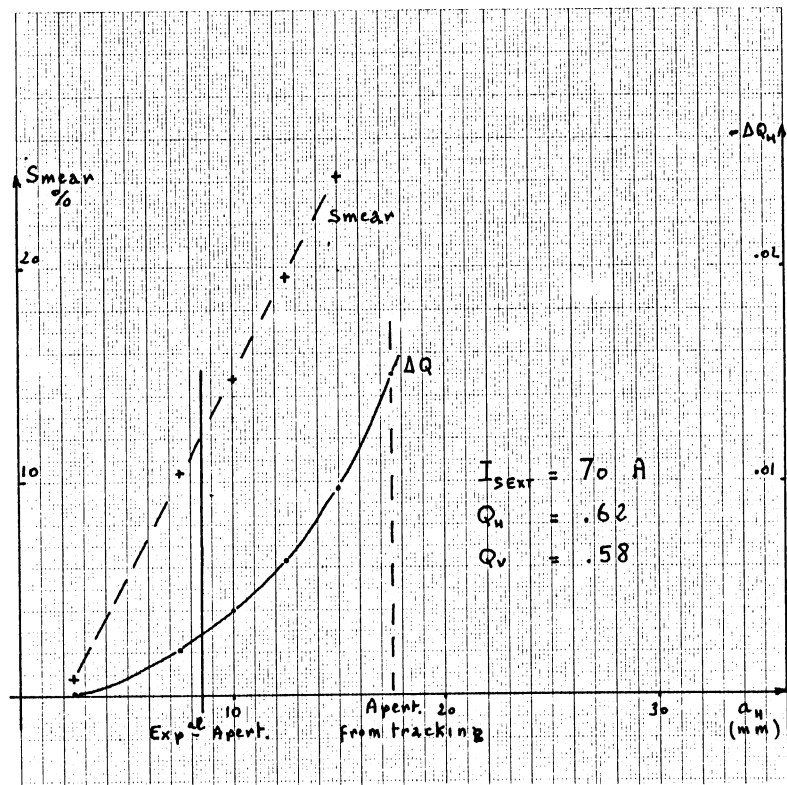


Fig. 6 ΔQ and smear from tracking

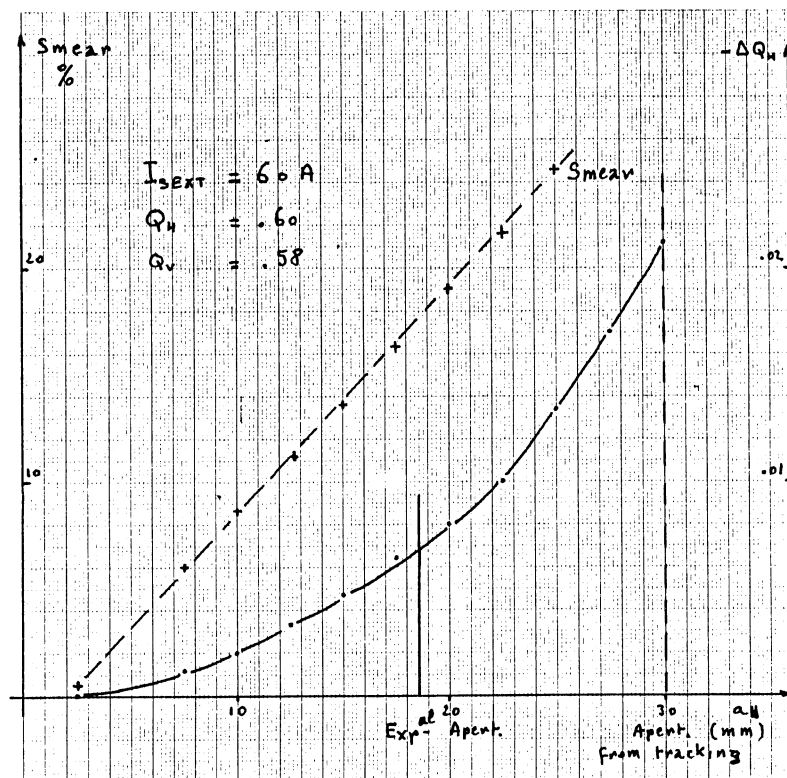


Fig. 7 ΔQ and smear from tracking

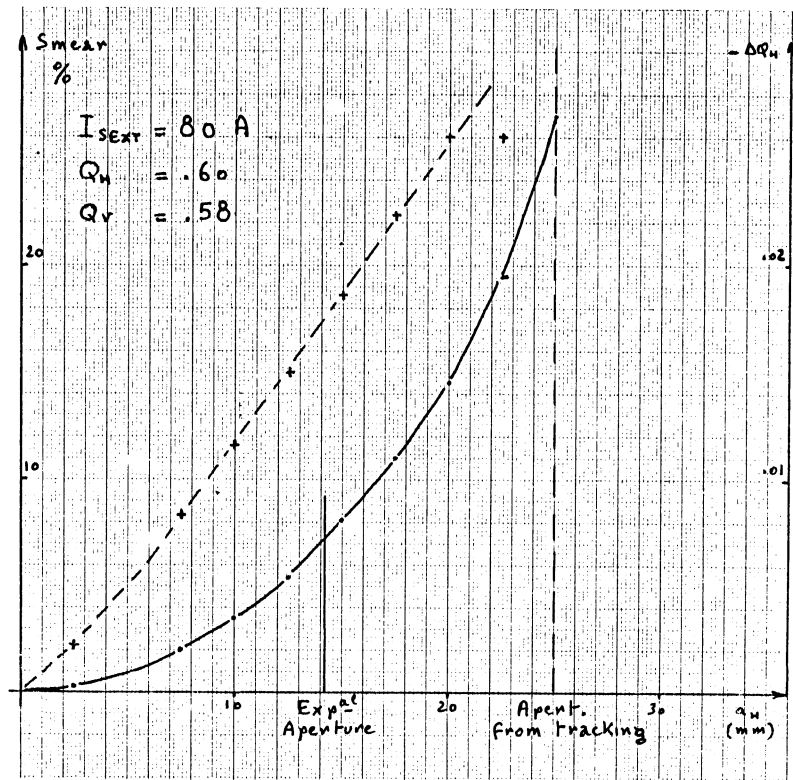


Fig. 8 ΔQ and smear from tracking

Second Sextupole Pattern
 + + + + - - - -

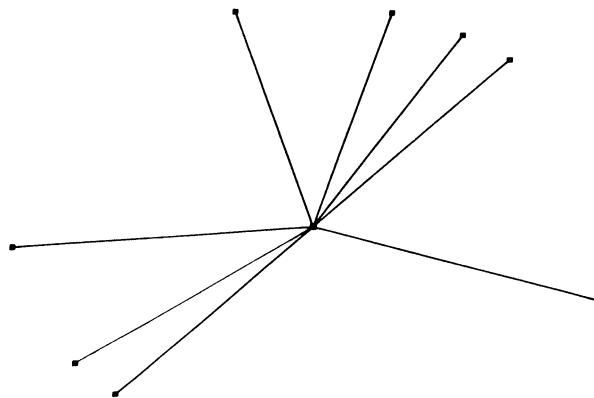


Fig. 9

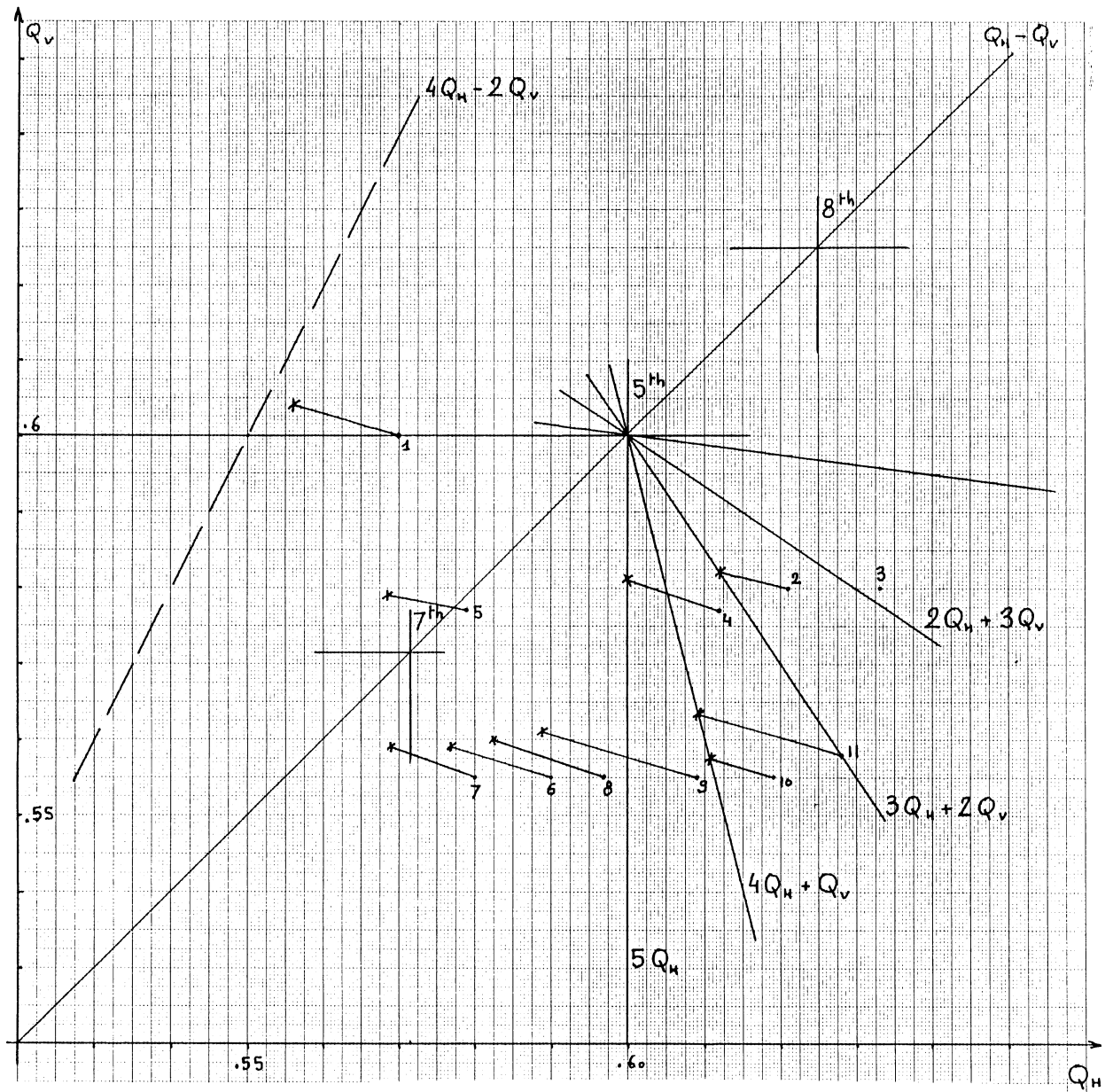


Fig. 10 Experimental points

Figure 10 shows the experimental results. On this figure, the dots represent the tunes of the beam measured before the kick (almost zero amplitude tune) and the crosses represent the tunes of the particle with the largest stable amplitude. These tunes cannot be measured and are calculated from tracking. As can be seen on this figure, for the majority of the experimental cases, the last stable particle is in the vicinity of the $Q_H = Q_V$ diagonal. This clearly reveals the important effect of the coupling in a machine with a flat vacuum chamber.

A few experimental points show the clear influence of one of the 5th order resonances.

Short term tracking has been performed, scanning the tune diagram. As shown on Fig. 11, all the particles are lost when their initial amplitude

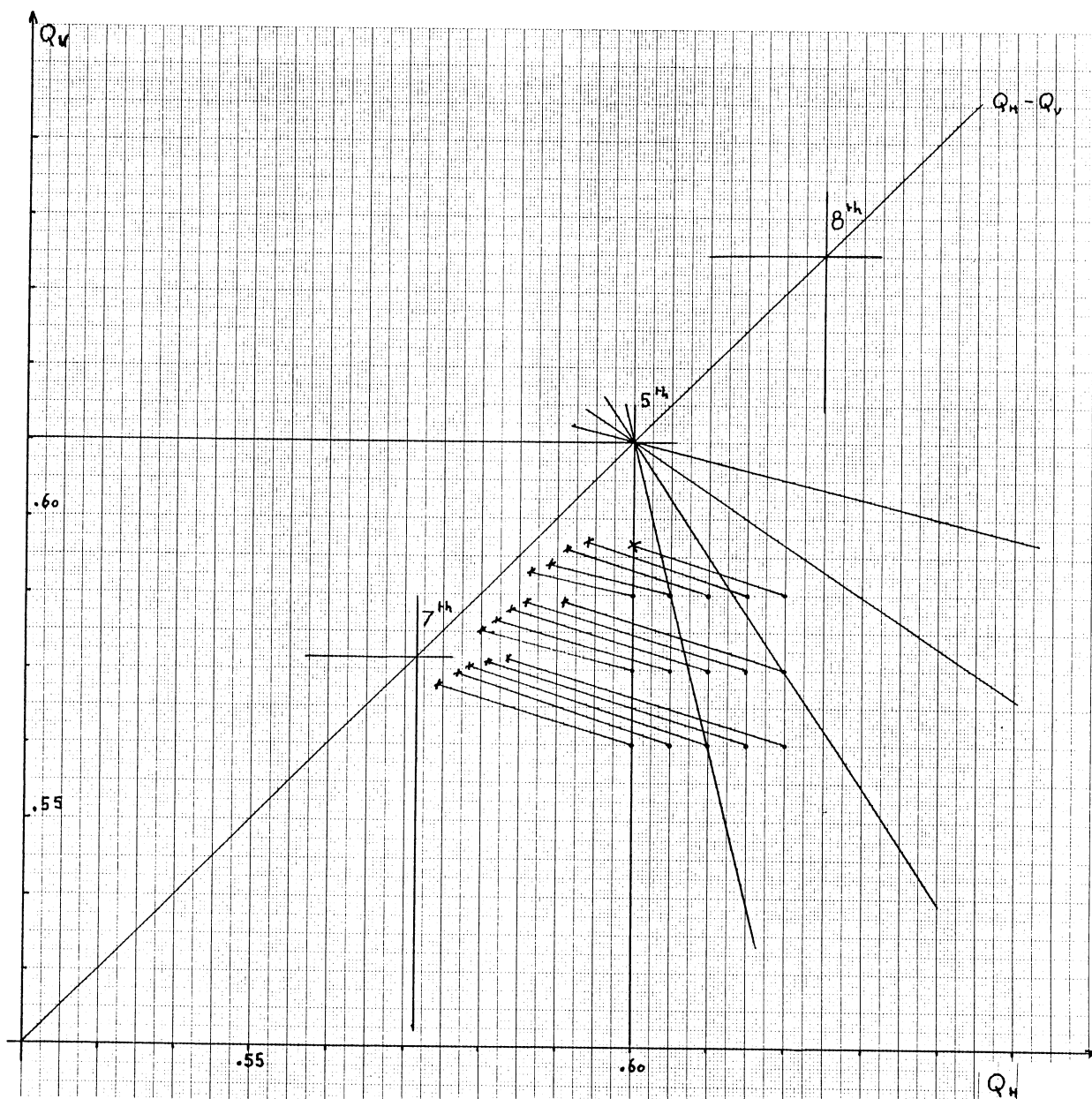


Fig. 11 Results from tracking

is such that their tunes approach the diagonal. The 5th order resonances excitation is clearly visible (Figs. 12-13).

In order to understand why the short term tracking does not show the loss on the 5th order resonances, one experimental point (No. 10) has been chosen and long term tracking has been performed. The results can be seen on Fig. 14 where the amplitude of the particle has been plotted versus the turn numbers. While the first particle keeps a constant amplitude over 10^5 turns, the second one suffers two amplitude jumps before being

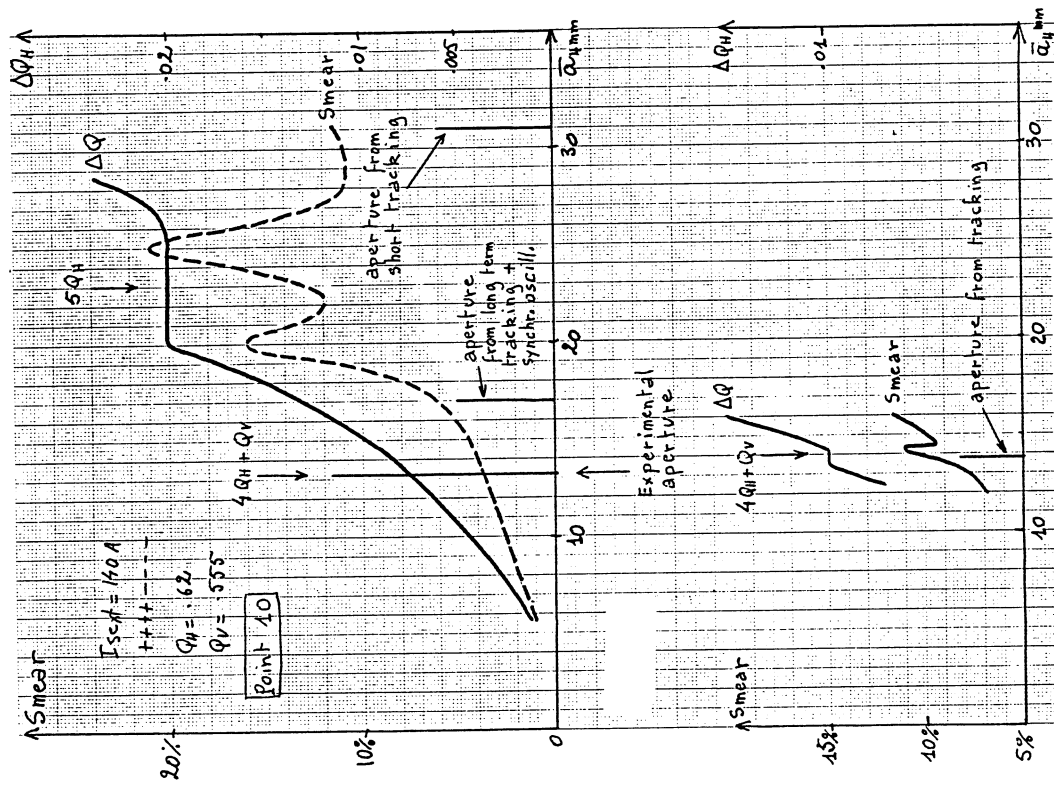


Fig. 13 Smear and ΔQ for experimental point No. 10

Tracking results.

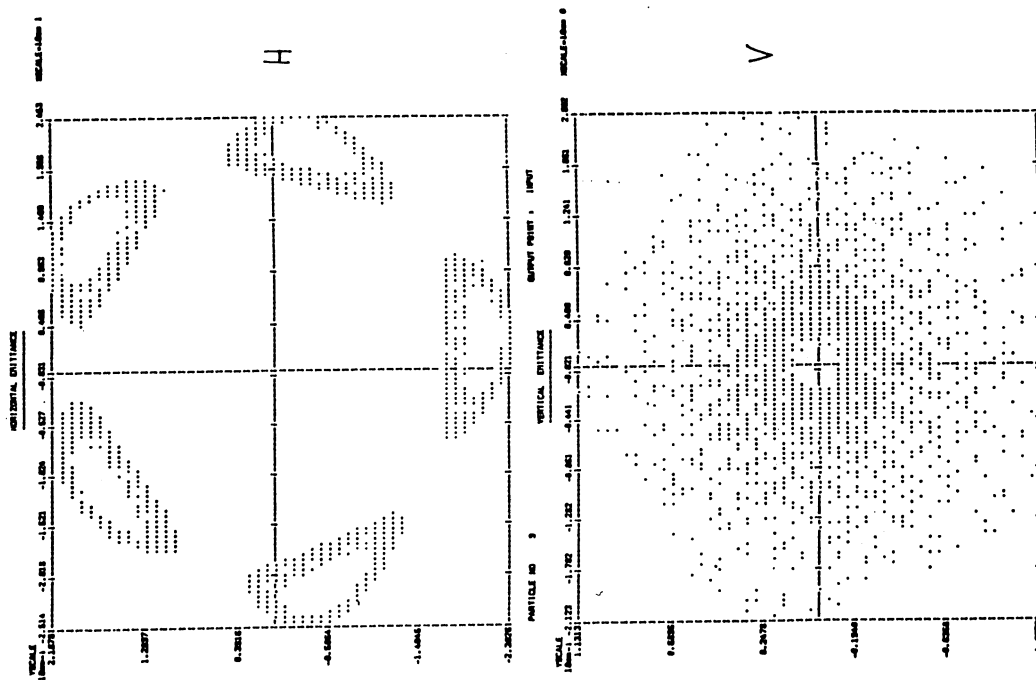


Fig. 12 Horizontal and vertical phase space from tracking



Fig. 14 Long term Tracking.
No closed orbit.
Synchrotron motion included.

lost. Still no evidence of the skew resonance $4 Q_h + Q_v = 133$ can be seen. To do so a vertical closed orbit has to be added in the tracking. Doing this the aperture predicted from long term tracking agrees very well with the experimental one as can be seen on Fig. 13 bottom part.

7. EXPERIMENT IN COAST MODE

The experiments in pulsed mode are adequate to evaluate the stability of particles over a few seconds (this is about 10^5 turns), whereas in proton colliders, the useful lifetimes are of the order of 10h. In order to check the stability limits over longer times, an experiment has also been made in storage at 120 GeV/c. This experiment must be considered as preliminary but the experimental procedure has been developed and some results found.

The procedure for this experiment is the following:

When in storage the non linear elements are energised. Then the beam is blown up until losses occur. The scrapers are then moved towards the beam to find the beam edge, and the beam lifetime is noted. The position of the scrapers at this point gives the dynamical aperture corresponding to this lifetime.

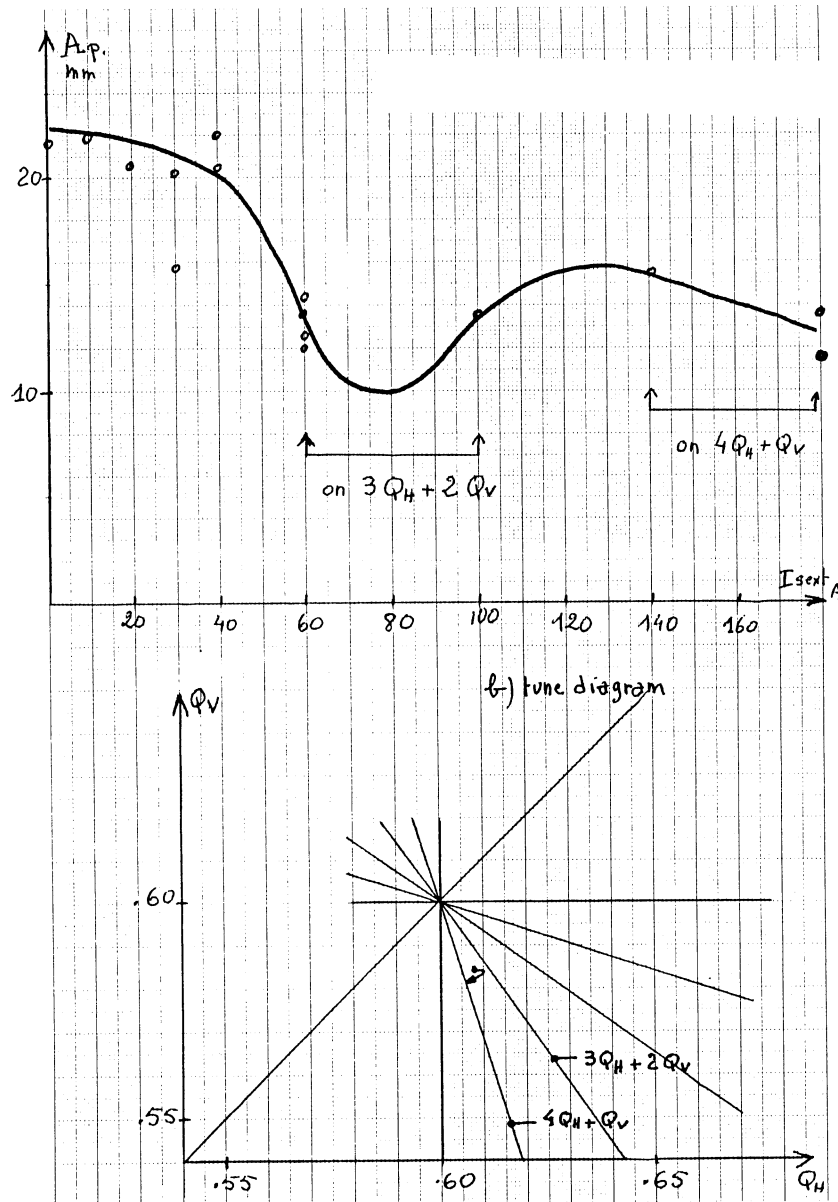


Fig. 15 Aperture study in coast mode.

Figure 15 gives a plot of the dynamical aperture versus sextupole currents. Because this experiment was very preliminary, these measurements are not very accurate, but some general features emerge:

- The dynamical aperture decreases as sextupole current increases.
- The influence of the 5th order resonance is important.

It is to be noted that during this experiment the tunes of the beam have been carefully measured using the Schottky receiver. This permits to identify the experimental points where the beam sits on a given resonance.

8. CONCLUSIONS

- The validity of the criterion used to define the "linear aperture" in the LHC studies is confirmed ($\Delta Q < .005$ and smear $< 3.5\%$).
- Dynamical apertures found by tracking over a few turns ($10^2 - 10^3$) are at least a factor 2 bigger than the experimental ones.
- The importance of the 5th order resonances excited by sextupoles is clearly demonstrated.
- The experiment in storage mode has to be done again to increase the precision of the results.

ACKNOWLEDGEMENTS

The experiments reported here have been carried out by a team comprising L. Evans, J. Gareyte, W. Scandale, L. Vos and the author. The SPS operation crews, and in particular K. Cornelis, A. Faugier, R. Lauckner and D. Thomas, were very helpful in setting up the machine in the special conditions required.

REFERENCES

- [1] SPS Improvement Report 209, 22nd July, 1987.
- [2] PATRAC: A program for single particle tracking, A. Hilaire A. Warman, CERN SPS/88-8 (AMS), 1988.

THE DYNAMIC APERTURE OF BESSY

Bettina Simon and Peter Kuske

BESSY GmbH, Berlin, Federal Republic of Germany

ABSTRACT

We measure the dynamic aperture of the electron storage ring BESSY. The experimental results are compared to tracking calculations.

1. INTRODUCTION

To provide a large enough dynamic aperture is one of the most difficult requirements in the design of low emittance storage rings for synchrotron radiation as they are planned e.g. in Berlin (BESSY II), Berkeley (1-2 GeV Synchrotron Light Source), Trieste (Sincrotrone Trieste) and Grenoble (European Synchrotron Radiation Facility). Usually the dynamic aperture is estimated by tracking calculations. We measure the dynamic aperture of the BESSY storage ring. The experiments and their results are presented and compared to tracking studies.

BESSY is a dedicated light source using an 800 MeV electron storage ring with a relatively low emittance of $4 \cdot 10^{-8} \pi \cdot m \cdot rad$. Though the beam itself is very small, single electrons reach large amplitudes when they are scattered at residual gas molecules. These electrons are either damped back into the beam or get lost as they eventually hit the vacuum chamber. The boundary between stable and unstable motion is called the dynamic aperture of the ring. The smaller the aperture the smaller the lifetime, as more scattered particles exceed the aperture and will get lost.

For the experimental determination of the dynamic aperture we measure the lifetime as a function of artificially restricted physical apertures. As long as this aperture limitation lies outside the stable area of electron motion, the lifetime should be constant. At the point where it restricts the motion of stable electrons a clear reduction of the lifetime should be observable. This point corresponds to the dynamic aperture of the ring.

2. THE MEASUREMENT

BESSY has been described in the literature [1], but for the present study we have collected updated data about the electron optic and other relevant storage ring parameters in Appendix 1.

The basic idea of our experiment is to measure the lifetime as a function of a variable aperture. The variation of the transverse aperture is accomplished with stepping motor driven mechanical scrapers which can be moved towards and away from the beam by the computer.

To keep the interpretation of the experimental results simple, the measurements were performed at very low beam currents ($< 1\text{mA}$) where current dependent instabilities, the Touschek effect, and the trapping of positively charged ions in the potential of the electron beam can be neglected [2]. The determination of

the lifetime is based on accurate current measurements. The current is measured through its synchrotron radiation with a windowless photodiode at one of the beamlines of the PTB [3]. This diode is sensitive enough to detect even a single stored electron, and its signal is proportional to the beam current. We have developed a fast lifetime monitor which determines the beam lifetime within 5-10 sec [4] from the photocurrent.

In the experiments the scraper is moved in small steps of a few tenth of a millimeter. For every step the lifetime is determined. The aperture restriction, the lifetime and the statistical error are stored in the computer for later data analysis. When the lifetime sinks to less than 100 min the scraper is moved back out, in order not to lose the beam, and the next measurement can start under nearly identical conditions. We can also vary the strength of one quadrupole family, in order to measure the aperture for different tunes. The whole experiment is done automatically, and it is possible to perform up to 40 scraper measurements for different quadrupole settings without injection.

2.1 Interpretation of the measurements

The decay rate of an electron beam in a storage ring as a function of an aperture restriction Δ is always given by a sum of two contributions - one independent (τ_0) and one dependent on the aperture ($\tau_1(\Delta)$):

$$\frac{1}{\tau_{total}} = \frac{1}{\tau_0} + \frac{1}{\tau_1(\Delta)} \quad (1)$$

In an actual measurement the effects contributing to τ_0 and τ_1 differ for the particular aperture restriction chosen. The current dependence can be neglected under the experimental conditions described above.

Two aperture dependent effects contribute to the lifetime. The first dominates for small and the second for large apertures. In an intermediate range of apertures the description is complicated as both effects overlap.

1. When the aperture is small enough to lie within the tails of the assumed Gaussian particle distribution the lifetime is dominated by the quantum lifetime $\tau_{quantum}$ [5]:

$$\tau_{quantum} = \tau \cdot \frac{\sigma^2}{\Delta^2} \cdot e^{\frac{\Delta^2}{2\sigma^2}} \quad (2)$$

with

- τ longitudinal or transverse damping time
- σ rms-width of longitudinal or transverse particle distribution function
- Δ transverse aperture or longitudinal acceptance

The quantum lifetime dominates for apertures smaller then six times the natural width of the beam: $\Delta < 6 \cdot \sigma$

2. For apertures much larger then the beam size ($\Delta > 10 \cdot \sigma$) the electrons scattered by residual gas particles determine the lifetime of the beam. The aperture dependence of the lifetime can then be calculated assuming a δ -distribution of the electrons.

2.a) Elastic Scattering

The interaction of an electron with the Coulomb field of the nucleus of a residual gas particle leads to an angular kick θ in the betatron motion. In linear theory, the emittance, E , of the scattered electron is

lost if the square of the aperture, Δ , at another location, s_0 , with beta function, β_0 , is equal to $E \cdot \beta_0$:

$$\Delta^2 = E \cdot \beta_0 = \theta^2 \cdot \beta_{scat} \cdot \beta_0 \quad (3)$$

The total scattering cross section is proportional to $1/\theta^2$. To include all scattering events, one has to integrate over the circumference of the ring. This leads to [6]:

$$\frac{1}{\tau_{coul}} = constant \cdot \left(\frac{\langle \beta_x \rangle \cdot \beta_x(s_0)}{\Delta_x^2} + \frac{\langle \beta_z \rangle \cdot \beta_z(s_0)}{\Delta_z^2} \right) \quad (4)$$

The lifetime increases quadratically with aperture. The constant depends on the energy, the residual gas, and other parameters [7].

2.b) Inelastic Scattering

In an inelastic collision the electron loses energy by emitting Bremsstrahlung. The electron will be lost if its energy deviation exceeds the longitudinal acceptance, Δ_{long} , of the ring or if the increased emittance in the dispersive plane exceeds the transverse aperture. In the second case, the longitudinal acceptance is a function of the transverse aperture. Usually the longitudinal acceptance is determined by the RF cavity voltage, but it can also be restricted by energy dependent tune shifts and the crossing of fatal resonances. The contribution to the lifetime for the interaction with a screened nucleus is given by:

$$\frac{1}{\tau_{brems}} = constant \cdot \left(\ln \frac{1}{\Delta_{long}} - \frac{5}{8} \right) \quad (5)$$

The lifetime grows only with the logarithm of the aperture. The constant does not depend on the energy but as in the case of elastic scattering depends on the residual gas [7].

The situation in an intermediate range of apertures ($6 \cdot \sigma < \Delta < 10 \cdot \sigma$) is complicated by the finite extent of the beam. In this region the lifetime should be smaller than expected when simply assuming a δ -distribution of the electrons.

2.2 Data analysis

In order to extract the dynamic aperture from a scraper measurement we need to know the position of the beam center with respect to the position of the scraper where it starts to reduce the lifetime. The dynamic aperture is given by the difference between these two positions, which can be determined by a fitting procedure. The fit function depends on the different contributions to the lifetime and might be very complicated.

The vertical profile of the electron beam is extremely small with a σ_z of 0.07 mm and the scraper is moved back out long before the intermediate range of apertures, 10σ , is reached. Therefore, we can assume a δ -distribution for the beam and disregard the quantum lifetime and the effects in the range of intermediate apertures. Thus the theoretical function for the fit is very simple [8]:

$$\frac{1}{\tau_{theo}} = P_1 + \frac{P_2}{D^2} \quad (6)$$

where D is the effective aperture, i.e. either the aperture of the machine, Δ_z , or the aperture determined by the mechanical scraper, if this is smaller than Δ_z . If Z is the variable position of the scraper and Z_0 denotes the center of the beam, then D is given by:

$$D = |Z - Z_0| \text{ for } \Delta_z > |Z - Z_0|$$

$$D = \Delta_z \text{ for } \Delta_z < |Z - Z_0|$$

The term P_1 contains all contributions to the lifetime independent of the vertical aperture, namely the losses in the horizontal plane or at the energy acceptance, whereas P_2 stems solely from the vertical elastic Coulomb scattering.

We use a linear least squares fit to determine the fit parameters P_1 and P_2 . The aperture Δ_z and the beam center Z_0 are varied until the sum of the squared errors, $(\frac{1}{\tau_{theo}} - \frac{1}{\tau_{exp}})^2$, over all individual lifetime measurements reaches a minimum. A satisfactory fit function for the horizontal measurement has not yet been developed.

3. RESULTS

3.1 Lifetime as a function of aperture

In Figure 1 we show the experimental and theoretical results for the lifetime as a function of vertical and horizontal aperture restrictions. For the vertical scraper measurement (left) the agreement between the theoretical fit function and experiment is excellent. From this measurement we can determine the vertical position of the beam and the vertical aperture with an uncertainty of only .1 mm: $\Delta_z=17.4$ mm. The fit parameter P_2 can be used to estimate the residual gas pressure. With an averaged nuclear charge of $Z=7$ it turns out to be 3.3 nTorr. We use these figures, the constants given by LeDuff [7] and the storage ring parameters as listed in Appendix 1 to calculate the theoretical lifetime for the horizontal measurement (right). In the horizontal plane the aperture, Δ_x , is approximately 10 mm.

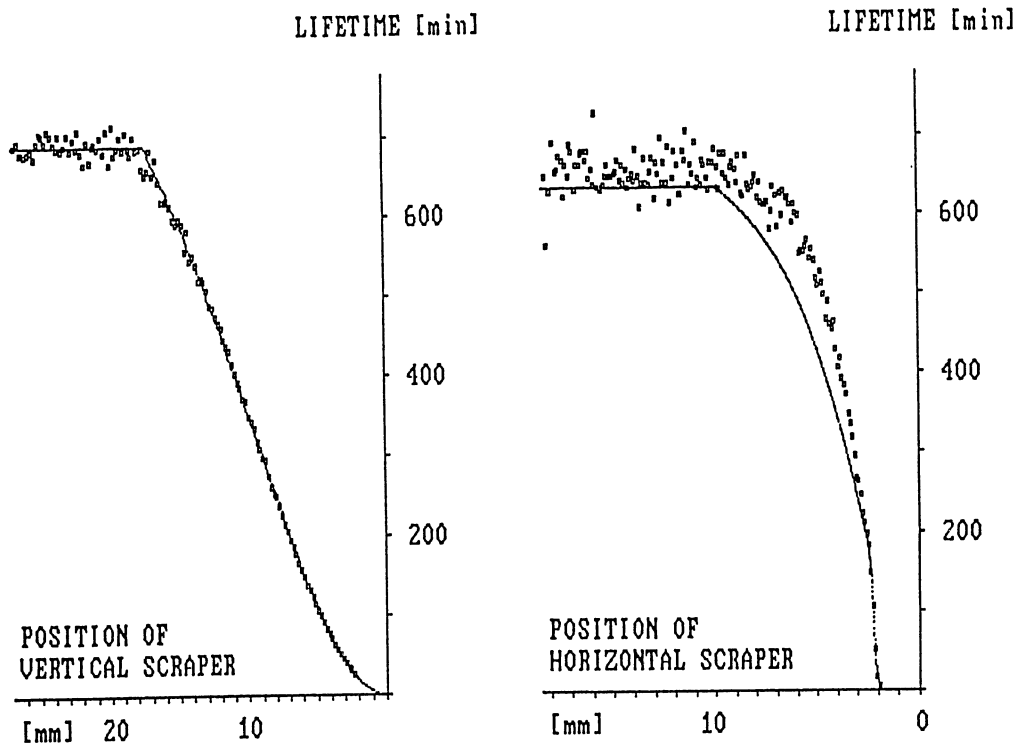


Figure 1: Experimental results and theoretical calculation of the lifetime as a function of transverse aperture restrictions.

In the case of horizontal aperture restriction, the quantum lifetime is dominant for small apertures. This shows up as a steep decrease in lifetime for apertures around 5 to 6 σ (right). We cannot expect to find more than general agreement between theory and experiment in the horizontal plane because of the large beam size ($\sigma_x=0.4\text{mm}$) and the energy dependent effects. It is obvious that the horizontal aperture of $\approx 10\text{ mm}$ is surprisingly small!

3.2 Tune dependent aperture measurements

The dynamic aperture of a machine is a property related to a whole area in the tune diagram and not relevant at a singular point. The dynamic aperture at the actual working point depends strongly on the nearby resonances, but might be influenced by far away structure resonances as well. Only the knowledge of the aperture at various tunes will yield an understanding of the mechanism that determines the aperture. Therefore, and in order to learn something about the existing non-linearities in the storage

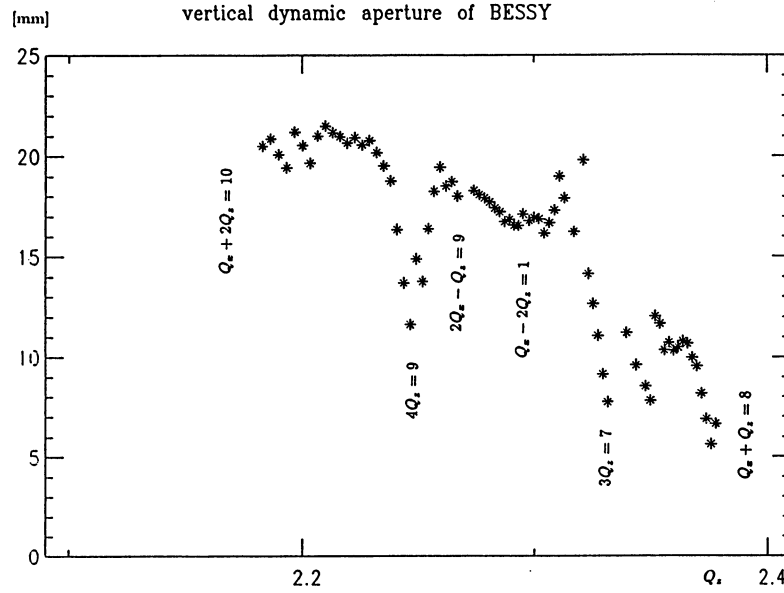


Figure 2: The measured vertical dynamic aperture of BESSY as function of the vertical tune

ring, we measured the dynamic aperture as a function of the linear tune.

In Figure 2 we show the vertical dynamic aperture of BESSY as a function of the vertical tune. Every star in the plot represents the result of one complete scraper measurement, each for a different quadrupole setting. The tune is moved through the tune diagram and crosses several resonances. This results in a strong tune dependent variation of the aperture.

Figure 3 shows the initial lifetime of each scraper measurement in Figure 2. The initial lifetime can be determined very accurately by averaging over all lifetime measurements taken before the scraper reaches the aperture. There is an obvious correlation between the lifetime and the aperture. This effect, which only occurs in the vertical dimension, can be explained by the fact that the lifetime at very low beam currents is dominated by the vertical losses. Any further reduction of the vertical aperture, here due to resonances, must immediately cause a shortage in lifetime. Lifetime measurements are much easier and faster to make

than aperture measurements. We used the correlation between the two to verify the identification of the various resonances seen in the aperture measurement. From the shift of corresponding dips in additional lifetime measurements with slightly changed horizontal tunes all resonances could be identified clearly.

The dynamic aperture and thus the lifetime shown in Figure 2 diminish towards higher vertical tunes. This decay is due to the influence of the structure resonance $Q_x + Q_z = 8$. This resonance is the strongest resonance in the surroundings of our regular working point, and has a stopband width of ≈ 0.04 .

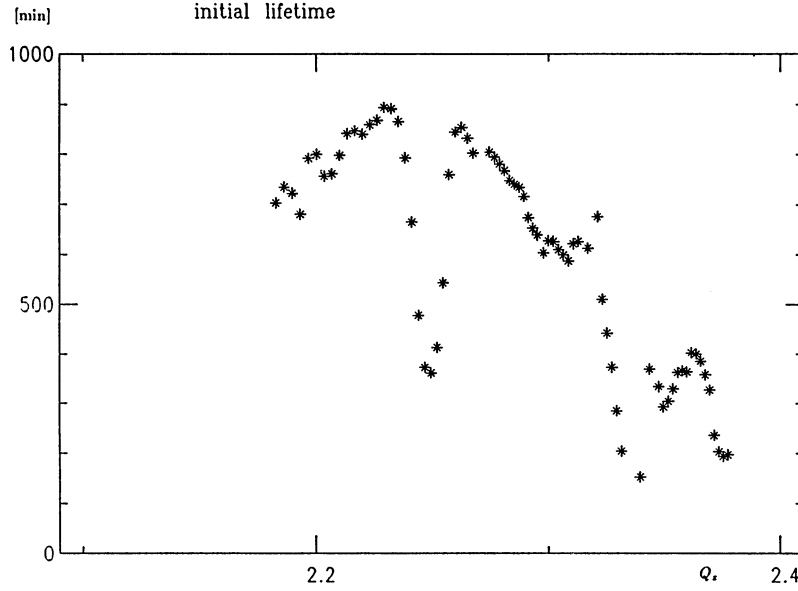


Figure 3: Initial lifetime extracted from the vertical scraper measurements shown in Figure 2

Towards lower vertical tunes the dynamic aperture gradually increases, until it reaches the physical aperture of the ring, which is ≈ 20 mm. The latter is determined by the vacuum chamber of the dipoles or the septum magnet for the vertical injection. The lower limit for the tune variation is set by the $Q_x + 2Q_z = 10$ resonance, which is also destructive. $Q_x + 2Q_z = 10$ is driven by random normal sextupole components. To check whether these components come from our regular sextupoles, we repeated the measurement with the sextupoles turned off. Without sextupoles the influence of the resonance is still very strong, but it no longer causes a beam loss. This means that our regular chromaticity compensating sextupoles only enhance another strong sextupole component in the ring. Whether it stems from the higher field components of the dipoles, which are not shimmed to improve the field quality, from the steerers or from the strong fringe fields due to the dense magnet structure of the BESSY ring, still has to be investigated.

Some other resonances can be clearly identified. $4Q_z = 9$ is a higher order normal sextupole resonance, and must be driven by our regular sextupoles, as it disappears when we turn the sextupoles off. The same is true for $Q_x - 2Q_z = 1$. As a difference resonance it is much weaker than the corresponding sum resonance, which cannot be crossed.

Two resonances are driven by skew sextupole components. $3Q_z = 7$ leads to a strong reduction of the lifetime, whether the sextupoles are turned on or off. $2Q_x - Q_z = 9$ can hardly be seen in this measurement, but one of the lifetime measurements proves its existence. Skew sextupole fields might stem from vertical steerers, from the last vertical injection dipole or again might be due to strong fringe fields.

We do not have any explanation for the decrease in aperture and in lifetime above the $3Q_z = 7$ resonance. Though this dip appears in all measurements with and without sextupoles, and is always rather strong, it does not coincide with any lower order resonance.

Though the actual sources of the field components driving these resonances still have to be located, one can say that the measured vertical dynamic aperture of BESSY can be understood on the basis of common knowledge about resonances. Choosing an appropriate working point, one can reach optimal lifetimes, as the dynamic aperture starts to become bigger than the linear aperture of the machine.

The situation is quite different in the horizontal plane. All horizontal scraper measurements indicate a frighteningly small aperture around 10 mm, independent of the tune and the settings of the sextupoles.

4. TRACKING CALCULATIONS

For all our tracking calculations we use the computer program RACETRACK written by A. Wrulich [10]. RACETRACK is a kick code using the thin lense approximation to transform the particle trajectories through higher order fields. Most of the calculations that involve more than one run of RACETRACK where automated by a package of command procedures. These procedures perform successive RACETRACK runs changing specific input parameters and store the desired results.

The dynamic aperture calculated with tracking programs for a given lattice depends strongly on the choice of the starting conditions, the number of tracked turns, and the other input parameters such as coupling or energy deviation.

RACETRACK can track up to 16 particles (4 per plane), distributed on the horizontal and vertical linear phase space ellipses. Using the equation of the phase space ellipse and the coupling parameter between the two planes, the initial conditions of all 16 particles can be related to one horizontal amplitude. This amplitude is only considered stable when all particles survive the specified number of turns.

Starting one particle with an amplitude only, ($p_x = 0$), the calculated dynamic aperture (5000 turns) for the BESSY lattice without any linear aperture limitations is 47.8 mm. The error is on the order of a couple of millimeters when the number of turns is reduced. Tracking a particle started with an initial phase of $p_x = 90^\circ$ and $x = 0$, the aperture reduces to 33.4 mm.

We track four particles lying equidistantly on the linear phase space ellipse. Thus our aperture will be symmetric for positive and negative amplitudes and phases. The determined aperture will correspond to the biggest linear phase space ellipse inscribed in the nonlinear phase space. We track this ensemble of particles for 50 turns. This yields a rather pessimistic dynamic aperture of 24 mm, but an error smaller than 1 mm.

The aperture limitations are set by the acceptance of the ring, which is defined by the 20 mm half gap of the dipoles or the septum magnet in vertical and the 40 mm quadrupole chamber of the second focussing quadrupole in horizontal direction.

In the lattice input the fringe field of the rectangular dipoles and the reduction of the quadrupole field due to the short distance between two oppositely poled quadrupoles [1] is taken into account. The dipole

fringe field and the optical length and field reduction of the quadrupoles where adjusted to reproduce the linear behaviour of the ring as it has been determined by measuring the linear tunes and the beta functions. The sextupoles were tuned by RACETRACK to yield a slightly positive chromaticity, $\xi_x = 2.0$ and $\xi_z = 0.7$.

As in the measurement, we vary one quadrupole family and calculate the variation of the aperture along a line through the tune diagram.

To determine the vertical aperture we start the particles with vertical amplitudes and phases only. The horizontal coordinates are set to zero. The regular sextupoles of the lattice will couple the vertical motion into the horizontal plane and the particle will develop some horizontal emittance.

We started tracking the regular lattice without any errors or extra higher order fields. The influence of the second order structure resonance, $Q_x + Q_z = 8$, is very pronounced as the aperture steadily increases from this resonance to the linear aperture of the ring. In a regular symmetric lattice, only structure resonances are driven, so no further shaping of the aperture curve could be expected.

The measurement indicated a strong random sextupole component. We introduced one additional normal sextupole ($2m^{-2}$) in the middle of the straight section and obtained the aperture curve shown in Figure 4. The decay of the aperture towards the structure resonance is still visible. As in the measurement, the strongest resonance aside from the structure resonance is $Q_x + 2Q_z = 10$. It reduces the aperture to a couple of millimeters, corresponding to a loss of beam. The related difference resonance, $Q_x - 2Q_z = 1$, is much weaker, as expected. The higher order sextupole resonance, $4Q_z = 9$, also occurs, but it is wider and less deep than in the measurement.

All resonances were determined by tracking single particles for the corresponding quadrupole setting

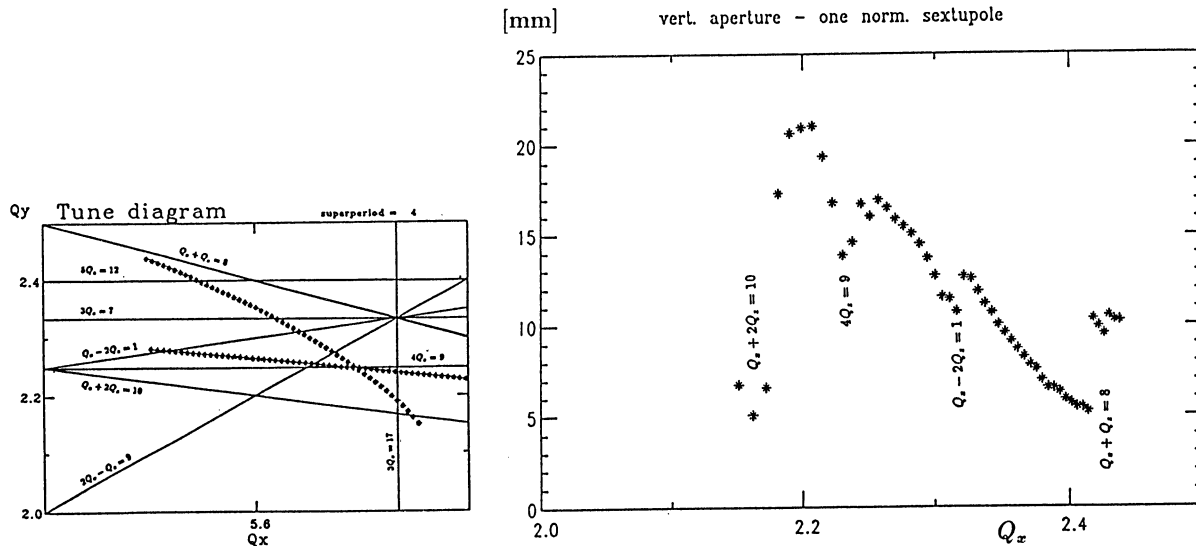


Figure 4: The vertical dynamic aperture of BESSY determined by tracking calculations as a function of the vertical tune. One random normal sextupole has been introduced into the lattice to drive the regular sextupole resonances.

and Fourier analysing their motion to determine the non-linear tune. Often a plot of the one dimensional phase space or a plot of the x,z-plane helps to identify the resonance.

To reproduce the skew sextupole resonances, one skew sextupole was inserted in the lattice, but the sharp and deep structure of the $3Q_z = 7$ resonance seen in the measurements could not be reproduced. The skew resonances do show up, but, in combination with the regular sextupole components, they lead to unrealistically broad dips of the aperture. One should track statistically distributed small skew sextupole components to see whether the interference of various sources yield results closer to the measurement.

As in the experiment, the horizontal plane is more complex than the vertical plane in the calculations. In order to avoid tracking purely horizontal motion, which doesn't occur in a real machine, we use a small coupling factor of 1%. Again four particles were spread on the horizontal phase space ellipse, but each particle was combined with four vertical initial conditions. Off energy particles have not yet been investigated.

As the limiting resonances in the measurements are not structure resonances, one has to introduce irregularities into the lattice in order to drive these resonances. Figure 5 (left) shows a tracking run (purely horizontal motion) for a lattice with randomly distributed quadrupole components. Introducing the coupling to the vertical plane and the one normal sextupole used in vertical tracking, the aperture shown in Figure 5 (right) results. The influence of the horizontal third order resonance is reduced, and coupling resonances like $Q_x - 2Q_z = 1$ appear. The importance of this run is to show that the small horizontal dynamic aperture of approximately 10 mm that we measured, does in principal agree with the tracking calculations. Using other random error distributions or energy deviation might reduce the aperture even further.

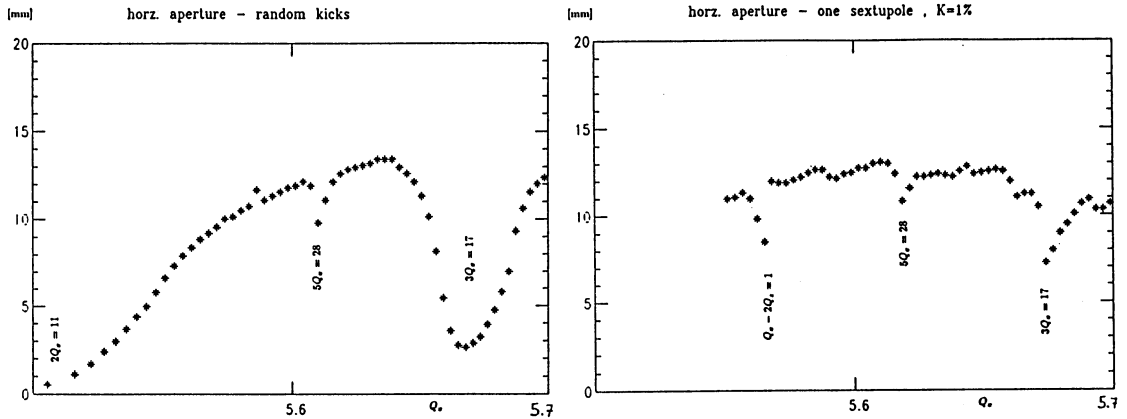


Figure 5: The horizontal dynamic aperture of BESSY determined by tracking calculations under variation of one quadrupole family. Left: tracking with purely horizontal motion and random kicks at every sextupole. Right: one random normal sextupole has been introduced into the lattice and the coupling to the vertical motion is 1%.

5. CONCLUSIONS

We show how to experimentally determine the dynamic aperture of a storage ring. The experiment is based on lifetime measurements as a function of a variable aperture. The fitting of the data involves only the known loss mechanisms of electrons in a storage ring. The theoretical background and the resulting problems in the analysis of the data have been explained. The measured dynamic aperture of BESSY is larger than the physical aperture in the vertical plane, but reaches only about 10 mm in the horizontal plane.

We have shown that the analysis of tune dependent measurements are an excellent tool to study the existing non-linearities of a ring. The simulation of the measured data by tracking calculations leaves space for much further work and requires a thorough understanding of the linear machine. We were able to explain and to calculate the principle behaviour of the measured dynamic apertures, but one should proceed to investigate which choice of input parameters for the tracking calculations yields the best agreement with reality.

6. ACKNOWLEDGEMENTS

We would like to thank Dr. G. Ulm from the Physikalisch Technische Bundesanstalt who allowed us to use the photodiode and always helped us with the setup. As most scientific work this paper is based on the continuous and reliable work of many people. We thank the BESSY machine group.

References

- [1] G. Mühlaupt et al., International Conference on Insertion Devices for Synchrotron Sources (1985), SPIE Vol. 582, p. 118
- [2] P. Kuske et al., Proceedings of the 1987 IEEE Particle Accelerator Conference, Vol. 1, p. 535
- [3] S. Bernstorff et al., BESSY, Technischer Bericht 1988 and Contribution to "The 3rd International Conference on Synchrotron Radiation Instrumentation: SRI-88" Tsukuba, Japan (1988)
- [4] P. Kuske, BESSY Jahresbericht 1987, p. 354
- [5] M. Sands, SLAC-121,UC-28 (1970)
- [6] H. Wiedemann, ESRP-IRM-10/83
- [7] J. Le Duff, Nucl. Instrum. Methods, Vol. A239 (1985) 83
- [8] P. Kuske et al., International Conference on Insertion Devices for Synchrotron Sources (1985), SPIE Vol. 582, p. 143
- [9] E. Weihreter et al., IEEE Trans. NS-32 (1985) 2317
- [10] A. Wrulich, DESY 84-026, March 1984

Appendix 1

Linear optic parameters

$E =$	$800 MeV$	electron energy
$\sigma_E =$	$5 \cdot 10^{-4}$	relative rms-width of the natural energy distribution
$U_0 =$	$20.8 keV$	energy loss by radiation in one revolution
$\alpha =$	$1.3 \cdot 10^{-2}$	momentum compaction factor
$h =$	104	harmonic number of the RF-system (500 MHz)
$\epsilon_x =$	$4 \cdot 10^{-8} \pi \cdot m \cdot rad$	natural horizontal emittance
$\epsilon_z =$	$4 \cdot 10^{-10} \pi \cdot m \cdot rad$	vertical emittance (1 percent coupling)
$\langle \beta_x \rangle =$	$3.8 m/rad$	average of the horizontal betatron function
$\langle \beta_z \rangle =$	$7.9 m/rad$	average of the vertical betatron function
$\beta_x =$	$3.5 m/rad$	horizontal betatron function at the scraper
$\beta_z =$	$13.5 m/rad$	vertical betatron function at the scraper
$\sigma_x =$	$0.38 mm$	horizontal beam size at the scraper
$\sigma_z =$	$0.07 mm$	vertical beam size at the scraper
$\tau_x =$	$17.4 msec$	horizontal damping time
$\tau_z =$	$16.1 msec$	vertical damping time
$\tau_l =$	$7.8 msec$	longitudinal damping time
symmetry	4 fold	

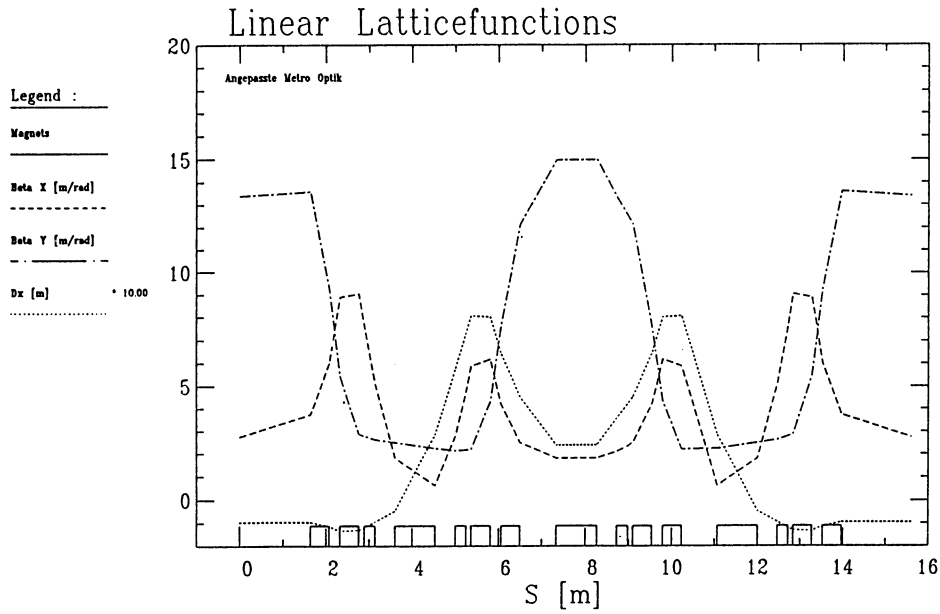


Figure 1: Linear latticefunctions of the BESSY METRO-optic

HAMILTONIAN THEORY OF THE E778 NONLINEAR DYNAMICS EXPERIMENT

S.G. Peggs

SSC Central Design Group, Berkeley, California, USA

ABSTRACT

Short, medium, and long time scale Hamiltonians describing the E778 experiment are presented, corresponding to smear, capture fraction, and tune modulation types of measurements. A one-turn "discrete" Hamiltonian representing motion in the presence of thin multipoles is derived from nonlinear projection maps, leading to expressions for distortion functions, Fourier spectra, normalized covariances, and smear. An N-turn Hamiltonian is derived representing motion at a tune near a rational fraction I/N , leading to expressions for detuning, resonance island width, resonance island tune, and persistent capture fraction. Generating functions appropriate to slow and fast tune modulation are presented, leading to four conditions which partition the tune modulation plane into four distinct "phases" of dynamical behavior.

1. INTRODUCTION

E778 is an accelerator physics experiment that has been performed in the Tevatron proton-antiproton collider, at Fermilab. The original motivation for the experiment was to check that tracking programs and reality agree on the variation of smear and tune shift with amplitude, and to ensure that a real storage ring performs well enough even when these quantities reach the maximum tolerances specified for the "linear aperture" in the Conceptual Design Report of the SSC[1]. Results from the analysis of data taken in May 1987, and preliminary results from the February 1988 data, are presented elsewhere in these proceedings[2], and in other publications[3]. The experiment investigated the behavior of the Tevatron in the presence of strong nonlinearities introduced by 16 special sextupoles. Most of these investigations focussed on the information provided by two neighboring beam position monitors (BPMs), after horizontal betatron oscillations with amplitudes of 2 to 6 millimeters were excited by a one turn kicker. Turn-by-turn information was read out, digitized, and written to magnetic tape, on each of (typically) 64k successive turns - about 1.4 seconds. Data analysis falls naturally into three different time scales - about 50 turns, about 500 turns, and about 50,000 turns. Fifty turns of data are usually sufficient to adequately measure the smear (defined below), and the tune at the amplitude of the kick. These measurements have been successfully completed.

The focus of E778 analysis has now turned to the phenomenon of resonance trapping, in which a persistent signal is seen on the BPM data, due to some fraction of the kicked beam being trapped on resonance islands. These signals often lasted from kick time until the Tevatron ended its two minute cycle. Untrapped beam decoheres in a time corresponding to the inverse of the tune spread - approximately 100 turns, as shown in Figure 1. Five hundred turns of data are sufficient to accurately measure the "capture fraction" - the ratio of persistent amplitude to initial amplitude - and to measure the size and locations of the resonance islands. The analysis of long time scale (1 second) behavior will examine how the persistent response depends on tune modulation of the form

$$Q = Q_0 + q \sin(2\pi Q_M t) \quad (1)$$

where t is the turn number. Tune modulation was externally introduced into the Tevatron by exciting fast response quadrupoles which are normally used to feedback on the tune during slow extraction. Different kinds of behavior are expected in different regions of the (q, Q_M) plane.

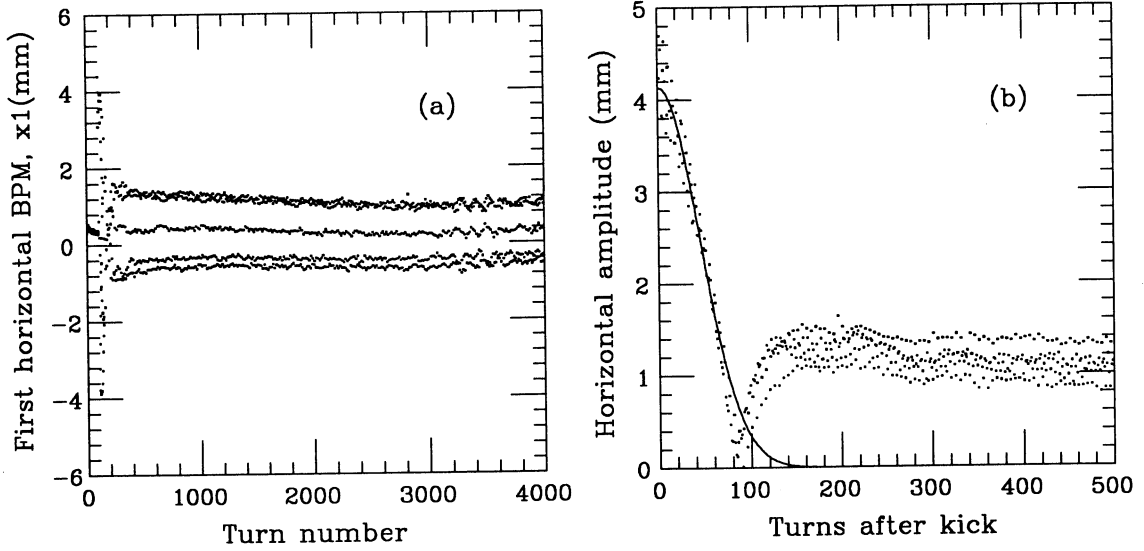


Figure 1. Raw BPM output, (a) for 4000 turns, and (b) for 500 turns after the kick, showing decoherence and a persistent signal. The smooth curve is a Gaussian fit, as expected theoretically

2. SHORT TIME SCALE - NONLINEAR DISTORTIONS

2.1 Projection maps, and the discrete one turn Hamiltonian H_1

Consider the general problem of transverse motion around an accelerator with many thin multipole nonlinearities. Although it is convenient (and appropriate for E778) to concentrate on normal sextupoles in what follows, it is straightforward to extend the results to include any and all multipoles, normal or skew. The angular impulse on a particle passing through a thin sextupole is

$$\Delta X' = g(X^2 - Z^2), \quad \Delta Z' = -2gXZ \quad (2)$$

where X and Z are horizontal and vertical displacements, a prime denotes differentiation with respect to the azimuthal coordinate, and g is the sextupole strength. In normalized coordinates, x and z , the perturbation is

$$\Delta x' = g_{xx} x^2 - g_{zz} z^2, \quad \Delta z' = g_{xz} xz \quad (3)$$

where

$$g_{xx} \equiv g \beta_x^{3/2}, \quad g_{zz} \equiv g \beta_x^{1/2} \beta_z, \quad g_{xz} \equiv -2g \beta_x^{1/2} \beta_z = -2g_{zz}$$

Linear motion from a fixed reference point at the origin of accelerator phases, $\psi_x = \psi_z = 0$, to a given sextupole, is given in this coordinate system by a rotation matrix,

$$R(\psi_x, \psi_z) = \begin{pmatrix} c_x & s_x & 0 & 0 \\ -s_x & c_x & 0 & 0 \\ 0 & 0 & c_z & s_z \\ 0 & 0 & -s_z & c_z \end{pmatrix} \quad (4)$$

where

$$c_x = \cos(\psi_x), \quad s_x = \sin(\psi_x), \quad \text{et cetera.}$$

The "projection" map P is defined as linear motion R from the reference point to a given sextupole, followed by the nonlinear kick, finally followed by inverse linear motion R^{-1} back to the reference point.

The net effect of a projection map P is found by combining equations (3) and (4), to give

$$\begin{pmatrix} \Delta x \\ \Delta x' \\ \Delta z \\ \Delta z' \end{pmatrix} = \begin{pmatrix} -s_x [g_{xx}(c_x x + s_x x')^2 - g_{xx}(c_x x + s_x x')^2] \\ c_x [g_{xx}(c_x x + s_x x')^2 - g_{xx}(c_x x + s_x x')^2] \\ -s_z g_{xz}(c_x x + s_x x')(c_z z + s_z z') \\ c_z g_{xz}(c_x x + s_x x')(c_z z + s_z z') \end{pmatrix} \quad (5)$$

which has the remarkable property of leading directly to a "discrete projection Hamiltonian",

$$H_p = -\frac{g_{xx}}{3} (c_x x + s_x x')^3 + g_{zz} (c_x x + s_x x')(c_z z + s_z z')^2 \quad (6)$$

that exactly reproduces the map (5) under partial differentiation

$$\begin{pmatrix} \Delta x \\ \Delta x' \\ \Delta z \\ \Delta z' \end{pmatrix} \equiv \begin{pmatrix} \frac{\partial H_p}{\partial x'} \\ -\frac{\partial H_p}{\partial x} \\ \frac{\partial H_p}{\partial z'} \\ -\frac{\partial H_p}{\partial z} \end{pmatrix} \quad (7)$$

It is important to note that these are DIFFERENCE, and NOT DIFFERENTIAL, equations - explaining what is meant by a "discrete" Hamiltonian. If it is assumed that the difference vector is small, and if action-angle variables J and ϕ are introduced through

$$\begin{pmatrix} x \\ x' \\ z \\ z' \end{pmatrix} \equiv \begin{pmatrix} (2J_x)^{1/2} \sin(\phi_x) \\ (2J_x)^{1/2} \cos(\phi_x) \\ (2J_z)^{1/2} \sin(\phi_z) \\ (2J_z)^{1/2} \cos(\phi_z) \end{pmatrix} \quad (8)$$

then the projection Hamiltonian becomes

$$H_P = \frac{g_{xx}}{3} J_x^{3/2} [\sin(3\alpha_x) - 3 \sin(\alpha_x)] + \frac{g_{zz}}{2^{1/2}} J_x^{1/2} J_z [2 \sin(\alpha_z) - \sin(\alpha_x + 2\alpha_z) - \sin(\alpha_x - 2\alpha_z)] \quad (9)$$

where

$$\alpha_x = \psi_x + \phi_x, \quad \alpha_z = \psi_z + \phi_z \quad (10)$$

and powers of trigonometric functions have been expanded into multiple angle form. One-turn motion around the Tevatron is given by following map P_1 with P_2 , et cetera, up to P_{16} , and finally by applying $R(2\pi Q_{x0}, 2\pi Q_{z0})$, where Q_{x0} and Q_{z0} are the small amplitude linear tunes. The nonlinear part of the motion is described to first order in sextupole strengths – and not at all to higher order – by summing H_P for each sextupole, so that the discrete one-turn Hamiltonian is

$$H_1 = 2\pi Q_{x0} J_x + 2\pi Q_{z0} J_z + \sum_{\text{sextupoles}} H_P \quad (11)$$

H_1 is shorthand for a set of difference equations, NOT differential equations, which are

$$\begin{pmatrix} J_x \\ \phi_x \\ J_z \\ \phi_z \end{pmatrix}_{t+1} = \begin{pmatrix} J_x \\ \phi_x \\ J_z \\ \phi_z \end{pmatrix}_t + \begin{pmatrix} -\frac{\partial H_1}{\partial \phi_x} \\ \frac{\partial H_1}{\partial J_x} \\ -\frac{\partial H_1}{\partial \phi_z} \\ \frac{\partial H_1}{\partial J_z} \end{pmatrix}_t \quad (12)$$

The linear contribution on the right hand side – $\Delta\phi_x = 2\pi Q_{x0}$, $\Delta\phi_z = 2\pi Q_{z0}$ – is constant and (usually) large. Consequently, the value of H_1 is not a constant of the motion, and the motion cannot be graphically understood, (in one dimension) by plotting its contours. Projection maps appear to have been first used in nonlinear accelerator applications by Kobayashi in 1970[4], although they were also independently developed for application to linear coupling problems[5]. It remains to be shown that this formal structure is more than just academically interesting.

2.2 Distortion functions

It is conceptually natural and practically straightforward to rewrite the one-turn Hamiltonian (11) as

$$H_1 = 2\pi Q_{x0} J_x + 2\pi Q_{z0} J_z + \sum_{\{ijkl\}} V_{ijkl} J_x^{i/2} J_z^{j/2} \sin(k\phi_x + l\phi_z + \phi_{ijkl}) \quad (13)$$

where the sum is over

$$\{ijkl\} = \{3030, 3010, 1210, 1212, 121-2\}$$

The first two indices of the constants V_{ijkl} and ϕ_{ijkl} refer to the powers of $J_x^{1/2}$ and $J_z^{1/2}$, while the last two identify a particular harmonic. It is trivial to solve for the phase space "distortion functions", $J_x(\phi_x, \phi_z)$ and $J_z(\phi_x, \phi_z)$, after substituting (13) into the equations

$$J_x(\phi_x + 2\pi Q_{x0}, \phi_z + 2\pi Q_{z0}) - J_x(\phi_x, \phi_z) = -\frac{\partial H_1}{\partial \phi_x}$$

and

$$J_z(\phi_x + 2\pi Q_{x0}, \phi_z + 2\pi Q_{z0}) - J_z(\phi_x, \phi_z) = -\frac{\partial H_1}{\partial \phi_z}$$

(14)

This gives, to lowest order in sextupole strength,

$$J_x(\phi_x, \phi_z) = J_{x0} - \sum_{\{ijkl\}} \frac{k V_{ijkl}}{2 \sin[\pi Q_{kl}]} J_{x0}^{i/2} J_{z0}^{j/2} \sin(k\phi_x + l\phi_z + \phi_{ijkl} - \pi Q_{kl})$$

and

$$J_z(\phi_x, \phi_z) = J_{z0} - \sum_{\{ijkl\}} \frac{l V_{ijkl}}{2 \sin[\pi Q_{kl}]} J_{x0}^{i/2} J_{z0}^{j/2} \sin(k\phi_x + l\phi_z + \phi_{ijkl} - \pi Q_{kl})$$

(15)

where it is convenient to define the harmonic tune

$$Q_{kl} \equiv kQ_{x0} + lQ_{z0}$$

(16)

Note that the vertical sum in (15) only includes the three terms with 1 non-zero, $\{ijkl\} = \{1210, 1212, 121-2\}$, while the horizontal sum continues to include all five terms. Note also the presence of Q_{kl} in the resonance denominators. Although expressions for distortion functions have already been found by many other authors[6], their derivation in the formalism of discrete Hamiltonians is especially economical and conceptually clear. The extension of this description to include other multipoles is straightforward, and is left as an exercise for the reader.

2.3 Fourier spectra, normalized covariances, and smear

The lowest order solution for $J_x(t)$ and $J_z(t)$ on turn t is given by substituting

$$\phi_x = \phi_{x0} + 2\pi Q_{x0} t, \quad \phi_z = \phi_{z0} + 2\pi Q_{z0} t$$

(17)

into equation (15), giving

$$J_x(t) = J_{x0} - \sum_{\{ijkl\}} \frac{k V_{ijkl}}{2 \sin[\pi Q_{kl}]} J_{x0}^{i/2} J_{z0}^{j/2} \sin(2\pi Q_{kl} t + \phi_{0ijkl})$$

and

$$J_z(t) = J_{z0} - \sum_{\{ijkl\}} \frac{l V_{ijkl}}{2 \sin[\pi Q_{kl}]} J_{x0}^{i/2} J_{z0}^{j/2} \sin(2\pi Q_{kl} t + \phi_{0ijkl})$$

(18)

with

$$\phi_{0ijkl} \equiv k\phi_{x0} + l\phi_{z0} + \phi_{ijkl} - \pi Q_{kl}$$

Rewriting (18) in terms of amplitudes, rather than actions, gives

$$a_x(t) = a_{x0} - \sum_{\{ijkl\}} \frac{k V_{ijkl}}{2^{(i+j+2)/2} \sin[\pi Q_{kl}]} a_{x0}^{i-1} a_{z0}^j \sin(2\pi Q_{kl}t + \phi_{0ijkl})$$

and

$$a_z(t) = a_{z0} - \sum_{\{ijkl\}} \frac{l V_{ijkl}}{2^{(i+j+2)/2} \sin[\pi Q_{kl}]} a_{x0}^i a_{z0}^{j-1} \sin(2\pi Q_{kl}t + \phi_{0ijkl}) \quad (19)$$

Each term in the horizontal or vertical sum in (19) corresponds to one line in a discrete Fourier analysis of the amplitudes (not the displacements). While the lines are ideally narrow, in practice their width is proportional to the tune spread of the beam. It is nonetheless possible to reconstruct the single particle motion by properly summing the power and the phase of the bins under the broadened peaks - assuming that the peaks can be resolved. This summarizes the situation in terms of a small set $\{ijkl\}$ of physically important and theoretically predictable parameters, V_{ijkl} and ϕ_{0ijkl} .

The motion is further summarized by calculating three statistics, the "normalized covariances",

$$\begin{aligned} \sigma_{xx} &\equiv \frac{\langle a_x a_x \rangle}{\langle a_x \rangle \langle a_x \rangle} - 1 = \sum_{\{ijkl\}} \frac{k^2 V_{ijkl}^2}{2^{(i+j+3)} \sin^2[\pi Q_{kl}]} a_{x0}^{2i-4} a_{z0}^{2j} \\ \sigma_{zz} &\equiv \frac{\langle a_z a_z \rangle}{\langle a_z \rangle \langle a_z \rangle} - 1 = \sum_{\{ijkl\}} \frac{l^2 V_{ijkl}^2}{2^{(i+j+3)} \sin^2[\pi Q_{kl}]} a_{x0}^{2i} a_{z0}^{2j-4} \\ \sigma_{xz} &\equiv \frac{\langle a_x a_z \rangle}{\langle a_x \rangle \langle a_z \rangle} - 1 = \sum_{\{ijkl\}} \frac{kl V_{ijkl}^2}{2^{(i+j+3)} \sin^2[\pi Q_{kl}]} a_{x0}^{2i-2} a_{z0}^{2j-2} \end{aligned} \quad (20)$$

where angle brackets $\langle \rangle$ imply a time average. (These equations are incorrect if two members of $\{ijkl\}$ have identical kl values.) The covariances are "normalized" in the sense that they are dimensionless, and are zero for linear motion. Two of them, σ_{xx} and σ_{zz} , are positive-definite, but the cross term σ_{xz} can be negative, with

$$\sigma_{xz}^2 \leq \sigma_{xx} \sigma_{zz} \quad (21)$$

If one of the harmonics in the sum dominates - if V_{ijkl} is very large or Q_{kl} is very close to an integer for some $ijkl$ - then there is a simple invariant of the motion,

$$l a_x - k a_z = \text{constant} \quad (22)$$

and the equality holds in (21). In the most common E778 experimental conditions, motion was induced in the horizontal plane, with the tune Q_{x0} in the range from 19.37 to 19.42. The horizontal rms "smear" is then just

$$s \equiv \sigma_{xx}^{1/2} = \left(\frac{3 V_{3030}^2}{2^6 \sin^2(3\pi Q_{x0})} + \frac{V_{3010}^2}{2^6 \sin^2(\pi Q_{x0})} \right)^{1/2} a_{x0} \quad (23)$$

and is linear in the initial amplitude. Notice that $\sin(3\pi Q_{x0}) = 0.729$ at the upper end of the tune range, and the

resonance denominator in the first term in (23) is not small, showing that the E778 smear was not (necessarily) dominated by the $3Q_{x0}$ harmonic.

3.0 MEDIUM TIME SCALE - PERSISTENT SIGNALS

3.1 The N-turn Hamiltonian H_N

If the base tune of an accelerator is near a rational fraction, $Q_0 \approx I/N$, then the net phase space motion after N turns is comparatively small. For example, the E778 fractional tune was between $2/5 - 0.03$ and $2/5 + 0.02$, so the magnitude of the net phase advance was typically less than one tenth of 2π . It could also be argued that the E778 tune was close to $1/3$, although it remains to be seen how close is close enough. Consider, then, the general N -turn case, where the motion is described to lowest order by the N -turn Hamiltonian

$$H_N = 2\pi (Q_0 - \frac{I}{N}) J + \frac{1}{N} \sum_{n=0}^{N-1} \sum_{\{ik\}} V_{ik} J^{i/2} \sin[k(\phi + n2\pi Q_0) + \phi_{ik}] \quad (24)$$

All subscripts x are dropped from here on, and the set of indices $\{ijkl\}$ is contracted to $\{ik\}$, since only horizontal motion is treated. The N -turn difference equations of motion are now

$$\begin{pmatrix} J \\ \phi \end{pmatrix}_{t+N} = \begin{pmatrix} J \\ \phi \end{pmatrix}_t + N \begin{pmatrix} -\frac{\partial H_N}{\partial \phi} \\ \frac{\partial H_N}{\partial J} \end{pmatrix}_t \quad (25)$$

The crucial difference between H_N and H_1 - see equation (13) - is that now the difference step is small. To a reasonable approximation, H_N is a constant of the motion, and the difference equations can be replaced by the more common Hamiltonian differential equations,

$$\begin{pmatrix} \frac{dJ}{dt} \\ \frac{d\phi}{dt} \end{pmatrix} = \begin{pmatrix} -\frac{\partial H_N}{\partial \phi} \\ \frac{\partial H_N}{\partial J} \end{pmatrix} \quad (26)$$

Strictly speaking, the motion obtained by "integrating" (26) is only correct for values of t which are exact multiples of N . The outer sum in (24) is easily removed by using the trigonometric identity

$$\sum_{n=0}^{N-1} \sin(A + nB) \equiv \frac{\sin(NB/2)}{\sin(B/2)} \sin(A + \frac{N-1}{2} B) \quad (27)$$

so that

$$H_N = 2\pi (Q_0 - \frac{I}{N}) J + \sum_{\{ik\}} V_{Nik} J^{i/2} \sin(k\phi + \phi_{Nik}) \quad (28)$$

where

$$V_{Nik} \equiv \frac{\sin(NkQ_0\pi)}{N \sin(kQ_0\pi)} V_{ik}, \quad \phi_{Nik} \equiv \phi_{ik} + (N-1)k\pi Q_0 \quad (29)$$

A remarkable and important property of V_{Nik} is that

$$\begin{aligned} V_{Nik} &\approx V_{ik} && \text{if } \text{mod}(k,N) = 0 \\ V_{Nik} &\ll V_{ik} && \text{if } \text{mod}(k,N) \neq 0 \end{aligned} \quad (30)$$

provided that

$$|Q_0 - \frac{I}{N}| \ll \frac{1}{k\pi}$$

This defines when the tune is "close enough" - when most of the V_{Nik} terms are negligible. For example, if the maximum value of k is 3, then it is reasonable to drop most of the $\{ik\}$ terms in (28) if the base tune is within, say, 0.03 of I/N . This shows that E778 conditions were "close" to the 2/5 resonance, but not to the 1/3.

3.2 The three turn motion, and octupolar detuning

Suppose that the tune is between 0.33 and 0.36 (not true for E778), and that $\{ik\}$ is $\{33, 31, 44, 42, 40\}$, including both sextupolar and octupolar terms. If the extra terms come from true octupoles, their V_{ik} and ϕ_{ik} values are easily calculated. However, if, as in the E778 case, they come from cross terms between sextupoles, they are not calculable without resorting to second order perturbation theory. Combining (28) and (30),

$$H_3 = 2\pi (Q_0 - \frac{1}{3}) J + V_{33} J^{3/2} \sin(3\phi + \phi_{33}) + V_{40} J^2 \quad (31)$$

Since H_3 is a constant of the motion in this approximation, the distortion function is just

$$J(\phi) = J_0 - \frac{1}{2\pi (Q_0 - \frac{1}{3})} (V_{33} J_0^{3/2} \sin(3\phi + \phi_{33}) + V_{40} J_0^2) \quad (32)$$

in agreement with (15), if the constant term proportional to V_{40} is (legitimately) dropped. Equation (32) describes the classic (normalized phase space) topology, of small amplitude circles becoming more and more distorted at larger and larger amplitudes, out to a separatrix in the shape of an equilateral triangle. This description is accurately confirmed by tracking. The perturbed tune at an average action of J_0 is given by

$$Q(J_0) = \frac{1}{3} + \frac{1}{T} \quad (33)$$

where, using (26),

$$T = \int dt = \int_0^{2\pi} \left(\frac{\partial H_3}{\partial J} \right)^{-1} d\phi \quad (34)$$

After equation (31) is differentiated and substituted into (34), the integrand depends explicitly on J and ϕ . Next, the integrand is expanded in a Taylor series up to order J^1 , and then (32) is used to make the integrand depend solely on ϕ , allowing T to be evaluated. This gives

$$Q(J_0) = Q_0 - \frac{3}{8\pi^2} \frac{V_{33}^2}{(Q_0 - \frac{1}{3})} J_0 - \frac{V_{40}}{\pi} J_0 \quad (35)$$

which is correct to first order in J_0 . The presence of the resonance denominator in the V_{33}^2 term shows that it is unnecessary to consider the cross terms between sextupoles, if the tune is close enough to $1/3$.

3.3 The five turn motion, and experimental observables

Most of the persistent signals observed in E778 were due to the $2/5$ resonance, and so the five turn motion is very relevant. After expanding the $\{ik\}$ set even further, to be $\{33, 31, 44, 42, 40, 55, 53, 51\}$, but keeping only terms with $k=0$ and 5 according to (30), then the 5-turn Hamiltonian is written down as

$$H_5 = 2\pi (Q_0 - \frac{2}{5}) J + V_{40} J^2 + V_{55} J^{5/2} \sin(5\phi + \phi_{55}) \quad (36)$$

The decapole terms with $i=5$ coming from cross terms between sextupoles can also, in principle, be calculated in second order perturbation theory. However, as Taf says, "Beyond first-order results I know of no useful result from perturbation theory in (celestial) mechanics..."[7]. What is more, tracking results show that (36) is not an accurate description even at moderate amplitudes - V_{33} terms are still important in practice. Without minimizing these difficulties, it is possible to proceed with a general description by rewriting H_5 as

$$H_5 = 2\pi (Q_0 - \frac{2}{5}) J + U(J) - V_5(J) \cos(5\phi) \quad (37)$$

where

$$Q(J) \approx \frac{2}{5} + (Q_0 - \frac{2}{5}) + \frac{U'(J)}{2\pi} \quad (38)$$

and a prime now indicates differentiation with respect to J . This Hamiltonian exhibits island structure, with five stable and five unstable fixed points at local minima and maxima. They occur close to an action J_I which makes the tune exactly $2/5$, and which is found by solving (38).

It is illuminating to rewrite (37) in a Taylor expansion in I , the action displacement from the fixed points,

$$H_5(I, \phi) = \frac{1}{2} U''_I I^2 - V_{5I} \cos(5\phi) \quad (39)$$

where

$$I = J - J_I, \quad U''_I \equiv U''(J_I), \quad V_{5I} \equiv V_5(J_I) \quad (40)$$

Thus the stable and unstable fixed point phases are, respectively, even and odd integer multiples of $\pi/5$ (assuming U''_I and V_{5I} have the same sign). The island half width is found by solving $H_5(I_W, 0) = H_5(0, \pi/5)$,

$$I_W = 2 \left(\frac{V_{5I}}{U''_I} \right)^{1/2} \quad (41)$$

Small oscillations about the stable fixed point at the origin are described by

$$\frac{dI}{dt} = -5^2 V_{5I} \phi, \quad \frac{d\phi}{dt} = U''_I I \quad (42)$$

so that motion around the center of an island is characterized by the island tune

$$Q_I = \frac{5}{2\pi} (U''_I V_{5I})^{1/2} \quad (43)$$

These are the theoretical variables: what can be measured in E778?

The detuning function $Q(a)$ already measured in E778 is in good agreement with tracking at small and moderate amplitudes[2,3]. This leads to a measurement of U as a function of the action. The fraction of particles captured on fifth order islands is expected to be roughly proportional to the island half width in amplitude, a_W . Accepting the parameterisation in (36) for a moment,

$$a_W = 2^{-\frac{1}{4}} \left(\frac{V_{55}}{V_{40}} \right)^{\frac{1}{2}} a_I^{\frac{3}{2}} \quad (44)$$

in which case the capture fraction rises slightly faster than linear with the resonance amplitude, a_I . In any case, observation of the capture fraction leads to measurement of $\frac{V_{5I}}{U''_I}$ as a function of the action, after correction for systematic effects by comparison with multi-particle simulation. This measurement is being actively pursued. These two sets of observations are sufficient to measure the primary theoretical functions $U(J)$ and $V_{5I}(J)$. Knowledge of U and V_{5I} leads to a prediction for the island tune which, if Q_I can be measured independently, imposes a redundant test on the simple theory. When a single particle is captured close to the center of an island in a tracking program, a Fourier transform of its phase reveals a peak at Q_I , the island tune. Although the real signal caused by a beam of particles with finite size is weaker, it is hoped (with some justification) that Q_I can be measured as a function of a_I in the E778 data.

4. LONG TIME SCALE - TUNE MODULATION

The long time scale behavior of the Tevatron was probed, in E778, by observing the response of persistent signals under the tune modulation described in equation (1). Data were usually taken for 64k turns, but some were taken over one megaturn, at the limit of the instrumentation[8]. This is only two orders of magnitude short of the SSC storage time, about $3 \cdot 10^8$ turns in one day. The following description is broken into slow and fast regimes, where the modulation tune Q_M is much less, or much greater, than Q_I , the island tune.

4.1 Adiabatic tune modulation, and trapping

If the tune is changing slowly at a constant rate of \dot{Q} , then (39) is modified to become

$$H_5(I, \phi) = 2\pi \dot{Q} t I + \frac{1}{2} U''_I I^2 - V_{5I} \cos(5\phi) \quad (45)$$

This shows that the fixed point action I_{FP} , where $\frac{\partial H_5}{\partial I} = 0$, moves according to

$$I_{FP} = -\frac{2\pi \dot{Q}}{U''_I} t \equiv -\epsilon t \quad (46)$$

The explicit time dependence in the Hamiltonian is reduced to second order in the small quantity ϵ , defined above,

by performing a canonical transformation from (I, ϕ) to $(\bar{I}, \bar{\phi})$, using the generating function

$$W(I, \bar{\phi}, t) = I \bar{\phi} + \epsilon t \bar{\phi} \quad (47)$$

so that

$$\bar{I} \equiv \frac{\partial W}{\partial \bar{\phi}} = I + \epsilon t, \quad \phi \equiv \frac{\partial W}{\partial I} = \bar{\phi}, \quad \bar{H}_5 \equiv H_5 + \frac{\partial W}{\partial t} = H_5 + \epsilon \bar{\phi} \quad (48)$$

The new action variable \bar{I} is the action displacement from the moving fixed point, while the angle variable is unchanged. The new Hamiltonian is no longer periodic in the angle variable $\bar{\phi}$,

$$\bar{H}_5 = \frac{1}{2} U''_I \bar{I}^2 - V_{5I} \cos(5\bar{\phi}) + \epsilon \bar{\phi} - \frac{1}{2} U'' \epsilon^2 t^2 \quad (49)$$

and only has stable fixed points if there is a solution to $\frac{\partial \bar{H}_5}{\partial \bar{\phi}} = 0$, that is, if

$$2\pi \left| \frac{\dot{Q}}{U''} \right| < 5 |V_{5I}| \quad (50)$$

This is analogous to the well known problem of radio frequency acceleration, in which the stable buckets shrink, to become shaped like tear drops, or even to disappear, when $\frac{dE}{dt} = \frac{dI_{FP}}{dt}$ is non zero. If the tune modulation is sinusoidal, as in (1), then the maximum value of \dot{Q} is $2\pi q Q_M$, and, comparing equations (43) and (50), particles are only adiabatically trapped on resonance islands if

$$q Q_M < \frac{Q_I^2}{N} \quad (51)$$

(after generalization to the case of an N 'th order resonance). This condition is a factor of two more stringent than the one originally proposed by Chao and Month, which was based on a more heuristic model[9].

4.2 Rapid modulation, and synchrotron sidebands

When the sinusoidal nature of the tune modulation is explicitly included in the time independent Hamiltonian (39), the time dependent five-turn Hamiltonian is described, not by (45), but by

$$H_5 = 2\pi q \sin(2\pi Q_M t) I + \frac{1}{2} U''_I I^2 - V_{5I} \cos(5\phi) \quad (52)$$

This is canonically transformed by a generating function different from (47), namely

$$W(I, \bar{\phi}, t) = \bar{\phi} I + \frac{q}{Q_M} \cos(2\pi Q_M t) I \quad (53)$$

to give

$$\bar{I} = I, \quad \phi = \bar{\phi} + \frac{q}{Q_M} \cos(2\pi Q_M t), \quad \bar{H}_5 = H_5 - 2\pi q \sin(2\pi Q_M t) \quad (54)$$

The new action is unchanged, while the new angle is sinusoidally modulated with respect to the old angle, and the

tune modulation in the new five-turn Hamiltonian is shifted inside the cosine

$$\bar{H}_5 = \frac{1}{2} U_I'' \bar{I}^2 - V_{5I} \cos[5\bar{\phi} + \frac{5q}{Q_M} \cos(2\pi Q_M t)] \quad (55)$$

This is rewritten, without overbars, as

$$H_5 = \frac{1}{2} U_I'' I^2 - V_{5I} \sum_i J_i\left(\frac{5q}{Q_M}\right) \cos(5\phi + i2\pi Q_M t) \quad (56)$$

using the identity

$$\cos(A + B \cos(C)) \equiv \sum_{-\infty}^{\infty} J_i(B) \cos(A + iC) \quad (57)$$

where the J_i are Bessel functions. Now, if the action of a particular test particle is close to

$$I_k = k \frac{2\pi Q_M}{5 U_I''} \quad (58)$$

then its tune is close to

$$Q_k = \frac{2}{5} + k \frac{Q_M}{5} \quad (59)$$

and after five modulation periods, $5M$ turns, the net phase advance is small. All of the harmonic terms except one disappear in going to the $5M$ -turn Hamiltonian,

$$H_{5Mk} = \frac{1}{2} U_I'' (I - I_k)^2 + V_{5I} J_{-k}\left(\frac{5q}{Q_M}\right) \cos(5\phi) \quad (60)$$

due to the same averaging which made most terms disappear in going from the one turn (difference) map to the five turn (differential) map, equations (24) to (30). Note that this averaging is only valid if not much happens in $5M$ turns - if $Q_M \gg Q_I$. Just as the N -turn Hamiltonian motion was only correct every N turns, the motion found by "integrating" H_{5Mk} is only strictly correct at integral multiples of $5M$.

Equation (60) has stable fixed points and resonance island chains for every integer k , at a family of tunes with a spacing of $\frac{Q_M}{N}$, where N is the general resonance order. These "synchrobetatron" sidebands are strongly suppressed by small Bessel functions at large values of k , since

$$\begin{aligned} J_k(A) &\approx \left(\frac{2}{\pi A}\right)^{\frac{1}{2}} \cos\left(A - \frac{k\pi}{2} - \frac{\pi}{4}\right) & \text{if } A > k > 0 \\ J_k(A) &\approx 0 & \text{if } A < k \end{aligned} \quad (61)$$

Physically, this means that the test particle is hardly perturbed if its tune modulation amplitude q is insufficient to carry it the $\frac{kQ_M}{N}$ distance to the tune $\frac{I}{N}$ of the resonance. Only the fundamental $k = 0$ is present if

$$q < \frac{Q_M}{N} \quad (62)$$

The half width of a significant synchrobetatron island is given, in comparison with (41), by

$$I_{Wk} = 2 \left(J_k \left(\frac{Nq}{Q_M} \right) \frac{V_{5I}}{U_I} \right)^{\frac{1}{2}} \approx 2 \left(\frac{Q_M}{\pi N q} \right)^{\frac{1}{4}} \left(\frac{V_{5I}}{U_I} \right)^{\frac{1}{2}} \quad (63)$$

where the value of a Bessel function is approximated by its rms size. The action separating neighboring sidebands is given by (58), so the condition for synchrobetatron sideband overlap is just

$$I_{\text{separation}} = \frac{2\pi Q_M}{N U_I} < 2 I_{Wk} \quad (64)$$

or, using (43),

$$Q_M^{\frac{3}{4}} (Nq)^{\frac{1}{4}} < \frac{4}{\pi^{1/4}} Q_I \quad (65)$$

Large scale chaos is expected when this condition is satisfied.

4.3 Dynamical "phases" in the tune modulation plane. (Q_M, q)

Figure 2a shows how the (Q_M, q) tune modulation plane is broken into different regions by three solid boundaries corresponding to the conditions (51), (62), and (65), drawn here with $N = 5$ and $Q_I = 0.0053$. Assuming that the order of the resonance N is fixed, the only independent variables in these conditions are the three tunes q , Q_M , and Q_I . These three occur only in combinations of two more basic quantities, Q_M/Q_I and q/Q_I , which are the externally controlled tunes in units of the island tune. This shows that Q_I is a fundamental dimensionless measure of the resonance strength. The dashed boundary, $Q_M = Q_I$, roughly separates the zones where the slow and fast generating functions, (47) and (53), are valid.

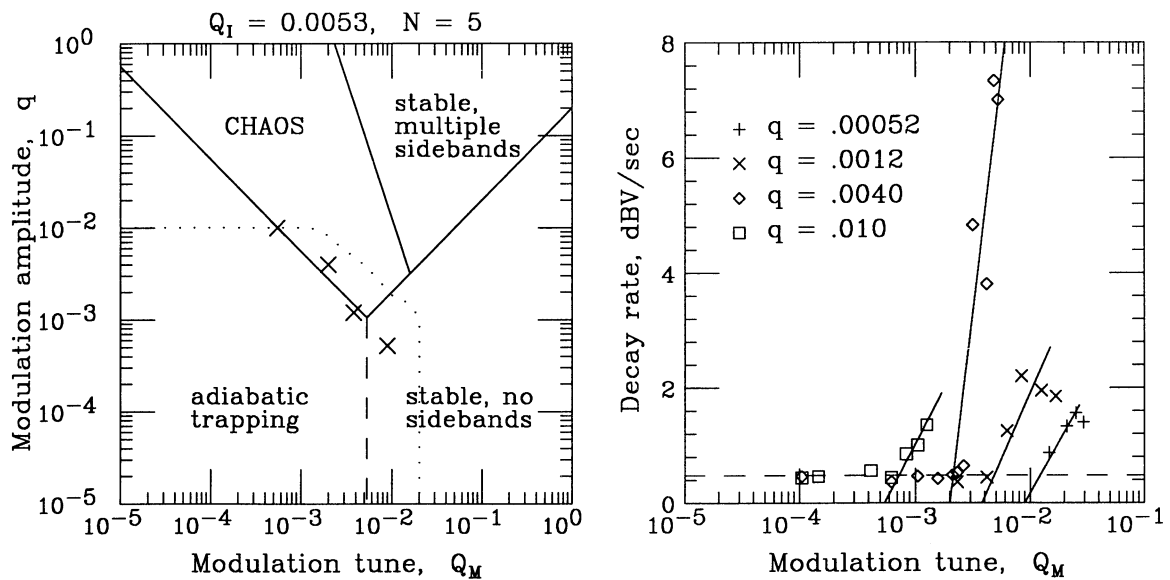


Figure 2 a) Tune modulation plane phases, and b) persistent signal decay rate versus modulation tune, Q_M

In the bottom left corner of this "phase" diagram, particles are trapped in a single fundamental island chain which "breathes" in and out, to larger and smaller amplitudes. Hence the strength of the persistent signal is amplitude modulated, in step with the tune modulation. In the bottom right corner there is still only a fundamental island chain, but trapped particles do not exhibit coherent amplitude modulations. Sideband island chains occur in the top right hand corner, in addition to the fundamental. If the size of the kicked beam in this region is large enough, then more than one sideband is populated at a time, and a Fourier transform of the persistent signal reveals peaks separated in tune by Q_M/N , without amplitude modulation. The fourth region, the top left, is chaotic. If "persistent" signals are observed there at all, they decay away very rapidly.

The dotted line in Fig. 2a shows the region which was physically accessible in the E778 experiment during the February 1988 run. Only the "adiabatic trapping" and "chaos" regions were accessible at values of Q_I where the persistent signals were significantly strong. The 64k turns of data typically taken per shot could not be analyzed on line (for example, in searching for amplitude modulation) in time for the next shot. Consequently, the main real time observable was the decay rate of the persistent signal. Figure 2b shows how, at a particular base tune Q_0 , and hence at a particular island tune Q_I , the decay rate increased dramatically above a critical value of Q_M . The four crosses drawn on Fig. 2a correspond to the four q values in Fig. 2b, showing behavior consistent with crossing the boundary between adiabatic behavior and chaos. Detailed analysis of the hundreds of megabytes of data taken in the tune modulation phase of the E778 experiment is only just beginning.

ACKNOWLEDGEMENTS

It is my pleasure to acknowledge all of the members of the E778 collaboration, who helped to write this paper in many different ways. In particular, I thank A. Chao and R. Talman for insightful discussions.

REFERENCES

- [1] J.D. Jackson et al., SSC-SR-2020, SSC-CDG, Berkeley, (1986)
- [2] D. Edwards, these proceedings, (1988)
- [3] A. Chao et al., SSC-156, SSC-CDG, Berkeley, (1988)
A. Chao et al., Experimental investigation of nonlinear dynamics in the Tevatron, submitted to Physical Review Letters, (1988)
N. Merminga et al., An experimental study of the SSC magnet aperture criterion, Proc. Rome EPAC, (1988)
J. Peterson et al., Dynamic aperture measurements at the Tevatron, Proc. Rome EPAC, (1988)
- [4] Y. Kobayashi, Nucl. Instrum. Methods 83 (1970) 77
- [5] S. Peggs, Particle Accelerators, Vol 12, 24 (1982) 219
S. Peggs, IEEE Trans. Nucl. Sci. NS-30 (1983) 2460
- [6] R. Talman, Cornell LNS Rep., Ithaca, (1976)
T. Collins, Fermilab Tech. Note 84/114, Batavia, (1984)
K.Y. Ng, Fermilab Int. Rep. TM-1281, Batavia, (1984)
- [7] L.G. Taf, Celestial Mechanics, New York, Wiley, (1985)
- [8] S. Peggs, C. Saltmarsh, and R. Talman, SSC-169, SSC-CDG, Berkeley, (1988)
- [9] A. Chao and M. Month, Nucl. Instrum. Methods 121 (1974) 129

DYNAMIC APERTURE AND INVARIANCE BEHAVIOUR IN THE CERN ANTIPROTON COLLECTOR

Patrick Krejcik

CERN, Geneva, Switzerland

ABSTRACT

The CERN Antiproton Collector ring is a strong focusing storage ring with a large acceptance for collecting the maximum number of antiprotons. The use of strong chromaticity correction sextupoles means that the yield of \bar{p} s is influenced by the nonlinear dynamics of particles with large amplitude motion. This is studied by measuring the oscillations of a test beam whose emittance is much smaller than the machine acceptance. Oscillations are made in both planes to observe the effects of nonlinear coupling. Results are compared with numerical tracking data from simulations. Fourier analysis is used as well as a technique for generating a 3-dimensional surface of the invariant of the motion.

1. INTRODUCTION

The CERN Antiproton Collector (AC) ring [1] has large transverse acceptances of 200π mm mrad in both planes for a momentum acceptance of $\pm 3\%$ in order to collect a maximum number of \bar{p} s from the production target. The nonlinear dynamics of the particle motion is of direct interest as it can affect the yield of \bar{p} s collected in the ring since many of the particles are injected into the ring with large amplitudes. In particular, the strong sextupole terms in the ring can excite nonlinear coupling resonances which will drive particles out of the ring if they are injected at large amplitudes in both planes. The mechanism by which this occurs is studied by numerical tracking. The tracking data are Fourier analyzed to reveal nonlinear resonances in the motion. This together with the invariant surfaces generated from the tracking data allows identification of the nonlinear coupling present in the machine. The Fourier analysis technique is very useful since it can be directly compared to the experimentally measured response of a small test bunch in the machine to a kick. The large coherent oscillations of a bunch when tracked turn by turn in the machine are similar in many respects to the idealized behaviour of a single macroparticle tracked in a numerical simulation.

Some notable features of the AC also make the measurements and analysis of large amplitude behaviour quite useful for the design of future accelerators. Some of these features complement experiments at the Tevatron [2] and at the SPS [3] which are specifically aimed at developing aperture criteria for future machines. The AC ring has an unusually large acceptance but in addition there exists the possibility for injecting proton test beams with a very small emittance of just a few π mm mrad. Very large amplitude oscillations can thus be studied in the ring under conditions where one can be sure that the measured response is coming exclusively from particles having large oscillation amplitudes. These are ideal conditions for measuring the large amplitude nonlinear behaviour of particles in a ring with strong sextupoles. A second notable feature is that the beam response is studied when it is kicked simultaneously in both planes. It is found both experimentally and in simulations that the dominant effect of the sextupoles in the AC is to induce nonlinear coupling between the horizontal and the vertical motion in the beam. This only becomes visible when the amplitude of the motion is large in *both* planes. The departure from the linear beam envelope calculations is quite severe under these conditions, strongly influencing the available aperture in the machine, even though the analysis of the behaviour of the invariant shows the motion to be regular and far from chaotic.

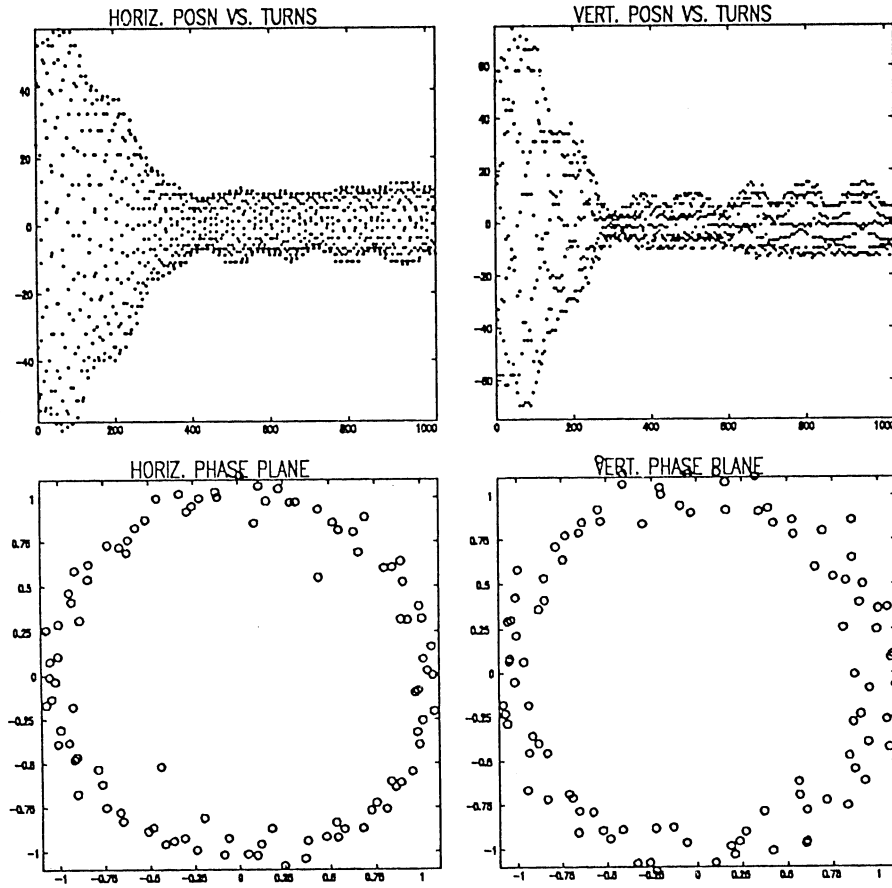


Figure 1. Large amplitude coherent oscillations excited in both the horizontal and the vertical planes. a.) Measured beam position versus turn number. b.) Normalized $x-x'$ and $y-y'$ phase planes reconstructed from the Inverse Fourier Transform.

2. MEASUREMENT AND ANALYSIS OF COHERENT OSCILLATIONS

The dynamic tracking of a single bunch in an accelerator has been tried at several machines [4–7]. On each revolution in the machine the transverse position of the bunch as measured by beam position pickups is recorded by a digitizer. The digitizer should only record the signal from the pickups at the instant that the charge centre of the bunch passes through the pickups. In the AC this is achieved by triggering the digitizer with a clock signal derived from the same rf signal exciting the cavities that keep the beam bunched during the measurement. A low-pass 3rd order Bessel filter for the beam position signal reduces the sensitivity to noise and jitter in the digitized signal [8]. If the bunch is injected with a slight phase error with respect to the rf small synchrotron oscillations will result which appear as a low frequency modulation to the data, but these are easily distinguishable in the subsequent Fourier analysis. A more sophisticated triggering system is in use at the LEAR accelerator [6] where the intensity signal from the beam position pickups is processed to supply the trigger for the digitizer.

The coherent oscillations can be excited in the horizontal plane by changing the injection kicker strength and in the vertical plane by missteering in the beam transfer line. The amplitude of the coherent oscillations is calibrated by measuring the emittance of the kicked beam. Off-momentum orbits are also investigated by first moving the beam with the rf to the desired orbit and then firing the kicker.

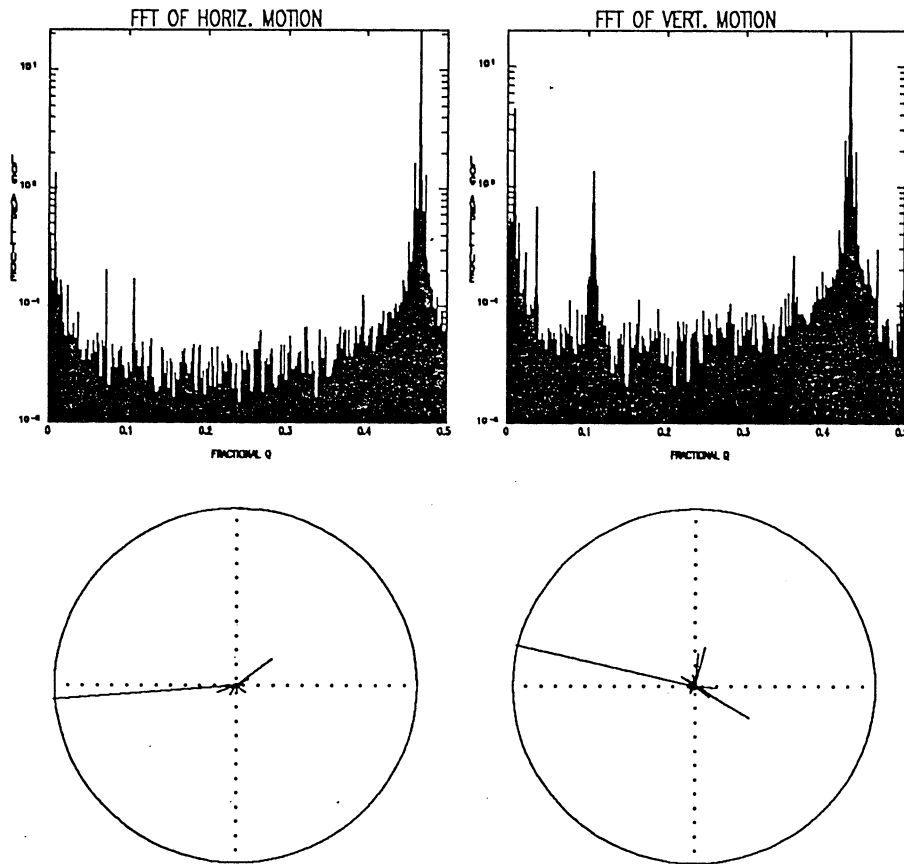


Figure 2. Fourier spectrum of the data in fig. 1. The phase of the peaks can be from the angle of the amplitude vector in the polar plot.

The on-line computer that reads the digitizer displays the acquired data, fig. 1, as well as making a Discrete Fourier Transform (DFT) of the motion. The data can also be analyzed off-line, where it is possible, for example to apply further noise reduction techniques in the frequency domain of the transformed data. The noise component of the data is mainly at high frequencies so limiting the number of data points used in the DFT is an effective way of applying a low-pass filter to the data. The oscillations of interest are at comparatively low frequencies compared to the noise so no loss of information occurs. However, if one would like to extract the amplitude and phase of a particular resonance there is an advantage in using a large number of data points since the transformed data has a finer frequency resolution between the discrete frequency steps. A fine frequency resolution means that one may not have to interpolate to find the exact amplitude and phase of a resonance whose frequency lies somewhere between adjacent frequency intervals in the DFT.

Various techniques of numerical analysis based on Fourier transforms are covered by Lanczos [9], for example. The IFT that yields the filtered oscillatory motion can also be differentiated allowing one to recreate the $x-x'$, $y-y'$ phase space of the motion, fig. 1, even though only one pickup was used to record the beam position in each plane. The convergence of the Fourier series is not a sufficient condition to guarantee the convergence of its derivative, but Lanczos shows how to solve this problem by deriving a smoothing factor that is applied to the series. The finite window used to analyse the original N events also introduces errors into the transform because of the discontinuities in the function and its derivative at the boundaries of the window. One solution, proposed by Lanczos, is to subtract from the original data a quantity of the form $\alpha + \beta t$, where α and β are chosen so that at the boundaries $t = 0$ and

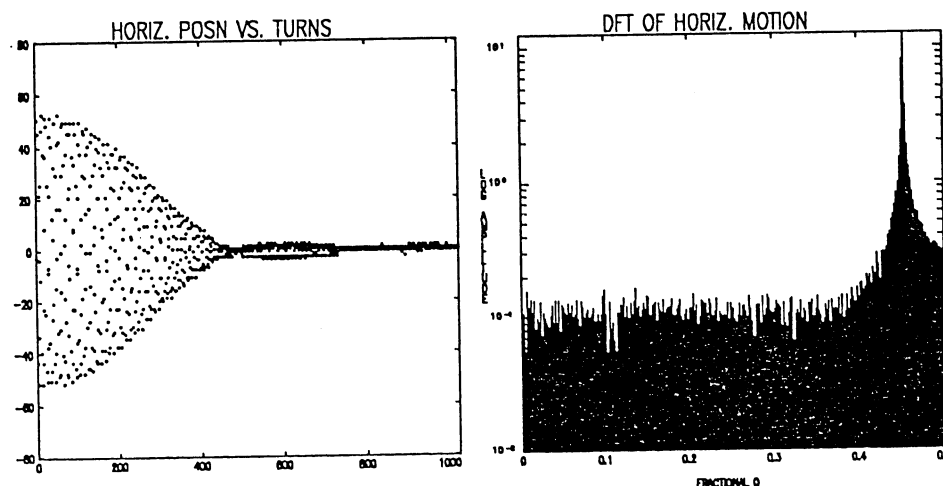


Figure 3. Large amplitude coherent oscillations excited in the horizontal plane only together with their Fourier spectrum.

$t = N\Delta t$ the function is zero. If the data is then reflected about $t=0$ as an odd function one ends up with a new function for which both it and its derivative are continuous at the boundaries. An alternative approach using sine windows is discussed in [6].

3. EXPERIMENTALLY OBSERVED NONLINEAR RESONANCES

For the maximum attainable kicks, horizontally 200 and vertically 100π mm mrad, the measured coherent oscillations are shown in fig. 1. The spectra from the DFTs of these data reveal, in addition to the fundamental frequencies of the motion, Q_H , Q_V , several peaks at frequencies $Q_H - Q_V$, $Q_H + Q_V$, $2Q_H + Q_V$. These are harmonics of certain resonances and their phase is determined from the angle of the amplitude vector in the polar plot accompanying the spectra.

If the beam is kicked in only one plane the Fourier spectra, fig. 3, do not reveal the nonlinear coupling resonances as these only appear when the particle has a large amplitude in both planes. This type of measurement is used on other occasions to measure the strength of the linear coupling in the machine.

A further difference between the measurements in figs 1 and 3 is the decoherence of the beam position signal. The decoherence is due to the tune spread in the bunch, but in the case of large transverse oscillations in both planes there is a persistent oscillation that remains long after the coherent part has decayed. This can be attributed to resonance trapping of the beam, a phenomena also observed in the Tevatron experiment [12]. In the 4-dimensional phase space of the beam there can be resonance islands and if the beam is kicked out to these amplitudes it may continue to oscillate about these points indefinitely. The fraction of the beam trapped is a measure of the strength of the resonance. In the case of the beam kicked in both planes as in fig. 1, the persistent oscillations were observed to disappear as the strengths of the kicks were reduced.

4. NUMERICAL TRACKING SIMULATIONS

Numerical tracking was used in a model of the machine where all known nonlinear effects are included. The chromaticity correction sextupoles are integrated in the arc quadrupoles [1], and are modelled accordingly. The end-fields of the quadrupoles are known to contribute a 3rd order term to the particle motion [13] and have been incorporated in the MIRKO program [14] to produce the tracking data in fig. 4. The Fourier transform of the tracking data gives peaks at the same frequencies as were observed

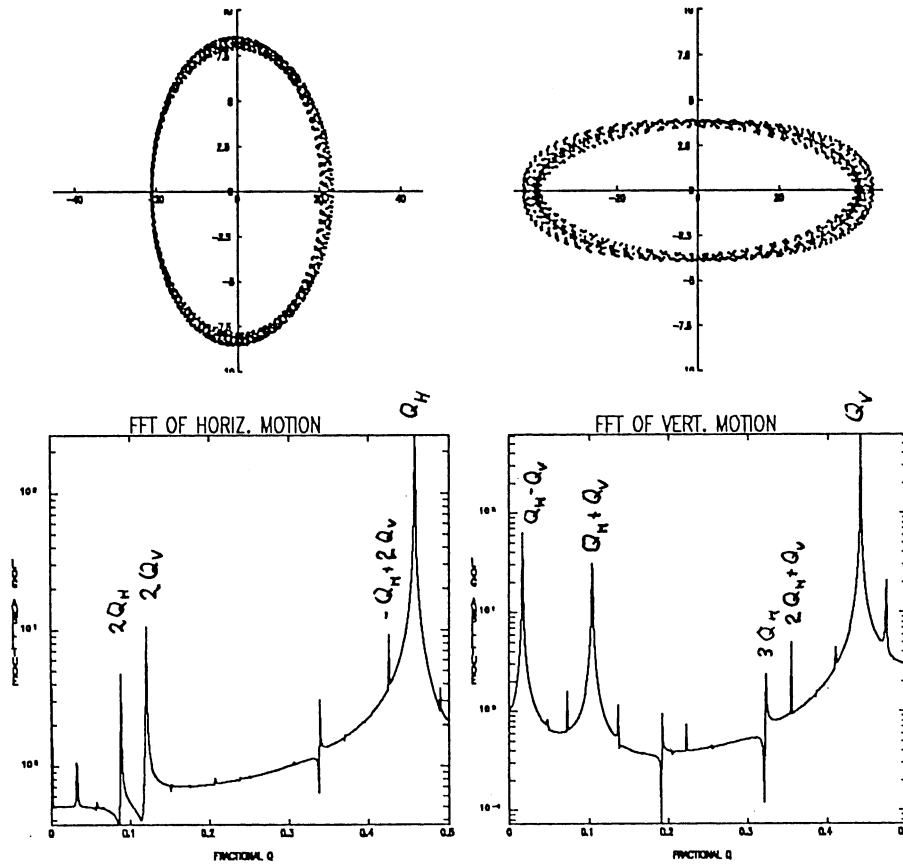


Figure 4. Numerical tracking of a single particle near the aperture limit in both planes. The Fourier spectra below show similar features to the measured data in fig. 2.

in the measured spectra, confirming the relationship of the nonlinear resonances to the multipole distribution in the machine. A resonance $mQ_H + nQ_V = p$ will cause distortions in the beam envelope with frequencies $\pm mQ_H \pm nQ_V \pm p$ [10]. The coupled motion of a single particle when viewed in one plane, as is the case with tracking, has frequencies which are modulated by the amplitude variation in the other plane. In the horizontal plane the observed frequencies are $(m \pm 1)Q_H + nQ_V \pm p$ and in the vertical plane $mQ_H + (n \pm 1)Q_V \pm p$ [11]. For example, the line at $Q_H + Q_V$ in the vertical plane in figs 2 and 4 corresponds to the resonance $Q_H + 2Q_V$ in the tune diagram. The frequency line $Q_H + 2Q_V$ of the resonance itself is found instead in the Fourier spectra of the invariants, fig. 5.

The Courant-Snyder invariant can be calculated from the phase plane coordinates of the particle after each turn and plotted either as a function of turn number or, as in fig. 5, as a function of the betatron phase. The invariance is expressed in the same units as emittance and hence indicates how much acceptance is lost due to the nonlinear coupling between the two planes. A Fourier analysis of the invariant behaviour, fig. 5, shows just those resonances which cause distortions in the beam envelope, namely at the frequencies $\pm mQ_H \pm nQ_V \pm p$. Each spectral line in fig. 5 has a corresponding line at a different frequency in fig. 4. The peaks occur at the same frequencies in the two planes in fig. 5 as there is coupling between the emittance in each plane such that the total 4-dimensional emittance remains constant.

This becomes plainly apparent when the invariant is plotted as a function of both the horizontal phase and the vertical phase so that it appears as a 3-dimensional surface, fig. 6. This is the surface of

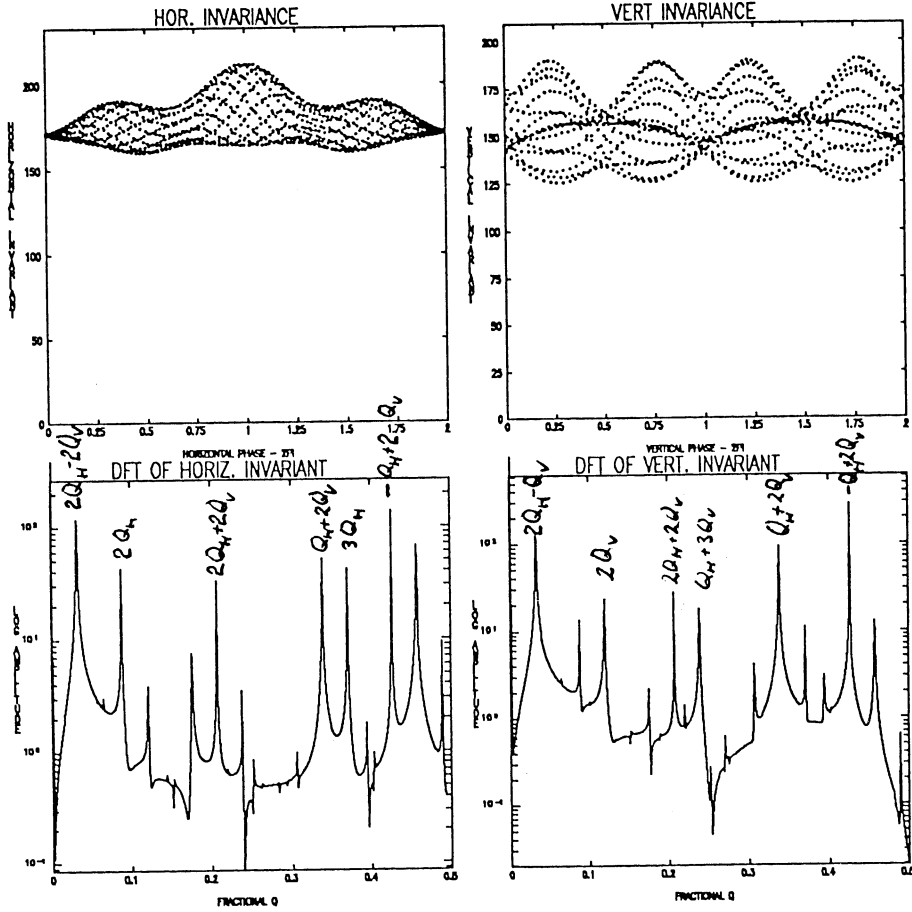


Figure 5. Invariant of the particle motion in fig. 4 plotted as a function of betatron phase. The Fourier spectrum of the invariant shows resonances in the beam envelope.

section when the invariant tori J_H and J_V are projected into a 3-dimensional subspace (ϕ_V, ϕ_H, J_H) and (ϕ_V, ϕ_H, J_V) [15]. A program has been written [16] for computing the invariant surfaces from arbitrary tracking data. New invariants of the form $mJ_H \pm nJ_V$ can also be computed, which is a very useful technique for distinguishing between sum and difference resonances in the motion. For the nominal tunes in the AC when the *sum* of the horizontal and vertical invariants is taken, in fig. 5, the surface modulations that resulted from the coupling between the planes do not vanish. The surface corresponding to the *difference* between the horizontal and vertical invariants is also modulated, but in a direction orthogonal to the modulations on the sum surface. This indicates that both sum and difference resonances are driven by the nonlinearities in the ring. Evidence of this can also be found when scatter plots are made of J_H versus J_V and also ϕ_H versus ϕ_V .

The usefulness of these surfaces is apparent for such cases since the classical techniques of perturbation analysis have difficulties when two resonances overlap. The whole phenomena of coupling becomes clear on such surfaces. The "smear" present in the original tracking data resolves itself into clearly regular motion on a single-valued surface.

ACKNOWLEDGEMENTS

Thanks to H.-O. Kuylenstierna for his help with coherent oscillation measurements [8], as well as to the members of the AR Group for their stimulating comments and criticisms.

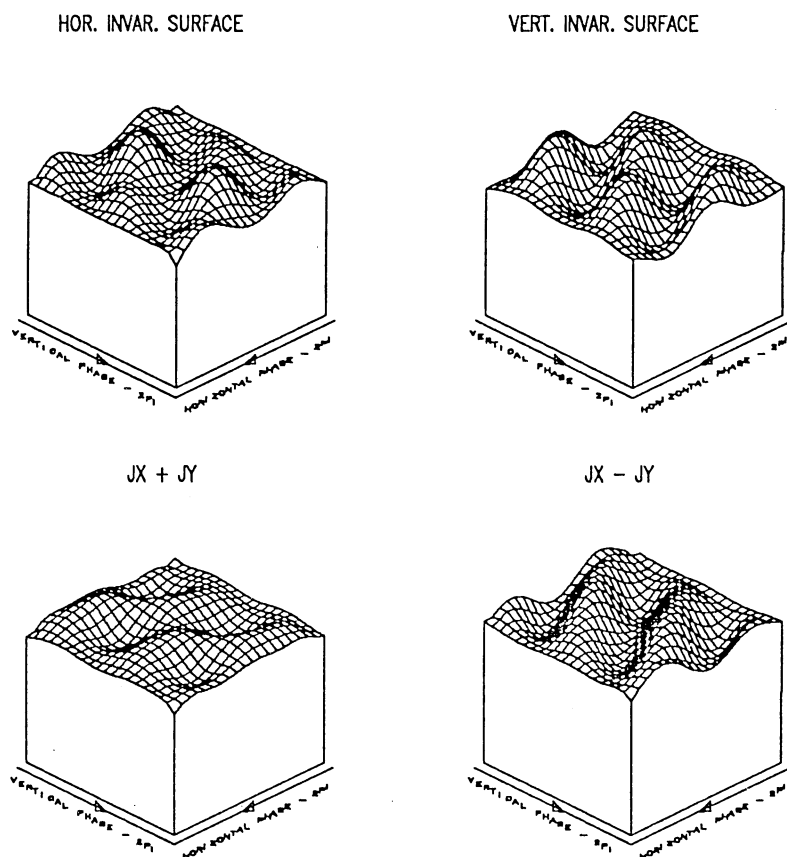


Figure 6. The horizontal and vertical invariant surfaces (top). The difference and sum of the invariants are shown below.

REFERENCES

1. B. Autin et al, Proc. European Particle Accelerator Conference, Rome, June, 1988; and B. Autin, AIP Conf. Proc. 153, SLAC, (1985), 290-347.
2. D. Edwards, "Overview of the Experiment E778", these proceedings.
3. A. Hilaire, "Dynamical Aperture Measurement at the SPS", these proceedings.
4. F. Willeke, Fermilab TM-1309, April 1985.
5. P.L. Morton et al, IEEE Trans. Nucl. Sci., NS-32, (1985), 2291-2293.
6. E. Asseo, J. Bengtsson and M. Channel, Proc. European Part. Accel. Conf., Rome, June, 1988.
7. R. Cappi, CERN/PS/87-48 (PSR).
8. H.O. Kuylenstierna, Student Report, CERN PS/AA/NOTE 87-13.
9. C. Lanczos, "Applied Analysis", Prentice-Hall (1956).
10. G. Guignard, CERN 78-08 (CERN, Geneva 1978)
11. J. Bengtsson CERN PS/LEA/Note 87-3 (1987).
12. S. Peggs, "E778 Phase Space Dynamics and their Interpretation", these proceedings.
13. P. Krejcik, Proc. European Part. Accel. Conf., Rome, June, 1988
14. B. Franczak, Proc. Europhysics Conf. on Computing in Accelerator Design and Operation, Lecture Notes in Physics, Springer Verlag (1984), 170-175.
15. R. Ruth, Proc. of Nonlinear Dynamics Aspects of Particle Accelerators, Lecture Notes in Physics, Springer Verlag (1985), 37-63.
16. SURFIN', A Program for Computing 3-dimensional SURFace INvariants, P. Krejcik.

THE CRITERIA WORKING GROUP SUMMARY

P. Audy (CEN, Saturne), *M. Cornacchia* (LBL), *A. Chao* (SSC/LBL), *M. Harrison* (FNAL), *A. Hilaire* (CERN), *C.S. Hsue* (SRRC, Taipeh), *H. Kugler* (CERN), *S. Ohnuma* (Univ. of Houston), *C. Planner* (Rutherford Appleton Lab.), *B. Simon* (BESSY), *S. Thomson* (Daresbury Lab.), *A. Verdier* (CERN)

(reported by A. Chao)

The working group identified four issues to be addressed during the workshop. These are:

1. How to determine the needed aperture? (1)
2. What quality the needed aperture must have (e.g., what are the figures of merit)?
3. The "linear aperture."
4. What help do we need from the theorists and experimentalists?

Impact of collective effects on aperture is considered outside the scope of the present study. Discussions of the four issues in our group were led by Mike Harrison, Max Cornacchia, Alex Chao and Alain Hilaire, respectively. In addition, Ferdi Willeke, Jacques Gareyte, Swapan Chattopadhyay, Sam Heifets and Mike Harrison delivered talks to the group [1].

ISSUE 1. APERTURE NEEDS

The aperture need depends on the type of accelerator. Three types are identified: synchrotron radiation sources, electron colliders, and proton colliders. Table 1 gives the aperture needs for the first two types.

For synchrotron radiation sources, the aperture need is most demanding at injection. One of the needs is therefore to accomodate the injection amplitude, which preferably takes place horizontally (x) rather than vertically (y) [2]. The need for closed orbit distortions is obvious.

However, the important considerations (the fun part) are the Toushek lifetime for the x-aperture and beam-gas lifetime for the y-aperture; both effects are stronger at injection energy. It

Table 1
Horizontal and vertical aperture needs
in synchrotron radiation sources and electron colliders.

	Horizontal	Vertical
synchrotron radiation sources	<ul style="list-style-type: none"> - injection amplitude - Toushek lifetime > 8 hrs - closed orbit - closed orbit 	<ul style="list-style-type: none"> - beam-gas lifetime > 8 hrs for vacuum of a few $\times 10^{-9}$ torr
electron colliders	<ul style="list-style-type: none"> - $10 \sigma_x$ at maximum beam energy - closed orbit 	<ul style="list-style-type: none"> - $10 \sigma_y$ at maximum beam energy - closed orbit

is interesting to note that the x- and y-aperture needs are determined by completely different physical mechanisms. The beam-gas lifetime is more important in the y-dimension because the vertical aperture is usually restricted by the insertion devices. This in principle could give an odd-shaped aperture whose width is, say, very much larger than its height. It is also interesting to note that quantum lifetime is of absolutely no concern for modern synchrotron radiation sources. This is because the beam emittance has been made so small that the aperture determined by other needs turns out to be very much larger than the rms beam size.

On the contrary, in an electron collider, aperture need is dominated by the (boring) quantum lifetime requirement. The aperture is then determined by its need at the maximum beam energy when the beam size is the largest and quantum lifetime the shortest. The vertical beam size is that given by a fully coupled beam (as done in PEP) or nearly fully coupled beam (as done in LEP). The aperture determined is more or less round because the x- and y-aperture needs are approximately the same.

The aperture need in proton colliders tends to be most stringent at injection due to the larger beam size [3] and potential injection errors. Table 2 is a comparison of the "aperture budgets" made in the designs [4] of the SSC, the LHC and the HERA proton ring. The relatively large emittance in the LHC compared with the SSC is for the option of colliding electron and proton beams. The last row of the table gives the criteria presently taken by the respective designers to judge whether the aperture is acceptable in terms of meeting the needs. For example, a constraint on tune shift Δv means that the tune shift with amplitude and momentum of all particles inside the needed aperture will have to be within the limit imposed. More on the aperture criteria will be discussed later.

Table 2
Aperture needs for three proton collider storage rings SSC,
LHC and HERA. The normalized emittance is defined to be $\epsilon_N = \gamma \sigma_x \sigma_{x'}$.

	LHC	SSC	HERA
Beam size	4σ with $\epsilon_N = 5 \times 10^{-6}$ m	$\sqrt{6}\sigma$ with $\epsilon_N = 1 \times 10^{-6}$ m	$\sqrt{6}\sigma$ with $\epsilon_N = 3 \times 10^{-6}$ m
Closed orbit	4 mm	1.5 mm	1.5 mm
Energy spread $\Delta E/E$	1.5×10^{-3}	1×10^{-3}	0.8×10^{-3}
Miscellaneous	—	Injection errors, β -function mismatch, mechanical errors	Injection error of $\pm 2-3$ mm
Criteria	1. Survival of tracking for 100 turns 2. $\Delta v < 0.005$	1. $\Delta v < 0.005$ 2. smear $< 6.4\%$ 3. $> 30\%$ away from the 400-turn dynamic aperture	Particle motion is not chaotic in 10^5 turns

Special consideration may be needed to deal with the beam-beam tails when the beams are colliding. A suggestion by Jacques Gareyte, not discussed as much as it deserves during the workshop, was to impose the following condition for colliding beams:

$$\begin{aligned} \text{the } 10^3 \text{ turn dynamic aperture} &> 12 \sigma \\ \text{the } 10^5 \text{ turn dynamic aperture} &> 8 \sigma \end{aligned} \quad (2)$$

It is suggested then that a collimator positioned at 8σ would be able to clean up the beam tail without producing undesirable background for the high energy physics detectors.

ISSUES 2 AND 3. FIGURES OF MERIT, AND THE LINEAR APERTURE

Once the needed aperture is given, the next question is what qualities does it have to have before it is judged satisfactory. In practice, one must identify a set of figures of merit that characterizes the optical quality of the storage ring on the one hand, and is easy to calculate on the other hand. The hope for easy calculation is of great practical importance. For example, a figure of merit that is to be obtained by executing 10^8 turn trackings would not be desirable.

During the workshop, 6 possible figures of merit were identified. Arranged in order of decreasing grossness, or increasing intricateness, these are: the betatron tunes, the dynamic aperture, tune shifts, the smear, resonance widths, and Arnold diffusion rates. Aside from the Arnold diffusion rates, they are discussed below.

1. The betatron tunes

The tunes remain the most important aperture parameters. They must be chosen carefully so as to avoid resonances — the integral part chosen to avoid the systematic resonances, and the fractional part chosen to avoid the non-systematic resonances.

2. The dynamic aperture

In this paper, “dynamic aperture” refers to that obtained by tracking simulations. Limited by computer power, these simulations are typically limited to 100 to 10^5 turns.

Electron storage rings are “short term” (10^2 – 3 turns) machines due to radiation damping. Proton storage rings are “long term” (10^8 – 9 turns) machines. They have very different aperture criteria. In particular, the dynamic aperture is much more relevant to electrons than to protons.

Before turning a tracking program loose to calculate the dynamic aperture, it pays to be reminded how to do it “properly.” The group has considered the following points:

- Tracking must be performed on more than several particles distributed along the phase ellipse corresponding to a given emittance. When any one of these particles is lost during tracking, the emittance is identified as the dynamic aperture. This is due to the observation, of which Figure 1 is an example, that the dynamic aperture may be sensitive to the initial betatron phase while it is the limiting betatron amplitude that is of interest. One consequence is that the dynamic aperture will then be in units of mm-mrad, rather than mm.
- The number of turns tracked must be comparable or larger than the radiation damping time.
- It may not be sufficient to study the stability at the working point alone. It is suggested that exploration around the working point be made to make sure the stability is not excessively sensitive to the tune choices.

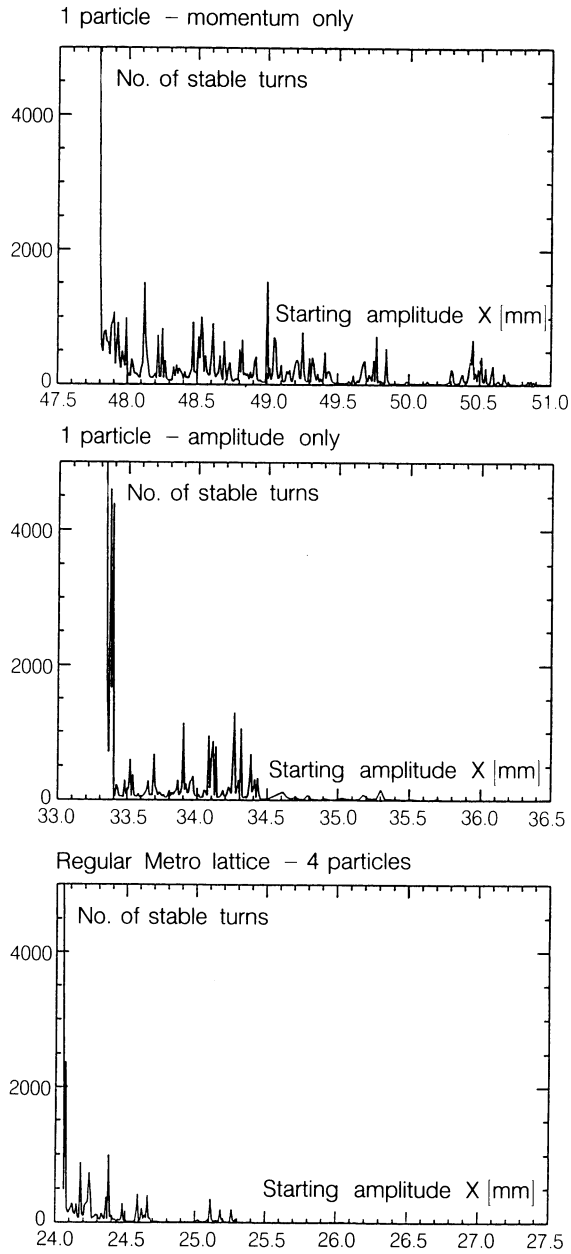


Fig. 1. Simulation of the BESSY ring by Betina Simon. Dynamic aperture varies between 24 to 48 mm depending on the initial betatron phase.

- A concern was raised by Andrei Verdier that real physical aperture limits may have to be imposed in order to find the true dynamic aperture. The consensus of the group is that one ought to do both cases with and without these real physical apertures.

For electrons, the dynamic aperture is of great relevance. This is not necessary the case for protons. Figure 2 is a schematic illustration of what might happen. The dynamic aperture reached in 10^2 - 10^4 turns would be relevant for the electron storage rings. It has been observed,⁵ however, that the dynamic aperture could take a sudden loss when the number of turns is increased to, say, 10^5 turns in a simulation. The relevant number of turns for the proton colliders is 10^8 turns; the typical tracking power misses this by 3 orders of magnitude. It is conceivable that more such sudden losses (shown as the dashed curve in Figure 2) may occur between 10^5 and 10^8

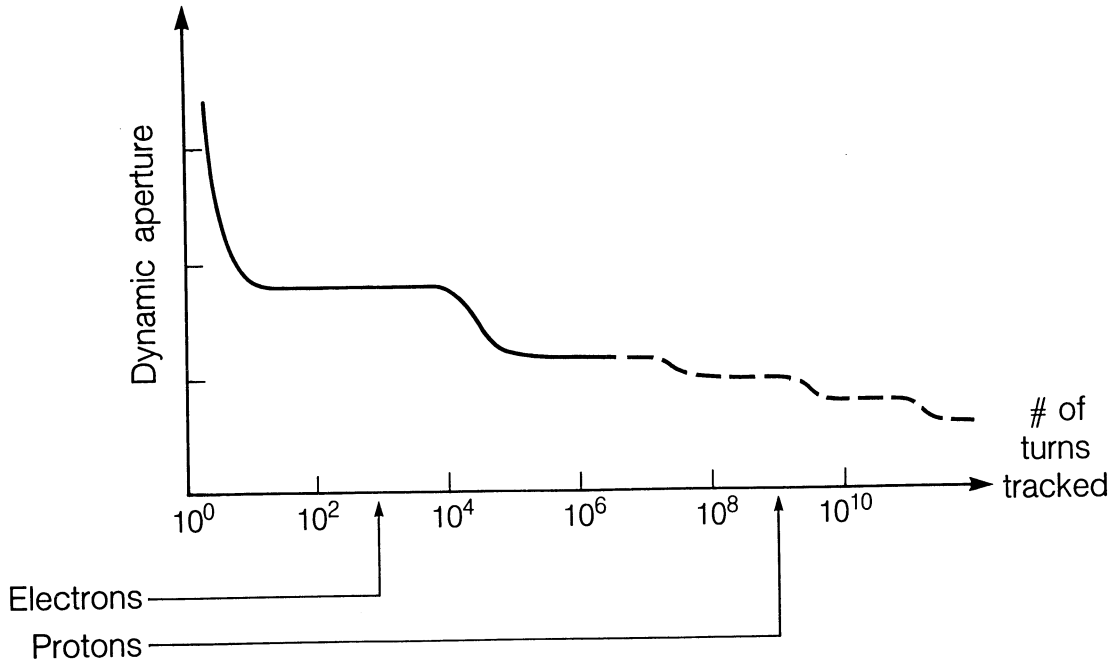


Fig. 2. Schematic illustration of possible behavior of dynamic aperture as a function of the number of turns tracked in a simulation program.

turns. Partly for this reason, the short-term dynamic aperture criterion is not sufficient for proton storage rings.

According to the KAM theorem, the motion of a particle is bounded provided it executes 1-D motion and has a “small” amplitude. In practice, the small amplitude could be very small indeed, and in any case particles usually move in a 3-D space. So even the mighty KAM does not seem to rescue the protons from possible long term loss.

3. Tune shifts

It is conventional wisdom that the tunes must be chosen to avoid resonances. One implication is that the tunes of all particles inside the needed aperture must not deviate from their nominal values by more than a certain limit. (Remember that the nominal tunes have been carefully chosen.) For example, PEP had taken the condition $|\Delta\nu| < 0.01$ and LEP, LHC and SSC have taken $|\Delta\nu| < 0.005$.

An issue is how to include the beam-beam tune shift as part of the criterion. Two possibilities were suggested with no consensus on which to adopt:

- Impose the criterion $|\Delta\nu_{BB}| + |\Delta\nu_{SR}| < \text{limit}$, where $\Delta\nu_{BB}$ is the beam-beam induced tune shift, summed over all interaction points, and $\Delta\nu_{SR}$ is the tune shift due to nonlinearities in the storage ring. If this is adopted, one might study a possible trade-off between field quality tolerance and luminosity.
- Impose two separate criteria $|\Delta\nu_{BB}| < (\text{limit } 1)$ and $|\Delta\nu_{SR}| < (\text{limit } 2)$.

In either case, the values of some of these limits are different for electrons and protons. Their proper values may require more inputs from the theory and experiments.

4. The smear, its equivalents, or its substitutes

The short-term dynamic aperture is a sensitive, elusive quantity. For example, Figure 2 showed its possible sensitivity to the number of turns tracked. Figure 3 is a schematic illustration of the dynamic aperture in the phase space. It is meant to define an “edge of the cliff” beyond which particles are lost quickly. It may be advisable to back off from this cliff edge to

- Provide safety margin.
- Stay in a region that is “understood” (e.g., by some version of perturbation theory).
- Stay in a region where long-term stability is better assured.

(The last item is for protons only.) For these purposes, a “linear” or “quasi-linear” aperture has been suggested to replace the dynamic aperture as a more conservative estimate of the relevant aperture.

The question is then how to determine the linear aperture. In particular, what is the figure of merit that provides the indication that a linear aperture is reached? One suggestion for such a figure of merit is the “smear” [6,7].

To obtain the smear, the tracking result (x, x', y, y') for each turn is processed to give the x - and the y -amplitudes $A_{x,y}$, and the results are plotted in the (A_x, A_y) phase space as a collection of dots, each representing the result for one turn. In a perfectly linear system, the dots all fall on one and the same point. In a system with nonlinearities, these dots spread out as sketched in Figure 4. The ratio of the rms spread in the quantity $A = (A_x^2 + A_y^2)^{1/2}$ and its average value is then the smear [8].

Note that the detailed distribution of the dots in Figure 4 also contains useful information. For example, a distribution that looks like a thin, long, tilted ellipse could indicate the influence of a single coupling resonance. It is therefore possible to consider extracting more parameters (e.g., the second moments) from the plot than the smear alone. In a moderately linear region, the smear hopefully suffices.

Qualitatively speaking, near the dynamic aperture, the smear is $\approx 100\%$. Perturbation theory breaks down here. A possible linear aperture criterion is therefore

$$\text{smear} < \text{several } \% \quad (3)$$

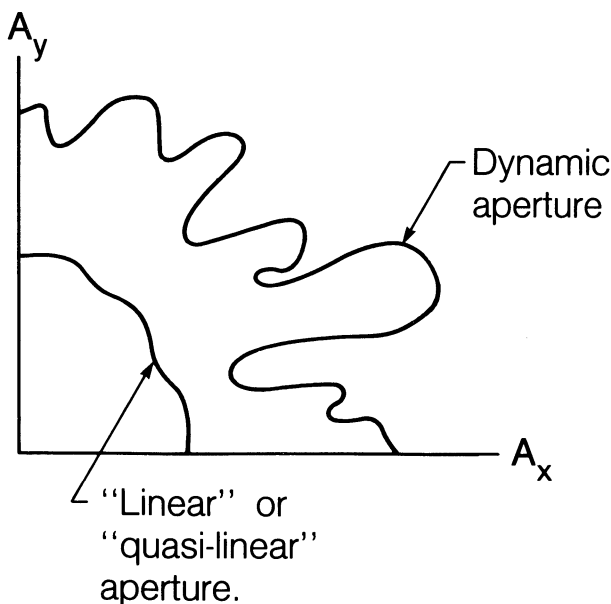


Fig. 3. Schematic illustration of the dynamic aperture versus linear aperture in the phase space. A_x and A_y are the betatron amplitudes in the x - and y -dimensions.

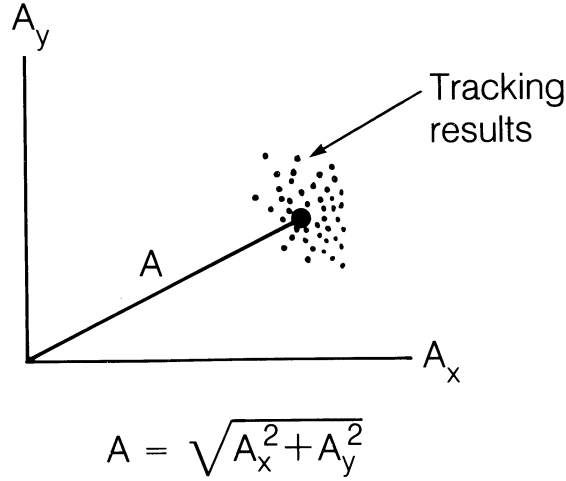


Fig. 4. Definition of smear.

The present SSC design takes 6.4%, while the LHC takes 3.5%. (They also have somewhat different definitions of smear.) Both these values are still tentative. More theoretical and experimental studies are needed to set the best value. In addition to the smear, the linear aperture also requires imposing a limit on the tune shift. Both the SSC and the LHC have taken 0.005 to be the tune shift limit.

Figure 5 shows the proposed linear aperture region in the ($\Delta\nu$, smear) space, as well as some experimental results from SpS [9] and Tevatron (E778) [10,11]. Neither experiment is designed to

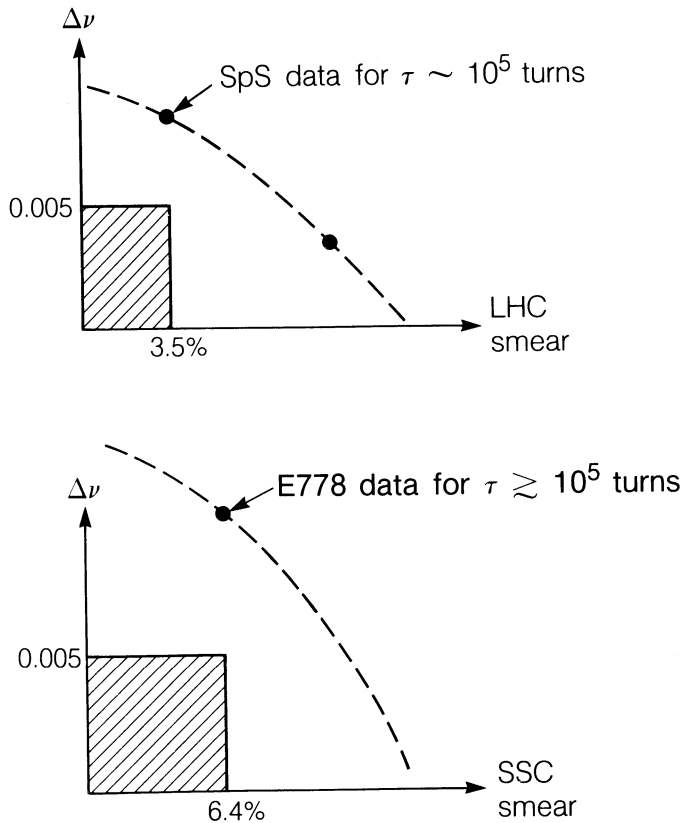


Fig. 5. Proposed linear aperture is shown as shaded regions. Experimental data corresponding to 10^5 turns lifetime are shown for the SpS. A data point for $>10^5$ turns lifetime is also shown for the Tevatron, but it is only to be considered very preliminary. (a) SpS and (b) Tevatron.

explore the long term effect in the $(\Delta v, \text{smear})$ space, but figure 5 seems to say the linear aperture as defined by Δv and the smear is so-far-so-good.

In figure 5, an imagined dashed curve was drawn to represent the contour corresponding to 10^5 turn lifetime. Presumably the curve moves inward as the number of turns of stability increases. One may try to experimentally map out these contours for various values of beam lifetimes. Hopefully, the linear aperture criterion ultimately chosen will be inside the contour that corresponds to 10^8 turns.

Smear is a parameter devised to characterize the strength of nonlinearity. One of its advantages is that it is easily calculable in a tracking program. It is not meant to rigorously assure the long term stability, or even if it is unique for the purpose.

HERA has adopted a different criterion to back off from the dynamic aperture [12]. The criterion used (mentioned in Table 1) is that particle motion must not be chaotic in 10^5 turns. As sketched in Figure 6, this means the shaded region, even if stable in 10^5 turns, is not considered within the aperture. In practice, this may require judgement as to where chaotic motion has started.

5. Resonance strengths

The resonance strengths contain the most detailed information of the nonlinear optics. Knowing the strengths of all resonances of all orders, in principle, implies knowing the entire nonlinear optical map. But in practice, one is limited to only a small number of figures of merit. For example, one might compute

$$\sigma_n = \text{sum of the strengths (in tune units) of all } n\text{-th order resonances} \quad (4)$$

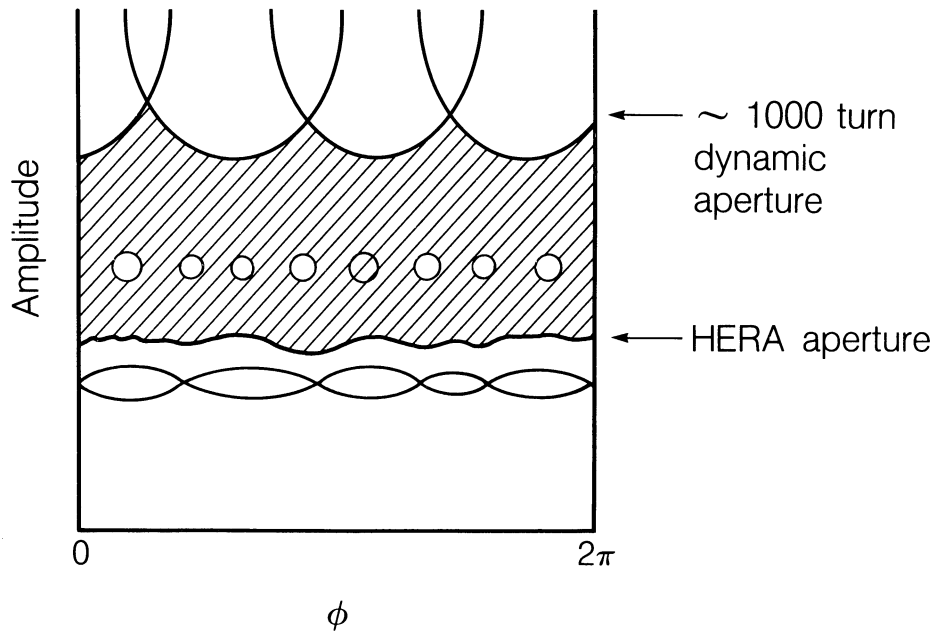


Fig. 6. HERA aperture is quoted below the chaotic region (shaded area) even if the chaotic region is stable for 10^5 turns.

The computation is to be carried out even when the lower order resonances have been avoided by proper tune choices. Examples being explored along this line are

$$\sigma_n < 0.02 \text{ for } n = 3,4,5,6 \text{ for the SSC}$$

$$\begin{aligned} \sigma_n &< (\text{limit yet to be determines}) \text{ for } n = 3,4,5,6 \\ &\text{and monotonically decreases with } n \text{ for } n > 6, \\ &\text{and } \sigma_{n>6} \approx 10\% \text{ of } \sigma_{3-6} \text{ for the ALS [13].} \end{aligned} \tag{5}$$

For example, if adopted, an amplitude at which σ_n stops to decrease monotonically with $n > 6$ will be considered outside the acceptable aperture for the ALS. Whether these are to be developed further as aperture criteria remains to be seen.

ISSUE 4. MORE EXPERIMENT AND THEORY FOR PURPOSE OF CRITERIA

During the workshop, several activities were suggested for the theorists and the experimentalists. A few of such suggestions are listed below.

- Does the short term dynamic aperture suffice for electron storage rings? An experiment is suggested to measure the dynamic aperture and compare with the “proper” tracking as discussed earlier. Include magnet errors and orbit errors if necessary. The hope is that the stability region is indeed accurately predicted by the short term tracking. If not, it will have a serious impact for the electron designers.
- Experimentally determine the stability boundary in the $(\Delta v, \text{smear})$ space as discussed in Figure 5. The hope is to obtain the numerical values of the tune shift and smear limits.
- Analytically estimate the Arnold diffusion rate sufficiently accurately and identify a corresponding figure of merit [14]. The hope is that an easily calculable figure of merit can be identified, and it either replaces or supplements the smear as far as long-term stability is concerned.
- Measure the beam emittance blow-up versus tune in an electron storage ring (suggested by Susan Thomson). Correlate the blow-up with smear. Agreement would imply understanding of the sextupole solution and checking of the tracking program with reality. For synchrotron radiation sources, this experiment may be repeated with insertion devices.

CONCLUDING REMARKS

The issue of aperture criteria was brought to the attention of a wide spectrum of experts (theory & experiment, electrons & protons, colliders & synchrotron radiation sources). Four issues, eq. (1), were identified, and opinions exchanged (sometimes heatedly) among the participants.

Underlying the study of these issues is the wish that a universal set of aperture criteria could be established. Despite the high caliber of our group, we failed to accomplish this wish. This means a certain degree of arbitrariness and uncertainty will be with us for some time to come, and individuals still end up to be the sole decision makers about the aperture of their own accelerator.

However, we are making progress. A set of figures of merit are identified and discussed; aperture experiments are yielding encouraging results; theoretical tools are being improved. The insight gained in the workshop hopefully would help the individual efforts in the future.

REFERENCES

1. See their contributions to the workshop proceedings.
2. This is partially because of the wish to keep the vertical aperture small for the insertion devices.
3. Proton beam size goes like $E^{-1/2}$. Electron beam size goes like E .
4. Information collected from participants during the workshop.
5. For example, in SpS tracking, reported by Jacques Gareyte in these proceedings.
6. Don Edwards, SSC-22 (1985).
7. Tom Collins, SSC-26 (1985).
8. It turns out there has been a proliferation of the definition of the smear, but the differences are too detailed to be discussed here.
9. Jacques Gareyte, these proceedings.
10. Don Edwards, these proceedings.
11. Steve Peggs, these proceedings.
12. Frank Schmidt, see Ferdi Willeke, these proceedings.
13. Swapan Chattopadhyay and E. Forest, private communications. See also contribution of Chattopadhyay to these proceedings.
14. Talk by Sam Heifets to the criteria group.

APERTURE AND MULTIPOLE CRITERIA FOR LEP

A. Verdier

CERN, Geneva, Switzerland

ABSTRACT

For e^+e^- colliders the aperture is determined by lifetime considerations at high energy. The multipole content of any magnet in such a machine has to be as small as not to perturb too much the dynamic aperture associated with the chromaticity correction sextupoles.

1. APERTURE CRITERIA

In a given lepton circular machine, the transverse beam dimension is proportional to energy. Therefore, the aperture requirements are defined at high energy (physics conditions).

Lifetime considerations lead to leaving at least a 10σ margin for the beam. This must include both transverse amplitude (emittance) and momentum spread. In addition, some clearance for closed orbit distortion and for systematic energy loss due to synchrotron radiation has to be added.

For the present LEP [1] the aperture definition resulted from these considerations at 100 GeV. It had to be checked that the particles with amplitudes corresponding to the aperture so defined are within the dynamic aperture (see below). In fact, in a lepton machine there is some safety margin : the transverse emittance of the beam can be adjusted within certain limits by an adjustment of the damping partition numbers and the systematic energy loss makes an excursion which can be reduced by increasing the number of RF stations.

2. MULTIPOLE CRITERIA

The acceptable multipole contents of the LEP magnets have been determined from their influence on the dynamic aperture and on the non linear resonances.

The dynamic aperture is defined as the maximum emittance for which the betatron motion including synchrotron oscillations remains stable over 400 turns (i.e. a little more than one damping time at 55 GeV which is the smallest physics energy and thereby has the largest damping time). This maximum emittance is closely related to the multipole magnets present in the machine. The maximum emittance is determined by tracking trajectories which are started with initial conditions corresponding to the same number of standard deviations in both planes; tracking starts at a symmetry point and the slopes are taken to be zero.

In order to quantify the influence of the dynamic aperture on performance, a procedure was established [2]. It is based on filling the dynamic aperture with 10σ 's in 3 directions (transverse and momentum), with an emittance adjustment depending on the energy and working at a given beam-beam limit. This makes it possible to compute the luminosity as a function of the energy. Doing this, we can establish that there is : firstly a maximum energy due to the fact that for large momentum deviations there always appears a betatron instability due to the off-momentum mismatch of the lattice (this in turn touches the chromaticity correction problem which is tackled in another communication to this workshop [3]), and secondly a maximum luminosity.

Under these conditions, two multipole studies have been done. One study concerned the systematic parasitic sextupole and octupole components in dipoles compatible with the non-interleaved sextupole scheme which has a large sensitivity to the introduction of multipoles inside the sextupole pairs [4]. The tune shift with amplitude associated with tolerable components was deduced from this study and made it possible to infer tolerable high order multipole components in all LEP dipoles and quadrupoles. The tolerances found were easily met with the conventional magnet design. A second study was done for the superconducting low- β quadrupoles [5]. The effect of both random and systematic high order multipoles in the superconducting quadrupoles on the dynamic aperture was investigated. Indeed, these magnets have larger multipole components than steel magnet and the tolerances must be estimated to their very maximum and not taking very safe margins. It was checked that the expected multipole content of these quadrupoles did not need any compensation. The analysis was done in the same way as for the first study.

Tolerances associated with random multipole components everywhere in the machine were computed from their influence on tune shifts with amplitude (and compared to the ones found above as well as to those given for PETRA) and from the resonance bandwidths they produce (and compared to the ones produced by the beam-beam interaction) [6]. All these requirements could be met for the LEP magnets.

REFERENCES

1. LEP Design Report, Vol. II, The LEP Main Ring, CERN-LEP/84-01 (section 2.4).
2. E. Keil, 'High energy performance of LEP', LEP Note 337 (1981).
3. A. Verdier, 'Chromaticity correction for LEP: how did we get there?', this workshop.
4. A. Verdier, 'Non interleaved sextupole schemes for LEP and related effects on systematic multipole components in the lattice magnets, 12th Int. Conf. on High Energy Accelerators, FNAL, Batavia (1983).
5. S. Chen and G. Guignard, 'The effects of high order multipole imperfections on the LEP dynamic aperture, CERN-LEP-TH/85-37.
6. G. Guignard, 'Tolerances for the magnetic elements of the LEP lattice, 12th Int. Conf. on High Energy Accelerators, FNAL, Batavia (1983).

SUMMARY OF WORKING GROUP ON COMPENSATION SCHEMES

F. Willeke

Deutsches Elektronen-Synchrotron (DESY), Hamburg, Federal Republic of Germany

Contributors of the Working Group:

B. Autin	C.-S. Hsue	C. Planner	A. Verdier
R. Brinkmann	D. Neuffer	A. Ropert	F. Willeke
M. Cornacchia	S. Ohnuma	B. Simon	
E. Forest	Y. Orlov	R. Talman	
M. Harrison	A. Piwinski	S. Thompson	

1. COMPENSATION SCHEME ISSUES

By compensation schemes, we mean procedures to compensate the effects of nonlinear fields in circular accelerators. Two main cases may be distinguished: There are **chromaticity dominated** machines, where the main contributions to the nonlinear fields come from chromaticity compensating sextupole fields. This is in contrast to **error dominated** machines, where the field errors of the (bending) magnets are the most important source of nonlinearities. In general, we expect that the machines like electron and proton synchrotrons, low emittance electron storage rings and large electron colliders which are all built from normal conducting iron magnets to be chromaticity dominated. Large superconducting proton accelerators or colliders are error dominated machines. The TEVATRON is a machine in which chromaticity compensating sextupoles and magnet errors contribute to nonlinearities by approximately the same amount.

Among the chromaticity dominated machines, one may distinguish between large machines with **regular FODO arcs** and smaller machines with a more **irregular structure**. Compensation schemes are likely to differ in these cases. In error dominated machines, we have two kinds of errors: systematic field errors which are dominated by persistent current effects at low excitation, and random field errors which are produced by manufacturing tolerances of the superconducting magnets. These two types of errors apparently need different compensation strategies.

It turns out that in these different cases the goals of compensation are different too. In large electron colliders, the goal of compensation is to provide a large dynamic aperture which is proportional to the luminosity (in the case where the machine is operated at the beam-beam tune shift limit).

The same goal is pursued in synchrotron light sources. In these machines, the beam life time is determined by single scattering at the rest gas which can be overcome by a large dynamic aperture. Dynamic aperture may also be an issue for low energy proton synchrotrons where the beam has a large cross section and it occupies a large area in tune space.

In large, error-dominated proton machines, another goal is being developed [1]: The dynamic aperture cannot be defined in an unambiguous way that is valid for all cases. Furthermore, there are no analytical methods to calculate dynamic aperture. This makes systematic investigations very difficult and time consuming because it must be done by numerical simulations. Therefore, in order to arrive at an optimum magnet design for large superconducting proton colliders, a quantity has been defined which is better calculated by analytical methods. This is the distortion of the linearity of the motion of a particle. The quantity can well be calculated to high accuracy analytically [2]. Having this quantity in mind, the goal of compensation in large proton colliders may be formulated as to achieve almost linear behaviour of the particles within the aperture needed by the beam.

It is relevant for all cases that compensation schemes must be both feasible and practical. This means that the number of correction elements and the number of logical and physical circuits must be minimized.

Correction schemes should be tunable so that they can be adapted to a changing environment. Furthermore, they have to be robust in the sense of sensitivity against errors and imperfections.

2. CHROMATICITY COMPENSATION IN LARGE ELECTRON COLLIDERS

2.1 SEXTUPOLE COMPENSATION SCHEMES FOR LARGE e^+e^- COLLIDERS

The luminosity of electron colliders is inversely proportional to the β -function at the collision point (IP) and therefore also proportional to the chromaticity contributions ξ^* produced in the low- β quadrupoles. The limitation of ξ^* arises from the need to compensate it with sextupole fields which causes a dynamic aperture reduction due to the additional nonlinearity. If the chromaticity is compensated with two sextupole families, the maximum allowed ξ^* can be expressed by the chromaticity contribution from the arcs ξ^a and the needed dynamic aperture using a scaling law for the dynamic aperture[3]:

$$\xi^* = \xi^a \left[\frac{n^a}{n^n} - 1 \right]$$

(where n is the dynamic aperture measured in standard deviations; the superscript "n" means needed and the superscript "a" means no chromaticity contribution from the insertions).

However, besides the linear dependence of the tune due to the momentum deviation $\frac{\Delta p}{p}$, the variation of the β -functions with $\frac{\Delta p}{p}$ has to be compensated also. The latter is responsible for a nonlinear tune shift with $\frac{\Delta p}{p}$ and it may excite synchrotron resonances via the beam-beam interaction. For this reason, at least six sextupole families have to be introduced to cancel the six chromatic integrals

$$\begin{aligned} \xi_z^{(mc)} &= \oint ds \beta_z (k_z(s) - B_2(s) D_x(s)) \cos m\phi_z(s) \\ \xi_z^{(ms)} &= \oint ds \beta_z (k_z(s) - B_2(s) D_x(s)) \sin m\phi_z(s) \end{aligned}$$

B_2 : sextupole strength $m = 0, 2$ $z = x, y$
 $\phi_z(s)$: β -tron phase advance β_z : β -functions

This increases - not the mean but - the peak sextupole strengths. Therefore, the dynamic aperture might be further decreased which will reduce the maximum allowable ξ^* and thereby the luminosity. Thus the goal of a sextupole compensation scheme is to compensate the higher order chromatic effects without creating large additional nonlinear effects so that the above relationship between ξ^* and dynamic aperture is preserved.

In large machines with regular lattices and repeating structures, the nonlinear effects are well characterized by the strengths of nonlinear resonances. They are expressed in terms of "resonant harmonics" κ of the nonlinear potential A_{nm} (vector potential of the magnetic field B):

$$\begin{aligned} A_{nm} &= \frac{(-1)^m (n+m-1)!}{n!m!} \cdot \frac{d^k B_y}{dx^k} = \frac{(-1)^m k!}{n!m!} \cdot B_k \\ \kappa_{nm\nu\mu q} &= \frac{1}{\pi} \oint ds \left(\frac{\beta_x}{2} \right)^{n/2} \left(\frac{\beta_y}{2} \right)^{m/2} \binom{n}{\frac{n-\nu}{2}} \binom{m}{\frac{m-\mu}{2}} A_{nm} \cos(\nu\phi_x(s) + \mu\phi_y(s) - (\nu Q_x + \mu Q_y + q)2\pi s/L) \end{aligned}$$

B_k : multipole coefficients ; $k = n + m - 1$: multipole order
 $0 \leq |\nu| + |\mu| \leq n + m$: nonlinear resonance order ; $\nu Q_x + \mu Q_y + q \simeq 0$
 s : pathlength along design orbit ; L : circumference

The concept which is widely used in the design of sextupole compensations for large colliders is the interleaved sextupole placement with intrinsic resonance compensation. For this scheme a β -tron phase advances per FODO cell like

$$\phi_c = \frac{2\pi}{4}, \quad \frac{2\pi}{6}, \quad \dots$$

are needed. Ususally 60° and 90° degree lattices are considered (see for example LEP chromaticity compensation[4]). However, other rationals are also possible. For example, for the HERA electron ring, phase advances of

$$\phi_c = \frac{3}{16} \cdot 2\pi ; \quad \frac{5}{24} \cdot 2\pi \quad \dots$$

have been proposed. The general rule is that sextupole-driven, nonlinear resonances are not excited ("intrinsically compensated") in first order if the lattice is built up of **complete** supercells with an odd **integer** **β -tron phase advance** consisting of **two identical subsections**. Thus many phase advances are possible between 60° and 90° as it has been demonstrated for HERA. They all provide excellent sextupole correction, and the dynamic aperture obeys the scaling law as quoted above[3].

2.2 RESIDUAL NONLINEAR TUNE SHIFTS WITH AMPLITUDE IN INTRINSICALLY RESONANCE COMPENSATED SCHEMES

It is well known, that it is not sufficient to consider cancellation of only a few resonant harmonics to compensate the nonlinear effect as produced by sextupoles. However, if the resonance driving terms are compensated section wise, the length of a section is inversely proportional to the width of a band of cancelled harmonics around the resonant one. Thus, correcting a nonlinearity locally means that the width of the cancelled band becomes infinitely wide and the nonlinear effect is completely corrected.

In order to parameterize the effect of the noncancelled harmonics, the nonlinear tune shift with amplitude produced by the cross terms between sextupoles may be considered.

$$\Delta Q = \frac{J}{24\pi} \sum_{m=1,3} m \cdot \left(\frac{3}{\frac{3-m}{2}} \right) \left(\frac{3}{\frac{3+m}{2}} \right) \oint \oint ds ds' (\beta(s)\beta(s'))^{3/2} B_2(s)B_2(s') \frac{\cos m(|\phi(s') - \phi(s)| - \pi Q)}{\sin m\pi Q}$$

$$\begin{array}{ll} B_2 & : \text{sextupole strength} \\ \phi(s) & : \text{horizontal } \beta\text{-tron phase advance} \\ \epsilon, \psi & : \text{Courant Snyder invariant and phase} \end{array} \quad ; \quad \begin{array}{ll} \beta & : \text{horizontal } \beta\text{-function} \\ J & = \frac{1}{2} \oint d\psi \epsilon \end{array}$$

Like any higher order nonlinear effect, the tune shift involves a sum over all harmonics. It can be considered as a measure for all the other higher order nonlinear effects. (It should be mentioned that on one hand the tune shifts, besides being a measure, provide stabilization of nonlinear resonances but, on the other hand, lead to chaotic motion and instability because they cause stabilized island chains to overlap.) The question which one may ask is how much tune shift is excited in intrinsically resonance compensated, chromaticity-correction schemes. For regular FODO structures with two sextupole families, the tune shift excited by sextupoles in second order can be completely analytically calculated as a function of the phase advance per FODO cell. The result for different phase advances between 60° and 90° is that for the intrinsically resonance-compensated structure as discussed above, the residual tune shifts with amplitude are of the same order of magnitude. A detailed discussion of residual tune shifts is included in these proceedings[5].

3. CHROMATICITY CORRECTION IN SMALLER MACHINES

The concept described in the previous sections can not in general be applied to small machines with more irregular lattices or lattices with particularly strong chromatic effects. In low emittance machines like synchrotron light sources or damping rings, and also in low energy proton machines like \bar{p} -accumulators and damping rings intrinsically resonance-compensated schemes are usually not possible, as dedicated circuits have to be designed to cancel out the dangerous harmonics which drive the nonlinear resonances. This, however, leads to extremely nonlocal compensation with strong additional circuits which only cancel out the resonant harmonics. Because all the other harmonics are potentially harmful too, it is very likely that such a procedure will not improve the dynamic aperture. In the working group, two schemes to overcome this problem have been presented which are discussed below.

The first scheme is the compensation of distortion functions. The second scheme consists of the compensation of resonant harmonics and simultaneous compensation of the nonlinear tune shift with amplitude

excited by sextupoles in second order. The aim of both schemes is to compensate a large band of harmonics as it is in the case in large regular structures. Both methods, which are summarized below, are discussed in more detail in separate contributions to these proceedings[6,7].

3.1 COMPENSATION OF DISTORTION FUNCTIONS

If nonlinear fields are added to a linear lattice, the Courant Snyder invariants and phases are distorted. These distortions may be calculated order by order in the strength of the nonlinear field coefficients by means of perturbation theory[8,10,11,6]. Other methods like Lie algebra are being used also[2,12]. The parameter of the distortion of the Courant Snyder invariants,

$$\epsilon_z = \gamma z^2 + 2\alpha z z' + \beta z'^2 \quad z = x, y ,$$

are the Poincaré invariants

$$J_z = \frac{1}{2} \oint d\psi_z \epsilon_z ,$$

The distorted emittances can be expressed in the form

$$\frac{1}{2} \epsilon_x = J_x + \sum_{nm\nu\mu} J_x^{n/2} J_y^{m/2} (\sigma_{nm\nu\mu}^c \cos(\nu\phi_x + \mu\phi_y) + \sigma_{nm\nu\mu}^s \sin(\nu\phi_x + \mu\phi_y)).$$

$n, m \in 0, 1, \dots, \infty$

$\nu \in n, n-2, \dots, 1(0)$

$\mu \in m, m-2, \dots, 2-m, -m$

The distortion functions $\sigma_{nm\nu\mu}$ are the sum over all harmonics of the nonlinear potential weighted by $1/\nu Q_x + \mu Q_y - q$ (distance from the resonance). The coefficients $\sigma_{nm\nu\mu}$ are explicitly given in terms of the multipole coefficients and the linear lattice functions. One of the 10 terms proportional to the strength of the sextupole coefficient B_2 ($n = 3, m = 1, 3$) is:

$$\sigma_{3m}^c = \frac{m}{3} \left(\frac{3}{\frac{3-m}{2}} \right) \oint ds B_2(s) \left(\frac{\beta_x(s)}{2} \right)^{3/2} \frac{\cos m(|\phi_x(s) - \phi_x(s_o)| - \pi Q_x)}{\sin m\pi Q_x}$$

Dedicated sextupole correction circuits may be tuned so as to minimize the ten distortion coefficients. The procedure is in fact not very different from the minimization or compensation of driving terms, but the result may be quite different. Minimization or compensation of distortion functions is at present successfully used in various laboratories. The effect of compensated phase space distortions is expected to give significant improvement of the dynamic aperture.

3.2 RESONANCE COMPENSATION WITH SIMULTANEOUS TUNE SHIFT COMPENSATION

An alternative to the method described in the previous section is to not only compensate resonant harmonics in the usual way but also to compensate the nonlinear tune shift with amplitude driven by sextupoles in second order. From the expression for the tune shift it is apparent that the latter one is composed of a sum of distortion functions. On the other hand, the resonant harmonics which are cancelled one by one, are in the center of the band of harmonics included in the distortion functions . Thus the two methods are in fact only two variants of the same procedure, cancelling bands of harmonics around the resonant one. As it is demonstrated in ref.[7] the dynamic aperture of the ESRF-design has been drastically improved by this procedure which underscores its usefulness.

4. THE USE OF OCTUPOLES FOR COMPENSATION OF NONLINEAR EFFECTS EXCITED BY SEXTUPOLES IN SECOND ORDER

Another possibility to control the octupolar contributions to the resonance driving terms or phase space distortion functions excited by sextupoles in second order is to use octupoles. However, if one compares for example the driving terms for the $4Q_x$, $2Q_x$ -resonance and $0 \cdot Q_x$ detuning term as excited by octupoles,

$$\kappa_{4omq}^{cos} = \frac{1}{4\pi} \left(\frac{4}{\frac{4-m}{2}} \right) \oint ds \left(\frac{\beta_x(s)}{2} \right)^2 B_3(s) \cos(m\phi_x(s) - (mQ_x + q)\frac{2\pi s}{L})$$

B_3 : octupole strength

with the corresponding terms excited by sextupole cross terms[13]

$$\kappa_{4omq}^{cos} = \sum_{m'} \frac{3m'}{2\pi} \oint ds \oint ds' h_{\alpha-\alpha'}^{(s)} h_{\alpha'}^{(s')} \frac{\cos(m'|\phi_x^{(s')} - \phi_x^{(s)}| - m'\pi\tilde{Q}_x + m\phi_x(s) - (mQ_x + q)\frac{2\pi s}{L})}{\sin m'\pi\tilde{Q}_x}$$

$m' = 1, 3; \quad m = 4, 2, 0; \quad \alpha' = 3, 0, m', 0$

$$h_{3omo} = \left(\frac{3}{\frac{3-m}{2}} \right) \left(\frac{\beta_x(s)}{2} \right)^{3/2} \frac{B_2(s)}{3}$$

Q_x : linear tune; \tilde{Q}_x : amplitude dependent tune

it is apparent that the ratios of the three terms ($m = 4, 2, 0$) are not the same for sextupole excitation and octupole excitation. The same is true for the vertical terms ($4Q_y$, $2Q_y$ and $0Q_y$) and the mixed ones $2Q_x \pm 2Q_y$, $0Q_x + 2Q_y$, $2Q_x + 0Q_y$, $0Q_x + 0Q_y$. As a consequence, 22 orthogonal octupole circuits would have to be provided to cancel out exactly the sextupole-excited octupolar resonances.

It is not impossible to invent such a compensation scheme: (for example, for the $(4, 2, 0 \times Q_x)$ terms, a scheme with 16 octupoles in 6 families ABCDEF would work spaced by a 45° horizontal phase advance placed at identical β_x values in the order EF EF AB CD AB CD EF EF) but there is no doubt that such a scheme would be highly impractical, especially for small machines where it is unlikely that appropriate positions in the lattice can be found. On the other hand, by providing three independent families of octupoles placed at positions $\beta_x > \beta_y$, $\beta_x = \beta_y$ and $\beta_y > \beta_x$, it should be possible to compensate at least the detuning terms excited by the sextupoles which are usually the dominant and potentially most harmful higher order effects. In particular, it is possible to compensate the detuning terms quasi-locally in large periodic lattices under this condition. If less than 3 octupole families are used, a substantial improvement of the dynamic aperture is not very likely as it has been demonstrated in ref.[14]. If one or two additional circuits are available and the octupole correctors are placed at appropriate positions, it should always be possible to cancel one of the 22 different terms which is particularly strong and dominant in the situation considered. This has been proposed for the CERN antiproton collector ACOL[6].

5. COMPENSATION OF SYSTEMATIC MAGNETIC FIELD ERRORS IN LARGE SUPERCONDUCTING PROTON STORAGE RINGS

Global chromatic effects are less important in large superconducting proton storage rings like SSC or LHC. That is simply due to the fact that since these machines are so large in terms of the number of FODO cells, the chromaticity limit as defined above can never be reached because the low- β quadrupole aperture would be unrealistically large and the local optical distortions for off-momentum particles would become intolerably large. Moreover, because the arcs are by far the most costly part of such machines, the dipole aperture and field quality has to be a compromise between low costs and the requirements for single particle stability. Thus, large superconducting proton machines are error dominated.

5.1 LOCAL CORRECTION OF SYSTEMATIC FIELD ERRORS

When thinking about compensation of systematic field errors in extremely large lattices, it is important to realize that such systems have much in common with transport channels. That is because the distortion which is building up during a single revolution can become extremely large. The tune shifts with momentum and with amplitude may be as large as an integer and more. Thus, even without any resonant effect which would build up over many revolutions, the distortions would be intolerably large.

Compensation of nonlinear effects includes the range from local correction of the error at its origin to extremely nonlocal and lumped corrections, e.g. with just one correction element in the whole machine. From what has been said above, it is clear that compensation of field errors in large proton machines has to be closer to the first of these two extremes.

A technical solution for complete correction of nonlinear field errors of the superconducting magnets are correction coils, mounted directly on the beam pipe within a magnet. This is being done to correct the large persistent-current sextupole component, for example in the HERA superconducting dipole magnet [15]. However, such a solution – especially if it also includes the correction of higher order multipoles as is necessary for the SSC or a similar large hadron machine – will complicate the production of the s.c. magnets and considerably increase the costs. Thus alternative concepts are needed. In the working group recent work done at the Central Design Group for the SSC has been presented and discussed [16].

One solution consists of 3 or more lumped correctors in a correction coil package at different locations in a FODO half-cell. Such a lumped correction scheme works well so long as the course of the nonlinear potential can be approximated by a parabola which is true for not too high order multipoles between two quadrupole magnets. Lumped correction schemes as proposed for the SSC fully satisfy the SSC linearity criteria.

It is, however, not clear that an even more lumped correction scheme where correctors are placed only in every 2nd, 3rd, ... cell would yield sufficient compensation of the nonlinear effects. This question could not be answered within the working groups; but it is recommended that some attention be given to such options, which could possibly provide sufficient compensation for less costs, be simpler to operate and maintain.

5.2 PERSISTENT CURRENT EFFECTS

The strongest nonlinear field distortions of superconducting magnets are due to persistent currents. These are eddy currents induced in the superconducting filaments inside the magnet coils. The magnetic field produced by the coil penetrates the type II superconducting filaments, a change of the magnetic field changes the flux through the filaments which induces an eddy current to counteract that flux change. In dipole magnets, persistent currents excite all allowed (even order) multipoles from which the sextupole contribution is dominant. At low excitation, persistent-current field distortions tend to be very large. For the HERA proton ring, for example, which has a very low injection energy the persistent current sextupoles exceed the strengths of the chromaticity compensating sextupoles by a factor of 3. That is the reason why it has been decided to compensate them locally inside the HERA superconducting dipoles. But higher order persistent-current excited multipoles are also important in HERA. Effects from duodecapole components in the superconducting quadrupoles have to be corrected by local coils inside the quadrupoles, whereas for the rather strong decapole component in the dipoles (which has a strength of 1/3 of the persistent current sextupole at $r = 25$ mm), a lumped compensation with one 3m-long correction coil close to the middle of each half FODO cell is sufficient (see [17]).

Besides these well-known and well-understood [18] effects, a new phenomenon related to persistent currents has been reported recently. In the TEVATRON, it has been observed that the chromaticity changes as a function of time for a beam stored at injection energy ($E = 150$ GeV) within several minutes by 10 units [19]. This has been confirmed as a persistent current effect by magnet measurements at FERMILAB [20]. If the beam is then accelerated, the original value of the chromaticity is restored by a very quick change. The speed of this change depends on the ramp speed. Although the reason for the time dependence of persistent currents is not yet fully understood (though some promising work is being published [21,22]), the very quick change of persistent-current sextupoles at the beginning of the ramp can be explained as a consequence of the special hysteresis behaviour of the persistent-currents (see also Fig.1).

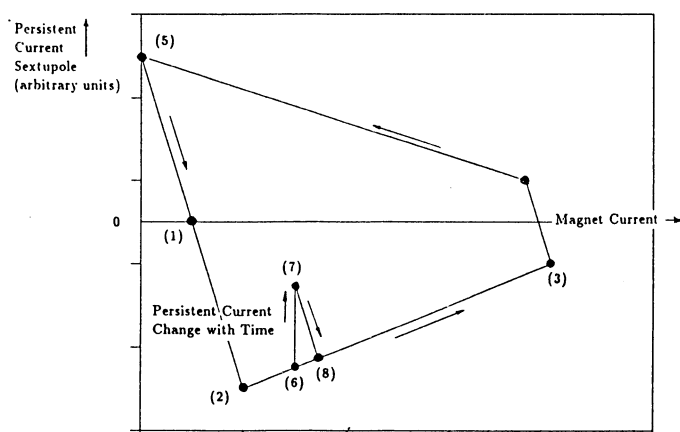


Figure 1: Persistent Current Sextupole Hysteresis (schematically). If the main current is increased persistent eddy currents are excited in the s.c. filaments in order to counteract the flux change. This continues until the critical current density of the superconductor is reached in the filaments (point 2). If the main field is increased further, the capability of the filaments to carry persistent currents decreases due to decreasing critical current density with increasing magnetic field and decreases due to the larger excitation current which is forced in addition through the filaments. If the change of the field is reversed at maximum excitation (3) eddy currents get induced in the other direction until the saturation point (4) is reached. Reducing the excitation further, the persistent current slowly increases and reaches its maximum at zero excitation. If the persistent current decays away during a store at injection energy (6 \rightarrow 7), the filaments get charged up with the full persistent current by the change of excitation at the beginning of the ramp due to this hysteresis behaviour (7 \rightarrow 8)

The phenomenon just described can cause a big operational problem if one is not prepared for it. Meanwhile at FERMILAB, the problem is meanwhile under control by ramping very slowly at the beginning and programming the chromaticity controlling power supplies appropriately[23].

6. COMPENSATION OF RANDOM ERRORS

Besides systematic field errors, superconducting magnets are subject to imperfections which vary between individual magnets due to manufacturing tolerances. Because it would be much too expensive to correct these errors individually, especially the higher order multipole errors, there are two strategies which have to be considered: (1) magnet sorting, which means that the magnets are installed in such a sequence in the machine so as to minimize the combined nonlinear effect, and (2) magnet binning which means that magnets with similar errors are connected to the same correction circuits.

6.1 MAGNET SORTING

It is obvious that in magnet sorting thus installing the magnets in a sequence so as to minimize the nonlinear distortions excited by nonsystematic magnet errors requires the knowledge of the field distortions of each individual magnet.

From the discussion of the systematic field errors and their influence on beam dynamics, it is clear that by a sorting scheme the compensation of nonsystematic errors should be as local as possible. The general principle remains the same: The shorter the period within which the contributions to the nonlinear

resonances and phase space distortions are compensated, the broader the band of cancelled harmonics. That means that the magnets have to be sorted in rather small groups. Fortunately, this is also preferable from an organisation point of view considering magnet storage space.

Magnet sorting as a strategy to minimize the effect of nonsystematic magnet errors on beam dynamics has been applied to the TEVATRON. The magnet sequence selected for installation minimizes the strongest driving terms of nonlinear resonances driven by sextupoles [24]. However, in particle tracking calculations for the TEVATRON in which the chosen magnet sequence was compared with a randomly shuffled magnet sequence[9,25] it did not show a significant advantage for the ordered sequence. The reason for that somewhat disappointing result has been discussed in the working group. Apparently it is not sufficient to rely completely on the concept of a small compensation period. A scheme which – at least for sextupoles – minimizes bands of harmonics more explicitly[26] was presented in the working group. The scheme is rather simple: a group of magnets which fills a period corresponding to a betatron wave length (assume $\phi_x = \phi_y$) is ordered so that the sextupole increases monotonically from the lowest to the largest value within this group. In the section which follows, the procedure is inversed so that there is a periodicity with twice the β -tron wave length. Thus the harmonic content of the nonlinear potential is shifted to Fourier components which are close to odd multiples of half the tunes ($Q/2, 3Q/2, 5Q/2, \dots$), whereas the harmonics close to the resonances ($Q, 2Q, 3Q, 4Q = \text{integer}$) are depopulated. It also should be mentioned, that this sorting scheme has been tested for the SSC with satisfactory results [27].

An alternative scheme is proposed for the HERA proton ring[28]. Here a broad band of harmonics is minimized by taking into account the driving terms for resonances driven in 2nd order when ordering the magnets in small groups to minimize the nonlinear resonance driving terms. This scheme which is implemented to take into account resonances up to order 12 is expected to give good results for the HERA proton ring.

6.2 MAGNET BINNING

An alternative concept which works in connection with correction elements powered by several correction circuits is magnet binning. Magnets with similar nonsystematic multipole errors will be connected to the same correction circuit. As with sorting, it has in common that the field quality of all the individual magnets needs to be measured.

It has been demonstrated in the working group that just as in case of constant, systematic field errors, a correction scheme as proposed by D. Neuffer[16] also works for nonsystematic errors which vary along the orbit in a half FODO cell.

Using perturbation theory, it can be shown that the distortion Δ of the linear motion $q_o^{(s)}, p_o^{(s)}$,

$$\bar{q}(s) = \bar{q}_o(s) + \Delta(s, \bar{q}_o, \bar{p}_o)$$

can be written in the form[29]

$$\Delta = \sum_n \int_o^l ds f(s) s^n \cdot \frac{H_o^n}{n!} V(\bar{q}_o, \bar{p}_o)$$

provided that the unperturbed linear motion $q_o(s), p_o(s)$ is described by a Hamiltonian function which does not explicitly depend on the path length s along the closed orbit, and that the nonlinear distortion potential factors in an s -dependent and a coordinate dependent part

$$H_1 = f(s) \cdot V(\bar{q}, \bar{p})$$

These conditions are met (in very good approximation) for the motion of charged particles through a half FODO cell between the quadrupoles. Thus, for correction of the nonlinear effects, it is sufficient to add correction elements of strength f_c in such a way to the half-cell so as to minimize the moments

$$G_n = \int_o^l ds (f(s) - f_c(s)) s^n$$

This is the generalization of Neuffer's scheme[16] which will be described in more detail in a separate contribution to these proceedings [29].

7. CONCLUSIONS

In the working group concerning compensation schemes, a wide range of problems in compensating the effects of nonlinear fields in accelerators has been presented and discussed. In the discussion of the various subjects, it was confirmed that the new concepts which have been proposed in the last few years such as nonlinear distortion functions, effects of cross terms between nonlinear elements, and the concepts of linear aperture, are being used successfully in various laboratories with compensation schemes being modified to take into account these new criteria. Concepts which have been used in the past like resonance compensation have been developed to a certain degree of sophistication. We hope that the one-week discussions of the workshop will further stimulate and encourage accelerator scientists to use the new tools to improve the performance of accelerators with respect to nonlinear beam dynamics.

References

- [1] A. W. Chao: "Magnet Field Quality Requirements for the SSC", SSC-75 (1986)
- [2] E. Forest: "Analytical Computation of Smear", SSC-95 (1986)
- [3] R. Brinkmann and F. Willeke, "Chromaticity Compensation in the HERA Electron Ring", these proceedings
- [4] E. Keil, CERN-LEP note 350 (1981)
A. Verdier, these proceedings
- [5] B. Autin and F. Willeke, these proceedings
- [6] B. Autin, these proceedings
- [7] A. Ropert, these proceedings
- [8] F. Willeke: "Study of the Nonlinear Acceptance of the TEVATRON by Computer Simulations", FERMILAB TM 1220 (1983)
- [9] F. Willeke: "Determination of the Dynamic Aperture in Circular Accelerators by the Perturbation Theory Method", Proceedings of the Workshop on the SSC, Ann Arbor (1983)
- [10] F. Willeke: "Analytical Study of the TEVATRON Nonlinear Dynamics", FERMILAB FN-422 (1985)
- [11] T. Collins: "Distortion Functions", FERMILAB Publ. 84-114 (1984)
- [12] L. Michelotti: "Deprit's Algorithm, Green's Functions and Multipole Perturbation Theory", Part. Accelerators, Vol 19 no 1-4 p205 (1985)
- [13] F. Willeke and F. Schmidt, to be published in the proceedings of the European Accelerator Conference, Rom (1988)
- [14] M. Cornacchia and Y. Chin: "A Study of the Dynamic Aperture Limit in TRISTAN", Part. Accelerators Vol 17 (1985), p191-213
- [15] HERA Proposal, DESY Hamburg (1981)
- [16] D. Neuffer: "Lumped Correction of Systematic Multipoles in Large Synchrotrons", SSC-132 (1987)
D. Neuffer, these proceedings
R. Talman, these proceedings
- [17] R. Brinkmann and F. Willeke: "Persistent Current Field Errors and Dynamic Aperture of the HERA Proton Ring", these proceedings
- [18] M.A. Green: "Residual Fields in Superconducting Magnets", Proceedings of the Magnet Techn. Conf., MT-4 p339 (1972), Brookhaven Natl. Lab.

- [19] D. Finley et al: "Time Dependent Chromaticity Changes in the TEVATRON", 1987 IEEE Part. Acc. Conf., Washington (1987)
- [20] R. Hanft, private communication
- [21] D. Edwards, private communication
- [22] H. Brück et al, DESY-HERA, to be published
- [23] M. Harrison , R.P. Johnson, private communication
- [24] H. Edwards: "The Energy Saver Test and Commissioning History", Proceedings of the 12th Internat. Conf. on High Energy Accelerators FERMILAB (1983)
- [25] N. Gelfand: "Calculation of the Dynamic Aperture of the TEVATRON", Proceedings of the Workshop on the SSC, Ann Arbor (1983)
- [26] R. Gluckstern and S. Ohnuma: "Reduction of the Sextupole Distortion by Shuffling Magnets in Small Groups", IEEE Trans on Nucl. Science Vol NS32 No p2314 (1985)
S. Ohnuma, these proceedings
- [27] S. Peggs: "Accelerator Physics in Large Proton Storage Rings", Proceedings of the 13th Internat. Conf. on High Energy Accelerators, Novosibirsk (1986)
L. Schachinger (1986), unpublished
- [28] F. Willeke: "A Magnet Ordering Procedure for the HERA Electron-Proton Collider", DESY HERA 87-12 (1987)
- [29] E. Forest, these proceedings

THE APERTURE OF THE HERA PROTON RING

F. Willeke

Deutsches Elektronen-Synchrotron (DESY), Hamburg, Federal Republic of Germany

1. Introduction

In this report the criteria and the methods on which the aperture decision for the HERA superconducting magnet is based on, is reviewed from a beam dynamics point of view. A large number of people have been working on that problem during the last decade: R. Brinkmann, E. Karanzoulis, J. Maidment, H. Mais, G. Ripken, J. Rossbach, Frank Schmidt, P. Wilhelm, A. Wrulich and F. Willeke.

For those who are not familiar with the HERA electron proton collider, a summary of the main parameters is given in table 1.

Table 1: Parameters of the HERA storage rings					
	Electrons	Protons		Electrons	Protons
Max. Energy/GeV	30	820	Inject. Energy/GeV	14	40
Circumference/m	6336	6336	Number of IPs	3 (4)	3 (4)
Straight Sect./m	4 × 360	4 × 360	Bending Field /T	0.185	4.53
rf Frequency /Mhz	500	52/208	Harmonic Number	10560	1100/4400
Circumf. Volt./MV	165	0.3/2.4	Number of bunches	210	210
σ_x /mm (IP)	0.27	0.24	σ_y /mm (IP)	0.06	0.07
Beam current/mA	60	150	Long.Spin Polariz.	87%	-
Polariz. Time/min	24	-			
Luminosity $L = 1.6 \times 10^{31} sec^{-1} cm^{-2}$					

The considerations which will follow are restricted to the superconducting proton ring. There are of course other important non-beam-dynamics issues which have played a role in the aperture decision but they will not be considered here.

2. The aperture need of the HERA Proton Storage Ring

The HERA proton acceleration chain starts in a **50 MeV linac**, a copy of the CERN Alvarez linac, which will deliver a $10mA$ H^- beam with a transverse normalized 2.5 sigma emittance of $\epsilon = 8 \cdot 10^{-6} \pi rad m$ and an energy spread of $\Delta E = 120 keV$. The H^- beam is injected in multi turns into the DESY III - booster through a carbon stripping foil and accelerated as a proton beam up to $7.5 GeV/c$. It then gets transferred to PETRA which accelerates the protons up to the HERA injection energy of $40 GeV$. A careful adjustment of this acceleration chain will lead to the developement of beam density as presented in table 2.

It should be mentionend that the largest aperture in HERA is needed at injection, even if the large amplitude functions in the low β quadrupoles have been reduced to ease injection. Based on the numbers shown in table 2, the aperture requirements for the HERA proton ring are as follows: The injected beam occupies transversly a phase space area of $\epsilon_{x,y} = 0.5 \pi radm$ (95% of the beam). If one allows for an accidental blow up of 100% in order to avoid frequent injection quenches of the superconducting magnets, a phase space area of $\epsilon_{x,y} = 1.0 \pi radm$ must be provided. This corresponds to maximum horizontal and vertical beam sizes in the arc of $(\beta_{x,y}^{max/min} = 80/13m)$ $\sigma_{x,y} = 9mm$. Additional space must be provided due to a beam momentum spread of $\frac{\Delta p}{p} = 4 \cdot 10^{-4}$. Allowing here also for an accidental blow up of 100% the transverse amplitude increase due to momentum spread is $\Delta \sigma_x = 1.6mm$ so that we have to assume a transverse beam size in the arc of $\sigma_x \times \sigma_y = 10mm \times 9mm$. In addition one has to provide space for extraordinary injection errors. It is very difficult to predict how large the injection errors will be in a new

machine. All the injection elements and also the injection diagnosis is specified such that the injection errors don't contribute significantly to the beam emittance.

Transfer	Momentum [GeV/c]	ϵ_{long} [eV sec]	long. blow up	$\epsilon_{x,y}$ [$\pi rad m$]	transv. blow up
Linac → DESYIII	0.3 → 0.30	0.003 → 0.072	20.0	8.0 → 8.0	1.0
DESYIII → DESYIII	0.3 → 7.50	0.072 → 0.090	1.25	8.0 → 9.6	1.2
DESYIII → PETRAII	7.5 → 7.50	0.090 → 0.112	1.25	9.6 → 11.5	1.2
PETRAII → PETRAII	7.5 → 40.0	0.112 → 0.140	1.25	11.5 → 13.9	1.2
PETRAII → HERA	40. → 40.0	0.140 → 0.175	1.25	13.9 → 16.9	1.2
HERA → HERA	40. → 820.	0.175 → 0.300	1.70 ^{*)}	16.7 → 20.0	1.2
*) includes intra beam scattering during injection time					

Experiences with existing machines show that an injection orbit deviation of about $\Delta X_{c.o.} \simeq 2mm$ is what one has to expect after some time of operation without fine tuning of the injection elements. Two numbers are presented which give an impression of the sensibility of the machine with respect to errors. If one assumes that the quadrupoles move between two proton injections by $10\mu m$ the injected beam will miss the closed orbit likely by $2mm$. If the injection septum has a small failure so that it misses its correct value by 0.1% (specification is 10^{-4}), the resulting orbit error is $\Delta x = 2mm$. The conclusion is that a good field aperture of $a = (20 - 30)mm$ is needed for the HERA proton ring.

3. The Relevance of the TEVATRON

The experience made during construction and commissioning of the TEVATRON have been observed carefully by the DESY designers and they played an important role in the HERA aperture decision. Table 3 shows a summary of the Fermilab magnet measurements[1] which have been taken as a reference of the magnet errors expected for HERA.

Low Field (Injection Energy 150GeV)					High Field (1TeV)				
Normal Component			Skew Component		Normal Component			Skew Component	
n	average	sigma	average	sigm	n	average	sigma	average	sigm
1	0.0	0.0	0.0	0	1	0.0	0.0	0.0	0
2	0.0	0.63	0.0	0.79	2	0.0	0.63	0.0	0.69
3	-4.71	3.75	-0.11	1.29	3	-0.99	3.50	0.38	1.29
4	-0.23	0.89	-0.04	1.67	4	-0.27	0.87	-0.07	1.69
5	0.12	1.42	-0.04	0.56	5	-0.76	1.60	-0.07	0.53
6	-0.02	0.41	-0.15	0.69	6	-0.05	0.37	-0.10	0.67
7	6.69	1.03	0.15	0.41	7	5.48	1.01	-0.13	0.46
8	0.02	0.29	0.25	0.44	8	-0.12	0.29	0.45	0.35
9	-15.69	1.98	-0.73	0.87	9	-15.43	2.01	-0.68	0.88
Values in Units of 10^{-4} at $r=25.4mm$									

There are certain remarkable details one learns from those measurements: First, the persistent current sextupole which is rather large at low fields, does not have a significant nonsystematic component. This is important because of the large persistent current effects in HERA due to the low injection energy (40 GeV for HERA, 150 GeV for the TEVATRON). Furthermore there are no higher order persistent current multipole components, except the persistent current decapole. The latter one however which is about $\frac{1}{5}$ of the p.c. sextupole, has been neglected by the DESY designers at the time. Fig 1a shows tracking calculations [2] made with the RACETRACK computercode [3] for the TEVATRON. The dynamic aperture was calculated as a function of constant momentum deviation assuming high field errors as quoted above. The result is that a beam with horizontal and vertical amplitudes of $\sqrt{x^2 + y^2} = 22mm$ remains stable (particles survive 200 turns). This is in agreement with TEVATRON experience. The conclusion one can draw from these measurements, experiences and calculations is that a TEVATRON like magnet with a

coil diameter of $D_{coil} = 73mm$ and a free space inside the beam pipe of $D_{beam} = 60mm$ corresponds to the HERA needs, provided that one compensates the much higher persistent current sextupole in HERA which is due to the much lower injection energy. Therefore it was decided to compensate the persistent current sextupole locally by correction coils which are wound on the beam pipe inside the dipole magnet. This however leads to a further reduction of the aperture to $D_{beam} = 56mm$. Another safety factor with respect to the TEVATRON magnet is achieved by improving the field quality of the magnet considerably by wedges between the cables of the coil. The cross section of the HERA magnet is shown in fig 1b, preliminary results of the measurements of $\Delta B/B$ on prototypes of the HERA superconducting dipole is shown in table 4. No multipole errors higher than order $n=5$ have been detected.

Table 4 $\Delta B/B$ of HERA S.C. Dipole Prototypes				
	normal component		skew component	
n	average	sigma	average	sigma
2	-0.4	0.7	1.7	1.2
3	-3.1	2.0	-0.6	0.9
4	-0.3	0.40	-0.7	1.2
5	-1.02	0.6	-0.05	0.4
Values in units of 10^{-4} at $r=25mm$				

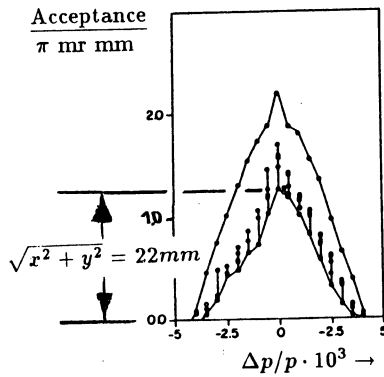


Figure 1a: TEVATRON Dynamic Aperture
Determined by Particle Tracking as a
Function of Constant $\Delta p/p$ with Multi-
pole errors in the dipoles, o: system., +:
random

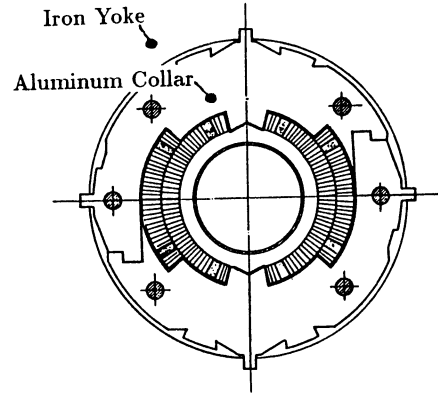


Figure 1b: The HERA Superconducting
Dipole

4. Stability Assurance

4.1 Computational Tools

Numerical particle tracking codes as well as analytical methods have been used to assure stability in the HERA proton ring. One of the most important tools is the "kick"-code RACETRACK written by A. Wrulich [3]. This code which was restricted to two degrees of freedom and in which the longitudinal momentum amplitude was modulated "externally", has been extended to include synchrotron oscillations [4] using a symplectic six-dimensional formalism [5]. Among the analytical tools, the model of isolated nonlinear resonances [6] was used to estimate the strengths of the nonlinear effects. A deeper understanding of the reduction of dynamic aperture was obtained by the use of higher order perturbation theory [7]. A

systematic theory of nonlinear synchrotron resonances was developed to understand the impact [8] of coupling between longitudinal and transverse motion. Finally methods which are summarized as "qualitative theory of dynamical systems" [9] are used in connection with tracking to explore the boundary of stability of the motion. This includes the concept of the Lyapunov exponent to detect global chaos. Examples for the use of these methods will be given below.

4.2 Particle Tracking

The particle tracking code RACETRACK takes nonlinearities into account as localized kicks which are separated by purely linear elements. The dynamic aperture is defined as the largest starting amplitude in the phase space $(x, x'\beta_x + x\alpha_x, y, y'\beta_y + y\alpha_y)$ which survives a few hundred turns. A large number of systematic tracking calculations has been performed to determine the field quality requirements of the HERA magnets. Various parameters have been scanned such as tunes, momentum offset, size of the closed orbit errors, and sets of random errors. Figs 2a,b show typical examples of such a parameter scan. They have been taken from ref [10].

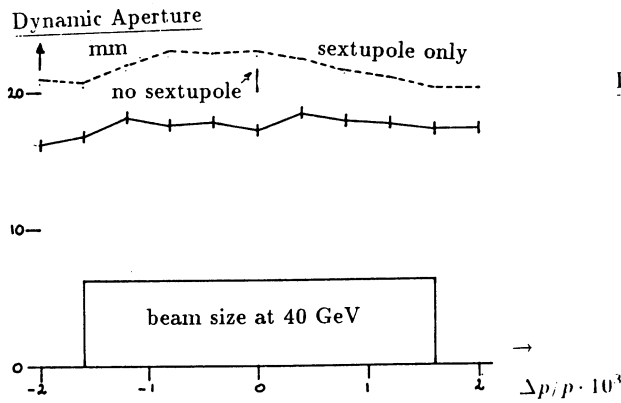


Figure 2a: Dynamic Aperture of the HERA Proton Ring as a Function of Constant Momentum Deviation With and Without Systematic and Nonsystematic Multipole Errors in the Dipoles

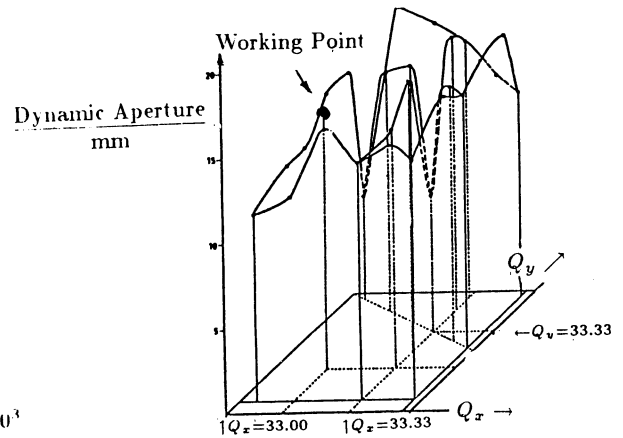


Figure 2b: Dynamic Aperture of the HERA Proton Ring as a Function of the Machine Tunes With 3rd Integer Resonance Compensation

4.3 Example of the Use of Perturbation Theory

An interesting question is whether the dynamic aperture of the TEVATRON is determined by the large 14-pole and 18-pole components of the dipole field (see table 2). These multipole components have been avoided in the HERA design. This question cannot be trivially answered by particle tracking. In perturbation theory however, the phase space distortions can easily be decomposed into contributions from different multipoles. From fig 3a, which shows the relative distortion of the Courant Snyder invariant in the TEVATRON (systematic field errors only) and which is taken from ref[7] it is apparent that at amplitudes close to the dynamic aperture the phase space distortions are dominated by 14-pole and 18-pole contributions which overweight the other ones by almost an order of magnitude.

4.4 Chaos as a Criterion for the Boundary of Stable Motion

Long time particle tracking for the HERA proton ring over up to several 10^5 turns confirmed that the particle motion can become unbounded even after such a long time of quasi stable motion. Therefore the onset of such chaotic (because unpredictable) trajectories which form a quasi stable layer around the stable inner core of the phase space is defined as the dynamic aperture. In principle everywhere, also in the inner part of the phase space, there are chaotic trajectories in vicinity of periodic orbits which may be connected

part of the phase space, there are chaotic trajectories in vicinity of periodic orbits which may be connected to the outer chaotic layer due to the complicated topology of high dimensional nonlinear phase space. Thus particles could diffuse out of the inner part of the phase space and might get lost. However for HERA, Arnold diffusion could be excluded whenever such trajectories have been detected.

In order to use chaos as a practical mean to determine the border of stability, a procedure for early detection of chaos is needed. The distance of two close phase space trajectories diverges exponentially if the motion is chaotic (see for example [11]) The exponent which describes this divergence is called Lyapunov exponent. For HERA a numerical procedure was developed which allows the detection of a non vanishing Lyapunov exponents already after a few 10^3 turns (see fig 3b)[4].

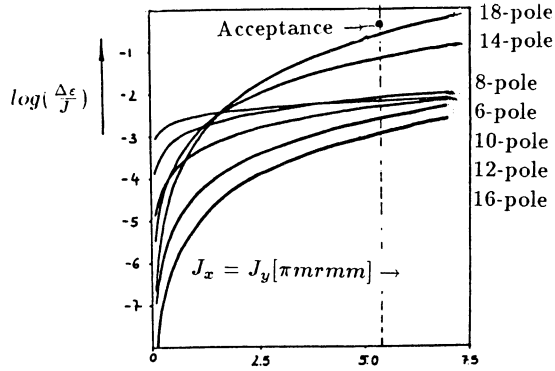


Figure 3a: Distortion of the Horizontal Emittance ε_x due to Systematic Field Errors in the TEVATRON as a Function of Phase Averaged Emittance $J = 1/2 \int d\Phi$

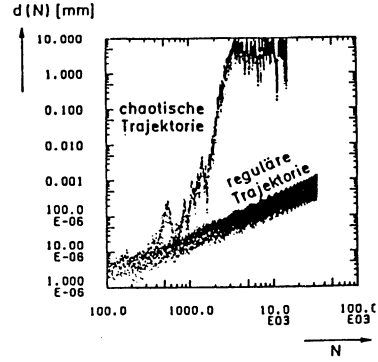


Figure 3b: Detection of Chaos in HERA by Analyzing the Evolution of The Distance of two Close Phase Space Trajectories

References

- [1] R. Hanft et al, IEEE Trans Nucl Science Vol NS-30 no 4 (1983)
- [2] F. Willeke, FERMILAB TM 1220 (1983)
- [3] A. Wrulich, DESY 84-026 (1984)
- [4] F. Schmidt, Thesis, University of Hamburg, DESY HERA 88-02 (1988)
- [5] G. Ripken, DESY 85-084 (1985)
- [6] G. Guignard: "A General Treatment of Resonances in Accelerators", CERN MA-78-11 (1978)
- [7] F. Willeke: "Analytical Study of the TEVATRON Nonlinear Dynamics", FERMILAB FN-422 (1985)
- [8] D. Barber et al: "Nonlinear Theory of Coupled Synchro-Betatron Motion", DESY 86-147 (1986)
- [9] H. Mais et al: "Particle Tracking", Cern Accelerator School CERN 87-03 (1985)
- [10] A. Wrulich, in Acc. Phys. Issues for a Supercond. Super Collider, Ann Arbor (1983)
- [11] A.M. Lyapunov: "Stability of Motion", Academic Press New York (1966)

MULTIPOLE CORRECTION IN LARGE SYNCHROTRONS*

David Neuffer

Los Alamos National Laboratory, Los Alamos, New Mexico, USA

ABSTRACT

A new method of correcting dynamic nonlinearities due to the multipole content of a synchrotron such as the Superconducting Super Collider is discussed. The method uses lumped multipole elements placed at the center (C) of the accelerator half-cells as well as elements near the focusing (F) and defocusing (D) quads. In a first approximation, the corrector strengths follow Simpson's Rule. Correction of second-order sextupole nonlinearities may also be obtained with the F, C, and D octupoles. Correction of nonlinearities by about three orders of magnitude are obtained, and simple solutions to a fundamental problem in synchrotrons are demonstrated. Applications to the CERN Large Hadron Collider and lower energy machines, as well as extensions for quadrupole correction, are also discussed.

INTRODUCTION

The Superconducting Super Collider (SSC)¹ requires adequate linearity for beam stability and reliable operation. Linear motion is required over a working region sufficient to include the beam size and momentum spread with closed orbit deviations and injection errors. Orbit nonlinearity can be measured by the amplitude and momentum-dependent tune shifts per turn $\Delta\nu_x, \Delta\nu_y$. An SSC linear aperture tolerance (SLAT) has been set by requiring $\Delta\nu_x, \Delta\nu_y \leq \pm 0.005$ for orbits with amplitudes A_x, A_y , up to 0.5 cm in the SSC arcs and with momentum offsets $\delta \equiv \frac{\Delta p}{p} \leq \pm 0.001$.¹ (The SSC also requires small amplitude distortion.) The magnetic fields in the dipoles may be represented by the complex expression

$$B_y + iB_x = B_o \{1 + \sum [b_n(s) + ia_n(s)](x + iy)^n\} ,$$

where B_o is the bending field and $b_n(s)$ and $a_n(s)$ are the normal and skew multipole components. The transverse motion may then be described by a Hamiltonian,

$$H = \frac{I_x}{\beta_x(s)} + \frac{I_y}{\beta_y(s)} + \Re \sum_n \frac{B_o [b_n(s) + ia_n(s)](x + iy)^{n+1}}{B\rho (n+1)} ,$$

where $\beta_x(s)$ and $\beta_y(s)$ are the betatron functions of linear motion. The coordinates x and y of particle motion are represented in action-angle variables (I, ϕ) by $x = \sqrt{2\beta_x I_x} \cos(\phi_x) + \eta\delta, y = \sqrt{2\beta_y I_y} \cos(\phi_y)$; the off-momentum orbit at δ determined by the dispersion $\eta(s)$ is included. The terms $A_x = \sqrt{2\beta_x I_x}$ and $A_y = \sqrt{2\beta_y I_y}$ are the amplitudes.

The tune shifts are obtained to first order by averaging the phase advance caused by the field perturbation

$$\Delta\nu_{x,y} = \frac{1}{2\pi} \int \frac{d\phi_{x,y}}{ds} ds = \Re \left(\frac{dH}{dI_{x,y}} \right) . \quad (1)$$

In first order in the coefficients b_n and a_n , only systematic normal multipoles (\bar{b}_n) contribute; the resulting expressions for the tune shifts as a function of the variables I_x, I_y , and δ due to sextupole (b_2), octupole (b_3) and decupole (b_4) components are

$$\begin{aligned} \Delta\nu_x &= \langle b_2 \beta_x \eta \delta \rangle + \left\langle \frac{3}{4} b_3 \beta_x^2 I_x - \frac{3}{2} b_3 \beta_x \beta_y I_y + \frac{3}{2} b_3 \beta_x \eta^2 \delta^2 \right\rangle \\ &\quad + \langle 3b_4 \beta_x^2 \eta I_x \delta - 6b_4 \beta_x \beta_y \eta I_y \delta + 2b_4 \beta_x \eta^3 \delta^3 \rangle \\ \Delta\nu_y &= -\langle b_2 \beta_y \eta \delta \rangle + \left\langle \frac{3}{4} b_3 \beta_y^2 I_y - \frac{3}{2} b_3 \beta_x \beta_y I_x - \frac{3}{2} b_3 \beta_y \eta^2 \delta^2 \right\rangle \\ &\quad + \langle 3b_4 \beta_y^2 \eta I_y \delta - 6b_4 \beta_x \beta_y \eta I_x \delta - 2b_4 \beta_y \eta^3 \delta^3 \rangle . \end{aligned} \quad (2)$$

The tune shift criteria set tight tolerance limits² on uncorrected $|\bar{b}_n|$; see Table I.

The SSC dipoles are expected to have significant multipole content, particularly in the \bar{b}_n with n even, which are allowed in dipole symmetry. Estimates³ of the expected systematic and rms random multipole strengths as extrapolated from the measurements⁴ of the similar Tevatron dipoles or calculated from saturation and persistent current effects¹ have been collected in Table I. Serious deficiencies in $\bar{b}_2, \bar{b}_3, \bar{b}_4$ and possibly \bar{b}_6 are obtained. Consequently, initial SSC design included sets of multipole trim coils within every dipole for correction of \bar{b}_2, \bar{b}_3 , and \bar{b}_4 .

*Work supported by the US Department of Energy, Office of High Energy and Nuclear Physics.

TABLE I. Tolerances and estimated strengths of systematic multipole content in the SSC dipoles. All multipole strengths are in units of 10^{-4} cm^{-n} . The tolerances are obtained from the SLAT. Estimated strengths are extrapolated from Tevatron data or calculated from the magnet properties.

Multipole	Tolerance in SSC Lattice (230 m, 90° Cells)	Estimated Random Error (Tevatron)	Systematic Strength (Tevatron)	Persistent Current Multipole Strength	Saturation Multipole Strength
b_2	0.0097	2.0	0.45	-4.7	1.2
b_3	0.017	0.35	-0.14	-	-
b_4	0.031	0.60	-0.33	0.30	-0.05
b_5	0.054	0.06	-0.024	-	-
b_6	0.096	0.08	1.57 ^a	0.07	-0.01
b_7	0.17	0.16	0.009	-	-
b_8	0.29	0.02	-2.1 ^a	<0.02	0.02

^a The higher allowed multipoles (b_6 , b_8) were not minimized in the Tevatron design; the SSC conductor placement should reduce these within tolerances.⁵

The trim coil correction requires separately powered sextupole, octupole, and decupole windings within the bore tube of every dipole. They greatly complicate the dipoles by making the SSC dipoles multifunction magnets, restricting the physical aperture and adding difficulties in quench behavior. Also, the trim-coil correction is inflexible in that the trim coil multipoles and strengths must be fixed before the dipoles are built; they may therefore be insufficient. Recently, a better correction method using separated correction elements has been developed and that is the subject of this paper.^{6,7}

CORRECTION WITH DISCRETE CORRECTORS

The new method of multipole correction uses separate multipole elements placed at the Center (C) of the accelerator half-cells as well as elements near the focusing (F) and defocusing (D) quadrupoles.⁶ Figure 1 shows an idealized picture of the correction method, with three correctors per half-cell. In practice, the correctors on opposite ends of the quads would be combined in lumped elements on either side of the short F and D quads (see Fig. 2), where chromaticity sextupoles and trim dipoles and quads are already planned. There are, therefore, only two physical corrector elements per half-cell.

The first-order correction of tune shifts can be quite impressive. Table II shows the correction of octupole (b_3) and decupole (b_4) tune shifts. Correction with only F and D correctors reduces tune shifts by only a factor of ~ 2 . Adding C correctors and setting the corrector strengths naively by Simpson's Rule for three-point integration reduces tune shifts by two orders of magnitude. Some further tuning of the corrector strengths about the Simpson's Rule values can reduce the tune shifts by another order of magnitude. The correction is more than adequate for the SSC.

Consideration of the form of the terms that appear in the tune shifts [see Eq. (2)] indicates why the Simpson's Rule correction is so accurate. For example, the first-order amplitude-dependent 1-D tune shift caused by octupoles may be written as

$$\Delta\nu_x = \frac{3I_x}{4L} \left\{ \int_0^L b_3(s) \beta_x^2(s) ds + \left[\frac{S_{3,F}}{B_o} \beta_x^2(0) + \frac{S_{3,C}}{B_o} \beta_x^2(L/2) + \frac{S_{3,D}}{B_o} \beta_x^2(L) \right] \right\} \quad (3)$$

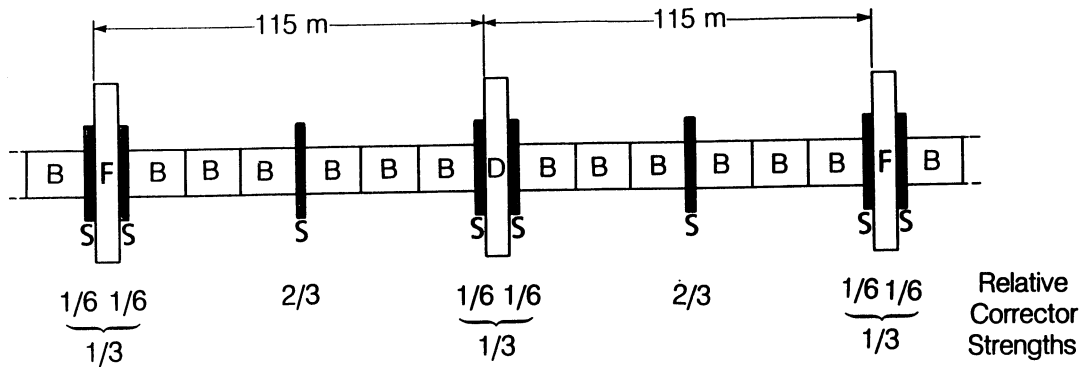


Fig. 1. A symmetrical SSC cell. The element labels are: B – dipoles, F and D – quadrupoles, S – slots for correctors, C – center corrector slot. The correctors on opposite sides of the F and D quads may be combined on either side and exact symmetry is not necessary.

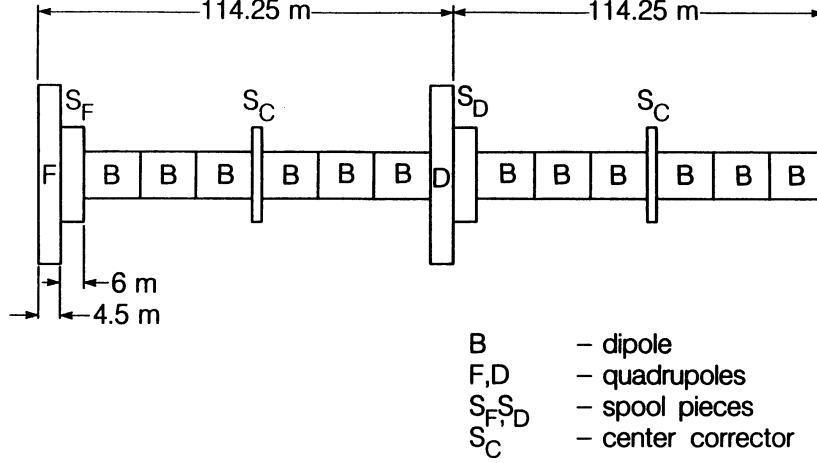


Fig. 2. An actual SSC cell with the added center correction.

in a simplified lattice. All first-order $\Delta\nu$ terms are of similar form. The corrector multipole strengths $S_{n,i}$ are defined by $S_{n,i} \equiv B_{n,i} l_i = -f_{n,i} B_0 \tilde{b}_n L$, where $B_{n,i}$ and l_i are the corrector lengths and strengths, and L is the half-cell length. The Simpson's Rule solution⁸ is $f_F = f_D = 1/6$ and $f_C = 4/6$ per half-cell and corrects all $\Delta\nu$ terms by approximately two orders of magnitude.

The correction [Eq. (3)] is equivalent to approximating integrals of powers of betatron functions by a sum over discrete points, and Simpson's Rule is a third-order integration that is very accurate for smoothly varying functions. Figure 3 shows β_x, β_y , and η , over a full cell; they are smoothly varying over half-cells with a derivative discontinuity at the quadrupoles. Figures 3 and 4 show the specific functions that appear in b_2 and b_3 , tune shifts. These functions are smoothly varying on the half-cell level; F, C, and D correctors provide local three-point, Simpson's Rule type cancellation on the half-cell level.

The first-order correction is insensitive to betatron function perturbations, because Simpson's Rule requires only smooth variation on the half-cell level. Amplitude distortion is greatly reduced by the correction. Second-order effects are also reduced by first-order correction, although second-order effects for multipoles above sextupole are not large at current parameters. More exact consideration of the actual terms that appear in the tune-shift expressions also provides guidelines for improving the correction from Simpson's Rule values. For example, the octupole terms are relatively enhanced at the F, C, D positions, and a small reduction in all corrector strengths improves the correction. The decupole terms all include powers of the dispersion function and are consequently overweighted toward the F quad; a 5% reduction in the F corrector strength greatly improves correction (see Table II). These improvements are not necessary for the SSC at current parameters, but they do provide an additional order of magnitude in margin of safety. They also improve the degree of correction to a level above that which can be obtained with the less flexible trim-coil correctors.

Higher-order multipoles can also be corrected using the same method. For example, b_6 tune shifts are corrected by a factor of ten by a naive application of Simpson's Rule correctors; the method can be extended to include other multipoles if necessary.

SEXTUPOLE CORRECTION

Because there are only two first-order sextupole tune-shift terms (the linear chromaticity terms), only two (F and D) correctors are needed for their complete correction. In first-order, F, D and F, C, D correction methods are equal.

However, superconducting dipoles have a very large b_2 content, and second-order terms are important. Identification of second-order terms requires perturbation theory.¹⁰⁻¹² As a result, second-order sextupole tune-shift terms are of the same form as the first-order octupole terms:

$$\Delta\nu_x = aI_x + bI_y + c\delta^2 \text{ and } \Delta\nu_y = dI_y + bI_x + e\delta^2 . \quad (4)$$

The coefficients a through e scale as b_2^2 and are naturally positive after first-order correction. The coefficients may be expressed as double integrals with phase factors and internal discontinuities and are not closely fitted to Simpson's Rule half-cell integration. The first-order b_2 correction with only F and D elements reduces second-order terms by a factor of ~ 5 ; however, the b_2 tolerance is only increased to $2.7 \times 10^{-4} \text{ cm}^{-2}$, somewhat below the desired level of $\sim 5 \times 10^{-4} \text{ cm}^{-2}$. Addition of a C sextupole corrector reduces these terms by a factor of ~ 5 , increasing b_2 tolerance by a factor > 2 to a level above the estimated SSC dipole levels. Setting the C corrector strength by Simpson's Rule or by equal weights ($f_C = 1/2$) obtains similar correction (Table II).

TABLE II. First-order correction of b_3 , b_4 and second-order b_2 correction. The correction factor is the ratio of uncorrected to corrected $\Delta\nu$ in the SLAT aperture. The tolerance is the maximum corrected b_n permitted under the SLAT.

Correction Condition	Correction Factor	Tolerance (10^{-4}cm^{-n})
b_3 (Octupole) Correction		
No correction	1.0	0.018
F, D chromatic correction ⁹ ($f_F = 0.28, f_D = 0.70$)	1.9	0.033
F, C, D Simpson's Rule (f_F, f_C, f_D) = (1/6, 4/6, 1/6)	93	1.6
F, C, D correction (0.165, 0.66, 0.165)	370	6.7
b_4 (Decupole) Correction		
No correction	1.0	0.029
F, D chromatic correction ⁸ ($f_F = 0.24, f_D = 0.93$)	1.4	0.04
F, C, D Simpson's Rule (f_F, f_C, f_D) = (1/6, 4/6, 1/6)	31	0.9
F, C, D correction (0.158, 0.663, 0.168)	800	24
Second Order b_2 (Sextupole) Correction		
No correction	1.0	1.2
F, D chromatic b_2 correction	5.1	2.7
F, C, D chromatic b_2 correction, equal weights ($f_C = 0.5$)	24	5.9
F, C, D chromatic correction, Simpson's Rule ($f_C = 0.667$)	23	5.7
F, D first-order b_2 correction ($f_{C,2} = 0$), and F, C, D octupoles	120	13
F, C, D first-order b_2 correction ($f_{C,2} = 0.5$ to 0.67), and F, C, D octupoles	700	32

Because the second-order terms are not ideally suited to Simpson's Rule integration, the improvement in correction is not dramatic. The remanent tune shifts scale as

$$\Delta\nu \propto \frac{b_2^2}{N^2},$$

where N is the number of corrector elements. The SSC linearity requirements imply that $N \gtrsim 2$ correctors per half-cell is required, provided that no correction beyond sextupole elements is permitted.

Second-order b_2 correction can be greatly improved by using the F, C, D octupoles.¹³ The tune shifts due to the octupoles ($i = F, C, D$) are

$$\Delta\nu_x = -\frac{1}{2\pi B\rho} \sum B_{3,i} l_i \left(\frac{3\beta_{x,i}^2}{8\beta_0} A_x^2 - \frac{3\beta_{x,i}\beta_{y,i}}{4\beta_0} A_y^2 + \frac{3}{2}\beta_{x,i}\eta_i^2\delta^2 \right) \quad (5)$$

$$\Delta\nu_y = -\frac{1}{2\pi B\rho} \sum B_{3,i} l_i \left(\frac{3\beta_{y,i}^2}{8\beta_0} A_y^2 - \frac{3\beta_{x,i}\beta_{y,i}}{4\beta_0} A_x^2 - \frac{3}{2}\beta_{y,i}\eta_i^2\delta^2 \right) \quad (6)$$

Unlike b_2^2 terms, first-order octupole terms have opposing signs and there are only three correctors for five terms. However, the negative terms in Eq. (2) have similar dependence with relatively enhanced values at the C correctors (see Fig. 3). The correction strategy is to use the C octupoles to correct the b and e terms in Eq. (4) and the F and D octupoles to correct the others; the ratios of F, C, and D strengths per half-cell are $\sim (1 : -2.7 : 1)$. The reduction in nonlinearity can be very impressive. The correctors can be tuned to correct completely either amplitude or chromatic $\Delta\nu$ with the remanent terms reduced by $\geq 10\times$. The SLAT tune shifts can be reduced by a factor of ≥ 30 , increasing b_2 tolerances to $\geq 30 \times 10^{-4}\text{cm}^{-2}$ providing an extremely large safety margin (see Table II). Other nonlinear effects such as orbit distortion remain small, provided cell resonances are avoided. Because the octupole tune shifts are linear, there is no interference between their b_2^2 and b_3 correction roles. The use of F, C, and D octupoles to correct second-order sextupole nonlinearities adds an extra operational dimension, conceptually similar to the use of F and D sextupoles to correct quadrupole chromaticity. The use of the octupoles may be extended to control nonlinearities from other elements; for example, all A_i^2 tune shifts can be cancelled to zero, regardless of their sources.

The accuracy of the correction of all terms can be understood by noting that the first-order octupole Hamiltonian has three terms:

$$H_3 \propto B_3(s) [x^4 - 6x^2y^2 + y^4]$$

(The second-order sextupole Hamiltonian has similar terms with different coefficients.) The F corrector has the greatest effect on the x^4 term, while the cross term (x^2y^2) is relatively more controlled by the C octupole, and the D octupole controls the y^4 term. Therefore the F, C, D corrector scheme directly controls all of the amplitude dependent terms in the Hamiltonian. The horizontal chromatic tune-shift term ($\Delta\nu_x \propto \delta^2$) derives from the x^4 term, and the vertical chromatic tune shift is obtained from the cross term (x^2y^2) and their dependences follow closely, but not precisely, the corresponding amplitude-dependent terms (see Fig. 4); correction of one set reduces the other by an order of magnitude. Lattice parameters may be fine-tuned to provide

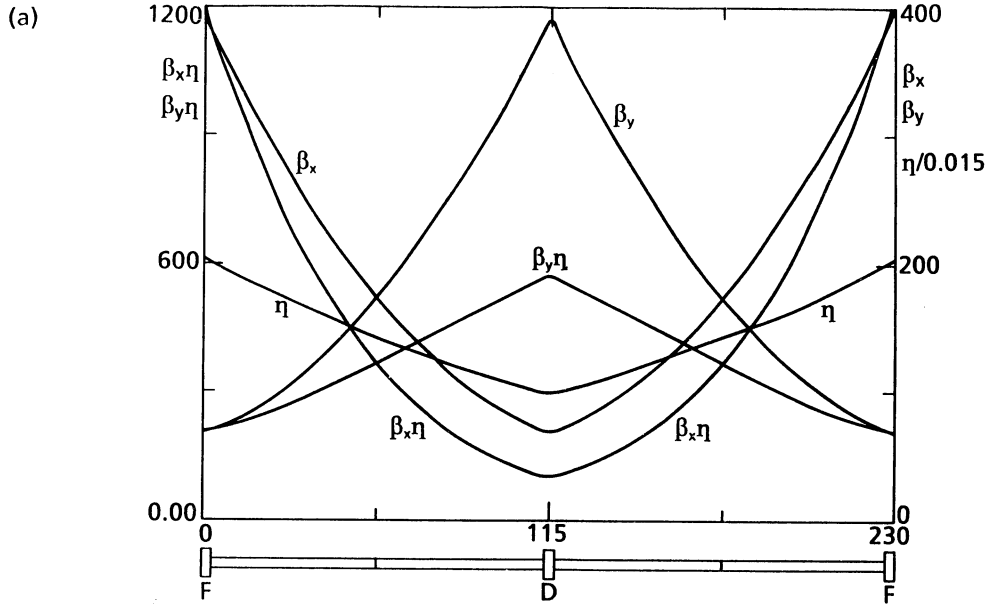


Fig. 3. Betatron functions (β_x, β_y, η) for a full SSC cell. The functions that appear in the sextupole tune shifts ($\beta_x\eta, \beta_y\eta$) are also shown. Note the derivative discontinuity and the reflection symmetry at the D quadrupole.

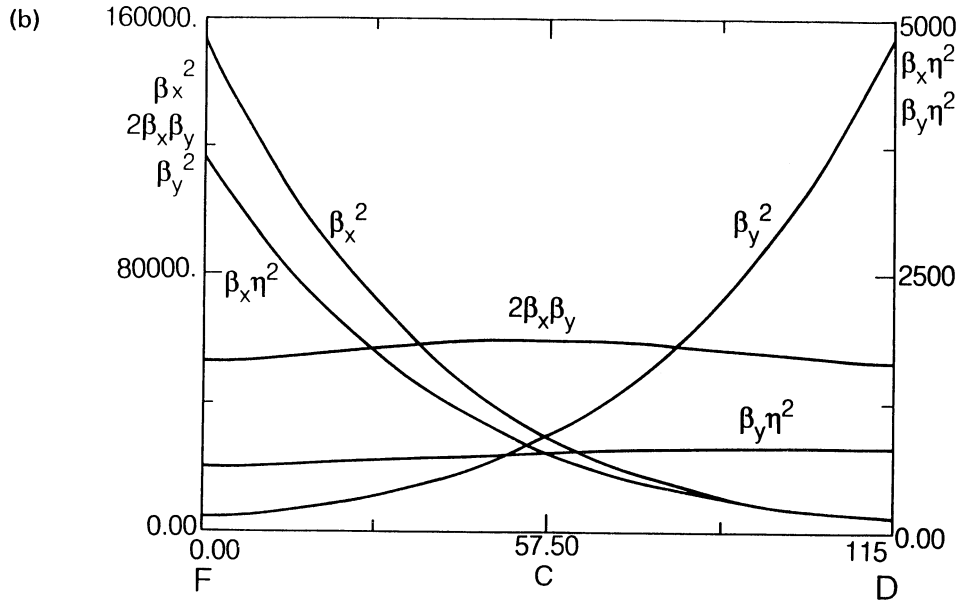


Fig. 4. Octupole $\Delta\nu$ functions on a half-cell. The β_x^2 and $\beta_x\eta^2$ terms are derived from x^4 in the Hamiltonian, $2\beta_x\beta_y$ and $\beta_y\eta^2$ from $(-x^2y^2)$, and β_y^2 from y^4 .

more precise cancellation. We note here that the less flexible trim-coil correction, which lacks tunable F, C, and D octupoles, cannot achieve a similar level of correction.

We note that the procedure of using F and D octupoles to control general second-order chromaticity is nonoptimal; the D corrector disproportionately affects vertical motion. Use of octupoles at F and C positions for horizontal and vertical chromaticity, respectively, would minimize the nonchromatic effects.

CORRECTION OF RANDOM MULTIPOLES

Extension of the F, C, D corrector concept to include quasi-local correction of random multipoles has been obtained by E. Forest and J. M. Peterson,¹⁴ and was described by Forest at the Workshop.¹⁵ They developed an algorithm in which the corrector strengths are set by requiring that the following moments of the multipole content be zero on the half-cell level:

$$\sum S_{n,i} = 0, \quad \sum S_{n,i} z = 0, \quad \sum S_{n,i} z^2 = 0$$

Here, $S_{n,i}$ are the integrated multipole strengths and include both dipole and F, C, D corrector contributions, and z is position along the half-cell. As with systematic multipoles, F and D strengths for adjacent half-cells are combined in units on one side of the quadrupole; there are only two physical correctors per half-cell. If all dipole multipole strengths ($b_{n,i}$ or $a_{n,i}$) are equal, the algorithm obtains Simpson's Rule for the corrector strengths.

The nonlinear effects of random multipole content are dominated by amplitude distortion or "smear." Application of the algorithm reduces "smear" from random a_n and b_n by an order of magnitude at SSC parameters and provides more than adequate correction. The economics of corrector power supply "binning"¹⁶ can be applied to the F, C, D correctors. In an optimally economic application, C coils would be longer than F and D coils but would share the same current sources. After consideration of the variations induced by binning and the power of the algorithm, it is found that the present method is as effective and more efficient than previously proposed corrections that placed a corrector with every dipole.

APPLICATION TO THE LHC

The same correction methods can be applied to any synchrotron; as an example, we consider the CERN Large Hadron Collider (LHC).¹⁷ The LHC has current-dominated superconducting magnets with a relatively large multipole content as in the SSC. The LHC has somewhat larger aperture requirements because of lower injection energy and plans to operate with a higher emittance beam. However, it has a much stronger focusing lattice ($L = 50\text{m}$, $\phi = 90^\circ$ cells). The tolerances are somewhat greater than for the SSC; however, correction of b_2 , b_4 , and possibly b_3 is desirable. (See Table III). In Table IV, the effects of F, C, D correction of b_3 , b_4 , and b_2^2 tune shifts are displayed. As in the SSC, tolerances are greatly increased, but greater safety margins are obtained for the smaller, stronger-focusing LHC.

TABLE III. Systematic multipole tolerances in LHC magnets.
Tolerance at the aperture ($A_x = 0.7\text{cm}$, $\frac{\delta P}{P} = \pm 0.15\%$).

Multipole	Strength (10^{-4} cm^{-n})
b_2	0.025
b_3	0.03
b_4	0.045
b_5	0.069
b_6	0.10
b_7	0.15
b_8	0.21

TABLE IV. LHC octupole, decupole, and second-order sextupole correction.

Correction Parameters	Correction Factor	Tolerance (10^{-4} cm^{-n})
b_3 , no correction	1.0	0.03
b_3 , (f_F, f_C, f_D) = (1/6, 4/6, 1/6)	90	2.8
b_3 , (f_F, f_C, f_D) = 0.99 (1/6, 4/6, 1/6)	260	7.9
b_4 , no correction	1.0	0.045
b_4 , (f_F, f_C, f_D) = (1/6, 4/6, 1/6)	30	1.3
b_4 , (f_F, f_C, f_D) = 0.99 (0.16, 67, 0.17)	450	19.0
Second-Order Sextupole Correction		
No Correction	1.0	1.6
F and D correctors only	5.3	3.7
F, C, D correctors	25	8.0
$f_C = 0.667$ (Simpson's Rule)		
F, C, D correctors	34	9.3
$f_C = 0.50$ (equal weights)		
F, C, D sextupoles and octupoles	700	40

The greater margin of safety can be exploited in obtaining greater operational flexibility and performance. Alternatively or concurrently, the margin of safety can be used to permit a weaker-focusing lattice with shorter quads and sextupole requirements and therefore permit more dipole length in the fixed LHC circumference, even after allotting adequate space for the correctors. For example, going from a 50-m, 90° lattice to a 70-m, 90° lattice would permit an ~5% increase in LHC energy.

DISCUSSIONS AND EXTENSIONS

In the previous discussion, only one corrector configuration was considered. R. Talman⁶ has initiated a study in which the number and location of correctors are varied; results are discussed in other workshop papers. The correction cases assumed identical corrector systems in every cell. A sparser corrector scheme with stronger correctors in fewer cells has been suggested by Willeke¹⁸ for further investigation. The same correction techniques may be applied to provide quasi-local correction of nonlinear fields in interaction region (IR) quads. An initial, nonoptimal configuration of lumped correctors placed within SSC IR quads reduces nonlinear effects by ~50%. Further investigation is indicated.

A key ingredient of the present corrector scheme is the inclusion of correctors at the C location; where $\beta_x \cong \beta_y$ (away from the quads). This addition permits accurate correction of multipole effects, as well as separate operational control of horizontal, vertical, and coupled motions. For example, this permits the use of F, C, D octupole compensation of b_2^2 -like effects. Exploitation of this new degree of freedom in these or other applications would be a useful option in all accelerators.

An extremely powerful method of nonlinear correction has been described. Elements (F, C, D) are introduced to provide local compensation of multipole content on the half-cell level, reducing all systematic and random multipole effects by orders of magnitude. The F, C, D elements may be further adjusted for precise control of the motion. The compensations are more than adequate for present and future synchrotrons.

REFERENCES

- ¹ Superconducting Super Collider Conceptual Design, SSC-SR-2020, March 1986, edited by J. D. Jackson, (unpublished).
- ² D. Neuffer and J. M. Peterson, Proc. 1987 IEEE Particle Accelerator Conf., E. R. Lindstrom and L. S. Taylor, Eds., IEEE Catalog No. 87CH2387-9, p. 1502 (1987).
- ³ Superconducting Super Collider report, SSC-7, April 1985, edited by J. M. Peterson, (unpublished).
- ⁴ R. Hanft, B. C. Brown, W. E. Cooper, D. A. Gross, L. Michelotti, E. E. Schmidt, and F. Turkot, IEEE Trans. Nucl. Sci. 30 (4), 3381 (1983).
- ⁵ S. Caspi, W. Gilbert, M. Helms, L. J. Laslett, and C. Taylor. IEEE Trans. Magn. MAG-23, 1219 (1987).
- ⁶ D. Neuffer, "Lumped Correction of Systematic Multipoles in Large Synchrotrons," to be published in *Particle Accelerators* (1988).
- ⁷ D. Neuffer, "A Novel Solution to the SSC Multipole Problem," submitted to Phys. Rev. Lett.
- ⁸ M. Abramowitz and I. A. Stegun, Handbook of Mathematical Functions, National Bureau of Standards, Washington, DC (1972).
- ⁹ A. Jackson, Superconducting Super Collider report SSC-107, February 1987 (unpublished).
- ¹⁰ S. Ohnuma, in *Intersections between Particle and Nuclear Physics*, edited by R. Mischke, AIP Conf. Proc. No. 123 (American Institute of Physics, New York, 1985), p. 415.
- ¹¹ R. D. Ruth, in *Physics of Particle Accelerators*, edited by M. Month and M. Dienes, AIP Conf. Proc. No. 153 (American Institute of Physics, New York, 1987), p. 152.
- ¹² L. Michelotti, in *Physics of Particle Accelerators*, p. 260.
- ¹³ D. Neuffer, Superconducting Super Collider report SSC-N-384 (1987).
- ¹⁴ J. M. Peterson and E. Forest, Superconducting Super Collider report SSC-N-383 (1987) (unpublished).
- ¹⁵ E. Forest, these proceedings.
- ¹⁶ R. Talman, these proceedings.
- ¹⁷ G. Brianti and K. Hubner, CERN 87-05 (1987).
- ¹⁸ F. Willeke, these proceedings.

ACKNOWLEDGMENT

I would like to thank E. Forest, J. M. Peterson, R. Talman and P. Channell for extremely helpful discussions.

CHROMATICITY CORRECTION FOR LEP: HOW DID WE GET THERE

A. Verdier

CERN, Geneva, Switzerland

ABSTRACT

Since the beginning of the LEP studies in 1975, the chromaticity correction was a concern. The arguments developed to come to a satisfactory solution of this problem influenced the choice of the LEP lattice. This is what we show here.

1. FIRST DESIGN : LEP 100 [1]

The first LEP design aimed at a machine with "round number" parameters. The beam energy was 100 GeV, the luminosity $10^{32} \text{ cm}^{-2}\text{s}^{-1}$, the free space around the crossing points was $\pm 10 \text{ m}$ in 8 interaction regions. The circumference was 51.5 km, found by cost optimisation. The tunes which were equal in both planes, were chosen to be half way from the half integer resonances, and so that the phase advance per cell be close to 60° .

The lattice was made from four basic structures which contain all quadrupoles : regular cell with dipole and sextupole magnets, dispersion suppressor insertion, regular cell with zero dispersion for RF, low- β insertion. All the subsequent LEP design follow the same scheme, except that there may be two sets of low- β insertions.

If the sextupoles are not powered, the tune derivatives with respect to momentum are, for LEP 100 [1] :

$$Q'_h = -248, \quad Q'_v = -307$$

and consequently the vertical betatron motion becomes unstable for $\Delta p/p = 0.8^\circ/_{00}$ which is strongly unacceptable since $\sigma_E/E = 1.08^\circ/_{00}$.

If the Q 's are made zero with two sextupole families, the variations of the tunes with momentum deviation are such that a vertical betatron instability occurs at $\Delta p/p \sim -6^\circ/_{00}$ as shown on Fig. 1, which is still unacceptable for life time.

It was tried to improve this situation by splitting each sextupole families into three regularly arranged families. The improvement was effective in the horizontal plane but not in the vertical plane. In order to understand this, we have to remember that a sextupole is a Δp -acting quadrupole. Hence, the β -functions on off-momentum closed orbits have to be inspected. An example is given on Table 1 : a modulation of the β -function occur on the off-momentum closed orbits. The reason of this modulation is that the matching of the low- β quadrupole is not valid for $\Delta p \neq 0$, which makes a strong gradient perturbation.

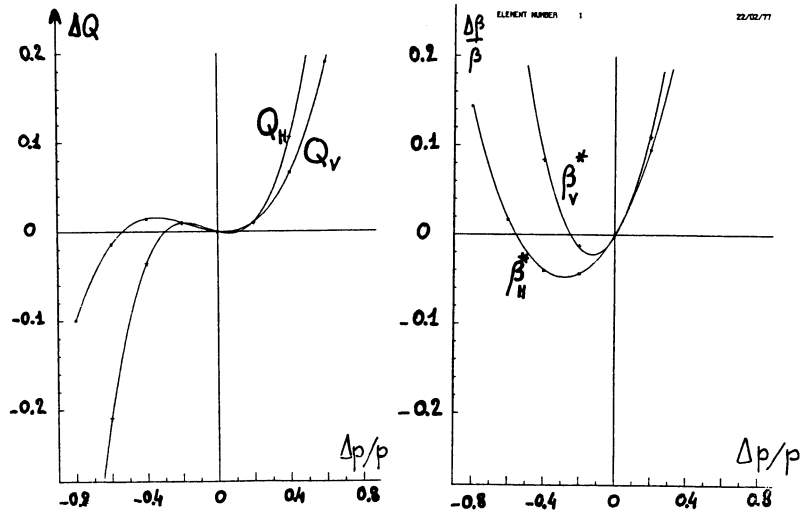


Fig. 1 - Variation of the tunes (left) and β -functions at interaction point (right) with momentum deviation for LEP 100 when the chromaticity is corrected with 2 sextupole families.

BETAH				BETAV			
				-0.006	0	+0.006	
DELTA P/P	-0.006	0	+0.006				
SF	241,114	132,720	192,089	SD	61,832	139,979	177,001
SF	164,154	132,720	70,861	SD	269,411	139,970	331,117
SF	78,408	132,716	221,504	SD	295,163	139,993	107,963
SF	228,747	132,719	185,035	SD	74,047	139,989	135,508
SF	177,588	132,720	72,614	SD	178,970	139,966	340,523
SF	225,276	132,720	196,719	SD	112,760	139,996	84,062
SF	189,695	132,720	69,500	SD	121,681	139,982	314,182
SF	71,145	132,717	220,018	SD	328,082	139,981	218,079
SF	215,338	132,719	197,840	SD	182,166	139,981	61,763
SF	201,904	132,720	69,343	SD	72,506	139,982	277,697
SF	70,023	132,717	218,949	SD	291,078	139,982	268,825
SF	204,038	132,719	199,279	SD	256,331	139,981	59,709
SF	213,283	132,720	69,144	SD	60,688	139,982	228,341
SF	70,779	132,717	217,809	SD	224,829	139,982	308,343
SF	192,083	132,719	200,386	SD	311,646	139,981	78,380
SF	223,546	132,720	69,024	SD	89,994	139,982	174,639
SF	73,482	132,717	216,718	SD	149,967	139,982	331,028
SF	179,235	132,719	201,809	SD	332,031	139,981	115,274
SF	232,530	132,720	68,870	SD	151,719	139,982	123,725
SF	77,958	132,717	215,552	SD	88,888	139,982	332,904
SF	166,257	132,719	202,899	SD	310,779	139,981	164,149
SF	240,000	132,720	68,787	SD	226,556	139,981	84,318
SF	84,253	132,718	214,440	SD	60,491	139,982	314,291
SF	152,934	132,718	204,305	SD	254,548	139,982	218,391
SF	245,830	132,720	68,677	SD	292,364	139,981	61,679
SF	92,085	132,718	213,249	SD	73,230	139,982	277,360
SF	140,014	132,718	205,377	SD	180,538	139,982	268,775
SF	249,894	132,720	68,632	SD	328,558	139,981	59,691
SF	101,440	132,718	212,116	SD	123,292	139,982	228,426
SF	127,326	132,718	206,764	SD	111,045	139,982	308,599
SF	252,076	132,720	68,566	SD	324,390	139,981	78,585
SF	111,980	132,718	210,900	SD	195,476	139,982	174,280
SF	115,541	132,718	207,816	SD	67,467	139,982	330,910
				SD	281,247	139,981	115,196

Table 1

Table of the β_H values at the SF sextupoles and β_V values at the SD sextupoles for LEP 100 when the chromaticity is corrected with two sextupole families.

It appears that the modulation of β_H has grosso modo a periodicity of 3 cells. Hence, affecting each third SF sextupole to the same family (which is called a regular arrangement) makes it possible to produce an off-momentum tune shift with a mere change of the family excitations, whilst keeping the sum of the excitations (i.e. Q') constant, thanks to the different values of the average off-momentum β 's associated with the different families.

Inspecting the off-momentum β_v 's at the SD sextupoles, we notice that any nice modulation does not exist. The difference in behaviour between the horizontal and vertical plane comes from the phase advance per cell which is 59.2° in the horizontal-plane and 55.5° in the vertical-plane. In order to make an off-momentum tuneshift with the SD sextupoles as we did for the SF, we have to group them into families as shown in Table 2 for instance.

SD2	SD3	SD0	SD2	SD3	SD0	SD0	SD2	SD3	SD1	SD2	SD3	SD1	SD2	SD3	SD1	SD2	SD3
SD1	SD3	SD2	SD1	SD3	SD2	SD1	SD1	SD2	SD0	SD1	SD2	SD2	SD1	SD0	SD2	SD1	

Table 2
Arrangement of SD sextupoles for a superperiod of LEP 100 in 3 families.
SD0 means : not excited.

This arrangement is based on grouping sextupoles separated by 3 cells (i.e. by nearly a π phase advance) so as to minimise the second order geometric aberrations of the pairs.

It is worth mentioning that in a first trial, the SD sextupoles had been grouped into 3 families according to the values of the off-momentum β 's. The variation of tunes with momentum was almost as good as with the above arrangement but the stability of betatron oscillation was poor because the geometric aberrations were too large.

The variation of the tunes with momentum with 3 SF regular families and the SD families given in Table 2 is shown on Fig. 2. The sextupole strengths have been obtained by computing off-momentum tune shifts with the sum of the K 's kept constant in each plane so that $Q'_{h,v}$ remains zero and that $\Delta Q(\delta = -0.006) = \Delta Q(\delta = +0.006) = 0$ (ΔQ is the variation

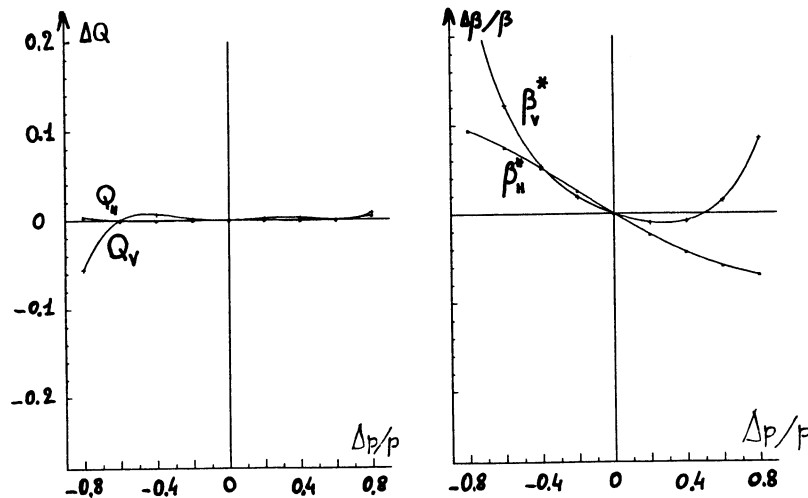


Fig. 2 - Variation of the tunes (left) and β -functions at the interaction point (right) with momentum deviation for LEP 100 with 6 sextupole families. The sextupole strengths are calculated so that $Q_{h,v}(\delta = -0.006) = Q_{h,v}(\delta = +0.006) = Q_{h,v}(\delta = 0)$ with the simple tune shift formula.

with reference to the on-momentum tune value). We notice that the variation of β^* with momentum deviation is made smaller (compare Fig. 1 and Fig. 2). This can be understood with the second order tune shift formula in [2], from which it appears that Q'' and β' are related.

2. INTERMEDIATE LEP DESIGN

2.1 "Blue book" design [3]

This machine was smaller than the previous one with 22.2 km circumference and 4 intersection points. The phase advance per cell were 60° horizontal and 62.12° vertical. This needed twelve regular sextupole families for chromaticity correction. Two computation methods were tried for obtaining the sextupole strengths : firstly the program HARMON developped for PEP [4] and secondly a minimisation of the derivative of the TWISS matrix w.r.t. momentum deviation [5].

2.2 "Pink book" design [6]

The circumference was larger than the previous one : 30.6 km with 4 intersection points. The phase advance per cell was set to exactly 60° for each plane thanks to a more flexible design of the dispersion suppressors. The chromaticity correction was possible with 6 sextupole families and was better than for all other LEP versions. The variation of tunes and β^* with momentum deviation are shown on Fig. 3, the sextupole strengths having been computed with HARMON [4].

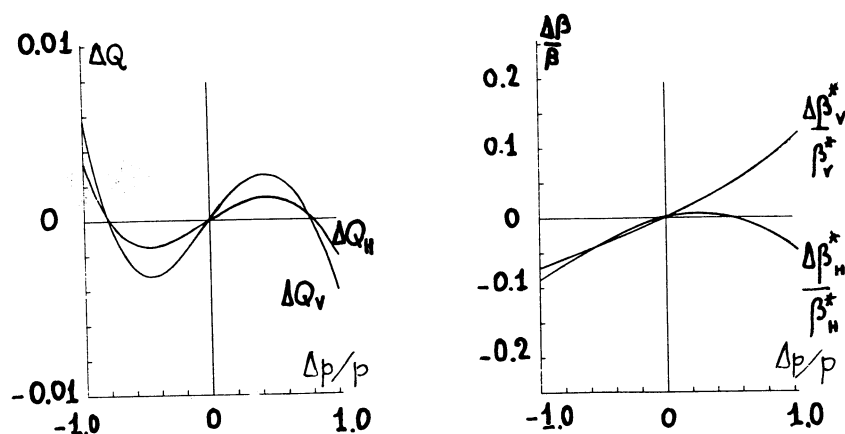


Fig. 3 - Variation of the tunes (left) and β -function (right) at the interaction point with momentum deviation for the "pink book" machine. 6 sextupole families. $Q_H = 70.31$, $Q_V = 74.54$.

This LEP design was the first for which the linear machine was adjusted to have a favourable condition for chromaticity correction [7].

3. FINAL LEP LATTICE [8]

Its design is very similar to that of Ref.[6], except that the circumference was brought down to 26.6 km for construction reasons. The influence of the sextupole phase, which is the main parameter in [7], was investigated to really find the optimum which leads to the best performance [9]. The variation of the tunes and β^* with momentum deviation is shown on Fig. 4 when the chromaticity correction is done with 6 regular sextupole families. Several attempts were done to change the sextupole arrangements [9,10] which led to the conclusion that putting the maximum number of them was the best solution.

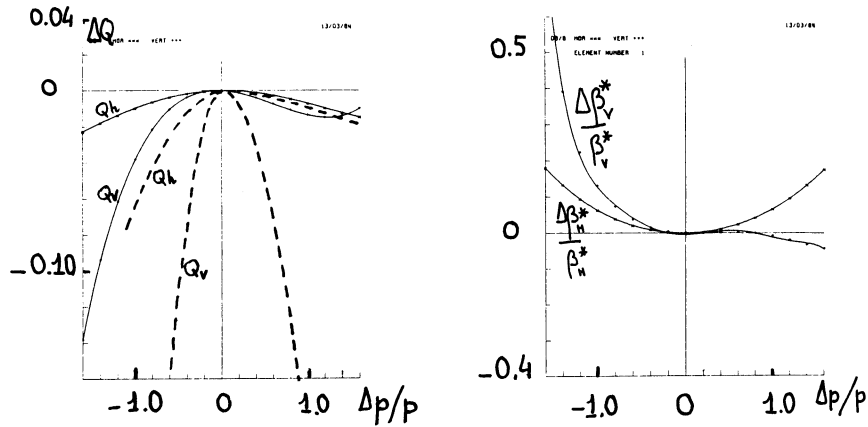


Fig. 4 - Variation of the tunes (left) and β -functions (right) at the interaction point with momentum deviation for the final LEP design. 6 sextupole families. $Q_h = 70.35$, $Q_v = 78.20$. The dotted lines are for 2 sextupole families.

A lattice with 90° per cell was also studied. The optimisation of the chromaticity correction was done : for this case it is crucial that the sextupole phase be adjusted on order to maximize the dynamic aperture [11]. The variations of the tunes and β^* are shown on Fig. 5 for this machine.

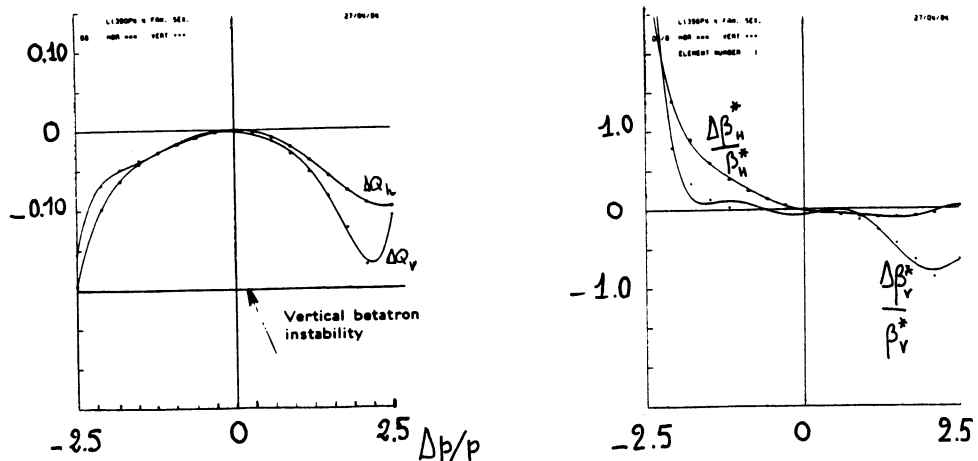


Fig. 5 - Variations of the tunes (left) and β^* 's (right) with momentum deviation for the 90° lattice. Chromaticity corrected with 2 SF and 3 SD sextupole families [11].

4. CONCLUSIONS

The LEP sextupole scheme for chromaticity correction was defined after many years of studies. The importance of the phase advance per cell was recognised as well as that of a proper linear design of the machine. After all these theoretical studies, the verdict of experience has now to come.

REFERENCES

1. J.R.J. Bennet et al, Design concept for a 100 GeV e^+e^- storage ring (LEP), CERN 77-14.
2. E.D. Courant, H.S. Snyder, Theory of the alternating gradient synchrotron, Ann. of Phys., Vol. 3 (1958) 1.
3. The LEP Study Group, Design study of a 15 to 100 GeV e^+e^- colliding beam machine (LEP). CERN/ISR-LEP/78-17.
4. M.H.R. Donald and D. Schofield, A user guide to the HARMON program, LEP Note 420.
5. M. Bassetti, Another chromaticity correction for LEP 70, Note LEP-70/97.
6. The LEP Study Group, Design study of a 20 to 130 GeV e^+e^- colliding beam machine (LEP), CERN/ISR-LEP/79-33.
7. B. Montague, Linear optics for improved chromaticity correction, LEP Note 165.
8. LEP Design Report, Vol II, The LEP main ring, CERN-LEP/84-01.
9. A. Verdier, Influence of the vertical phase of the sextupoles and their number on the chromaticity correction of LEP13, LEP Note 473.
10. M. Placidi, Comparison of performance for LEP Version 12 60° with interleaved sextupolar schemes for chromatic compensation, LEP Note 426.
11. A. Verdier, Optimisation of the sextupole scheme for the chromaticity correction of LEP13 with 90° per cell. LEP Note 503.

SECOND ORDER TUNE SHIFT IN A COMPENSATED SUPER CELL

B. Autin

CERN, Geneva, Switzerland

F. Willeke

Deutsches Elektronen-Synchrotron (DESY), Hamburg, Federal Republic of Germany

1. INTRODUCTION

In most modern storage rings, the dominant non linear fields limiting the single particle stability come from chromaticity correction sextupoles. In order to minimize the reduction of acceptance due to these non linearities, the phase advance per FODO cell in the arcs where the sextupoles are placed is chosen to be a rational fraction of 2π whenever this is possible and $\pi/2$ or $\pi/3$ are the favourite values. However it has been recently proposed for HERA [1,2] many phase advances between 60 and 90 degrees

$$\mu = \frac{2k+1}{n} 2\pi \quad (1)$$

The repetitive element of the lattice including the sextupoles is a *super cell* with the same phase advance $(2k+1)2\pi$ in each plane. Under these conditions, the first order sextupolar non linear terms are cancelled. The influence of the second order terms remains to be analyzed. The test parameter we have chosen to study is the horizontal betatron tune shift in the special case of a pure horizontal motion.

2. TUNE SHIFT EXPRESSION

In the first order perturbation theory, it can be shown that sextupolar fields excite modes whose characteristic phases are [3,4]

$$\mu_x, \mu_x + 2\mu_y, \mu_x - 2\mu_y, 3\mu_x$$

The virtue of the compensation is to annul integrals of the type

$$\int_0^L f(s) \cos(m\mu_x(s) + n\mu_y(s)) ds$$

over the length L of a super cell. However, there is a cross-talk between

the sextupoles of a super cell and, as a consequence, a net deformation of the particle trajectory which provokes a tune shift. The effect is quite similar to the variation of chromaticity induced by the alteration of the β -function on off-momentum orbits. Several formalisms have been used to derive the expression of the tune shift [5,6,7,8] that we write

$$\Delta_2 Q_x = \frac{J_x}{64\pi} \int_0^L ds \int_s^{s+L} k'(s) k'(s') \beta_x^{3/2}(s) \beta_x^{3/2}(s') \left[-3 \frac{\cos(-\pi Q_x + \mu_x(s') - \mu_x(s))}{\sin \pi Q_x} - \frac{\cos 3(-\pi Q_x + \mu_x(s') - \mu_x(s))}{\sin 3\pi Q_x} \right] ds' \quad (2)$$

J is the action variable, k' the sextupolar focusing strength, Q the betatron tune, β the β -function and μ the betatron phase advance. The expression can be simplified by taking the compensation assumption into account

$$\int_0^L k'(s) \beta_x^{3/2}(s) \exp im\mu_x(s) ds = 0 \quad m = 1 \text{ or } 3 \quad (3)$$

Let us note that

$$\int_L^{s+L} k'(s') \beta_x^{3/2}(s') \cos m(-\pi Q_x + \mu_x(s') - \mu_x(s)) ds' = \int_0^s k'(s') \beta_x^{3/2}(s') \cos m(\pi Q_x + \mu_x(s') - \mu_x(s)) ds' \quad (4)$$

By performing the substitution

$$\int_s^{s+L} = \int_0^L - \int_0^s + \int_L^{s+L}$$

and applying the rules (3) and (4), one finds

$$\Delta_2 Q_x = \frac{3J_x}{32\pi} \sum_{m=1,3} \int_0^L k'(s) \beta_x^{3/2}(s) ds \int_0^s k'(s') \beta_x^{3/2}(s') \frac{\sin m(\mu_x(s') - \mu_x(s))}{m} ds' \quad (5)$$

3. CORRELATIONS

A super cell is a string of n FODO cells each with a phase advance μ_0 . The self-correlation terms which represent the interaction of a sextupole with itself can only occur for thick elements; they are not treated here. For the cross-correlation terms there is no loss of generality assuming that the sextupoles are thin lenses of integrated strength $k'l$ and, for a more precise model, it is always possible to perform an analytical integration over each lumped element [9]. The double \int can then be replaced by a double \sum

$$\Delta_2 Q_x = \frac{3J_x}{32\pi} \sum_{m=1,3} \sum_{i=1}^n (k'l)_i \beta_{xi}^{3/2} \sum_{j=1}^i (k'l)_j \beta_{xj}^{3/2} \frac{\sin m(\mu_{xj} - \mu_{xi})}{m} \quad (6)$$

If all the sextupoles are different, the above expression has to be calculated numerically. When the chromaticity is corrected with two families of sextupoles, interesting simplifications appear. The cross-correlations belong to four classes: F-F, D-D, F-D, D-F. In (6), the part which depends on the summation indices is

$$S_m = \sum_{i=1}^{2n} \beta_{xi}^{3/2} (k'l)_i \sum_{j=1}^i \beta_{xj}^{3/2} (k'l)_j \sin m(\mu_{xj} - \mu_{xi}) \quad (7)$$

It can be split into the four contributions

$$S_m = [\beta_{xF}^3 (k'l)_F^2 + \beta_{xD}^3 (k'l)_D^2] \sum_{i=1}^{n-1} \sum_{j=1}^i \sin j(m\mu) + (\beta_{xF}\beta_{xD})^{3/2} (k'l)_F(k'l)_D [\sum_{i=1}^{n-1} \sum_{j=1}^i \sin (2j-1)(m\mu/2) + \sum_{i=1}^n \sum_{j=1}^i \sin (2j-1)(m\mu/2)] \quad (8)$$

The sum of the trigonometric series has a closed form which is derived from the expression

$$\sum_{j=j_1}^{j_2 j_3} e^{i(j-j_4)\mu} = \frac{\sin(1-j_1+j_2-j_3)(\mu/2)}{\sin(\mu/2)} e^{i(\frac{j_1+j_2-j_3}{2} - j_4)\mu} \quad (9)$$

which becomes

$$\sum_{j=j_1}^{n-j_3} e^{i(j-j_4)\mu} = \frac{\sin(1-j_1-j_3)(\mu/2)}{\sin(\mu/2)} e^{i(\frac{j_1-j_3}{2} - j_4)\mu} \quad (10)$$

when the compensation condition

$$e^{in\mu} = 1$$

is applied. It can thus be shown that

$$S_m = \frac{n}{\sin(m\mu/2)} [(\beta_{xF}\beta_{xD})^{3/2} (k'l)_F(k'l)_D + \frac{1}{2} (\beta_{xF}^3 (k'l)_F^2 + \beta_{xD}^3 (k'l)_D^2) \cos(m\mu/2)] \quad (11)$$

4. ROLE OF CELL PHASE ADVANCE

The discussion of the correlations shows that the tune shift in a super cell of n cells is

$$\Delta_2 Q_x = \frac{3J_x}{32\pi} \sum_{m=1,3} \frac{S_m}{m} \quad (12)$$

The analysis can be continued assuming that the sextupoles are superimposed to the quadrupoles and that they correct the cell chromaticity only

$$k' = k/D \quad (13)$$

where k is the quadrupole component of the integrated focusing strength kl related to μ and to the cell length L_c through the expression

$$kl = \pm (4/L_c) \sin(\mu/2) \quad (14)$$

+ or - signs standing for F- and D- elements respectively and D is the orbit dispersion

$$D = (\Phi L_c / 2) \frac{1 \pm (1/2) \sin(\mu/2)}{\sin^2(\mu/2)} \quad (15)$$

with Φ , the bending angle per magnet. The β -function is given by

$$\beta = L_c \frac{1 \pm \sin(\mu/2)}{\sin \mu} \quad (16)$$

After substitution of $k'l$ and β into (11), we get

$$\Delta_2 Q_x = \frac{3J_x n}{4\pi L_c \Phi^2} \sum_{m=1,3} F_m(\mu) \quad (17)$$

with

$$F_m(\mu) = \frac{\tan^3 \frac{\mu}{2}}{m \sin \frac{m\mu}{2}} \left\{ -\frac{\cos^3 \frac{\mu}{2}}{1 - \frac{1}{4} \sin^2 \frac{\mu}{2}} + \frac{1}{2} \cos \frac{m\mu}{2} \left[\frac{(1 + \sin \frac{\mu}{2})^3}{(1 + \frac{1}{2} \sin \frac{\mu}{2})^2} + \frac{(1 - \sin \frac{\mu}{2})^3}{(1 - \frac{1}{2} \sin \frac{\mu}{2})^2} \right] \right\} \quad (18)$$

This expression is better appreciated by applying it to a full ring of circumference C (the integer value of Q does not matter in the present discussion!). For N super cells, we have

$$\Delta_2 Q_{xt} = N \Delta_2 Q_x \quad (19)$$

$$C = N n L_c \quad (20)$$

$$\pi = N n \Phi \quad (21)$$

so that

$$\Delta_2 Q_x = \frac{3J_x (Nn)^4}{4\pi^3 C} G(\mu) \quad (22)$$

The function

$$G(\mu) = \sum_{m=1,3} F_m(\mu) \quad (23)$$

is plotted in Fig. 1, it presents a sharp peak near $\pi/2$ and decays quickly to zero. This behaviour is not intuitive and would deserve further investigations especially in the case of real machines like LEP which have to be retuned to work at high energy. The test would consist of calculating the sextupolar tune shift at various working points near $\pi/2$, finding when its sign changes and determining the dynamic aperture in these conditions.

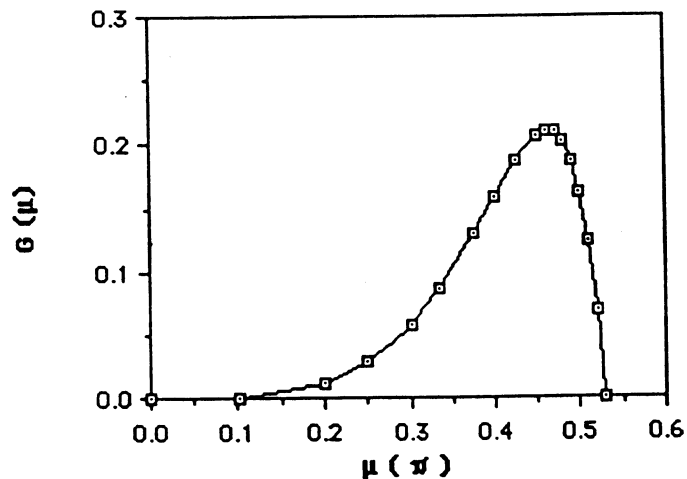


Fig. 1 Variation of the sextupolar tune-shift with the betatron phase advance per cell

REFERENCES

- [1,2] R. Brinkmann, F. Willeke, *Chromatic Corrections and Dynamic Aperture in the HERA Electron Ring, Part I and II*, DESY 87-037.
- [3] B. Autin, *Non Linear Betatron Oscillations*, AIP Conference Proceedings 153, SLAC Summer School 1985.
- [4] T. Collins, *Distortion Functions*, Fermilab 84/114 (1984).
- [5] F. Willeke, *Analytic Study of the Tevatron Non Linear Dynamics*, Fermilab FN-422.
- [6] J. Bengtsson, *Non Linear Transverse Dynamics for Storage Rings with the Application to the Low Energy Antiproton Ring at CERN*. Ph.D. Thesis.
- [7] W. Scandale, *Numerical Results on the Effect of the Parasitic Multipoles in the Superconducting Dipoles of LHC*. LHC Note 57.
- [8] A. Bazzani, P. Mayzanti, G. Servizi, G. Turchetti, *Normal Forms for Hamiltonian Maps and Non Linear Effects in a LHC Model*, LHC Note 66.
- [9] B. Autin, J. Bengtsson, *Application of Symbolic Computation to the Search of Complicated Primitives: the Example of the Betatron Integrals*, Computer Physics Communications 48, (1988).

CORRECTION OF SEXTUPOLAR BEAM ENVELOPE DISTORTION

B. Autin

CERN, Geneva, Switzerland

Introduction

In most machines the momentum dependence of the betatron tune, also called *chromaticity*, is controlled by sextupoles in such a way that a beam blow-up due to non linear resonances or to various types of instabilities is avoided. As a counter-part, the sextupolar fields produce a distortion of the particle trajectories. In contrast with the linear fields perturbations, the non linear distortions depend on the initial phase and amplitude of the betatron oscillation. They are corrected using one of the following three methods: self compensation in large colliders super-cells, the single resonance compensation which has been used for a long time in a variety of cases, and the *broad band* compensation which is the object of this paper. The principle which this method is based upon is similar to a global closed orbit correction [1] and uses a formalism [2,3] which is an extension of the classical Courant and Snyder's treatment of linear perturbations [4]. It has been applied to the CERN Antiproton Collector Ring which is an ideal test case since it is a small ring in which the strong sextupolar fields cannot be self compensated and whose linear acceptance exceeds 200π mm.mrad in the horizontal and vertical planes.

Beam envelope distortion

The betatron oscillations can always be described by the couple of equations

$$x = \sqrt{2J_x \beta_x} \cos(\mu_x - \mu_{x0}) \quad (1)$$

$$y = \sqrt{2J_y \beta_y} \cos(\mu_y - \mu_{y0}) \quad (2)$$

The actions (J_x, J_y) which are numerically equal to half the emittances, and the initial phases (μ_{x0}, μ_{y0}) are constants of motion in a linear machine. When a sextupolar field of integrated strength $k'l$ is present, actions and phases vary around the machine and the action distortion which is a measure of the beam envelope distortion is given after N turns by [3]:

$$\Delta J_x = \frac{k'l \sqrt{2J_x \beta_x}}{4} \sum_{i=1}^5 C_{xi} \sum_{n=1}^N \sin \bar{m}_i (\bar{\mu} - \bar{\mu}_0 + 2\pi n \bar{Q}) \quad (3)$$

$$\Delta J_y = \frac{k'1 \sqrt{2J_x \beta_x}}{4} \sum_{i=1}^5 C_{yi} \sum_{n=1}^N \sin \bar{m}_i \cdot (\bar{\mu} - \bar{\mu}_0 + 2\pi n \bar{Q}) \quad (4)$$

with

$$\bar{C}_x = (J_x \beta_x, -2J_y \beta_y, J_x \beta_x, -J_y \beta_y, -J_y \beta_y) \quad (5)$$

$$\bar{C}_y = (0, 0, 0, J_y \beta_y, -J_y \beta_y) \quad (6)$$

$$\bar{m} = ((1,0), (1,0), (3,0), (1,2), (1,-2)) \quad (7)$$

$$\bar{\mu}_0 = (\mu_{x0}, \mu_{y0}) \quad (8)$$

$$\bar{\mu} = (\mu_x, \mu_y) \quad (9)$$

$$\bar{Q} = (Q_x, Q_y) \quad (10)$$

The sum over the number of turns has the closed expression

$$\sum_{i=1}^N = \frac{\cos \bar{m} \cdot (-\pi \bar{Q} + \bar{\mu} - \bar{\mu}_0) - \cos \bar{m} \cdot [(2N+1)\pi \bar{Q} + \bar{\mu} - \bar{\mu}_0]}{2 \sin \pi \bar{m} \cdot \bar{Q}} \quad (11)$$

It consists, at a given position characterized by (μ_x, μ_y) , of an average term modulated by a sinusoidal term of frequency

$$f = \bar{m} \cdot \bar{Q} \quad (12)$$

This form is particularly interesting to interpret the results of a tracking program in which the output is presented as a plot of (J_x, J_y) at each turn. The action distortion depends upon the initial actions and phases; each particle trajectory has thus its specific deformation and the contour of the beam is no longer clearly delimited but transformed into a halo. A correction must be valid for all the particles and, for this purpose, it is preferable to write the action distortion in a different form. The action dependence is not a problem. The phase dependence requires a special treatment. The sine term in (3) or (4) is the imaginary part of

$$\exp i \bar{m}_i \cdot (\bar{\mu}_j - \bar{\mu}_0 + 2\pi n \bar{Q}) \quad (13)$$

for the j-th one of a set of M sextupoles and the action distortions can be re-written in a complex form

$$\Delta J_x^* = f(N, \bar{\mu}_0) \sqrt{2J_x} \sum_{j=1}^M (k'1)_j \sqrt{\beta_{xj}} \sum_{i=1}^5 C_{xij} \exp i \bar{m}_i \cdot \bar{\mu}_j \quad (14)$$

$$\Delta J_y^* = f(N, \bar{\mu}_0) \sqrt{2J_x} \sum_{j=1}^M (k'1)_j \sqrt{\beta_{xj}} \sum_{i=1}^5 C_{yij} \exp i \bar{m}_i \cdot \bar{\mu}_j \quad (15)$$

where f is some function which has not to be made explicit. An important simplification occurs when the sextupoles respect the mirror symmetry of the lattice. In this

case, the sextupoles located at μ and $2\pi Q - \mu$ can be associated and, using (11), the expressions (14) and (15) become real

$$\Delta J_x = g(N, \bar{\mu}_0) \sqrt{2J_x} \sum_{j=1}^{M/2} (k'l)_j \sqrt{\beta_{xj}} \sum_{i=1}^5 C_{xij} \cos \bar{m}_i \cdot (-\pi\bar{Q} + \bar{\mu}_j) \quad (16)$$

$$\Delta J_y = g(N, \bar{\mu}_0) \sqrt{2J_x} \sum_{j=1}^{M/2} (k'l)_j \sqrt{\beta_{xj}} \sum_{i=1}^5 C_{yij} \cos \bar{m}_i \cdot (-\pi\bar{Q} + \bar{\mu}_j) \quad (17)$$

Principles of correction

Ideally, one would like to group the chromaticity sextupoles in super cells [5] without caring about the cell symmetry and apply the compensation conditions

$$\sum_{j=1}^M (k'l)_j \sqrt{\beta_{xj}} \sum_{i=1}^5 C_{xij} \exp i \bar{m}_i \cdot \bar{\mu}_j = 0 \quad (18)$$

$$\sum_{j=1}^M (k'l)_j \sqrt{\beta_{xj}} \sum_{i=1}^5 C_{yij} \exp i \bar{m}_i \cdot \bar{\mu}_j = 0 \quad (19)$$

This approach is followed for large machines and guides the choice of the phase advance per cell. For smaller machines, it may not be possible to find enough space in the arcs to use this technique and another method has to be invented. The action distortion can be viewed as generated by the five modes m_i . Assuming that the lattice symmetry is respected, the components of the chromaticity sextupoles on each mode form a 5-vector

$$\bar{b} = \left[\sum_{j=1}^{M/2} (k'l)_j \sqrt{\beta_{xj}} C_{xij} \cos \bar{m}_i \cdot (-\pi\bar{Q} + \bar{\mu}_j) \right] \quad i = 1, \dots, 5 \quad (20)$$

which may be compensated by the combined action of S families of correction sextupoles located in zero orbit dispersion sections. Each family is characterized by the column vector of a correction matrix

$$A = [\bar{a}_k] \quad k = 1, \dots, S \quad (21)$$

with

$$\bar{a}_k = \left[\sum_{j=1}^{S_k} \sqrt{\beta_{xj}} C_{xij} \cos \bar{m}_i \cdot (-\pi\bar{Q} + \bar{\mu}_j) \right] \quad i = 1, \dots, 5 \quad (22)$$

The unknown integrated strengths are the components of a S -vector

$$\bar{x} = [(k'l)_i] \quad i = 1, \dots, S \quad (23)$$

which is a solution to the matrix equation

$$A\bar{x} + \bar{b} = 0 \quad (24)$$

Various strategies can be envisaged for the composition of the sextupole families

and for solving the equation (24). The MICADO algorithm which is widely used for orbit correction can still be applied to non linear corrections; at each iteration, it proposes a new sextupole family which, by combination with the previously selected families, gives the minimum norm of the residual vector

$$\bar{\mathbf{r}} = \mathbf{A}\bar{\mathbf{x}} + \bar{\mathbf{b}} \quad (25)$$

Example of correction

The CERN Antiproton Collector Ring [6] has two superperiods, each with a mirror symmetry, and betatron tunes per superperiod of (2.23 , 2.22). A quadrant is represented in Figure 1. The long straight sections at the end of the arc are dispersionless. The chromaticity sextupolar fields are produced by a special shaping of the pole profile of the focussing magnets in the arcs. The sextupolar component is characterized by a gradient index G'/G , ratio of the radial derivative of the field gradient to the central gradient, which is equal to .6 or 1.43 m^{-1} depending on the value of the orbit dispersion in the focussing magnets.

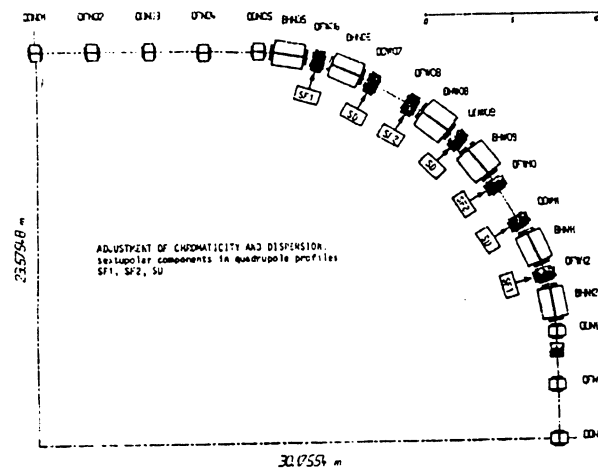


Figure 1. A quadrant of the CERN Antiproton Collector Ring.

The effect of the chromaticity sextupoles on the phase space dynamics is shown in Figure 2 for special initial conditions. In order to emphasize the importance of second order coupling effects [7], the linear tune split has been reduced to .001. Initially, correction sextupole families were composed of single elements and distributed in all the available quadrupoles. The application of the MICADO algorithm quickly showed that several elements had almost the same effect on the action distortion and it turned out that a single family grouping sextupoles in QDN03, QDN15 and their images in the lattice with a gradient index of 1.3m^{-1} would be sufficient to give a rather good compensation (Figure 3). The sextupolar field is obtained with twelve copper bars distributed in the quadrupole gap and connected in

series with the main quadrupole current [8].

The residual low frequency distortion can be corrected using an octupole scheme self compensated for 4-th order resonances (Figure 4). In practice, the octupole scheme was not installed because it was possible to tune the machine far enough from the line

$$Q_x - Q_y = 0 \quad (26)$$

in the working diagram.

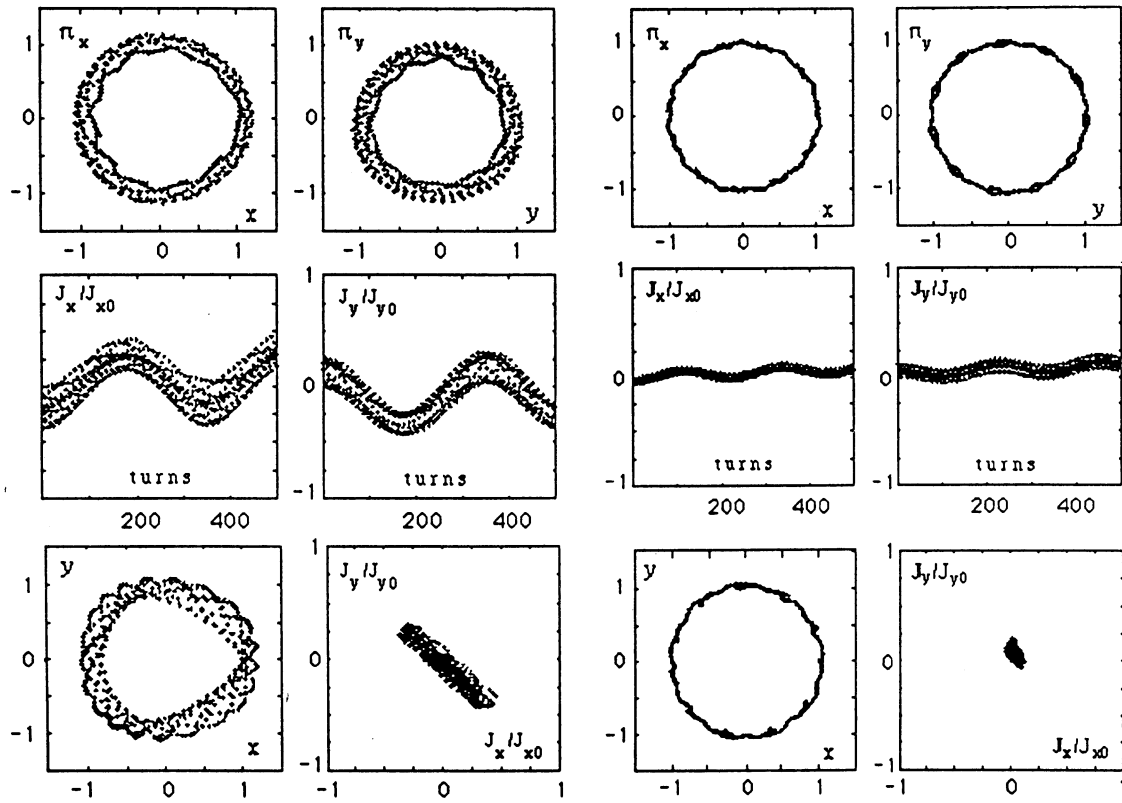


Figure 2. Phase space distortions produced by chromaticity sextupoles. Initial conditions: $J_x=J_y=100\pi$ mm.mrad, $\mu_x=0$, $\mu_y=\pi/2$.

Figure 3. Effect of a sextupole correction scheme (same conditions as in the case of Figure 2).

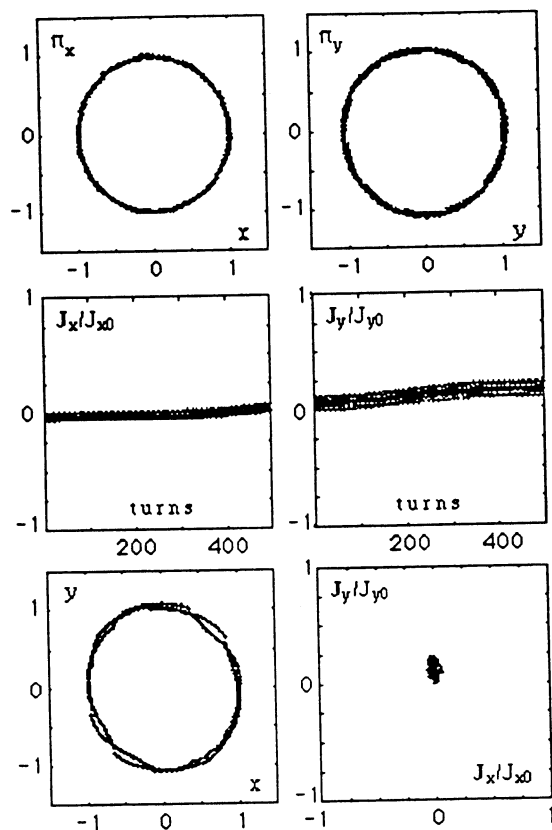


Figure 4. Combined effect of a sextupole and octupole correction scheme (same conditions as in the case of Figure 2).

References

- [1] B. Autin, *Lattice Perturbations*, AIP Conference Proceedings 127, pp.139, 200 (1983)
- [2] B. Autin, *Non Linear Betatron Oscillations*, AIP Conference Proceedings 153, pp.290, 347 (1985)
- [3] T. Collins, *Distortion Functions*, Fermilab-84/114 (1984)
- [4] E.D. Courant and H.S. Snyder, *Theory of the Alternating Gradient Synchrotron*, Ann. Phys.3, 1-48 (1958)
- [5] B. Autin and F. Willeke, *Second Order Tune Shift in a Compensated Super Cell*, These proceedings.
- [6] B. Autin *et al.*, *The CERN Antiproton Collector Ring*, Proceedings of the First European Conference on Particle Accelerators, Rome (1988)
- [7] M. Cornacchia, *Effect of Non Linear Coupling by Sextupoles in theSPS*, CERN LABII DI PA/74-3 (1974)
- [8] H.H. Umstätter, *Multipole currents in a Hyperbolic Mirror* (to be published).

PERSISTENT CURRENT FIELD ERRORS AND DYNAMIC APERTURE OF THE HERA PROTON RING

R. Brinkmann and F. Willeke

Deutsches Elektronen-Synchrotron (DESY), Hamburg, Federal Republic of Germany

Abstract

The influence of the magnetic field errors in the superconducting HERA proton ring on the nonlinear acceptance at injection ($E = 40\text{GeV}$) is investigated by tracking calculations. We find that the relatively strong multipole components caused by persistent currents would reduce the dynamic aperture to about half the physical aperture of the machine. The computer simulations have been compared to an analytical study using perturbation theory. It is concluded that a quasi local compensation of the strongest field components in every half FODO cell is necessary to achieve sufficient acceptance for an injected 40GeV beam.

1 Introduction

In a superconducting proton storage ring operated at its design energy, the linearity of the magnetic fields and thus the dynamic aperture is limited by systematic and random errors resulting from fabrication tolerances. Especially at low excitation of the magnets, the field quality is additionally reduced by persistent eddy currents in the superconducting filaments. For the case of the proton ring of the HERA e-p collider presently under construction at DESY, the latter effect is particularly important because of its low injection energy ($E_{inj} = 40\text{GeV}$ as compared to $E_{max} = 820\text{GeV}$). In extensive studies on nonlinear dynamics in HERA-p [1] [2] only the dominating distortion caused by the persistent currents namely the sextupole component in the superconducting dipoles has been taken into account. However recent measurements on magnet prototypes [3] have shown that the higher multipole components (the decapole in the dipoles and the duodecapole in the quadrupoles) are larger than originally anticipated (see table 1)

In this paper we investigate the influence of these additional field distortions on the acceptance of the machine and discuss the possibility to compensate them. In the next section a brief summary of the methods applied is given. This is followed by the presentation of the results of numerical simulation of the effect of the field distortions in dipole and quadrupole magnets. Finally results are discussed and compared with perturbation theory and conclusions are drawn.

2 Tracking Procedure

The nonlinear acceptance of the proton ring has been investigated using the particle tracking code RACE-TRACK [4]. Usually the acceptance as obtained from numerical simulation is defined as the maximum emittance (sum of the two Courant Snyder invariants) as calculated from initial conditions of a probe particle for which the trajectory is stable over a given number of turns. However since the acceptance defined that way depends rather strongly on the initial phase, many particles with different start phases would have to be tracked to obtain a safe estimate of the acceptance. This can be improved drastically by evaluating the emittance of the particle after each turn and remembering the minimum value reached during the run which will be considered as the acceptance. We found that with this procedure, tracking of only four particles (sin- and cos-like trajectories in both planes) lead to the same results as tracking a few tens of particles with the usual acceptance definition. Thus the needed computer time could be considerably reduced. As a compromise between computer time and reliability of the results the number of tracked turns was restricted to $n_{turn} = 1000$. According to reference [2], the dynamic aperture obtained by tracking up to 10^6 turns may be up to 30% – 40% smaller than the 1000-turn dynamic aperture.

The tracking runs have been performed with and without aperture limitations representing the beam pipe (we distinguish between "nonlinear acceptance" for the first case and "dynamic aperture" for the

latter one). This allows to compare the dynamic and the physical aperture as well as estimating how much the physical aperture is reduced by phase space distortions ("smear").

The particle momentum is kept constant during tracking. The investigated range is $\Delta p/p -0.002 \leq \Delta p/p \leq 0.002$. The closed orbit is adjusted to an r.m.s. error of 1mm. Each run is done with four different sets of random errors. Since it turned out that the tracking results don't vary significantly if the tunes are changed, most of the systematic investigations were carried out with fixed tunes of $Q_{x/z} = 31.15/32.18$

3 Effects of Persistent Current field errors and its compensation

We first study the machine with additional 12-pole components $b_6/b_2 = 4 \cdot 10^{-3}$ at $r_0 = 25\text{mm}$ in the superconducting quadrupoles (according to recent measurements [3]). The acceptance is compared to the one obtained for a machine with chromaticity correcting sextupoles and fluctuating higher order multipole components in the dipoles only (see table 1).

Table 1.									
Assumed Fluctuating Multipole Components of the HERA-p s.c. dipole magnets									
n	2	3	4	5	6	7	8	9	10
normal b_n	0.8	4.0	0.5	1.0	0.5	0.5	0.5	0.5	0.5
skew a_n	0.5	0.5	0.5	0.5	0.5	0.5	0.5	0.5	0.5
normalized to b_1 , in units of 10^{-4}									

The resulting dynamic aperture for both cases is shown in fig 1a.

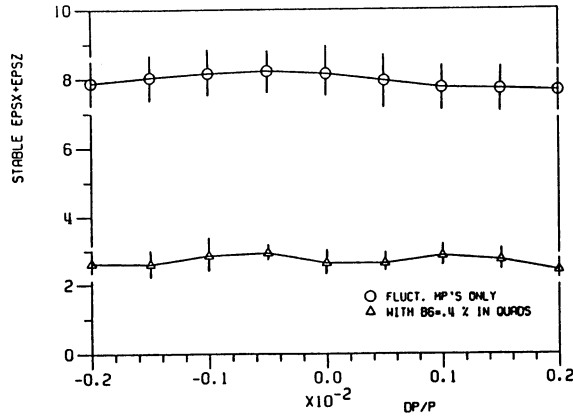


Figure 1a: Dynamic aperture for a machine with fluctuating multipoles only (○) and for a machine with an additional 12-pole component in the quadrupoles (△)

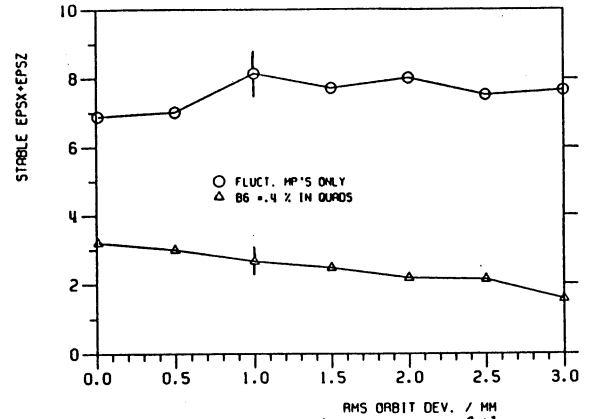


Figure 1b: Dynamic aperture of the machine with a 12-pole component $b_6 = 0.4\%$ in the quadrupoles as a function of r.m.s. orbit deviation (equal in both planes)

The presence of the persistent current 12-pole reduces the dynamic aperture by about a factor of three. Also in this case the acceptance is rapidly reduced with increasing r.m.s. orbit deviation (see fig 1b). For an orbit rms error of only 1mm, the dynamic aperture is already significantly smaller than the linear aperture over the full range of the momentum spread. An additional introduction of aperture limitation does not change the results any more.

We present next the influence of the persistent current decapole component in the superconducting dipole magnets. Its value at injection energy is $b_5/b_1 = -0.001$ at $r_0 = 25\text{mm}$ which is about 25% of the

persistent current sextupole component. The latter one is very well compensated by 6m long coils in each of the 9m long dipole magnets. As it can be seen in fig 2a, this additional multipole has only a small effect on the dynamic aperture for $\Delta p/p = 0$, but the acceptance drops rapidly with increasing momentum deviations resulting in a reduction of more than a factor of three.

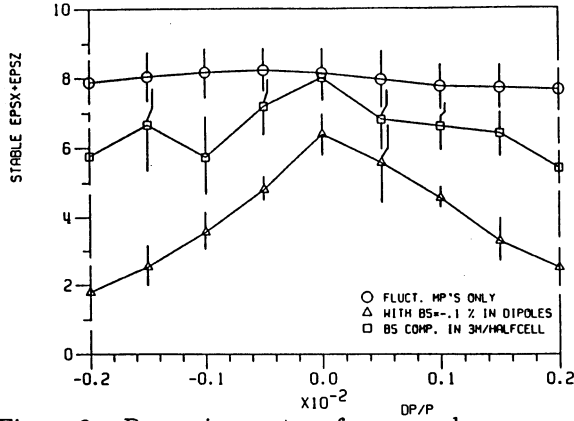


Figure 2a: Dynamic aperture for a machine with fluctuating multipoles only (o) and with $b_5 = -0.1\%$ in the dipoles without compensation (Δ) and with lumped correctors (□)

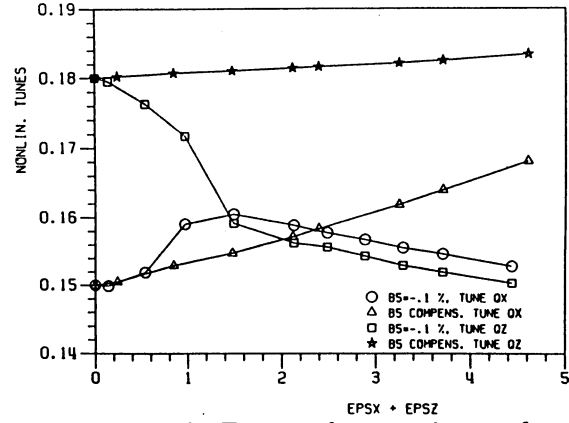


Figure 2b: Tunes vs beam emittance for the machine with an uncompensated de-capole $b_5 = -0.1\%$ in the dipoles without compensation (o, □) and with lumped correctors (Δ, *), $\Delta p/p = .002$

This is accompanied by a large nonlinear tune shift with amplitude as it can be seen from fig.2b

The 1000-turn dynamic aperture is for $\Delta p/p \leq 0.001$ larger than or comparable to the linear aperture. Therefore including the aperture limitation in the tracking calculations causes a further reduction of the nonlinear acceptance, except for large momentum deviations (fig 3a).

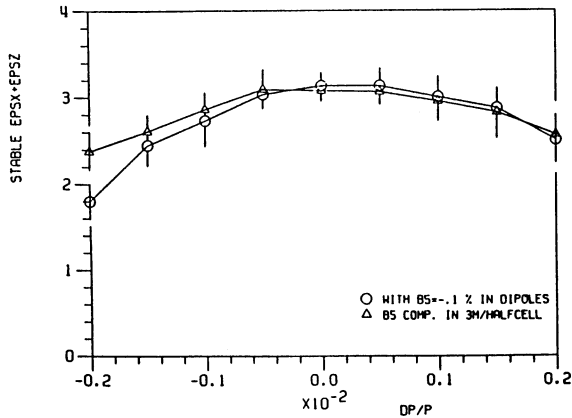


Figure 3a: Nonlinear Acceptance (physical aperture limitations) with an uncompensated (o) deca-pole $b_5 = -0.1\%$ in the dipoles and with lumped correctors (Δ)

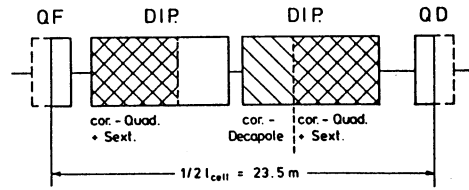


Figure 3b: Half FODO cell with sextupole and decapole correction coils

In case of the persistent current decapole a lumped compensation scheme with one 3m long correction coil in each half FODO cell was considered (fig 3b). The strength of the corrector is adjusted to cancel the integrated decapole strength of a half cell. The tracking results for this correction scheme without and with physical aperture restriction are shown in figs. 2a and 3a, respectively. The dynamic aperture is substantially improved but a small reduction for off momentum particles remains due to the fact that the scheme is only approximately local. For the case with aperture limitations, no significant improvement of

the nonlinear acceptance (except near $\Delta p/p = -0.002$) is observed. The nonlinear detuning is substantially smaller with compensations and linearity is improved in the range given by the nonlinear acceptance (see fig 2b).

4 Discussion of numerical results and comparison with perturbation theory

Because of the importance of the tracking results presented in the previous section and in view of the implication the proposed compensation scheme has on the construction of the superconducting magnets, it is very desirable to gain additional understanding how the results come about.

In case of the acceptance reduction by the 12-pole in the quadrupole, it is rather obvious that the resonant harmonics of order four must be rather strong, because they build up coherently due to the 90° betatron phase advance per FODO cell. The sensitivity of the dynamic aperture to orbit deviations in this case can be explained in the following way: An orbit deviation generated by many small random kicks looks locally very much like a betatron oscillation with a coherence length large compared to a betatron wavelength [5]. Thus the decapole and skewdecapole components due to the horizontal and vertical orbit deviation in the 12-pole field have a pattern which is in phase with the betatron oscillations for several wavelengths. The nonlinear distortion resulting from these decapoles and skew decapoles then add up coherently which explains the sensitivity of the dynamic aperture to orbit deviations. The consequence of the strong influence of the duodecapole in the quadrupole magnets on the beam dynamics is to provide a correction. The correction should be local, i.e. inside or at least close to each quadrupole. Correction coils placed at a few selected position in the ring would have to be extremely strong to account for the coherent effect from all the s.c. quadrupoles around the machine. This would in turn produce problems with positioning and orbit errors in the correctors, local optical distortions and higher order nonlinear effects.

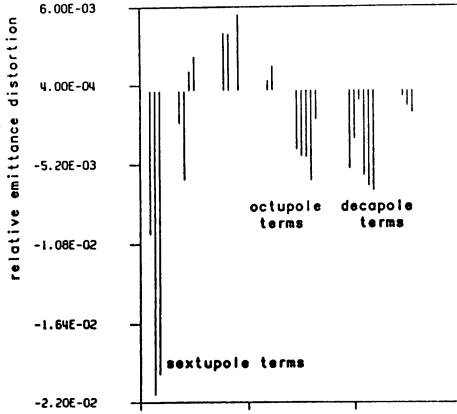


Figure 4a: Spectrum of Nonlinear phase space distortions $\Delta\epsilon/\epsilon$ without correction of the additional persistent decapole terms calculated for a HERA-p like FODO structure with 25 cells.

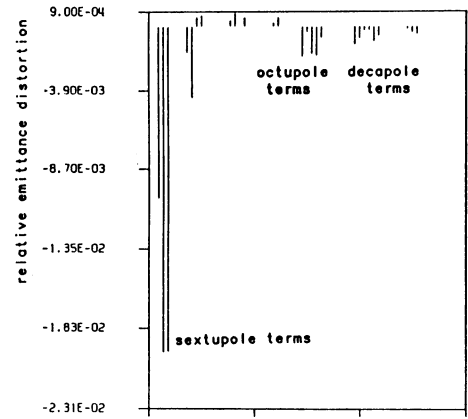


Figure 4b: Spectrum of Nonlinear phase space distortions $\Delta\epsilon/\epsilon$ with correction of the additional persistent decapole terms calculated for a HERA-p like FODO structure with 25 cells.

The situation for the decapole components in the dipoles is not so clear. On momentum, the reduction of dynamic aperture due to this field distortion is not very drastic. This is confirmed by the calculation of resonance driving terms and phase space distortions by perturbation theory (see [6]). The decapole driven terms never exceed the effect produced by the chromaticity correcting sextupoles. Analytical estimates of the dynamic aperture based on these calculations lead to a 25% aperture reduction due to the decapole component which corresponds to what is observed in tracking (see fig 2a).

Off momentum, the dynamic aperture decreases rapidly with a momentum deviation (a fact observed on earlier tracking calculations for the TEVATRON which also contains strong higher order multipoles [7]).

The octupole components resulting from feeddown due to the dispersion orbit in the decapole field add up coherently over the lattice just as the 12-pole components of the quadrupoles. However, calculation of the driving terms and distortion function shows, that they are not particularly strong compared with the sextupole and decapole terms. Large distortions result from the octupolar nonlinear coupling term $2Q_x - 2Q_z = 0$ which however is not expected to cause reduction of the dynamic aperture. The largest off momentum effect is the generation of octupolar detuning terms which exceed the sextupolar detuning terms by two orders of magnitude. A surprisingly strong effect is produced by the vertical dispersion which is not matched in the arcs. The nonlinear skew coupling resonance $Q_x - Q_z$ generated by the feeddown due to the vertical dispersion orbit is one of the strongest resonances at a 0.2% momentum deviation. All these calculations show that there is no single effect which is responsible for the strong off momentum aperture reduction but there is a large number of potentially harmful effects. Analytical estimation of dynamic aperture based on the distortion functions result in an acceptance of $A = 0.9\pi mrm$ at $\Delta p/p = 0.002$ which overestimates the acceptance drop by a factor of 2.

If the corrections are applied, the calculations show that the additional distortions of beam dynamics generated off/on momentum by the decapole component of the s.c.dipole are compensated by more than 75%, in most cases by an order of magnitude (see fig.4a,b)

5 Conclusion

The results and discussions presented in the proceeding sections have shown that the persistent current higher order multipoles at the low injection field in the HERA s.c. dipoles have a noticeable strong influence on the beam dynamics. The acceptance of the machine can be reduced to less than 0.5 of its original value (without the additional p.c. fields). These effect can be understood semi-quantitatively by analytical methods.

In the case of the 12-pole component of the quadrupole magnet it is very advisable to install local correction coils in or near the quadrupoles.

In the case of the 10-pole component of the dipole magnet the aperture reduction is only for off momentum particles ($\Delta p/p \geq 0.0005$). The total momentum spread of the 40 GeV beam is about $\Delta p/p \geq 0.0004$. This value will however be increased by a factor of four by bunch compression and intra beam scattering. It appears therefore in this case advisable to provide a quasi local correction in the middle of each half cell as described above (fig 6).

* * *

References

- [1] A. Wrulich, DESY-HERA 84-07 (1984)
- [2] F. Schmidt, Thesis, University of Hamburg, DESY-HERA 88-02(1988)
- [3] S. Wolff, H. Brück, private communication
- [4] A. Wrulich, DESY 84-026 (1984)
- [5] J. Kewisch et al, DESY 86-020 (1986)
- [6] F. Willeke, FERMILAB FN-422 (1985)
- [7] F. Willeke, FERMILAB TM-1220 (1983)

CHROMATIC CORRECTIONS AND DYNAMIC APERTURE IN THE HERA ELECTRON RING

R. Brinkmann and F. Willeke

Deutsches Elektronen-Synchrotron (DESY), Hamburg, Federal Republic of Germany

ABSTRACT AND CONCLUSION

The dynamic aperture of various sextupole correction schemes for the asymmetric HERA e^- lattice is investigated. Results show that it is important to restore the supersymmetry at least approximately by optics manipulations. Satisfactory sextupole configurations can be found for the whole range of lattices between 60° and 90° per FODO cell. They provide good chromatic behaviour. The beta functions change by less than 5 % and tunes change less than 0.01 in the momentum range between -1 % and + 1 %. The dynamic aperture considerably exceeds the necessary 6.5 standard deviations at 35 GeV for the whole range of solutions investigated.

1. INTRODUCTION

As in every large colliding beam storage ring, carefully optimized sextupole correction schemes are required in the HERA electron ring. In HERA, there are additional aspects:

The head-on-interaction scheme requires a special design for the straight section which is complicated by the need to have longitudinally polarized beams in the electron ring[1]. It became necessary to reserve one of the four straight sections for utilities like injection, proton dump etc. This results in a special optics in that quadrant. Owing to the broken supersymmetry, structure resonances are not suppressed automatically. This results in enhanced nonlinear effects in the beam dynamics.

Another aspect is that it is very desirable to be able to vary the electron beam emittance. This is achieved by variable focussing in the arcs: for optimum beam-beam interaction at high luminosity the transverse beam dimensions at the interaction have to be the same for electron and proton beams. The proton beam emittance, however, is not easy to adjust and predict. Also there is not much freedom left for changing the beta functions at the interaction point. Therefore, a variable electron beam emittance is necessary to achieve optimum conditions for colliding beams.

The adjustable optics in the arcs requires variable sextupole correction schemes to correct the chromaticity and the half integer off-momentum stop-band without exciting strong nonlinear resonances.

In this report we compare various optics which approximately restore the supersymmetry with respect to chromatic corrections and dynamic aperture. Furthermore, we present various sextupole correction schemes for betatron phase advances between 60° and 90° per FODO cell.

2. LINEAR OPTICS AND SEXTUPOLE DISTRIBUTIONS

The basis of the solutions discussed here is the linear lattice design presented in ref.[1,2].

There are two possibilities to restore approximately the symmetry in the HERA e-ring by means of the linear optics:

The first possibility is to give the modified insertion the same betatron phase advances as the supersymmetric ones. This restores 4 fold supersymmetry and suppresses structure resonances if the contributions to the chromaticity in the modified and in the standard insertion are not very different and if the nonlinear fields are located outside the insertion. However, in the HERA- e^- , the contributions to chromaticity from an interaction straight section are much larger than the contributions from the utility straight section. Furthermore, sextupole magnets are needed also in the matching sections at the ends of the arcs where the optics are different for utility and interaction straight sections.

Therefore, an alternative solution has been investigated: the quadrant containing the utility straight section has an integer phase advance N in both planes and the chromatic effects are compensated separately for interaction and utility quadrants. Thus, the beam transport matrix for the utility quadrant is a momentum independent unit matrix and the rest of the ring has a quasi 3-fold super-periodicity with

tunes of $(Q-N)/3$ per period. This solution is only satisfactory if the contributions to the driving terms of nonlinear resonances coming from the modified subperiod are small compared with the contributions from the other periods. This condition is in fact fairly well met in the modified utility quadrant: the short matching section between the periodic FODO structure of the arc and the straight section has rather smooth lattice functions so that sextupoles are placed essentially in a periodic FODO structure only. For certain phase advances/FODO cell it is then possible to arrange sextupoles so that there are no contributions to the driving terms of the lowest order nonlinear resonances no matter how the different sextupole families are excited. (This is explained in the next section).

The chromatic corrections are achieved by an interleaved sextupole scheme as proposed in ref.[3]. A horizontally focussing sextupole and a vertically focussing sextupole is placed in each FODO cell in the arcs. The members of the different families are distributed uniformly over the lattice.

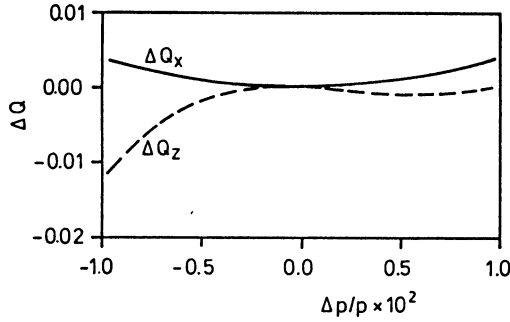


Figure 1a: Tune change vs $\Delta p/p$ for the 60° quasi 3-fold symmetric solution
solid line: horizontal tune
broken line: vertical tune

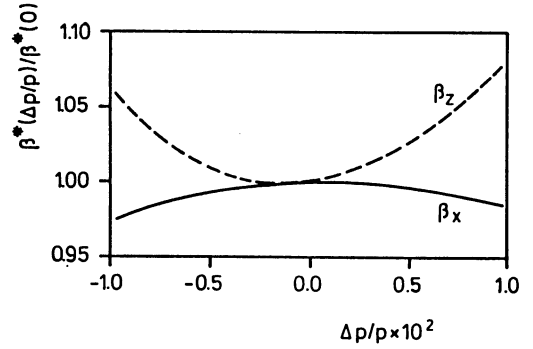


Figure 1b: change of β functions at interaction point, same optics
solid line: horizontal
broken line: vertical

In order to compensate the chromaticities in both planes and the off momentum β and α -beat factors (half integer stopband), at least 3 sextupole families per oscillation plane are needed. Because the beat factors have an amplitude and a phase which propagates with twice the betatron phase advance around the machine, we must provide two orthogonal correction circuits (if possible spaced by 45° phase advance) for each plane in addition to the chromaticity correction circuits.

The nonlinear effects of the sextupoles on the beam dynamics should be as small as possible. We expect that this will be the case if the driving terms of the lowest order nonlinear resonances (up to order 3) are zero. For a periodic FODO structure this is accomplished without any further sextupole circuits if the phase advance ϕ_c per FODO cell is an even fraction of an integer

$$\phi_c = n/m \cdot 2\pi \quad (m \text{ even})$$

and if the sextupoles are arranged in closed blocks extending over m FODO cells which have an integer phase advance $n \cdot 2\pi$ and which are composed of two identical parts each spanning a phase advance $n\pi$.

The intrinsic cancellation of driving terms is achieved for any excitation of the different families, because the sextupoles of the same family are spaced by $n \cdot \pi$ phase advance so that distortions cancel in first order.

We investigated the sextupole configurations for phase advances between 60° and 90° /FODO cell (equal phase advances in both planes are considered only).

Consider for example a phase advance of 60° /FODO cell: 6 FODO cells form a sextupole block with $\Delta\phi = 2\pi$. A HERA octant accommodates 4 sextupole blocks. The arrangement of the 3 families/oscillation plane is:

$$A - B - C - A - B - C$$

(where A includes two half FODO cells with a horizontally focussing sextupole family, "HA": and a vertically focussing sextupole family, "VA").

Orthogonality of the circuits for the compensation of beat factors is not perfect but it nevertheless allows the compensation of beat factors while deviations from the mean sextupole strength are smaller than 31 %. The driving terms for the nonlinear resonances up to the order 3 are not excited in the periodic part of the arcs.

In a 90° lattice, the 4-family sextupole blocks are as short as 4 cells. The configuration is A - B - A - B. For this phase advance only one of the two orthogonal circuits is available for stopband compensation. Therefore, the off momentum β -beats excited in the straight section can only be compensated if they arrive with a phase of zero or 180° at the first sextupoles in the periodic arc structure. This has been achieved by a proper distribution of phase advances in the straight sections. The lowest order driving terms are intrinsically compensated, but there is some concern about higher order effects. Contributions to the fourth order resonance driving from each cell build up over the whole HERA quadrant so that these resonances are expected to be strong (see below).

Therefore, we also investigated a nearby solution, a 88°, 4-family lattice where first and third integer resonances are not completely suppressed. The higher order resonances however are expected to be reduced. As an example for phase advances in between 60° and 90° we present 67.5°:

The sextupole block includes 16 FODO cells ($\Delta\pi = 3 \cdot 2\pi$). The arrangement of the 5 families per plane is

$$A - B - C - B - D - B - E - B - A$$

This configuration provides two perfectly orthogonal circuits combinations which allow correction of beat factors with only 25 % deviation from the mean sextupole strength. Stopband and chromaticity compensation are decoupled. The "B" families act on the chromaticities only, the A and D families form one of the orthogonal circuit combinations and C and E families the other one. Deviations of A and D from B have the same size but different signs thus $m_A + m_D = m_C + m_E = 2 \cdot m_B$ (m : sextupole strength). Resonances up to 3rd order are suppressed intrinsically. The contributions to 4th order resonance driving terms from each cell have a tendency to cancel so that we only expect small contributions from higher order effects on the beam dynamics.

Excellent chromatic properties are achieved for all phase advances. In the momentum range of

$$-1 \% < \Delta p/p < +1 \%,$$

the tune change does not exceed 0.01 and the β -functions at the interaction point change by less than 5 % (see fig. 1).

3. DYNAMIC APERTURE

The dynamic aperture is determined by particle tracking using the computer code RACETRACK[4]. Tracking is performed with synchrotron oscillations in the approximation of externally modulated momentum deviations. The program estimates the phase space areas in both planes which correspond to the maximum stable starting amplitude. These maximum stable phase space areas will be referred to as acceptances. For a more detailed discussion see ref.[5]. We always start with an initial emittance ratio of $\epsilon_z/\epsilon_x = 10$ %. As stability criterion, survival of a particle for 1000 machine turns within a given large aperture is assumed.

Firstly, we compare the dynamic aperture for the two quasi symmetric optical solutions for a phase advance of 60°/FODO cell. Sextupole fields are the only nonlinearities taken into account. In Fig. 2 we present the available number of standard deviations (square root of horizontal acceptance divided by equilibrium emittance) as a function of the momentum amplitude of the synchrotron oscillation. The shaded area represents the space needed by a 35 GeV electron beam. We recognize a significant advantage of the quasi 3fold-symmetric solution. The reason is that the quasi 4fold-symmetric solution does not suppress sufficiently the lowest order resonances. The resonance widths for $Q_x = 47$ and $Q_x + 2Q_x = 142$ are 5 times and twice as large respectively as the width in the 3-fold symmetric solution. In investigating the dynamic aperture in the vicinity of resonances we find a drastic reduction for both optics near $4Q_x = 189$ (which is a structure resonance for the 3fold quasi symmetric case). Near the third integer resonance, however, we find stability for the quasi 3-fold symmetric solution and an acceptance drop for the quasi 4-fold symmetric solution.

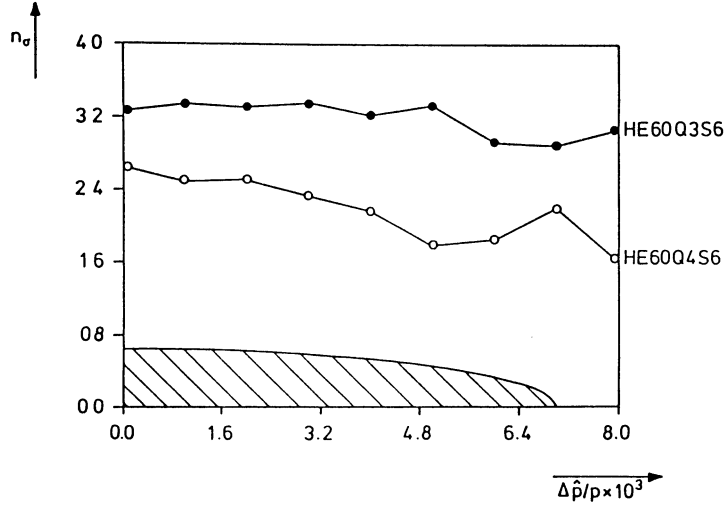


Figure 2: Sextupole acceptance A_x for quasi 4-fold (o) and quasi 3-fold (●) symmetric solutions.

Plotted is $n_\sigma = \sqrt{A_x/\epsilon_x}$ vs the amplitude of momentum oscillations $\Delta p/p$

Because of the advantage of the quasi 3-fold symmetric solution we restrict the investigation of the acceptance for different phase advances in the arcs to this case. In Fig. 3, the number of available standard deviations $n_\sigma = (A_x/\epsilon_x)^{1/2}$ ($E = 35$ GeV, on momentum) is plotted for different phase advances (dots). Acceptances are obtained for optimized sextupole correction schemes according to the description in the previous section.

The quality of the various sextupole correction schemes can be discussed by comparing the tracking results with an analytic scaling law: we take 60° as a reference point and scale the sextupole strengths to compensate the phase dependent chromaticity contributions $\xi^{cell} = \tan\phi_c/2$, produced in the arcs. From the equation of motion of a particle in sextupole fields it follows that for a sextupole distribution which is scaled only quantitatively but which is not changed qualitatively n_σ scales simply as

$$n_\sigma \propto 1/\sqrt{\epsilon_x(\phi_c)m(\phi_c)}$$

Expressing the equilibrium emittance ϵ_x and sextupole strength m in terms of the phase advance/cell ϕ_c (thin lens approximation) and taking the fixed chromaticity contributions from the straight sections into account we obtain the following scaling law:

$$m_{H/V}(\phi_c) \simeq \frac{\rho \sin^3 \phi_c / 2 (1 + 1.26 \cos \phi_c / 2)}{2\pi L^3 (1 \pm \frac{1}{2} \sin \phi_c / 2)}, \quad \epsilon(\phi_c) \propto \frac{(1 \frac{3}{4} \sin \phi_c / 2 + \frac{1}{60} \sin^4 \phi_c / 2) \sin \phi_c}{\sin^2 \phi_c / 2}$$

N number of FODO cells

ρ bend radius

L half cell length

This is represented by the solid line in Fig. 3. Results of tracking are close to the analytical scaling law (solid line). This shows that the quality of the excellent 60° sextupole configuration can be maintained for larger phase advances.

The only exception is the 90° solution where 2nd and higher order effects in the sextupole strengths are enhanced due to the special phase advance. For example, we found a strong acceptance reduction near the 5th order resonance $3Q_x + 2Q_z = 236$ which is excited by terms cubic in the sextupole strengths. Small deviations from 90° , however, are enough to reduce these lattice resonances as is demonstrated by the 88° point.

For all the optical solutions the dynamic aperture considerably exceeds the minimum required 6.5 standard deviations. Thus we may conclude that the lifetime in the HERA electron ring will not be restricted by the sextupole acceptance.

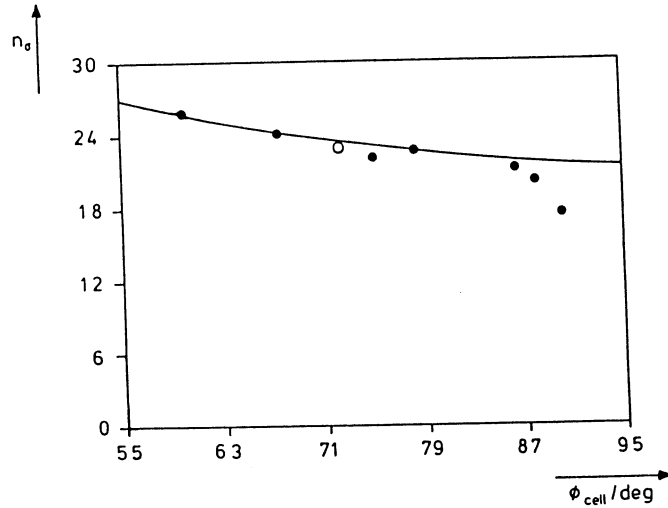


Figure 3: Dynamic aperture divided by equilibrium beam size (at $E = 35$ GeV), vs. phase advance per FODO cell.
Dots: tracking results
Curve: analytical scaling law (see text)
Open circle: 2-family-distribution (see chapter 3).

* * *

References

- [1] D. Barber, R. Brinkmann, R. Kose, J. Roßbach, K. Steffen and F. Willeke: "HERA Straight Sections for Head-On Electron-Proton Interactions", IEEE Trans. Nucl. Sc. Vol. NS 32-5, 1647 (1985).
- [2] D. Barber, R. Brinkmann, R. Kose, J. Roßbach, K. Steffen and F. Willeke: "The HERA Straight Section", Proc. Acc. Conf. Novosibirsk (1986).
- [3] A. Wrulich: "Various Sextupole Schemes for the HERA Electron Ring", DESY HERA 85-14, 1985.
- [4] A. Wrulich: "RACETRACK: A Computer Code for the Simulation of Nonlinear Particle Motion in Accelerators", DESY 84-026, 1984.
- [5] R. Brinkmann and F. Willeke: "Chromatic Corrections and Dynamic Aperture in the HERA Electron Ring, Part I, DESY 86-70 and Part II, DESY 87-037.

RECENT WORK ON ERROR CORRECTION AND RELATED ISSUES AT THE SSC

Richard Talman

LBL, Berkeley, California, USA

1. Introduction.

This will be largely restricted to being an enumeration of recent work on compensation of errors in the SSC. Much of this work is of a rather routine nature and will not be spelled out on that account. More fundamental new results by Neuffer on systematic corrections and by Forest on random corrections and other topics has been described by those authors at this workshop and will not be further described here.

Using the terminology of Willeke, the leader of the Compensation Scheme Group at this workshop, the SSC will be an "error dominated" not a "chromaticity dominated" machine. This means that some of the elegant, global compensation relationships described for small electron machines at this workshop are not really relevant. On the other hand, in large, error-dominated accelerators, it is important to understand the conspiracy between two (or more) bad effects, either of which, by itself, could be analysed simply. Two examples are coupling caused by orbit distortion, and random bend errors due to orbit shifts in elements possessing systematic errors.

Degradation due to nonlinear field errors has been quantified mainly by tune shifts and by "smear". A lengthy and inconclusive working session on standardizing usage as regards smear was held at the workshop and none of that discussion will be reported here. In analysing the SSC the following approximate "principles" have repeatedly been found to be valid:

- (i) systematic bend errors cause tune shifts and not smear, and
- (ii) random bend errors cause smear and not tune shifts.

Though these are obviously not universally valid they represent a useful rule-of-thumb on what to pay attention to.

2. Some Terminology of Error Correction.

The ideas behind various correction schemes are not at all deep and understanding them often requires little more than an understanding of the meaning of the terms employed in describing them. This itself is not necessarily easy as the terms are often a bit vague and describe points on a "continuous spectrum" of possibilities. Some of the terms are:

- (i) **local \simeq distributed \simeq bore tube correctors.** These are coils which, in the ideal limit, run the full length of the magnet and precisely "correct" the multipole element they are designed for. These have the effect of "fixing the magnet" itself rather than "fixing the accelerator". A bit of discussion at the workshop suggested that the former should be called "correction" while the latter should be called "compensation". Unfortunately, an appreciable minority felt the usage should be the reverse of that.
- (ii) **lumped \simeq remote correctors.** These are coils which are located in the lattice at points remote from the errors which they are "compensating". That is, they "fix the accelerator".

- (iii) **magnet sorting** consists of ordering the placement of elements in the ring based on bench measurements of one or more of their multipole errors and in such a way that their errors tend to be mutually compensating. The simplest scheme would match magnets in pairs having a particular multipole approximately equal in magnitude but opposite in sign; these would be placed side-by-side in the lattice. Such schemes have fervent supporters who were well represented at the workshop. They can be perceived to be “free” or at least “cheap”. For that very reason these schemes have been held “in reserve” in recent SSC investigations. They are not mutually exclusive of other schemes and can be used to compensate a lesser multipole if a greater multipole has been compensated (or corrected) some other way.
- (iv) **shuffling**. As applied to playing cards this means mixing them up. As applied to magnet laminations or other elements which have not been individually measured it means mixing them up to convert systematic errors (either feared or known) into much smaller random errors. At one large U.S. laboratory the barbarous use of this term to mean sorting has been all too common.
- (v) **binning correction**. This is just a minor variant of local correction. It works only to correct previously measured random errors and requires the existence of approximately local correction coils. Ideally every such coil would have an independent power supply powered to cancel the known error. After histogramming the measured values of the particular multipole error, one attaches all magnets falling in one bin to that power bus which cancels the center-of-bin value. This saves power supplies.
- (vi) **Neuffer scheme \simeq Simpson’s rule scheme**. Though not really synonyms these terms convey the same spirit. Neuffer uses traditional numerical integration weighting rules — for one likely configuration that means Simpson’s rule. Neuffer economizes further, with little degradation, by coalescing the corrections adjacent to quadrupoles, thereby getting the benefit of an integration formula of order higher by one than the number of lumped correctors appears to indicate.

Generally speaking local compensation is easy to analyse but may be expensive or impractical. Remote correction is cheaper but harder to analyse. Much of the recent work at the SSC has been devoted to analysing these trade-offs.

3. Diagnostic Developement.

Some other topics which have been of recent interest but which have been described by other participants in the workshop are hysteretic behaviour of persistent multipoles (described by M. Harrison) and developement of diagnostic capabilities performed in conjunction with the beam dynamics experiment E778. (These have been described by S. Peggs.) These last two are closely related since the expected slow chromaticity variation accompanying the drifting persistent currents are expected to demand continuous chromaticity control of the SSC with measurement times much less than a minute. (Chromaticity control is relatively more critical in a larger ring as tune variation tolerances are absolute; they become smaller relative to the integer tune.) By modulating the Tevatron R.F. frequency first plus then minus by one part in a million the tunes were measured within five seconds and the chromaticity calculated within about 30 seconds using the Sun workstation data aquisition instrument MIRABILE developed at the CDG by Saltmarsh, Peggs, and the author and described by Peggs. Comparison of the measured chromaticities with theoretical values is given in Fig. 1.

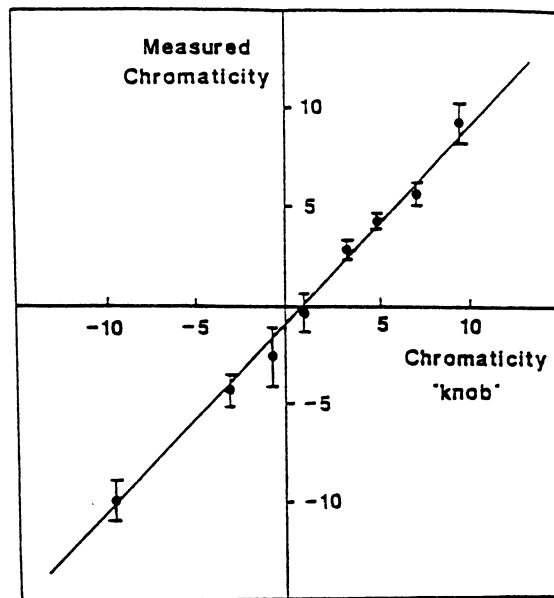


Figure 1. Comparison between chromaticity as calculated to calibrate a chromaticity "knob" with values measured and calculated on-line on the Tevatron.

4. Recent Reports on Multipole Compensation.

Some recent reports generated at the Central Design Group and describing different lumped schemes will now be enumerated. They are all mutually compatible and, as mentioned previously, are intended to replace sorting only in the sense of leaving that in reserve to compensate other multipoles.

Neuffer, SSC-132, June 1987, (and SSC-N-362, and other reports.) Lumped compensation of systematic multipoles is described and analysed.

Neuffer, SSC-N-384, March 1988, Compensation by octupoles of tunes shifts caused by second order sextupole tune shifts is described.

Forest and Peterson, SSC-N-383, September 1987. Using binning, lumped correction of random multipoles is shown to be effective.

Talman, SSC-N-413, December, 1987. Several lumped schemes are analysed and found to be effective both for randoms and systematics.

Neuffer and Talman, SSC-N-492, March, 1988. Of various lumped schemes of the same cost, the Neuffer scheme was found to be the most effective for systematics.

Sun and Talman, SSC-N-500, April, 1988. Of various lumped schemes of the same cost, using binning with strengths given by formulas of Forest, the Neuffer scheme was found to be the most effective for randoms.

5. Operational Simulation.

Work on interactive aspects of operational simulation is led by Schachinger. Computation is done on a cluster of Sun workstations. The analysis tool is the code TEAPOT, but, apart from the application to specific SSC design issues such as those just listed, recent work has been more in the area of graphical representation and development of interactive capabilities. As mentioned above it is the possibility of conspiracy between bad effects which necessitates the simultaneous inclusion of many different errors and imperfections. Areas in which reasonably complete work has been done are checked off in Table 1. Possible future projects are also indicated. Recent work includes

Schachinger, SSC-N-433, December 1987, Interactive Global Decoupling of the SSC Injection Lattice.

Schachinger and Talman, SSC-167, March 1988, Simulation of Chromaticity Control in the SSC.

Paxson, Peggs, and Schachinger, in preparation, Interactive Closed Orbit Control.

6. Data Organization.

Accelerator data are generated by diverse groups and they are of interest to diverse groups. It is important that the accelerators being designed, manufactured, positioned, measured, controlled, etc. are in fact the same machine. To insure this it is important that internal inconsistencies not develop and that requires that every parameter be recorded in a unique "sacred" record. Every user needing that number must obtain it from that source. At the same time most data "belong" most naturally to one particular group. That is the group having the greatest stake in their correctness, and, one supposes, the best motivation to keep them current. To meet these requirements a "hub-and-spoke" top level data organization, as shown schematically in Fig. 2, is planned.

The main features are

- (i) A **hub database** that manages the interaction between many spoke databases. It is primarily a "telephone directory" which contains addressing information permitting a worker in one spoke to locate information in another spoke.
- (ii) **Spoke Databases.** These contain real data from experiments, planning, design and so on, specialized applications for internal data presentation, and well-defined
- (iii) **public interfaces**, where responsibilities to and requirements from the wider user community can be specified without forcing inappropriate practices on specialized applications.

So far development of this structure has been restricted to the spoke labelled Accelerator Design DBMS (Database Management System.) A commercial database has been selected and rudimentary generation from the database of a lattice file in standard format has been achieved by Saltmarsh and Peggs. Plans are afoot to start work soon on the spoke labelled Magnet Construction and Measurement Database. Referring back to Table 1, it can be seen that, as yet, there is no mechanism for obtaining operational simulation input data from the shared database.

OPERATIONS SIMULATION	ORBIT			OPTICS			NONLINEAR SYSTEMATIC	RANDOM	MULTI- PARTICLE	DYNAMIC	CONTROL
	First turn	Iterated bump	Matrix inversion	Beta function adjustment	Global decoupling	Local decoupling	$Q(\delta, \epsilon_x, \epsilon_y)$	Smear, FFT, resonance	Tevatron simulation	Energy ramping Beta squeeze	Real control performance specification
Analytic description	Y	Y	Y	Y	Y	Y	Y	Y	Y		
"Batch" mode -- file input	Y	Y	Y		Y	Y	Y	Y	Y		
Useable for design decisions?	Y	Y	Y		Y	Y	Y	Y	Y		
Realistic, interactive, graphical, interface	Y	Y			Y	R	Y	Y			
Shared database											
"Real time" response*	Y	Y						Y			

Table 1. Checklist of SSC features which have been simulated. Y means "yes", R means "rudimentary", blank means "not yet", * means enough computer power so that the procedure being simulated takes roughly as long as the actual procedure will take.

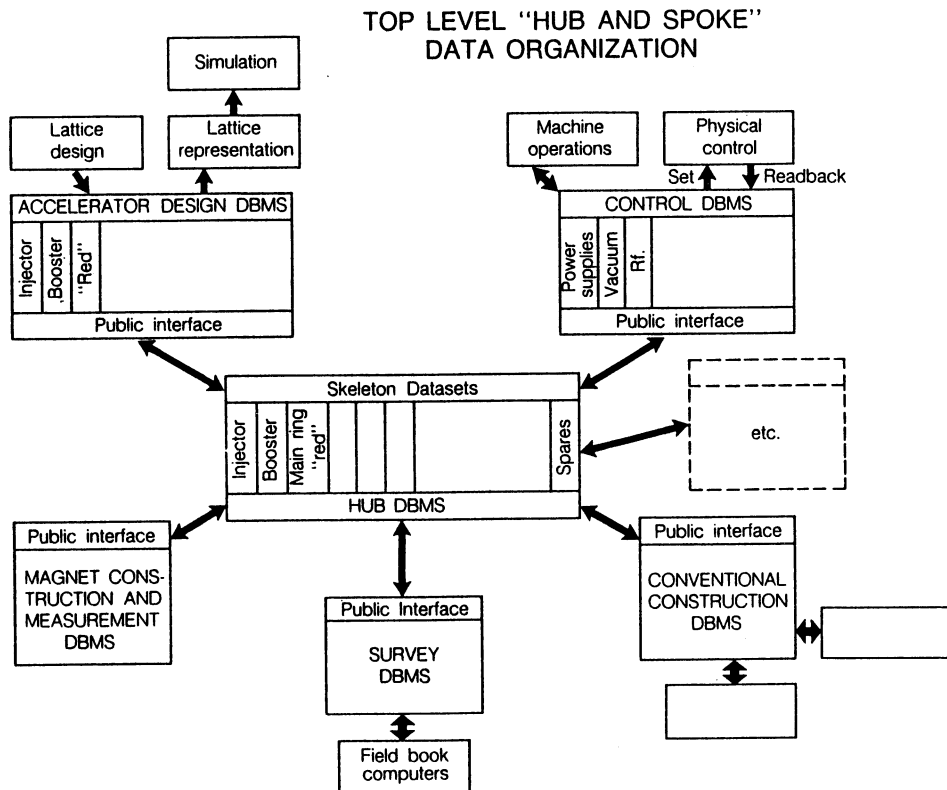


Figure 2.

FREQUENCY-DOMAIN CONSIDERATIONS IN MAGNET SORTING

S. Ohnuma

Department of Physics, University of Houston, Houston, Texas, USA

Summary

For large superconducting synchrotrons such as the Tevatron or the proposed SSC, the random normal sextupole component of dipoles is the most important factor in limiting their linear aperture. Since one selects the operating point in the tune diagram such that the third-integer resonances driven by particular harmonic components are not serious, the linear aperture cannot be enlarged by reducing these harmonic components alone. The magnet sorting scheme described in this note still depends on the harmonic description of the aperture-limiting effects but it tries to control a large number of harmonic components in the most troublesome regions. The scheme assumes that the sextupole component of each magnet is known and that, for each sorting group, there will be enough magnets to cover more than one betatron oscillation period. The "global" scheme is combined with the "local" sorting scheme such that the effectiveness of the scheme does not depend too strongly on a small change in tunes. An example is given to show that it is possible to achieve an order-of-magnitude reduction in the phase-space distortion ("smear") when some forty magnets are sorted as a group.

Introduction

If multipole components of all the dipoles to be used in the ring are measured and the data show nontrivial amount of fluctuations from magnet to magnet, as would be the case for superconducting magnets, one cannot afford to ignore the possible benefits expected from magnet sorting. The most attractive feature of any sorting is the fact that it is practically cost-free.

One must realize, however, that there is no unique way of sorting magnets. Factors that may influence the choice of sorting schemes are: total number of magnets in the ring, number in each cell, natural partition of the ring such as cryoloops and power supply stations, magnet installation schedules, magnet storage capacity, type and scope of correction systems, and allowance or non-allowance of magnets when one or two multipole components exceed the pre-determined values. It is also obvious that magnet sorting cannot cope with problems arising from very large systematic multipoles such as the normal sextupoles at injection induced by the persistent current in superconducting filaments. For these, there must be several families of correction packages and the system recently proposed by David Neufer¹ seems to be the most promising one. Another weakness of magnet sorting is that it is difficult to take into account more than one component and, at the same time, to control more than a handful of harmonic terms which drive resonances. One might perhaps depend on sorting for one component and use other compensating schemes such as "binning" for the second component. Binning, as proposed by R. Talman for the SSC, classifies all magnets in the ring into a number of groups ("bins"); magnets belonging to the same group are then all connected to the same power supply to excite the correction windings. Depending on how many bins one is willing to consider, the effective rms value of multipole component can be reduced substantially. A real two-component sorting for the SSC has been tried by L. Schachinger² to reduce the effects of skew quadrupole and normal sextupole errors simultaneously but the improvement over the one-component sorting is not clear from her report alone.

Since the Tevatron is the first superconducting machine, it is understandable that the first (recorded) magnet sorting was performed for it with a limited but well-defined goal in mind.³ The goal was simply to minimize the magnitude of several isolated resonance-driving terms, these resonances arising from sextupole components b_2 and a_2 and skew octupole component a_3 . The dimensionless figure-of-merit was the magnitude of each term relative to what one would expect from the distribution of these components if the sorting were not done. Since this sorting involves only one particular harmonic component for each resonance (altogether six), it is the simplest case of what one might call the "global" compensation.⁴ Although the effectiveness of this scheme is self-evident when the tune is very close to one of the resonances considered, it will be impossible to say how much the beam lifetime is enhanced by the sorting. One must be satisfied with the often-expressed feeling of Fermilab people that the Tevatron is a very "linear" machine. In "global" compensation schemes, it is important to note that cancellation of errors in two widely separated magnets would be destroyed by small changes in the tune or uncertainties in the lattice functions. Magnets to be sorted as a group should not cover too much betatron phase advance. For the Tevatron, thirty or so magnets were sorted as a group and they covered approximately 280° .

An entirely different scheme has been tried for the Relativistic Heavy Ion Collider (RHIC) in which the effect of normal and skew quadrupole components is considered to be serious.⁵ Since there are only two dipoles in each cell and the phase advance per cell is 90° , one is forced to sort a very small number (8 to 12 used) of magnets in order to avoid covering too much phase advance. With such a small number of magnets, global compensations controlling many harmonic components are not suitable and a "local" sorting scheme has been used. Local scheme is more appropriate when the source of errors is within a relatively small area of the ring. One tries to confine the effect of errors within this area. If the compensation is perfect, there will be no effect outside the area although the effect may not be too small inside.

Frequency-Domain Consideration

If it is allowed to ignore variations of machine parameters which are slow compared with the revolution time, any field perturbations in the ring are periodic with the period 2π in $\theta = \text{path length}/(\text{average machine radius})$. One can express the resulting change in quantities such as closed orbit, betatron amplitude functions, dispersion functions, the transition energy of the ring and the distorted functions⁷ associated with nonlinear perturbations in a Fourier expansion, i.e., frequency-domain formulas.^{4,6,8} The particular advantage of frequency-domain formulas is that they show explicitly the relative importance of each harmonic component by the denominators of the n -th harmonic term of the form

$$Q^2 - n^2, \quad (2Q)^2 - n^2, \quad 3Q - n, \quad \text{and} \quad (Q_1 \pm 2Q_2) - n, \text{ etc.}$$

Mathematically speaking, these frequency-domain expressions are of course completely equivalent to some closed forms, i.e., time-domain formulas. The time-domain formalism is convenient when the perturbation is confined within a small region of the ring and one tries to confine its effect within that region, or at least to minimize the disturbance propagating out of the region. Localized closed orbit bumps and beta-function bumps are typical examples.

When one or two well-identifiable resonances dominate the effect under consideration, it is easy to see from frequency-domain expressions what particular harmonic components must be controlled. The sorting performed for the Tevatron is based on the assumption that this is indeed what one must do in order to make the

machine more manageable than otherwise. Since there was no attempt to reduce the magnitudes of more than a handful of harmonic components, it is not really surprising that, according to a tracking study by N. Gelfand,⁹ the dynamic aperture of the sorted Tevatron does not exhibit any improvement over randomly arranged rings when the tune is away from third-integer resonances. One must conclude that a large number of harmonic components contribute to the aperture limitation and it is generally not enough to manipulate a few terms only. Harmonic correction magnets will be incapable of handling this situation unless one is willing to install and operate many independently controllable families. The sorting scheme proposed by Gluckstern and Ohnuma aims to control approximately M components ($M \approx Q$, tune value) around $n \approx Q$ and $3Q$ (actually around $n \approx$ any integer times Q where integers are either even or odd) when sextupole effects are considered.¹⁰ It is assumed here that two tunes Q_1 and Q_2 are close to each other so that $|Q_1 - Q_2|$ is much less than Q_1 and Q_2 .

Assume that there are N measured magnets available for installation at N consecutive locations. These N magnets should cover the betatron phase advance of 360° . For example, if the phase advance is 90° per cell and there are five dipoles in each half cell, N is 40. Magnets are numbered in the order of their sextupole contents, 1 for the most negative to N for the most positive. Note that the average part is not considered here. The arrangement of N magnets in N locations will be discussed later but it is by no means unique. In the next group of N magnets, they are numbered such that 1 is now the most positive and N the most negative. Their arrangement should be identical as far as the numbers are concerned; if the arrangement chosen for the first N magnets is 3,9,6,2,..., for example, the order for the second group should be identical although the numbering is now in descending order. It is obvious that the phase advance from the magnet \underline{n} in the first group to the magnet \underline{n} in the second group is 360° for all \underline{n} 's. It is also clear from this arrangement that one should like to have an even number of groups in each superperiod. In reality, this is not always possible and there will be some number of cells which are not paired. One of the easiest solution is to take aside good magnets from each group and use them in the unbalanced cells. For example, if there are $60\frac{1}{2}$ cells in each superperiod, fourteen groups of 40 magnets will be balanced but the remaining 45 magnets will not be balanced. One requests 43 or 44 magnets in each group, instead of the exact number 40, and set aside the extra three or four best magnets in each group. They can then be used in the unbalanced cells randomly or in some suitable arrangement. It can be shown¹⁰ that the expected average magnitude of harmonic component \underline{n} is zero unless $n = M/2, 3M/2, 5M/2, \dots$ and the rms values are all reduced by a factor

$$\left(\frac{2}{N+1} \right)^{\frac{1}{2}}$$

compared with the value expected for random arrangement.

The arrangement within each group can be arbitrary as long as the same order is maintained in all the groups. This statement of course ignores the importance of local cancellation and, for some arrangement, the effectiveness of sorting may depend too much on the choice of tune values. Uncertainties in the lattice parameters may also affect the performance. Common sense dictates that a large positive and a large negative sextupoles should be placed next to each other. Two large positive(negative) ones should be installed with phase advance of 180° so that they will contribute little to $n = M$ and $n = 3M$ which are still the most important harmonics. Even then, there are many equally effective arrangements and this flexibility can be used to control harmful effects arising from other multipole components in a few magnets.

An Example

Since the smears used by the SSC Central Design Group are proportional to distortion functions defined by Tom Collins,^{7,8} their rms magnitudes are used to compare the sorted ring with random ones. There are five pairs of functions and in each pair, one is cos-like and the other is sin-like. Cos-terms are continuous (as beta functions) but sin-terms change their values at each sextupole components (as alphas functions with thin lens). Their behavior is completely analogous to a closed orbit, for example; cos-term is like x or y and sin-term is like x' or y'. The difference is the phase angle one must use in moving from one sextupole to the next. For a closed orbit, the phase angle to be used from one dipole error to the next is the betatron phase angle itself, ψ_x or ψ_y . For distortion functions,

cos-term	B_3	B_1	\bar{B}	$B_S(B_+)$	$B_D(B_-)$
sin-term	A_3	A_1	\bar{A}	$A_S(A_+)$	$A_D(A_-)$
phase angle	$3\psi_x$	ψ_x	ψ_x	$\psi_x + 2\psi_y$	$\psi_x - 2\psi_y$

All ten functions are evaluated at each quadrupole location in the example given below. The magnitude of each pair is

$$C = (A^2 + B^2)^{\frac{1}{2}}.$$

Two figure of merits are used: MAX = maximum values of C's in the ring,

SIGMA = $(\sum C^2/N_Q)^{\frac{1}{2}}$ where the summation is for N_Q quadrupole locations in the ring. For ten rings with different magnets, the ratio of MAX(sorted)/MAX(unsorted) is averaged over ten rings. For SIGMA(sorted)/SIGMA(unsorted), the summation is taken for all ten machines before taking the square-root. The test lattice used is

90°/cell, 64½ cells/period, six superperiods with insertions,

5 dipoles/half cell, 40 dipoles/360°,

tune = 118 + (four different values of fraction)

arrangement within each group

((QD)19,23,15,27,11(QF)31, 7,35, 3,39 /((QD)1,37, 5,33, 9(QF)29,13,25,17,21/

((QD)20,24,16,28,12(QF)32, 8,36, 4,40 /((QD)2,38, 6,34,10(QF)30,14,26,18,22/

tune		C_3	C_1	\bar{C}	C_S	C_D
118.10	MAX	.11	.16	.11	.13	.16
	SIGMA	.087	.095	.072	.083	.068
118.25	MAX	.10	.14	.14	.10	.16
	SIGMA	.079	.11	.095	.070	.099
118.32	MAX	.067	.14	.14	.058	.17
	SIGMA	.056	.11	.10	.044	.10
118.40	MAX	.088	.14	.14	.10	.17
	SIGMA	.076	.11	.10	.068	.11

It would be interesting to find the amount of smear from tracking but this has has not been done.

References

1. D. Neuffer, SSC CDG Report SSC-N-384, September 1987.
2. L. Schachinger, SSC CDG Report SSC-N-123, January 1986.
3. L. Michelotti and S. Ohnuma, IEEE Trans. Nucl. Sci., NS-30, 2472 (1983).
4. S. Ohnuma, Interaction Between Particle and Nuclear Physics, AIP Conference Proceedings No. 123, 415 (1984).
5. S. Ohnuma, IEEE Trans. Nucl. Sci., NS-34, 1176 (1987).
6. S. Ohnuma, Fermilab \bar{p} Note No. 105, December 5, 1980.
7. T. Collins, "Distortion Functions", Fermilab Report Fermilab-84/114, October 23, 1984.
8. K.-Y. Ng, Fermilab Report FN-455, August 1987.
9. N.M. Gelfand, Accelerator Physics Issues for a Superconducting Super Collider, University of Michigan, UM HE 84-1, p. 124 (1984).
10. R.L. Gluckstern and S. Ohnuma, IEEE Trans. Nucl. Sci., NS-32, 2314 (1985).

SEXTUPOLE CORRECTION SCHEME FOR THE ESRF

A. Ropert

ESRF, Grenoble, France

ABSTRACT

The large chromaticities encountered in low emittance lattices designed for the new generation of synchrotron radiation sources require sophisticated sextupole corrections. These, in turn, tend to limit the dynamic aperture. The Chasman-Green lattice adopted for the 6 GeV ESRF storage ring was reputed to be very sensitive in this regard. We describe here the optimization of the sextupole correction scheme that has been applied to the ESRF lattice to improve considerably the performance.

1. DESCRIPTION OF THE LATTICE

The linear optics design of the ESRF storage ring has been governed by the requirement of obtaining a low emittance structure with a large number of long straight sections to accommodate insertion devices.

The unit cell (1/32 of the ring) consists of a single arc matched to a dispersion-free insertion straight section. The triplets at both ends of the straight sections are used to achieve the desired lattice functions at the insertion location. The dispersion in the arc is controlled by means of two quadrupole doublets. Compared to the basic Chasman-Green achromat with only one quadrupole between the two bending magnets, this scheme provides more flexibility and allows independent control of the horizontal and vertical chromaticities. The basic configuration has a 16-fold symmetry, with alternating low beta and high beta straight sections. The structure produces a natural emittance of 6.8×10^{-9} m.rad. The optical functions for one superperiod are shown in Fig. 1.

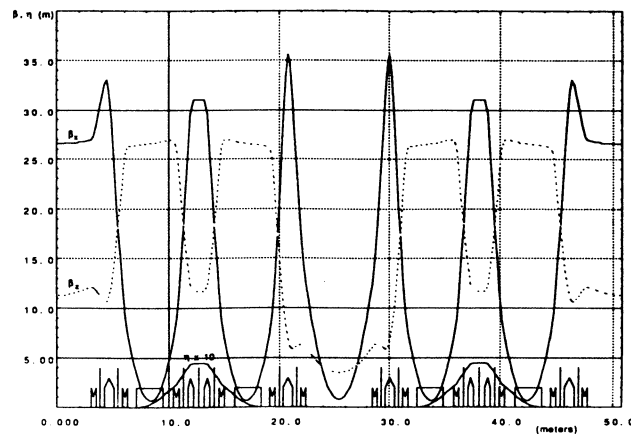


Fig. 1

It is of prime importance to choose the tune as far as possible from third-order systematic resonances driven by sextupoles. For the horizontal tune, the possible choices are rather limited since the requirement for low emittance induces a phase advance of the order of π per achromat. The choice of the vertical tune has been determined by the necessity of keeping the vertical chromaticity as small as possible. The tunes for the whole machine are therefore: $\nu_x = 36.2$, $\nu_z = 11.2$.

2. SEXTUPOLE CORRECTION SCHEME

The strong focusing required to obtain a low emittance results in large chromaticities. The natural chromaticities for the lattice, defined as $\xi = \Delta\nu/(\Delta p/p)$, are -113.9 and -34.5 in the horizontal and vertical plane respectively. Since the chromaticity-correcting sextupoles introduce non-linear effects that limit the dynamic aperture, additional sextupoles are generally used in the dispersion-free regions to improve the situation. The sextupole arrangement, as proposed in the original design [1], provided a small dynamic aperture. By properly selecting the location of the sextupoles and tuning them in order to compensate third-order resonance driving terms and tune shifts with amplitude, considerable enlargement of the dynamic aperture has been achieved.

2.1 Chromaticity correction

Two sextupole families are used to correct the chromaticity in both planes. The first criterion for choosing their location is the minimization of tune dependence on energy. The horizontal focusing sextupole is placed in the middle of the dispersive section. The two defocusing side sextupoles can be located either between the dipole and the defocusing quadrupole or between the doublet quadrupoles. This latter configuration gives better results, although the beta functions are not very well separated, which leads to higher sextupole strengths.

The energy range of interest at 6 GeV is dictated by quantum lifetime. An energy acceptance of $\pm 2\%$ is required, assuming bunch lengthening of a factor 3 in single bunch operation. The tune shifts are small within this energy range, as is shown in Fig. 2.

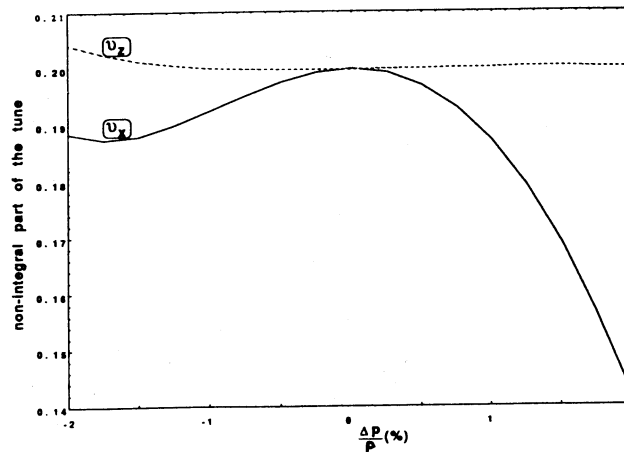


Fig 2

2.2 Compensation scheme

In order to minimize the driving terms of third-order resonances and enlarge the dynamic aperture, four additional sextupole families have been introduced into the dispersion-free regions. Two of them are located in the high beta straight sections; the other two families are in the low beta straight sections. In addition, the dependence of tune on amplitude has been considerably reduced by paying attention to the contribution of these sextupoles. When using Hamiltonian formalism and perturbation theory, the amplitude dependent tune shifts driven in second-order by sextupoles can be expanded in the form [2]:

$$\Delta v_x = A \epsilon_x + B \epsilon_z \quad (1)$$

$$\Delta v_z = B \epsilon_x + B \epsilon_z \quad (2)$$

with

$$A = -\frac{3}{4} \left\{ \sum_m \frac{|D_m|^2}{v_x - m} + 3 \sum_n \frac{|F_n|^2}{3 v_x - n} \right\} \quad (3)$$

$$B = \frac{1}{2} \left\{ \sum_q \frac{|H_q|^2}{v_x - 2 v_z - q} - \sum_r \frac{|L_r|^2}{v_x + 2 v_z - r} - \sum_m \frac{|D_m||G_m|}{v_x - m} \cos(d_m - g_m) \right\} \quad (4)$$

$$C = -\frac{1}{4} \left\{ \sum_q \frac{|H_q|^2}{v_x - 2 v_z - q} + \sum_r \frac{|L_r|^2}{v_x + 2 v_z - r} + \sum_p \frac{|G_p|^2}{v_x - p} \right\} \quad (5)$$

The minimization process which has been implemented in the tracking code BETA [3] allows the simultaneous compensation of the following quantities:

- i) resonant harmonic coefficients D_m , F_n , G_p , H_q , L_r driving the third-order resonances close to the machine tune, weighted by the distance of the tune from the resonance;
- ii) tune shifts Δv_x and Δv_z built up from a sum over a given number of harmonics.

This strategy has been successfully applied to the ESRF lattice, as demonstrated in Fig. 3 which shows a comparison between the dynamic aperture of the original ESRF lattice and the present design.

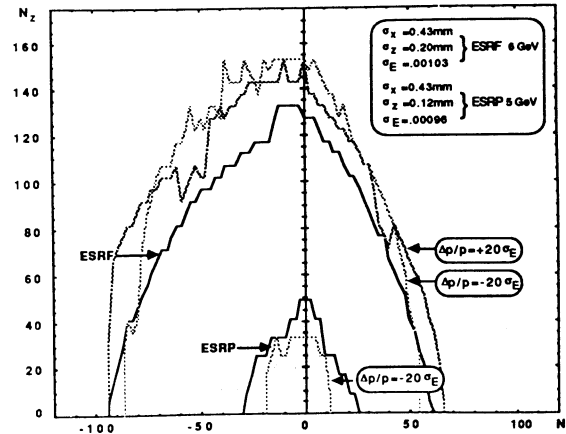


Fig. 3

The tune shifts with amplitude determined by tracking are plotted in Fig. 4. Their minimization within the whole dynamic aperture is an important figure of merit. In most cases, a lattice with large amplitude dependent tune shifts has an adverse behaviour when errors are introduced in the structure, since particles are driven to non-systematic resonances, leading to significant reduction of dynamic aperture. This is illustrated in Fig. 5, which shows the comparative response to quadrupole positioning errors of the ESRF structure and a Chasman-Green lattice which was not brought to the same level of optimization.

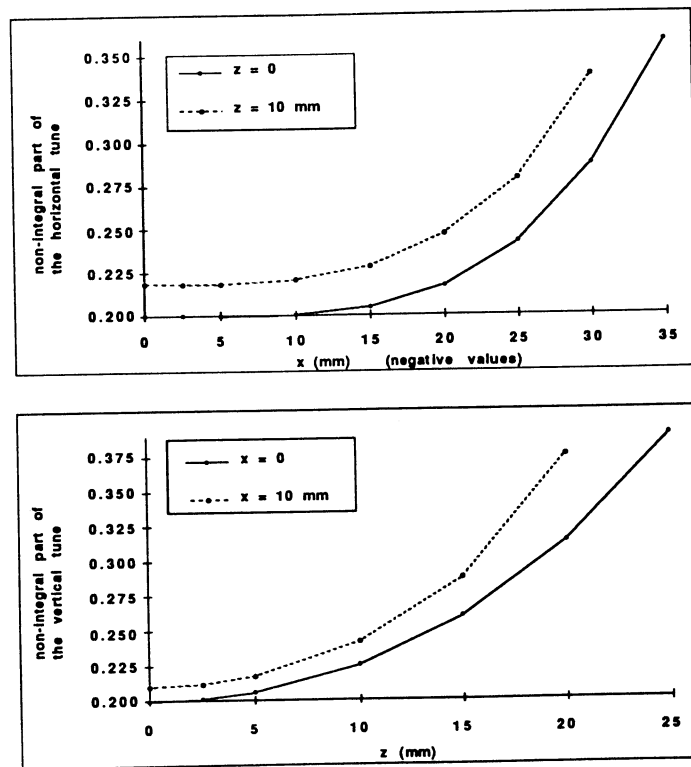


Fig. 4

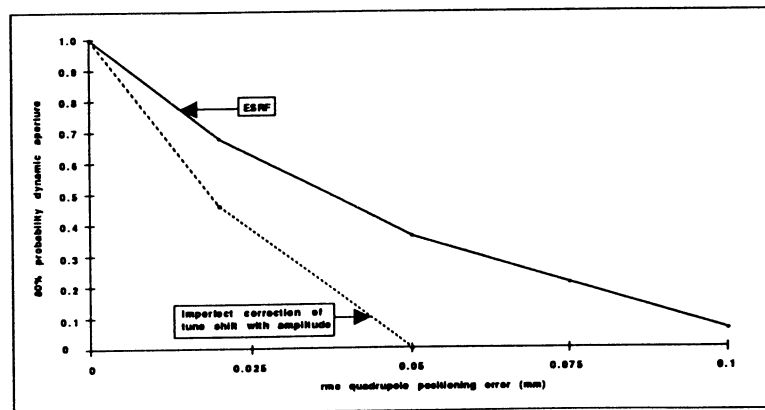


Fig. 5

Besides the enlargement of the dynamic aperture, the issue of flexibility of the lattice is very important. The results obtained when altering the periodicity of the machine by changing the number of high beta and low beta straight sections are shown in Fig. 6. If the sextupoles are not readjusted, the dynamic aperture of the detuned lattice is considerably reduced. This is mainly due to the excitation of additional driving resonances resulting from breaking down the symmetry. However, the dynamic aperture can be increased back to values comparable to the high periodicity scheme by switching the local correction sextupoles from one family to another and reoptimizing all four families.

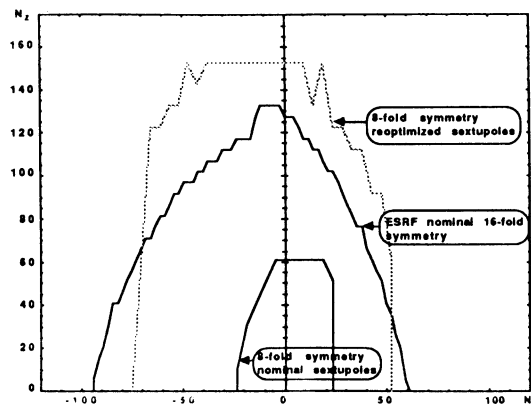


Fig. 6

3. CONCLUSION

The above results demonstrate that the simultaneous compensation of third-order resonances and tune shifts with amplitude greatly improves the performance of the ESRF lattice, as far as dynamic aperture, sensitivity to errors and flexibility are concerned.

REFERENCES

- [1] ESRP, Report of the ESRP, presented by B. Buras and S. Tazzari, Geneva (1984)
- [2] D. Poirier, Thesis, Orsay (1984)
- [3] L. Farvacque, J.L. Laclare, A. Ropert, BETA users' guide, ESRF-SR/LAT/88-08

LIST OF PARTICIPANTS

P. AUDY	CEN, Lab.Nat. Saturne <u>F-91191 GIF-sur-YVETTE</u>
B. AUTIN	CERN, PS Div. <u>CH-1211 GENEVA 23</u>
G. BRIANTI	CERN, DG Div. <u>CH-1211 GENEVA 23</u>
R. BRINKMANN	DESY, Notkestrasse 85 <u>D-2000 HAMBURG 52</u>
A. CHAO	SSC, LBL, Mail Stop 90.4040 <u>BERKELEY, CA 94720 U.S.A.</u>
S. CHATTOPADHYAY	LBL, Univ. of California <u>BERKELEY, CA 94720 U.S.A.</u>
M. CORNACCHIA	LBL, Univ. of California 50A-3115 <u>BERKELEY, CA 94720 U.S.A.</u>
E.D. COURANT	BNL, Physics Dept. <u>UPTON, N.Y. 11973 U.S.A.</u>
J. CRAWFORD	P.S.I. (SIN), <u>CH-5234 VILLINGEN</u>
D.A. EDWARDS	FNAL, P.O. Box 500 <u>BATAVIA IL 605 10 U.S.A.</u>
E. FOREST	SSC, LBL, Mail Stop 90.4040 <u>BERKELEY, CA 94720 U.S.A.</u>
J. GAREYTE	CERN, SPS Div. <u>CH-1211 GENEVA 23</u>
G. GUIGNARD	CERN, LEP Div. <u>CH-1211 GENEVA 23</u>
J. HAGEL	CERN, LEP Div. <u>CH-1211 GENEVA 23</u>
M. HARRISON	FNAL, P.O. Box 500 <u>BATAVIA IL 605 10 U.S.A.</u>
S. HEIFETS	CEBAF, 12070 Jefferson Ave. <u>NEWPORT NEWS, VA 23606 U.S.A.</u>
A. HILAIRE	CERN, SPS Div. <u>CH-1211 GENEVA 23</u>
K. HIRATA	CERN, LEP Div. <u>CH-1211 GENEVA 23</u>
G. von HOLTEY	CERN, LEP Div. <u>CH-1211 GENEVA 23</u>
C.-S. HSUE	Synchr.Rad.Res.Center, 6 Roosevelt Road, Sec. 1 <u>10757 TAIPEH TAIWAN.</u>
E. KAISER	CERN, LEP Div. <u>CH-1211 GENEVA 23</u>
E. KEIL	CERN, LEP Div. <u>CH-1211 GENEVA 23</u>
S. KHEIFETS	SLAC, P.O. Box 4349 <u>STANFORD CA 94305 U.S.A.</u>
P. KREJCIK	CERN, PS Div. <u>CH-1211 GENEVA 23</u>
H. KUGLER	CERN, PS Div. <u>CH-1211 GENEVA 23</u>
P. KUSKE	BESSY, Lentzeallee 100 <u>D-1000 BERLIN 33</u>
C. LEEMANN	CEBAF, 12070 Jefferson Ave. <u>NEWPORT NEWS, VA 23606 U.S.A.</u>

S. MAIO	CERN, LEP Div. <u>CH-1211 GENEVA 23</u>
H. MAIS	DESY, Notkestrasse 85 <u>D-2000 HAMBURG 52</u>
H. MOSHAMMER	Techn.Univ.Graz, Petergasse 16 <u>A - 8010 GRAZ</u>
D. NEUFFER	Los Alamos Nat.Lab., AT-6 MS H829 <u>LOS ALAMOS, NM 87545 U.S.A.</u>
S. OHNUMA	Univ. of Houston, Physics Department <u>HOUSTON, TX 77004 U.S.A.</u>
Y. ORLOV	Newman Lab.of Nucl.St., Cornell University <u>ITHACA, N.Y. 14853 U.S.A.</u>
S. PEGGS	SSC, LBL, Mail Stop 90.4040 <u>BERKELEY, CA 94720 U.S.A.</u>
C. PELLEGRINI	BNL, Physics Dept. <u>UPTON, NY 11973 U.S.A.</u>
F. PILAT	CERN, LEP Div. <u>CH-1211 GENEVA 23</u>
A. PIWINSKI	DESY, Notkestrasse 85 <u>D-2000 HAMBURG 52</u>
C. PLANNER	Rutherford Appleton Lab., Chilton <u>DIDCOT OX11 0QX</u>
J.P. POTIER	CERN, PS Div. <u>CH-1211 GENEVA 23</u>
A. ROBERT	ESRF, B.P. 220 <u>F-38043 GRENOBLE Cédex</u>
J. ROSSBACH	DESY, Notkestrasse 85 <u>D-2000 HAMBURG 52</u>
H. SCHOPPER	CERN, Director General <u>CH-1211 GENEVA 23</u>
T. SHERWOOD	CERN, PS Div. <u>CH-1211 GENEVA 23</u>
B. SIMON	BESSY, Lentzeallee 100 <u>D-1000 BERLIN 33</u>
T. SUZUKI	CERN, LEP Div. <u>CH-1211 GENEVA 23</u>
R. TALMAN	SSC, LBL, Mail Stop 90.4040 <u>BERKELEY, CA 94720 U.S.A.</u>
S. TAZZARI	Lab.Naz. INFN, P.O. Box 13 <u>I-00044 FRASCATI</u>
S. THOMSON	Daresbury Lab., Science Research Council <u>WARRINGTON WA4 4AD Cheshire, U.K.</u>
G. TURCHETTI	Univ.di Bologna, Dpt. Fisica, Via Irnerio <u>I 440126 BOLOGNA</u>
A. VERDIER	CERN, LEP Div. <u>CH-1211 GENEVA 23</u>
J.C. VIALIS	CERN, LEP Div. <u>CH-1211 GENEVA 23</u>
R. WARNOCK	SLAC, P.O. Box 4349 <u>STANFORD CA 94305 U.S.A.</u>
F. WILLEKE	DESY, Notkestr. 85 <u>D-2000 HAMBURG 52</u>
V. ZIEMANN	Universität Dortmund, Beschleunigerphysik <u>D-4600 DORTMUND</u>